The role of ClpC and its adaptor proteins in protein quality control systems of *Bacillus subtilis*

Von der Naturwissenschaftlichen Fakultät der
Gottfried Wilhelm Leibniz Universität Hannover

zur Erlangung des Grades
Doktorin der Naturwissenschaften (Dr. rer. nat.)

genehmigte Dissertation
von
Regina Maria Alver, geb. Kramer, M. Sc.

2020

Referent: Prof. Dr. rer. nat. Kürşad Turgay

Korreferent: Prof. Dr. rer. nat. Thomas Brüser

Tag der Promotion: 09.10.2020

Schlagworte: *Bacillus subtilis*, Proteinqualitätskontrollsysteme, McsB, Biofilmbildung

Keywords: *Bacillus subtilis*, Protein quality control systems, McsB, Biofilm formation

Zusammenfassung

In bakteriellen Zellen sind effiziente Proteinqualitätskontrollsysteme von zentraler Bedeutung, da sie die Anpassung regulatorischer Prozesse an wechselnde Umweltbedingungen unterstützen und an Stressantworten beteiligt sind. So können durch Hitzestress fehlgefaltete und aggregierte Proteine erkannt und durch Chaperone neu gefaltet oder durch Proteasen abgebaut werden. In *B. subtilis* ist das Hsp100/AAA+ Protein ClpC Teil des Proteinqualitätskontrollsystems und kann durch Kopplung mit ClpP einen Proteasekomplex (ClpCP) bilden, wobei die Substraterkennung und -auswahl von spezialisierten Adapterproteinen für ClpC vorgenommen wird. In dieser Arbeit konnte gezeigt werden, dass *in vitro* die komplette Disaggregation und wirksame Rückfaltung von Hitze induzierten Proteinaggregaten durch ClpC von Adapterprotein und Proteinargininkinase McsB, sowie von der Phosphatase YwlE abhängt. Als wesentlich für den Rückfaltungsprozess wurden insbesondere die Kinaseaktivität von McsB und die Phosphataseaktivität von YwlE identifiziert. Zudem wurde in Gegenwart von aktivem YwlE und McsB nicht die Degradation von Substraten durch ClpCP, sondern die Disaggregation und Rückfaltung bevorzugt. Es konnte gezeigt werden, dass die Eigenschaften der ClpCP Interaktionsschleife dazu beitragen Rückfaltung oder Degradation von Substraten zu ermöglichen. Folglich wurde hier ein bisher einzigartiges auf Argininphosphorylierung und -dephosphorylierung basierendes System für effiziente Disaggregation und Rückfaltung durch *B. subtilis* ClpC charakterisiert.

Das im Boden lebende Bakterium *B. subtilis* ist außerdem ein Modellorganismus für Studien der Regulation von Biofilmbildung und -komposition. Das Matrixprotein TasA bildet amyloid-ähnliche Fibrillen und ist essenziell für die Biofilmstruktur. Anhand von NMR-Spektroskopie Studien konnte gezeigt werden, dass im nativen Biofilm hauptsächlich homogene TasA Fibrillen vorkommen. Die Kristall-Struktur von TasA wies auf zwei Polyprolin II (PPII) Helices in dynamischen Regionen des Proteins hin. Mutationen in diesen PPII Helices zeigten, dass diese flexiblen Bereiche zu Faltung und Export von TasA beitragen. Außerdem wurde der Einfluss von ClpC auf die Regulation und Struktur des Biofilms untersucht. Eine erhöhte Faltenbildung der Matrix wurde immer beobachtet, wenn die Substratdegradation durch ClpCP beeinträchtigt war. Ein vergleichbarer Phänotyp im *ypbH* Deletionsstamm deutete auf eine Rolle dieses Adapterproteins in der ClpCP abhängigen Biofilmregulation hin.

Abstract

Efficient protein quality control (PQC) systems are crucial in bacterial cells since they support adjustments of regulatory processes under changing environmental conditions and are involved in stress response mechanisms. Under heat stress conditions many proteins are prone to misfold and aggregate, these impaired protein species are targeted by chaperones for refolding or proteases for degradation. In *Bacillus subtilis* the Hsp100/AAA+ protein ClpC is part of the PQC network and can interact with ClpP to form a protease complex (ClpCP), whereby substrate selection is carried out by specialized adaptor proteins for ClpC. During this work it was demonstrated that *in vitro*, the complete disaggregation and effective refolding of a heat aggregated substrate by ClpC depends on the adaptor protein and arginine kinase McsB as well as the phosphatase YwlE. The McsB kinase and YwlE phosphatase activities were identified to be essential for the refolding process. Furthermore, presence of active YwlE and McsB did not promote the degradation of substrates by ClpCP but disaggregation and refolding were favored. It was observed that the properties of the ClpCP interaction loop enable refolding or degradation of substrates. In conclusion, a unique arginine phosphorylation and dephosphorylation based system for effective substrate disaggregation and refolding by *B. subtilis* ClpC was characterized.

The soil-dwelling bacterium *B. subtilis* is an established model organism to study the regulation of biofilm formation and composition. The biofilm protein TasA forms amyloid-like fibrils and is essential for the matrix structure. NMR spectroscopic studies observed that in native biofilms predominantly homogenous TasA fibrils occur. The crystal structure of TasA revealed two polyproline II (PPII) helices in dynamic regions of the protein. Mutations in these helices demonstrated that these flexible segments are involved in TasA protein folding and export. Moreover, the influence of ClpC on regulation and structure of the biofilm was examined. An enhanced biofilm wrinkle formation was observed when no substrate degradation by ClpCP was possible. A similar phenotype was visible in an *ypbH* deletion strain, indicating that this adaptor protein might play a role in ClpCP dependent regulation of biofilm formation in *B. subtilis*.

Abbreviations

AAA+	ATPase associated with cellular activities
ADEP	acyldepsipeptides
ATP	adenosine triphosphate
BGSC	*Bacillus* Genetic Stock Center
BSA	bovine serum albumin
CC	Coomassie and Congo Red dye
cfu	colony forming units
Cs	citrate synthase
CV	column volumes
DMSO	dimethyl sulfoxide
DNA	deoxyribonucleic acid
DTT	dithiothreitol
DWB	double walker B
e.g.	*exempli gratia*, for example
EDTA	ethylenediaminetetraacetic acid
et al.	and others
FPLC	fast protein liquid chromatography
HEPES	4-(2-hydroxyethyl)-1-piperazineethanesulfonic acid
Hsp	heat shock protein
IPTG	isopropyl β-D-1-thiogalactopyranoside
kb	kilobase
kDa	kilodalton
LB	Luria Bertani
Mdh	malate dehydrogenase
MOPS	3-(N-morpholino)propanesulfonic acid
NADH	nicotinamide adenine dinucleotide
NBD	nucleotide binding domain
Ni-NTA	nickel nitrilotriacetic acid
NMR	nuclear magnetic resonance
NTD	amino (N)-terminal domain
OD	optical density at 600 nm
PAGE	polyacrylamide gel electrophoresis
pArg	phosphorylated arginine
PCR	polymerase chain reaction
PIPES	piperazine-N,N′-bis(2-ethanesulfonic acid)
PMSF	phenylmethylsulfonyl fluoride
PPII	polyproline II
PQC	protein quality control
PQK	Proteinqualitätskontrollsysteme
PTM	post translational modification

RNA	ribonucleic acid
rpm	revolutions per minute
SDS	sodium dodecyl sulfate
SigSeq	signal sequence
SMM	spizizen minimal medium
SUMO	small ubiquitin-like modifier
TCA	trichloracetic acid
TE	Tris-HCl EDTA
Tris	tris(hydroxymethyl)aminomethane
v/v	volume per volume
w/v	weight per volume
wt	wild type

Table of Contents

Zusammenfassung 1

Abstract II

Abbreviations III

Table of Contents V

1 Introduction 1

1.1 Phosphorylation as post-translational modification 1

1.1.1 Protein arginine kinase McsB in *B. subtilis* 3

1.2 Chaperones involved in protein homeostasis 6

1.3 Clp protein family 9

1.3.1 Clp proteases and protease complexes 9

1.3.2 Clp dependent protein un- and refolding 10

1.3.3 Adaptor proteins and recognition tags 12

1.3.4 Clp proteins in *B. subtilis* regulatory pathways 13

1.4 Biofilm formation in *B. subtilis* 15

1.4.1 Biofilm components 16

1.4.2 Regulation of biofilm formation 18

1.5 Aim of this work 21

2 Materials and Methods 22

2.1 Devices and reagents 22

2.2 Primers, plasmids and strains 23

2.3 Common media and solutions 28

2.4 Cloning 28

2.5 *B. subtilis* genomic DNA preparation 29

2.6 Transformation of *E. coli* and *B. subtilis* 29

2.7 Thermotolerance experiments 31

2.8 Biofilm cultivation 31

2.8.1 Biofilm reconstitution experiments 32
2.8.2 Biofilm sample fractionation and TasA protein level determination 33

2.9 Protein purification 34

2.9.1 His-tagged proteins 35
2.9.2 SUMO-His-tagged proteins 36
2.9.3 Desalting purified protein 37

2.10 SDS-PAGE & Western blotting 38

2.11 *In vitro* assays 40

2.11.1 Bradford assay 40
2.11.2 Malachite Green assay 40
2.11.3 Degradation assay 41
2.11.4 Light scattering assay 41
2.11.5 Malate dehydrogenase activity assay 42
2.11.6 Citrate synthase activity assay 43

3 Results 44

3.1 *In vitro* characterization of the ClpC disaggregation activity 44

3.1.1 YwlE enhances the McsB-induced ClpC disaggregation and refolding activity 47
3.1.2 McsB kinase and YwlE phosphatase activities are essential for efficient refolding 51
3.1.3 Disaggregation and refolding are triggered by McsA activation of McsB kinase ... 57
3.1.4 The influence of YwlE depends on protein dephosphorylation 61
3.1.5 The phosphatase YwlE assists protein refolding 65

3.2 Protein refolding or degradation with the protease complex ClpCP 67

3.2.1 Active YwlE enables substrate refolding rather than degradation by ClpCP 68
3.2.2 McsB C167S can act as adaptor protein for ClpCP 74
3.2.3 ClpC P-loop mutations affect the ClpCP degradation activity 78
3.2.4 Native Mdh is not significantly affected by the chaperone system components 85
3.2.5 Disaggregation and refolding of the model substrate citrate synthase 86

3.3 ClpC activation by adaptor proteins MecA and McsB 89

3.3.1 N-terminal ClpC mutations affect adaptor protein mediated activities 89
3.3.2 MecA and McsB facilitate distinct ClpCP activation 90

3.4 The role of ClpC and TasA in biofilm formation 93

3.4.1 The structure of TasA comprises two PPII helices 99
3.4.2 The intact PPII helix 1 is important for proper TasA export 101
3.4.3 Mutations in *tasA* PPII helix 2 impair biofilm formation 104
3.4.4 Biofilm formation is affected in *clpC* mutants 108
3.4.5 ClpCP dependent degradation is involved in pellicle formation 110
3.4.6 Adaptor protein YpbH could be involved in regulations via ClpCP 113

4 Discussion 117

4.1 McsB facilitates diverse ClpC dependent activities 117

4.1.1 Adaptor protein and arginine kinase activities of McsB 118
4.1.2 A refolding system based on arginine phosphorylation and dephosphorylation ... 119
4.1.3 Aggregate removal by protein rescue or degradation 124
4.1.4 The properties of the ClpCP interaction enable degradation and refolding 128
4.1.5 Differences in adaptor protein dependent ClpC activation 131

4.2 TasA and ClpC are important for pellicle biofilm formation 132

4.2.1 PPII helices contribute to the structural integrity of TasA 134
4.2.2 ClpC activities regulate biofilm formation 137

4.3 Summary and Conclusion 142

List of Figures 143

List of Tables 145

References 146

Curriculum vitae VIII

List of Publications IX

Danksagung X

1 Introduction

They are almost everywhere. Bacteria can adapt to enormous variances in e.g. temperature, pH, and nutrient supply. The ability to sense and to react to the environment is crucial for cellular survival. Movement to reach nutrients or evade unfavorable conditions, but also communication with other cells in a community is essential. Environmental changes can be sensed by different signaling pathways, resulting in regulation of cellular development and behavior (Fabret et al., 1999; Rodrigue et al., 2000). This machinery often depends on post-translational modifications (PTMs) altering regulatory proteins. Specific enzymes can attach various, often reversible modifications to amino acids of their substrate protein. Most common PTMs in bacteria are protein glycosylation, lipidation, acetylation and protein phosphorylation (Eichler and Koomey, 2017; Kim et al., 2013; Nakayama et al., 2012). It is usual that multiple modifications are attached to proteins, which change their chemical properties, such as binding characteristics, conformation, or charge (Macek et al., 2019; Mijakovic et al., 2016). Therefore, PTMs are an efficient way to trigger fast reactions and contribute to distinct processes, such as signal transduction, regulation of enzymes, cell division, and protein homeostasis.

1.1 Phosphorylation as post-translational modification

The relevance of protein phosphorylation as a PTM in bacteria, became clear with advances in detection and identification methods (Beltrao et al., 2013; Choudhary and Mann, 2010; Macek et al., 2019). In many regulatory and developmental processes specific kinases catalyze the phosphorylation of proteins, while dephosphorylation is carried out by according phosphatases. Phosphorylation of various amino acids have been reported as PTMs and most frequently observed were phosphorylation of histidine residues followed by phosphorylation of serine or threonine residues, facilitated by Hanks-type kinases (Macek et al., 2019; Stancik et al., 2018). Distinct chemical bonds can be formed by phosphorylation of different amino acids, which exhibit varying properties, such as altered stabilities or phospho-transfer potentials (Mijakovic et al., 2016). Thus, phosphorylation of serine, threonine and tyrosine (phosphoester bond) is considered to be more stable than the high-energy bonds in phosphorylated histidine or arginine (phosphoramidate bond) (Sickmann and Meyer, 2001). These characteristics can facilitate different functions, like the swift and efficient signal transduction in different regulatory networks (Mijakovic et al., 2016; Stock et al., 2000).

1.1 Introduction

Two-component systems

In the Gram-positive model organism *B. subtilis* many regulatory mechanisms, determining responses to the environment and cellular development, are well characterized. A wide range of signaling pathways entail so called two-component systems or more complex phosphorelays (Narula et al., 2016). In these networks, protein histidine kinases sense various signals, resulting in autophosphorylation and transfer of a phosphoryl group to the aspartate residue of response regulators (Fabret et al., 1999; Stock et al., 1989). This phosphorylation can cause conformational changes activating the regulator, which acts as a transcription factor or interaction partner adjusting gene expression. Since histidine kinase components are often embedded in the membrane, they can sense and react to environmental changes (Macek et al., 2019). Quorum sensing, for example, is a two-component system based process, enabling bacteria to detect and react to the cell density in communities (Kalamara et al., 2018; Miller and Bassler, 2001). Increasing concentrations of small molecules, so-called autoinducers or pheromones, which are secreted by bacteria, can be recognized by the sensor kinase (Figure 1 A). Subsequent phosphorylation of the response regulator results in coordinated initiation of cellular processes (Kumar and Singh, 2013; Wynendaele et al., 2015). In *B. subtilis* two-component systems are involved in chemotaxis by the Che signaling system (Rosario and Ordal, 1996), reactions to phosphate starvation by Pho (Fujisawa et al., 2007), as phosphorelay in initiation of sporulation by Spo0 systems (Burbulys et al., 1991; Hoch, 1993) or initiation of competence development (Grossman, 1995), among others.

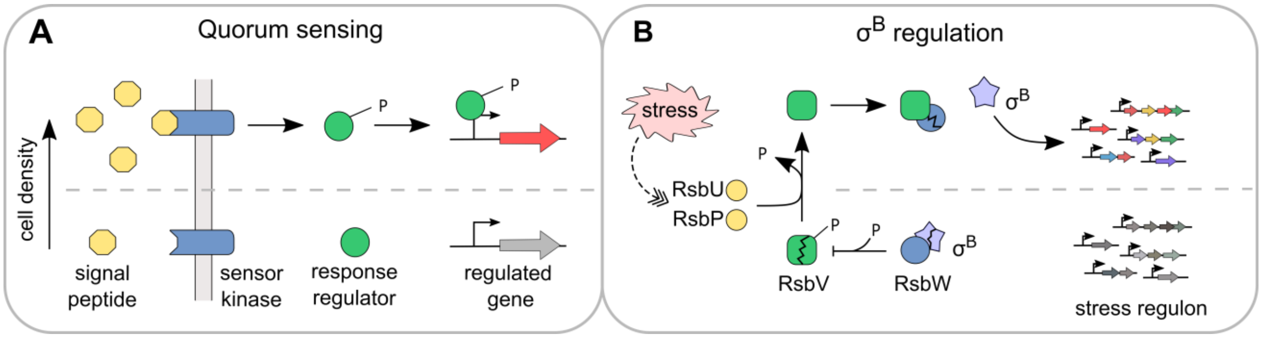

Figure 1 Model of Quorum sensing and σ^B regulation.

(A) In Quorum sensing, sensor kinases can detect increasing cell density through rising levels of signal peptide concentrations. Phosphorylation and activation of response regulators results in altered gene expression. (B) Under normal conditions, RsbW binds σ^B, acting as an anti-σ-factor and inactivates RsbV by phosphorylation. Upon stress, RsbU and RsbP dephosphorylate and activate RsbV that binds to RsbW, releasing and activating transcription factor σ^B. This results in upregulation of the general stress regulon.

1.1 Introduction

Phosphorylation of key regulators in bacterial stress response

Phosphorylation and dephosphorylation events also play a major role in cellular stress response pathways. One prominent example is the regulation of the general stress regulon including ~150 genes under control of stress response transcription factor sigma B (σ^B) (Petersohn et al., 2001; Price et al., 2002). This transcription factor alters promotor binding specificity of the RNA polymerase by binding to the core enzyme (Haldenwang and Losick, 1980). σ^B regulation underlies a complex partner switching mechanism dependent on Rsb (regulator of sigma B) proteins (Figure 1 B). Under normal growth conditions σ^B is bound and inhibited by the anti-σ-factor RsbW, which also possesses serine kinase activity to specifically inactivate RsbV by phosphorylation (Benson and Haldenwang, 1993; Dufour and Haldenwang, 1994). Dephosphorylation of the anti-anti-σ-factor RsbV by RsbU, under environmental stress, or RsbP, under metabolic stress conditions, leads to inactivation of anti-σ-factor RsbW by complex formation trough protein-protein interaction with RsbV and release and activation of σ^B (Brigulla et al., 2003; Vijay et al., 2000; Voelker et al., 1996). Similar partner-switching mechanisms are described for RsbT activation and regulation of sporulation by anti-σ-factor serine kinase SpoIIAB, managing σ^F activity by binding or phosphorylation of anti-anti-σ-factor SpoIIAA (Kang et al., 1998; Min et al., 1993; Yang et al., 1996).

1.1.1 Protein arginine kinase McsB in *B. subtilis*

The protein McsB plays a special role in protein homeostasis of *B. subtilis*, because of its dual function. On the one hand, McsB can act as adaptor protein for AAA+ chaperone ClpC. Thus, it regulates substrate selection, promotes ClpC activation and oligomerization as well as formation of the protease complex ClpC-ClpP (ClpCP) (Elsholz et al., 2012; Kirstein et al., 2007, 2005) (Figure 2). On the other hand, McsB specifically phosphorylates arginine residues, enabling PTM based influence on different regulatory pathways (Elsholz et al., 2012; Fuhrmann et al., 2009; Kirstein et al., 2007; Krüger et al., 2001). Recently, the structure and enzymatic mechanism for protein arginine phosphorylation by *Geobacillus stearothermophilus* McsB were described (Suskiewicz et al., 2019). This dimeric McsB has one catalytic domain targeting substrate proteins and one domain recognizing and binding already phosphorylated arginine residues, resulting in further enhancement of the McsB kinase activity (Suskiewicz et al., 2019).

B. subtilis McsB was shown to possess a low autophosphorylation activity, but full kinase activation and efficient substrate phosphorylation are only possible in presence of McsA (Kirstein et al., 2007, 2005). The specific role of the activator protein McsA, the interaction with McsB, and the exact mechanism of McsB activation have not been investigated in full detail so far. However, addition of McsA enhanced the McsB-induced ClpC ATPase activity as well as degradation of the adaptor protein McsB itself by the ClpCP protease complex *in vitro* (Kirstein et al., 2007). The McsB mediated ClpC activity was considered to be facilitated by phosphorylation of N-terminal arginine residues, whereas ClpC itself was shown to inhibit McsB kinase activity *in vitro* and *in vivo* (Elsholz et al., 2011a, 2012; Kirstein et al., 2005, 2007). Moreover, arginine phosphorylation of model substrates by McsB was demonstrated to act as targeting signal for ClpCP dependent degradation in absence of adaptor proteins in *B. subtilis* (Trentini et al., 2016). Consistently, binding of phosphorylated arginine by a conserved recognition site was also reported for ClpC1 from *Mycobacterium tuberculosis* (Weinhäupl et al., 2018). This intricate functional overlap of kinase and adaptor protein activities of McsB facilitates its involvement in regulatory processes as well as protein homeostasis in *B. subtilis*.

The arginine specific phosphatase YwlE was described to inactivate and antagonize McsB activity *in vitro* and *in vivo* (Elsholz et al., 2010; Fuhrmann et al., 2013a; Kirstein et al., 2005). Since YwlE and McsB do not form a stable complex and the impact of YwlE on McsB ATPase activity is low, it was predicted that the antagonism only depends the phosphatase activity (Fuhrmann et al., 2016). The strict control over McsB kinase activity by the activator McsA and the inhibitors ClpC and YwlE is important for correct cell physiology, as suggested by the severe influence of deletion mutants *in vivo* (Elsholz et al., 2011a). Examination of a Δ*ywlE* mutant revealed global changes in gene expression, demonstrating the significance of arginine phosphorylation and dephosphorylation for functional cellular regulation systems, such as competence development, stress response as well as regulation of spore germination (Figure 2) (Elsholz et al., 2012; Schmidt et al., 2014).

The phosphorylation of arginine modifies its charge from positive to negative and was considered to alter protein-protein, protein-DNA, and protein-RNA interactions (Fuhrmann et al., 2009; Mijakovic et al., 2016; Trentini et al., 2016). Moreover, the high energy of the phosphoramidate (P-N) bond might allow the transfer of the phosphate to other residues and the unstable nature of this bond was considered to complicate the detection (Elsholz et al., 2012; Schmidt et al., 2013;

Sickmann and Meyer, 2001; Teague and Dobson, 1999). Identification of protein arginine phosphorylation *in vivo* was only possible in a Δ*ywlE* mutant or with phosphatase inhibitor treatment in *B. subtilis* (Elsholz et al., 2012; Schmidt et al., 2014). Quantitative analysis of the arginine phosphoproteome of *B. subtilis* under different environmental conditions revealed that the main targets of arginine kinase McsB are members of the stress response system (Schmidt et al., 2014). Consistently, McsB expression is highly induced during heat stress in *B. subtilis* and ClpC interaction decreases, which leads to activation of McsB kinase activity, emphasizing the importance of McsB in heat stress response (Elsholz et al., 2011a). In *Staphylococcus aureus*, McsB is crucial for a successful stress response and accompanying virulence traits (Wozniak et al., 2012).

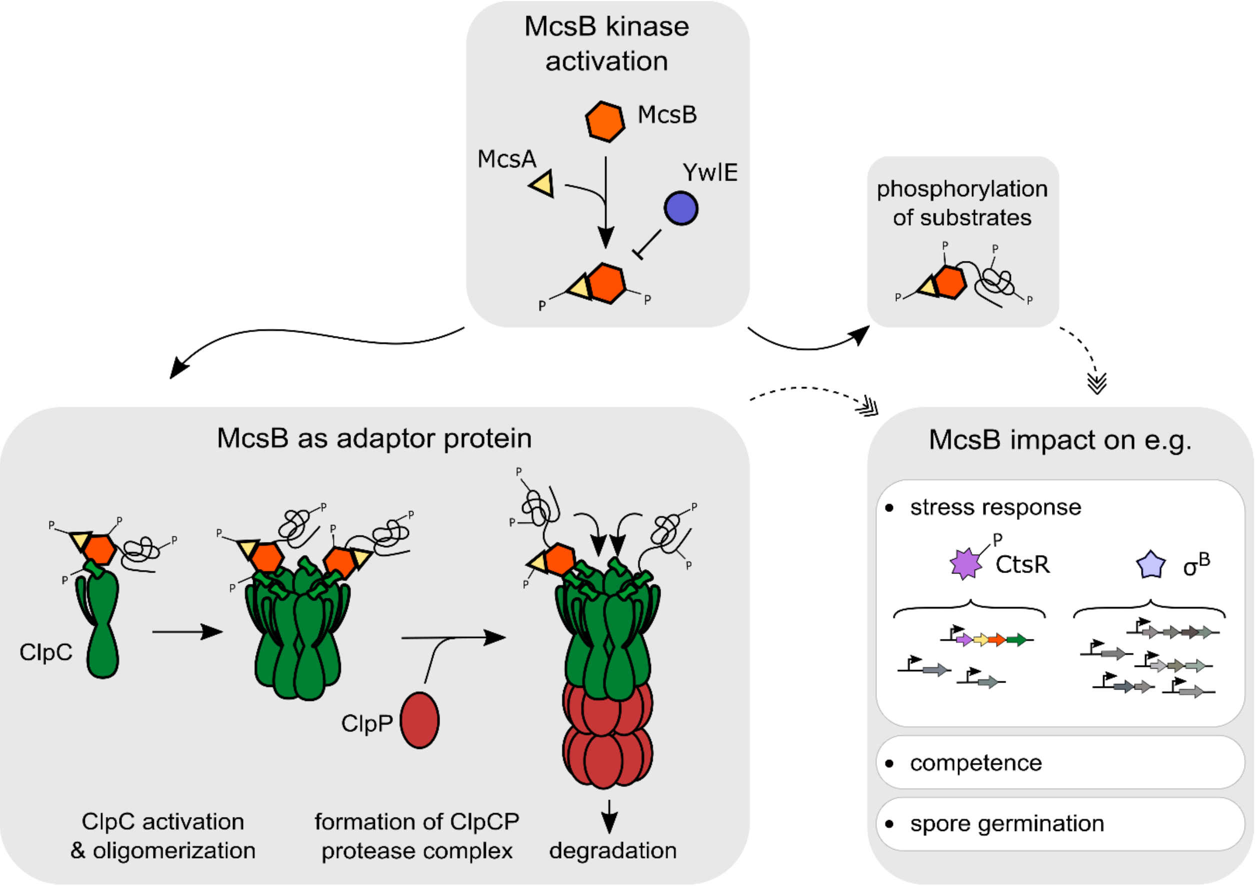
McsB kinase activation
McsB
McsA
YwlE
P
P
phosphorylation of substrates
P
P
P
P
McsB as adaptor protein
ClpC
ClpP
ClpC activation & oligomerization
formation of ClpCP protease complex
degradation
McsB impact on e.g.
stress response
P
CtsR
σB
competence
spore germination

Figure 2 McsB is an arginine kinase and ClpC adaptor protein.

The McsB kinase is activated by McsA and counteracted by YwlE. In its function as adaptor protein, McsB can facilitate the oligomerization and activation of ClpC and subsequent ClpCP complex formation. Substrate selection for ClpCP is carried out by McsB, whereby only phosphorylation of the substrate was shown to act as targeting signal (Trentini et al., 2016). The McsB activities, as arginine kinase and adaptor protein, enable impact on many cellular functions.

Sensing stress via McsA and YwlE in *B. subtilis*

Notably, both the activator of McsB, McsA, and the phosphatase YwlE have redox-sensitive traits. McsA contains two Cys2-Cys2 zinc finger motifs, forming disulfide bonds under oxidative stress conditions and thereby altering protein stability and function (Krüger et al., 2001; Wouters et al., 2010). The strong interaction between McsA and McsB is abolished during disulfide stress, resulting in free McsB targeting and inactivating CtsR, the repressor of class III heat shock genes in *B. subtilis* (Elsholz et al., 2011b; Krüger and Hecker, 1998). This pathway differs significantly from heat-stress induced CtsR regulation, where CtsR is inactivated by an intrinsic thermosensor and McsB facilitates subsequent ClpCP dependent degradation (see section 1.3.4) (Elsholz et al., 2011b). However, *Lactococcus lactis* lacks McsA and McsB so that the AAA+ protein ClpE, which contains a N-terminal zinc finger domain similar to McsA, can take their place in oxidative stress dependent CtsR regulation (Elsholz et al., 2011b; Varmanen et al., 2003).

The activity of *B. subtilis* phosphatase YwlE also depends on two cysteine residues, Cys7 and Cys12, that are flanking the active site pocket, as previously shown for comparable sequence motifs in *G. stearothermophilus* YwlE (Fuhrmann et al., 2013b). Under oxidative stress conditions a disulfide bridge is formed, inactivating YwlE reversibly and suggesting that YwlE can act as redox sensor in *B. subtilis* (Fuhrmann et al., 2016). It has been proposed that upon inactivation of YwlE dephosphorylation is halted and thus, McsB dependent arginine phosphorylation and induced expression of stress response genes could be enhanced (Fuhrmann et al., 2016).

1.2 Chaperones involved in protein homeostasis

One important system in a living cell, besides well-coordinated gene expression, is the control over protein homeostasis. Here, a rough separation between regulatory and stress induced operation systems can be made, whereas both are carried out by a highly conserved class of proteins, namely chaperones, which are often accompanied by proteases (Wickner et al., 1999). Chaperones are able to either hold substrate proteins and thereby prevent unintended interactions or formation of aggregates (“holders”) or support protein unfolding and refolding events (“folders”) (Mayer and Bukau, 1998). They are important in many different situations, such as assistance of protein folding directly after translation, by e.g. ribosome-associated trigger factor in *Escherichia coli*, the support of protein transport across membranes and recognition and refolding of incorrect folded proteins species (Hartl and Hayer-Hartl, 2002; Hoffmann et al., 2010; Zhou and Xu, 2005). Furthermore, proteases take an essential part in protein quality control (PQC) systems, because they are required for removal of irreversibly damaged proteins, generation of amino acids during starvation or for directed degradation of e. g. transcription factors in order to adjust different regulatory pathways (Goldberg and St. John, 1976; Gottesman, 2003; Jenal and Hengge-Aronis, 2003; Wickner et al., 1999).

Under normal but especially under stress conditions, such as heat, proteins are endangered to unfold and misfold. Thereby, hydrophobic regions can be exposed and possibly toxic protein aggregates emerge (Tyedmers et al., 2010; Vabulas et al., 2010) (Figure 3). Many chaperones and associated proteins counteracting this aggregate formation are called "heat shock proteins" (Hsp), because of their high occurrence during heat stress conditions (Lee and Tsai, 2005). Nevertheless, Hsp are not only involved in stress dependent but also in regulatory processes.

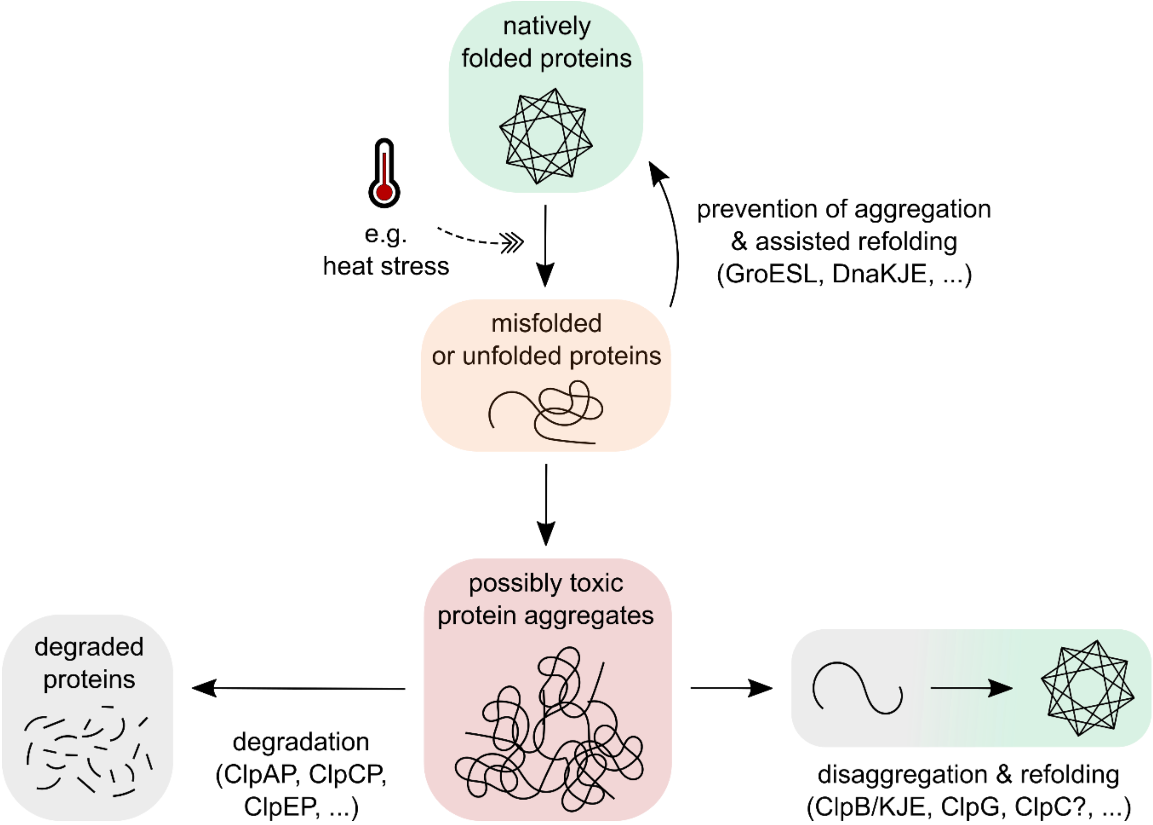
natively folded proteins
e.g. heat stress
prevention of aggregation & assisted refolding (GroESL, DnaKJE, ...)
misfolded or unfolded proteins
possibly toxic protein aggregates
degraded proteins
degradation (ClpAP, ClpCP, ClpEP, ...)
disaggregation & refolding (ClpB/KJE, ClpG, ClpC?, ...)

Figure 3 Schematic overview of PQC systems in aggregate removal and prevention.

PQC systems are involved in prevention and removal of e.g. heat induced protein aggregates. Hsp systems like GroESL or DnaKJE mostly act on mis- or unfolded protein species, whereby the unfolding of tight aggregates is often supported Clp chaperones. Proteases and protease complexes can degrade those possibly toxic protein aggregates.

1.2 Introduction

In many eukaryotic and prokaryotic organisms different Hsp families were identified and often termed according to their estimated molecular weight, e.g. Hsp100, Hsp90, Hsp70, Hsp60 and small Hsp families (Gupta et al., 2010). The well-studied prokaryotic chaperonines, GroEL (Hsp60) and GroES (Hsp10) (GroESL), were shown to prevent heat induced protein aggregation and promote protein folding in *E. coli* (Ziemienowicz et al., 1993) (Figure 3). Here, the cylindrical shaped chaperone GroEL binds mis- and unfolded substrate proteins via hydrophobic residues (Farr et al., 2000). Subsequent attachment of the fitting lid GroES leads to encapsulation and folding of the substrate by ATP-dependent conformational changes of the ATPase GroEL (Chen et al., 2013; Clare et al., 2012). Substrate folding and GroESL activity underlie a well-coordinated cycle by either sequential or simultaneous action of two stacked GroEL rings (Ye and Lorimer, 2013). ATP binding to one ring leads to release of substrate from the other GroEL (Ranson et al., 2001). If the substrate is not completely folded, several capture, folding and release cycles can be performed (Hayer-Hartl et al., 2016; Saibil et al., 2013). Similarly, eukaryotic and prokaryotic Hsp70 proteins perform several ATP-dependent substrate binding and release cycles, partially unfolding substrates and thus allowing independent refolding to the native state (Hartl and Hayer-Hartl, 2002; Mayer and Bukau, 1998). DnaK, a Hsp70 homologue from *E. coli*, acts together with co-chaperones DnaJ and GrpE. They stimulate DnaK ATPase activity, support substrate targeting and binding as well as subsequent refolding of substrates (Laufen et al., 1999; Liberek et al., 1991; Mayer and Bukau, 2005). Nevertheless, high disaggregation and refolding efficiency as well as destabilization of large aggregates depends on interplay with Hsp100 chaperones, like Hsp104 in *Saccharomyces cerevisiae* or ClpB in *E. coli* (Diamant et al., 2000; Glover and Lindquist, 1998; Mogk, 1999).

In eukaryotes proteolysis is mainly performed by the proteasome. Substrate entry into the compartmentalized complex is strictly controlled to prevent undesired degradation of native proteins. Specific regulatory proteins flanking the catalytic core can allow access of posttranslational modified proteins, which are labeled with a specific ubiquitin tag (Fort et al., 2015; Hershko et al., 1983). The catalytic core of the proteasome consists of stacked ring structures performing ATP-dependent proteolysis (Groll and Huber, 2003; Voges et al., 1999). These barrel-shaped proteins with a conserved ATPase module belong to the superfamily of AAA+ (ATPase associated with cellular activities) proteins (Ogura and Wilkinson, 2001; Walker et al., 1982).

1.3 Clp protein family

Different types of Hsp100/Clp ("caseinolytic proteins") AAA+ proteins are involved in PQC systems of bacteria. These proteins are subdivided in two classes according to the presence of either two (e.g. ClpA, ClpB, ClpC) or one (e.g. ClpX, ClpY) AAA+ "nucleotide binding domain" (NBD) (Schirmer et al., 1996). Two NBDs are connected by a module called "spacer" or "linker" domain and each NBD includes Walker A and B nucleotide-binding elements. Furthermore, Hsp100/Clp proteins are distinguished by different "amino (N)-terminal domains" (NTDs), which are crucial for specific recognition and binding of substrates and adaptor proteins (Battesti and Gottesman, 2013; Sauer and Baker, 2011). Clp proteins form barrel-like ring structures that can unfold substrate proteins by ATP-dependent threading through the axial pore. Substrate binding and translocation are carried out by axial-pore loops, as shown for *E. coli* ClpX (Iosefson et al., 2015; Martin et al., 1999). ATP dependent conformational changes facilitate coordinated movement of the pore loops, which pull substrate down the pore (Mogk et al., 2018).

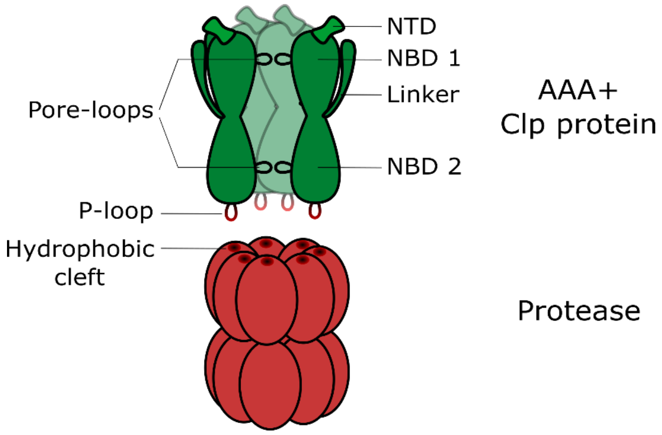

Figure 4 Schematic model example of AAA+ protein structure.

Model of barrel shaped AAA+ Clp protein (e.g. ClpA, ClpB, ClpC) in that the NTD recognizes substrate and adaptor proteins and the two NBD domains are connected by a linker domain. Pore-loops facilitate substrate translocation and P-loops of the AAA+ chaperone interact with hydrophobic clefts of according proteases.

1.3.1 Clp proteases and protease complexes

The Hsp100/Clp family also includes proteases, such as Lon and FtsH, which consist out of one AAA+ NBD linked to a metalloprotease-domain (FtsH) or a serineprotease-domain (Lon) (Ito and Akiyama, 2005; Tsilibaris et al., 2006). These AAA+ proteases form hexameric ring structures that recognize and unfold proteins in an ATP-dependent manner and can transfer the substrate to the intrinsic protease for degradation. Besides these merged AAA+ proteases other AAA+ chaperones can form protease complexes by association to separate proteases such as heptameric ClpP or hexameric ClpQ (Singh et al., 2001). Both proteases form double ring structures, with narrow pores through which substrates access the active sites inside the barrel (Baker and Sauer, 2006; Sauer et al., 2004). NMR studies showed, that degraded substrate exits ClpP through dynamic side pores, emerging upon conformational changes (Sprangers et al., 2005). The AAA+ Clp proteins (e.g. ClpA, ClpC, ClpE and ClpX) interact with ClpP via specific and flexible hydrophilic loops at the C-terminus. These P-loops possess a highly conserved tripeptide [LIV]-G-[FL] and can interact with hydrophobic pockets on the surface of ClpP (Kim et al., 2001). Mutations in the *E. coli* ClpX P-loop resulted in impaired substrate degradation activity of ClpXP *in vivo* and *in vitro* (Kim et al., 2001). In *B. subtilis*, Clp proteases and protease complexes are involved in different cellular processes by directed regulatory proteolysis (see section 1.3.4) (Jenal and Hengge-Aronis, 2003; Storz et al., 2011). However, the general degradation of impaired proteins, especially the removal of irreparably damaged proteins under stress conditions is also essential for the cell.

Substrate selection and degradation of complete proteins by ClpP depends on the associated AAA+ chaperones (Schlothauer et al., 2003; Thompson et al., 1994; Woo et al., 1989). Notably, a new class of antibacterial compounds, acyldepsipeptides (ADEP), were identified bypassing this protease regulation (Brötz-Oesterhelt et al., 2005; Schweitzer, 2008). By targeting ClpP, ADEP blocks the P-loop docking sites, opens the entrance pore and hinders the interaction between e.g. ClpX and ClpP in *E. coli* and *B. subtilis* (Lee et al., 2010). Thereby substrate selection and protease activation via Clp chaperones is overcome, resulting in uncontrolled substrate proteolysis by ADEP activated ClpP (Brötz-Oesterhelt et al., 2005; Kirstein et al., 2009a). This unrestrained protein degradation is especially toxic for the cell because regulatory proteolysis is prevented, and many essential proteins are damaged.

1.3.2 Clp dependent protein un- and refolding

Besides proteolysis, the un- and refolding of impaired proteins is a fast and efficient way to reactivate proteins and remove protein aggregates (Mogk et al., 2018; Wallace et al., 2015). Some AAA+ chaperones were already shown to act in a ClpP independent manner and participate in different regulatory processes. ClpX for instance is involved in remodeling the Mu transposome by unfolding subunits and thereby destabilizing the complex (Levchenko et al., 1995). In contrast to this, ClpA specifically targets and disassembles the replication initiator protein RepA, resulting in its activation (Pak and Wickner, 1997; Wickner et al., 1994). Apart from this regulatory involvement, the disaggregation and refolding activities of Clp chaperones are significant mechanisms in the bacterial stress response.

The *E. coli* Hsp100 protein ClpB, that is also present in many other bacteria, plays a major role in heat shock response and rescue from heat-induced damage (Weibezahn et al., 2004). ClpB takes a special place in the Clp family, because it lacks the ClpP interaction loop and acts as disaggregase (Weibezahn et al., 2004). In cooperation with Hsp chaperones DnaK, DnaJ and GrpE disaggregation and refolding of denatured protein aggregates is possible *in vitro* and *in vivo* (Laufen et al., 1999; Zolkiewski, 1999). In this system, DnaK acts as adaptor protein promoting substrate recognition and disaggregation by ClpB (Seyffer et al., 2012; Winkler et al., 2012). Efficient refolding of the unfolded substrates in return is again dependent on DnaK, DnaJ and GrpE (Glover and Lindquist, 1998; Rosenzweig et al., 2013). In addition to ClpB different stand-alone Clp disaggregases were identified in various bacterial species. ClpG for example, possesses even higher unfolding power than the ClpB, DnaK, DnaJ, GrpE (ClpB/KJE) system, enabling the disaggregation of firm aggregates under severe heat stress (Katikaridis et al., 2019). Furthermore, two ClpG disaggregase homologues were identified in *Pseudomonas aeruginosa*, which also lack a ClpP interaction loop and are important for heat tolerance and support heat resistance when expressed in *E. coli* (Lee et al., 2018). The cognate AAA+ protein ClpK, present in *Klebsiella pneumoniae* and *Cronobacter sakazakii* promotes heat resistance and is therefore assumed to be involved in persistence of these pathogens (Bojer et al., 2010; Gajdosova et al., 2011). However, despite absence of the conserved tripeptide described for the P-loop, the ClpK mediated thermoresistance is still dependent on the presence of ClpP *in vivo* (Bojer et al., 2013). Furthermore, many Gram-positive bacteria including *Staphylococcus spp.* contain AAA+ protein ClpL or ClpL homologues (Park et al., 2015). In these species ClpL promotes thermotolerance development by folding of the heat shock repressor CtsR, prevention of protein aggregation under heat stress and by protein disaggregation without assistance of adaptor proteins (Frees et al., 2004; Kwon et al., 2003; Tao and Biswas, 2013). Comparable to ClpK, ClpL lacks the ClpP interaction loop but co-precipitation under heat shock conditions suggested collaboration of this chaperone with the protease (Park et al., 2015).

An exclusive disaggregase acting without interplay to the protease ClpP, like ClpB or ClpG, is not present in the Gram-positive model organism *B. subtilis*. Nevertheless, other chaperone systems are considered to cover this function. So far, *in vitro* disaggregation and refolding of heat inactivated substrate was only described for ClpC, activated by adaptor protein MecA or its paralog YpbH, in absence of ClpP (Schlothauer, 2004; Schlothauer et al., 2003).

1.3.3 Adaptor proteins and recognition tags

The targeting of substrates for either degradation or disaggregation and reactivation by chaperone systems depends on different mechanisms. For many substrates simple tag and recognition site systems fulfill this role and lead AAA+ chaperones and proteases to their substrate. Incomplete transcription or damaged mRNA can result in tagging of the emerged proteins with the so called SsrA-tags by cotranslational switching to a tmRNA, encoded by the *ssrA* gene (Keiler et al., 1996; Tu et al., 1995). In *E. coli*, ClpXP, ClpAP and FtsH recognize and degrade these tagged substrates (Karzai et al., 2000). A special factor, SspB, can even increase the degradation efficiency of SsrA-tagged proteins by ClpXP (Levchenko et al., 2000). In addition to the SsrA-tag other substrate recognition motifs are recognized by ClpA, ClpX and Lon (Flynn et al., 2003; Gur and Sauer, 2008; Hoskins et al., 2002). However, many Hsp100 Clp proteins strictly require adaptor proteins to promote and enhance substrate specificity and recognition. These adaptor proteins therefore play a significant role in activation and alteration of chaperone functions and affiliated protease activities. In *E. coli* for example, degradation of general stress response factor σ^S by ClpXP depends on the adaptor protein RssB (Muffler et al., 1996; Zhou et al., 2001). Furthermore, the adaptor protein ClpS is responsible for recognition and subsequent ClpAP dependent degradation of N-end rule substrates, carrying destabilizing N-terminal residues (Erbse et al., 2006). Additionally, ClpS inhibits degradation of not recognized substrates and redirects ClpAP degradation activity from SsrA-tagged substrates to aggregated proteins (Dougan et al., 2018, 2002; Erbse et al., 2006). Furthermore, down regulation of protease activity by adaptors, like Lon by bacteriophage T4 protein PinA or ClpAP degradation of SsrA-tagged substrate by SspB, was reported (Flynn et al., 2003; Hilliard et al., 1998).

1.3.4 Clp proteins in *B. subtilis* regulatory pathways

The function and specificity of AAA+ proteins and their adaptor proteins in *B. subtilis* is one important topic of research since they can influence many regulatory pathways. The swarming ability, for example, depends on flagellar synthesis. This process is under control of the master activator SwrA, which is targeted by the adaptor protein SmiA for degradation by LonA in liquid environment (Mukherjee et al., 2015) (Figure 5). ClpXP dependent degradation of anti-sigma factor RsiW regulates the cell envelope stress response and initiation of sporulation is facilitated by degradation of checkpoint protein Sda, whereas the ClpXP adaptor protein CmpA ensures correct spore maturation (Burkholder et al., 2001; Ruvolo et al., 2006; Tan et al., 2015; Zellmeier et al., 2006). A specific C-terminal LCN sequence was observed to facilitate ClpCP dependent degradation of anti-σ^F factor SpoIIAB, which is also involved in regulation of sporulation (Pan et al., 2001; Pan and Losick, 2003). Nevertheless, an unknown adaptor protein of ClpC is considered to enable the recognition of SpoIIAB with this unique LCN-tag (Hantke, 2019; Pan and Losick, 2003). Furthermore, competence development and heat stress response are both influenced by the adaptor protein induced activity of Hsp100 AAA+ protein ClpC and affiliated protease complex ClpCP in *B. subtilis*.

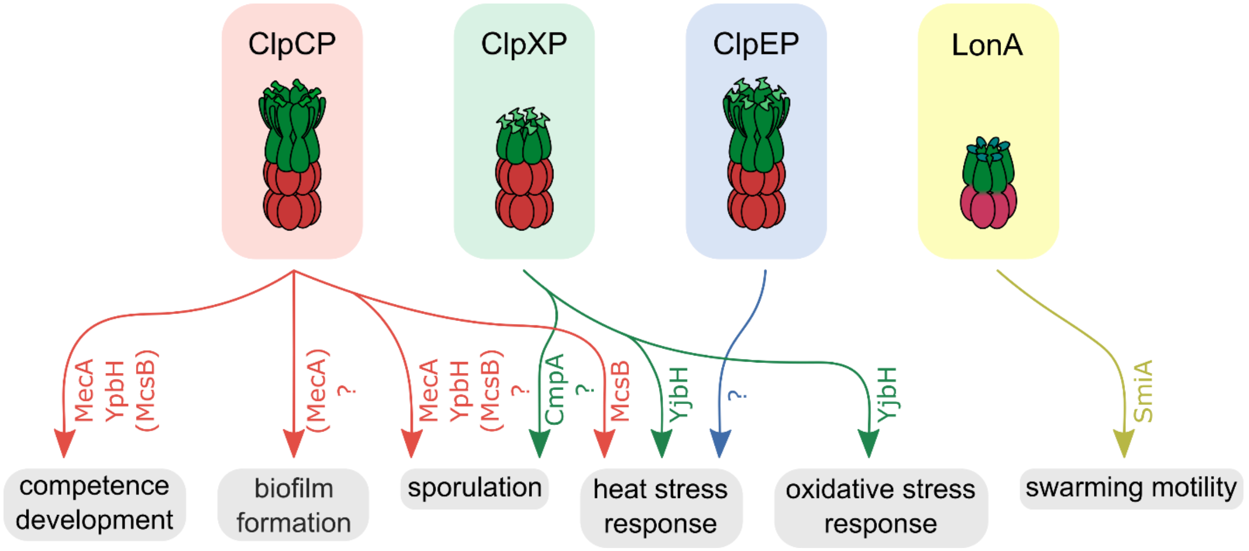
ClpCP
ClpXP
ClpEP
LonA
MecA
YpbH
(McsB)
(MecA)
?
MecA
YpbH
(McsB)
?
CmpA
?
McsB
YjbH
?
YjbH
SmiA
competence development
biofilm formation
sporulation
heat stress response
oxidative stress response
swarming motility

Figure 5 Involvement of selected Clp proteins in regulatory pathways.

B. subtilis Clp protease complexes, ClpCP (red), ClpXP (green), ClpEP (blue) and protease LonA (yellow) are involved in regulation of different cellular pathways (grey). Corresponding adaptor proteins that are known to facilitate Clp functions are listed beside related arrows. A selected set of regulatory pathways and pivotal connections to Clp are illustrated.

1.3 Introduction

Competence development of *B. subtilis*

Cells in a competent physiological state are able to take up and internalize external DNA and thereby benefit of additional genetic information, like antibiotic resistances, or of a further nutrient source (Chen, 2005; Finkel and Kolter, 2001). *B. subtilis* competence development is triggered in 5-10 % of the cell community by pheromones ComX and CSF, which accumulate at high cell density (Haijema et al., 2001; Magnuson et al., 1994; Storz et al., 2011). Expression of *srfA* operon, including *comS*, is induced via quorum sensing of these pheromones (D'Souza et al., 1994; Solomon et al., 1996). Under non-competent conditions the competence regulator ComK is targeted by adaptor protein MecA for degradation by ClpCP protease complex. Upon competence induction, ComS is produced and targeted by MecA, thus releasing ComK (Prepiak and Dubnau, 2007; Turgay et al., 1998, 1997). Subsequent positive autoregulation of ComK expression results in fast increasing protein concentrations and accompanied transcription of competence determining genes (Ogura et al., 2002; Sinderen et al., 1995). Escape from competence is mediated by retargeting of ComK by MecA for degradation by ClpCP (Turgay et al., 1998). The regulatory key player Spx was shown to counteract competence development by enhancing interactions between ClpC, MecA and ComK (Nakano et al., 2002). In addition to the adaptor protein MecA, its paralog YpbH was found to interact with ClpC and to be also involved in sporulation and competence development in *B. subtilis* (Persuh et al., 2002).

Heat shock response of *B. subtilis*

Heat shock response in *B. subtilis* is based on a complex network of sensor proteins, signal transduction factors and transcriptional regulators controlling expression and functions of Hsp, e.g. chaperones and proteases. Heat shock proteins are classified according to their regulation model, whereby class I-III are well-characterized in *B. subtilis* (Hecker et al., 1996). Class I includes *dnaK* and *grpE* operons that contain inverted repeats called CIRCE elements by which GroESL-activated HrcA can bind and negatively regulate their transcription (Mogk et al., 1997; Schulz and Schumann, 1996). Upon heat stress HrcA acts as a thermosensor, undergoing conformational changes leading to the expression of class I heat shock genes, whereby the reactivation of HrcA as repressor depends on GroESL (Hitomi et al., 2003; Roncarati et al., 2014). Over 150 general stress genes count to heat shock class II and are induced by growth-inhibiting stress conditions via σ^B dependent promotors in *B. subtilis* (Hecker et al., 2007, 1996). Regulation of σ^B underlies a complex partner switching system described in detail in section 1.1. Class III heat shock genes are under the control of CtsR, the first protein encoded in *clpC* operon (Krüger and Hecker, 1998). The expression of *clpP*, *clpE* and the *clpC* operon (*ctsR-mcsA-mcsB-clpC*) is repressed by binding of active CtsR to a specific promotor region under normal growth conditions (Derré et al., 1999; Krüger et al., 2001). *In vitro* studies showed, that CtsR can be inactivated and targeted for ClpCP degradation by McsA-activated McsB (Fuhrmann et al., 2009; Kirstein et al., 2005; Krüger et al., 2001). However, *in vivo* a highly conserved tetraglycine loop of CtsR is responsible for thermosensing and de-repression of heat shock genes upon heat stress (Derré et al., 2000; Elsholz et al., 2010). The adaptor protein function of McsB is still important for directed degradation of inactive CtsR *in vivo* and only arginine phosphorylation of CtsR is not sufficient for degradation *in vitro* (Elsholz et al., 2010; Kirstein et al., 2007). In *B. subtilis*, as well as bacteria lacking the McsB kinase, it was shown that ClpEP is involved in CtsR degradation and aggregate clearance under heat stress conditions (Ingmer et al., 1999; Miethke et al., 2006). With adaption to permanent heat stress new synthesized active CtsR rebinds and represses class III heat shock genes, implying that inactivation of CtsR only occurs due to temperature upshifts (Elsholz et al., 2017, 2010; Krüger et al., 1994). However, many of these regulations are not only connected to heat stress, but also part of various intricately interwoven stress response networks as the involvement of CtsR in thiol-specific oxidative stress response or the global stress response regulator Spx indicate (Elsholz et al., 2011b; Runde et al., 2014; Schäfer and Turgay, 2019). The adaptor protein YjbH can target Spx for degradation by ClpXP. This ClpXP activity governs upregulation of multiple genes concerning thiol-specific oxidative stress and heat induced stress as well as downregulation of energy-consuming cell functions during these conditions (Garg et al., 2009; Nakano et al., 2003; Runde et al., 2014; Schäfer and Turgay, 2019).

1.4 Biofilm formation in *B. subtilis*

Bacterial cells can develop different types of lifestyle depending on their environment. Movement is achieved by either swimming motility, in a three dimensional liquid as individual or by swarming motility, on a two dimensional solid surface as cell-group (Mukherjee and Kearns, 2014). The most abundant lifestyle is a sessile type, forming biofilms in highly diverse bacterial communities (Davey and O’Toole, 2000). These biofilms are classified in three groups based on their ground substrate being solid, an air-liquid interface (pellicle biofilm) or if they are formed by cellular clusters submerged in liquid (Terra et al., 2012; Vlamakis et al., 2013). In general, biofilms are produced by secretion of different proteins, “exopolysaccharides” (Eps) and eDNA to form an extracellular matrix in which the cells are embedded in different layers, performing specific tasks (Sutherland, 2001). The formation of biofilm facilitates the exchange of genetic material, improves nutrient supply and promotes cell to cell communication for coordinated growth (Davies, 1998; Gilbert et al., 1997; Hausner and Wuertz, 1999; Shapiro, 1998). Moreover, a higher tolerance against outer influences such as antibiotics, host immune responses or antimicrobial agents is conferred, indicating the importance of biofilm research in the medical field (Ceri et al., 1999; Donlan, 2002; Mah, 2012; Olsen, 2015).

The soil-dwelling Gram-positive bacterium *B. subtilis* is a model organism for studies of biofilm formation. In its natural habitat, *B. subtilis* colonizes on plant roots, whereby this biofilm formation can be induced by plant polysaccharides (Beauregard et al., 2013). Notably, these polysaccharides serve as carbon source for matrix formation and in return *B. subtilis* can promote plant growth and protect against salt stress or a huge variety of plant pathogens (Arkhipova et al., 2005; Choudhary and Johri, 2009; Ongena et al., 2005; S. Wang et al., 2009; Zhang et al., 2008). The bacterial community in a biofilm can be divided in different subpopulations which, despite similar genome, express a distinct set of genes. During biofilm maturation, cells differentiate depending on the environmental conditions, resulting in a big variety of phenotypic characteristics (López and Kolter, 2010; Vlamakis et al., 2013). Along with matrix-producing cell types, motile and sporulating cells emerge, localizing in different regions of the biofilm (Vlamakis et al., 2008).

1.4.1 Biofilm components

Biofilm formation is triggered by different external factors, such as already mentioned polysaccharides or surfactin, which is produced by a subpopulation of cells and can be detected by quorum sensing mechanisms leading to increased expression of matrix genes (Lopez et al., 2009). The main components of *B. subtilis* biofilms are Eps, products of the *eps*A-O operon (*eps* operon), but the distinct functions of many *eps* genes remain to be investigated. However, mutations in *eps*J-*eps*N can cause severe defects in pellicle formation and inactivation of some *eps* genes inhibits swarming in strain 168 (Nagorska et al., 2010). Furthermore, EpsE promotes Eps biosynthesis by gycosyltransferase activity, while at the same time inhibiting motility by arresting flagellar rotation (Blair et al., 2008; Guttenplan et al., 2010). With this bifunctionality, EpsE can support the transition from motile cells to sessile biofilm forming cells. Notably, osmotic pressure gradients generated by secretion of Eps are considered to support spreading of *B. subtilis* biofilm on agar plates, whereas pellicle biofilms are formed by vortex-like motion of aggregates composed of Eps secreting cells and motile cells (Seminara et al., 2012; Steinberg et al., 2018).

Moreover, the formation of a robust biofilm matrix depends on expression of all genes of the *tapA-sipW-tasA* operon (Branda et al., 2006; Chu et al., 2006). TasA ("translocation-dependent antimicrobial spore component") is a major component of *B. subtilis* biofilms and responsible for stabilization of the extracellular matrix in colony and pellicle biofilms (Branda et al., 2006; Romero et al., 2010). Recently, influences on membrane dynamics by TasA were observed to be important for cell viability (Cámara-Almirón et al., 2020). Moreover, TasA has high structural similarity with camelysins, which are metalloproteases involved in pathogenicity of *Bacillus cereus*, but no protease activity could be detected for *B. subtilis* TasA so far (Diehl et al., 2018; Fricke et al., 2001; Grass et al., 2004). *In vivo*, TasA was observed to form amyloid-like fibrils, which are highly stable and display structural changes under different pH or surface conditions *in vitro* (Chai et al., 2013; Romero et al., 2010). Addition of recombinantly produced and purified TasA to a *tasA* deletion strain with impaired biofilm formation results in reconstitution of the matrix (Romero et al., 2010). NMR analysis of TasA from those reconstructed biofilms recently showed that TasA is present in a homogenous, β-sheet-rich fibril form *in vivo*. The crystal structure of monomeric TasA revealed two polyproline II (PPII) helices, which were considered to be relevant in amyloid-like fibril formation and thus, biofilm maturation (Diehl et al., 2018).

In *B. subtilis* biofilms TapA ("TasA anchoring/assembly protein") is present in lower levels than TasA (Chu et al., 2006). Nevertheless, TapA is essential for robust matrix formation and localizes on the cell surface and anchors TasA fibrils to the cell (Romero et al., 2011). Moreover, the polymerization of TasA fibrils in the matrix structure is supported by TapA, but only a short N-terminal sequence of TapA is required for these functions (Earl et al., 2019; Romero et al., 2014).

In addition to TasA and TapA, the type I "signal peptidase W" (SipW) is encoded in the *tapA-sipW-tasA* operon (Tjalsma et al., 1998). SipW is crucial for biofilm formation in *B. subtilis*, because it processes both TasA and TapA (Chu et al., 2006). With recognition and cleavage of N-terminal signal sequences by SipW, the proteins are secreted and can support matrix formation and biofilm maturation (Romero et al., 2011; Stöver and Driks, 1999a, 1999a). Additionally, SipW has a regulatory function in activation of *eps* gene expression and is therefore required for submerged, surface adhered biofilm formation (Terra et al., 2012).

Furthermore, the surface layer protein BslA and the extracellular polymer “γ-poly-DL-glutamic acid” (PGA) are necessary for the biofilm structure of *B. subtilis*. BslA can form a hydrophobic layer on pellicle biofilms and contributes to complex colony development (Kobayashi and Iwano, 2012; Kovács and Kuipers, 2011; Verhamme et al., 2009). PGA is only involved in formation of submerged and surface-adhered biofilms by enhancing cell-surface interactions (Branda et al., 2006; Kobayashi, 2007a; Morikawa et al., 2006; Stanley and Lazazzera, 2005).

1.4.2 Regulation of biofilm formation

The regulation of biofilm formation is a sophisticated network under control of different master regulators (Molle et al., 2003) (Figure 6). The activity of master controller Spo0A is regulated by a phosphorelay, which is a complex two-component system. Here, five histidine kinases, KinA, KinB, KinC, KinD and KinE can phosphorylate and thereby activate Spo0A over a relay by transmitting the phosphoryl group over Spo0F and Spo0B to Spo0A (Jiang et al., 2000). KinA and KinB are involved in sporulation initiation, whereas KinC and KinD are required for production of the extracellular biofilm matrix (LeDeaux et al., 1995; Perego et al., 1989). The influence of phosphorylated Spo0A (Spo0A-P) on cellular development depends on its concentration (Fujita et al., 2005). Low levels of Spo0A-P repress e.g. matrix gene repressor AbrB and subsequently *eps* and *tapA-sipW-tasA* operons are expressed (Strauch et al., 1990). Besides AbrB, the activity of SinR, a second repressor of *eps* and *tapA-sipW-tasA* operons, is under the control of Spo0A-P. Increasing levels of Spo0A-P lead to expression of *sinI*, the anti-repressor of *sinR* (Shafikhani et al., 2002). By complex formation of SinI-SinR the repressing impact on matrix genes is relieved and biofilm formation is initiated (Bai et al., 1993; Kearns et al., 2005). With rising levels of Spo0A-P, sporulation is induced and matrix expression is halted by repression of *sinI* by high Spo0A-P levels (Chai et al., 2011; Vlamakis et al., 2013). Moreover, the transcriptional activity of Spo0A-P is under control of MecA, an adaptor protein for ClpC. By direct binding of Spo0A-P and inhibition of the transcription factor, without leading it to ClpCP for degradation, MecA and ClpC are involved in downregulation of *eps* genes (Prepiak et al., 2011).

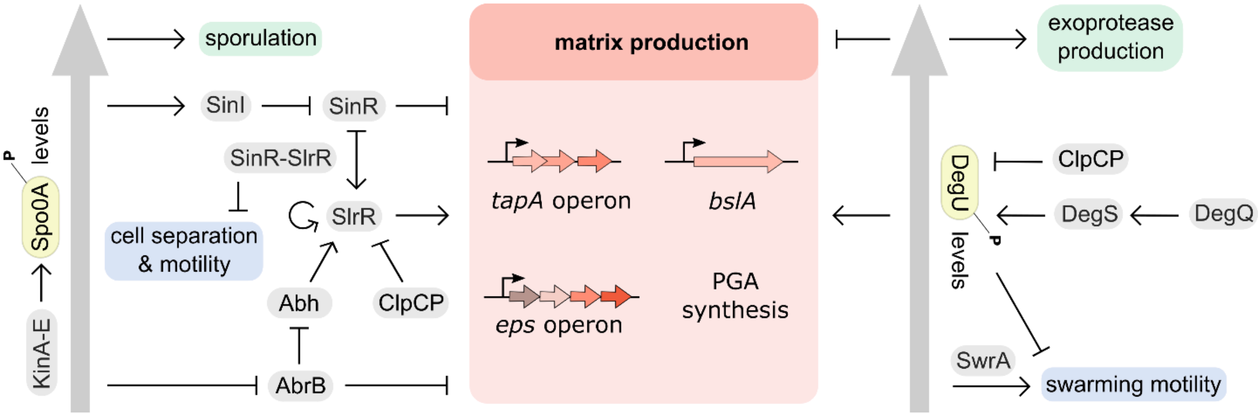
sporulation
SinI
SinR
SinR-SlrR
SlrR
cell separation & motility
Abh
ClpCP
AbrB
KinA-E
Spo0A
P
levels
matrix production
tapA operon
bslA
eps operon
PGA synthesis
exoprotease production
ClpCP
DegU
DegS
DegQ
P
levels
SwrA
swarming motility

Figure 6 Regulation model of biofilm matrix production under control of Spo0A-P and DegU-P.

Phosphorylation of both Spo0A and DegU is performed by their specific kinases. The respective levels of phosphorylated regulators alter their influence on various cellular developmental processes, e.g. motility, matrix production or sporulation.

Furthermore, the expression of regulator SlrR is under the control of AbrB and SinR (Chu et al., 2008). Complex formation of SlrR and SinR, similar to SinI and SinR, results in derepression of SinR controlled *eps* and *tapA-sipW-tasA* operons and higher expression of SlrR (Chai et al., 2009; Kobayashi, 2008). While high concentrations of SlrR promote matrix formation, the SinR-SlrR complex does additionally repress cell separation and motility genes (Chai et al., 2010b). This leads to a chain forming phenotype, essential in the early stages of biofilm formation. Notably, it was proposed, that this SlrR switch can be reversed by autocleavage of unstable SlrR as well as by ClpCP dependent degradation of SlrR in *B. subtilis* (Chai et al., 2010a).

In addition to these regulation mechanisms, further influences of AbrB homologue Abh on expression of matrix genes must be considered. Expression of *abh* is dependent on different sigma factors, like σ^{x}, which are stimulated by environmental signals (Eiamphungporn and Helmann, 2008; Huang et al., 1998; Murray et al., 2009b). Through positive control of *slrR* expression, Abh has indirect influence on expression of *eps* and *tapA-sipW-tasA* operons (Murray et al., 2009b). Furthermore, AbrB directly represses *abh* expression that is thereby indirectly under the control of Spo0A-P (Strauch et al., 2007).

Additional to control over *eps* and *tapA-sipW-tasA* operons, the expression of *bslA* and PGA synthesis are highly regulated. Both *bslA* and PGA production are under the control of two-component system DegS-DegU. DegS is a histidine kinase that, once stimulated by DegQ, phosphorylates response regulator DegU *in vitro* (Kobayashi, 2007b). Comparable to Spo0A-P, different concentrations of phosphorylated DegU (DegU-P) control various developmental processes. Very low levels of DegU-P, produced independently of DegS, promote swarming motility in presence of SwrA (Mordini et al., 2013). Complex colony development and BslA expression are induced by low levels of Deg-P under control of DegS and accumulation of high concentrations DegU-P inhibit previous regulations and enhance exoprotease production (Kobayashi, 2007b; Murray et al., 2009a; Verhamme et al., 2007). Notably, the ClpCP protease complex can degrade DegU-P *in vivo* and *in vitro* and thus affects flagellar gene expression (Molière et al., 2016; Ogura and Tsukahara, 2010).

Differences in biofilm formation of *B. subtilis* strain DK 1042 and strain 168

B. subtilis is a model organism to examine various cellular processes and during laboratory cultivation different domesticated strains evolved, with more and less severe defects in submerged, surface-adhered and pellicle biofilm phenotypes (McLoon et al., 2011; Nye et al., 2017). Compared to its wild ancestor, strain NCIB 3610, the DK 1042 strain comprises a *comI*$^{\mathrm{Q12L}}$ point mutation on the pBS32 plasmid, impairing the competence inhibitor and facilitating genetic studies (Konkol et al., 2013; Miras and Dubnau, 2016; Nye et al., 2017). In the laboratory strain 168 several mutations and loss of the plasmid pBS32 lead to swarming motility defects, deficient production of surfactant and antimicrobials as well as a disturbed biofilm formation (Butcher et al., 2007; Kearns et al., 2004; Kinsinger et al., 2003). Due to mutations in the coding region of *swrA*, the strain 168 is no longer able to produce PGA, affecting submerged and surface-adhered biofilm formation (Branda et al., 2006; Kobayashi, 2007a; Morikawa et al., 2006; Stanley and Lazazzera, 2005). Furthermore, mutations in the promotor region of *degQ* disturb the regulation of phosphate transfer in two-component system DegU-DegS (Kobayashi, 2007b). The biofilm formation of strain 168 is impaired by mutations in *epsC* and *sfp* genes (McLoon et al., 2011). EpsC was suggested to be membrane associated and possesses epimerase or dehydrogenase activity, while *sfp* is necessary for surfactin production (Lopez et al., 2009; McLoon et al., 2011; Nakano et al., 1992). Nevertheless, the strain 168 produces pellicle biofilms, albeit less robust than strain DK 1042. Introduction of *rapP*, a response regulator aspartate phosphatase from plasmid pBS32, and wild type *degQ*, *swrA*, *epsC* and *sfp* resulted in restored pellicle robustness of strain 168 (McLoon et al., 2011).

1.5 Aim of this work

The control over protein homeostasis is crucial under stress conditions, such as heat exposure, which can cause the formation of subcellular protein aggregates. The main objective of this work was to provide further insight into aggregate removal mechanisms by the AAA+ chaperone ClpC in *B. subtilis*. By characterization of ClpC activities *in vitro*, it was intended to investigate whether the adaptor protein McsB can facilitate efficient disaggregation and refolding of heat inactivated substrates. Since McsB has a second function as protein arginine kinase, an additional focus lay on the arginine phosphatase YwlE. Furthermore, ClpC forms a protease complex with ClpP and with mutations in the interaction loop it was intended to examine the dual role of ClpC in protein refolding and in protein degradation.

The biofilm component TasA forms amyloid-like fibrils and is essential for pellicle formation in *B. subtilis*. The crystal structure of TasA was observed to comprise two flexible polyproline II helices. Therefore, the second aim of this work was to study the function of these dynamic segments as well as the possible role of the chaperone ClpC in TasA fibril folding and biofilm maturation.

2 Materials and Methods

2.1 Devices and reagents

Table 1: List of devices

Device	**Manufacturer**
Äkta protein purification system FPLC	GE Healthcare
Autoclave VX150	Systec
Centrifuge Sorvall RC 6+	Sorvall/Thermo Scientific
ChemiDoc XRS+ Imager	Biorad
Corio CD-200F	Julabo
Fastblot B44	Biometra
FastPrep-24^{TM} 5G	MP Biomedicals
French Press	Heinemann
Gel Stick UV and scanner	INTAS
Heraeus Centrifuge	Thermo Scientific
Heratherm Incubator	Thermo Scientific
Incubator MaxQ7000	Thermo Scientific
Lynx 40000 Centrifuge	Sorvall
Micro centrifuge	Peqlab
Minigel-Twin	Biometra
Monolith NT.115	Nanotemper
Nanodrop 2000	Thermo Scientific
Photometer	Eppendorf
Safe2020 Clean Bench	Thermo Scientific
Scanner	Epson
Sonication needle and instrument	Bandelin
SpectraMax M3	Molecular Devices
Spectrofluorometer FP-6500/FP-8500	Jasco
SpeedVac	Eppendorf
Standard Power Pack P25	Biometry
Synergy H1 microplate reader	BioTek
T Gradient Thermocycler	Biometra
Thermo shaker	Eppendorf
Trans-Blot Turbo	Biorad

Table 2: List of chemicals and reagents

Chemicals and reagents	Manufacturer
Basic chemicals	Carl Roth, Sigma Aldrich
MasterPure DNA purification Kit (Gram-positive)	Epicentre
NucleoSpin PCR clean-up Kit	Macherey & Nagel
PCR/Cloning buffers/Restriction enzymes/Ligase	New England Biolabs
peqGOLD plasmid miniprep Kit	Peqlab
Phusion Polymerase	New England Biolabs
Primary antibodies	Pineda
Primers	Biomers
Protino Ni-NTA	Macherey & Nagel
Roti-Nanoquant	Roth

2.2 Primers, plasmids and strains

Table 3: List of primers

Primer	Fragment description	Sequence
1	NcoI-*clpC* for	catgccatggggtttggaagatttacaga
2	XhoI-*clpC* rev	ccgctcgagattcgttttagcagtcgtt
3	NcoI-m*ecA* for	catgccatggaaattgaaagaattaacgagc
4	NM356 XhoI-*mecA* rev	ccccctcgagtgatgcaaagtgtttttttatcg
5	BsaI-*ywlE* for	ggtctcccatggatattatttttgtctg
6	XhoI-*ywlE* rev	ccgctcgagtctacggtcttttttcagctg
7	NM351 BsaI-*mcsB* for	ccagtgggtctcaggtggtatgtcgctaaagcattttattcag
8	NM352 XhoI-*mcsB* rev	ccccctcgagtcatatcgattcatcctcctg
9	BsaI-*ywlE* C7S for	ggtctcccatggatattatttttgtcagcactggaaatacgtgc
10	NcoI-*clpP* for	catgccatgggt ttaatacctacagtcattgaac
11	XhoI-*clpP* rev	ccgctcgagctttttgtcttctgtgtga
12	*clpC* VGF::IGF for	ggagcaagtgagctaaaacgcaataaatatattggctttaacgttcaggat
13	*clpC* VGF::IGF rev	gtctttatgattttgagtttcatcctgaacgttaaagccaatatatttattgcg
14	NcoI-*clpC* R9A for	catgccatgg ggtttggaagatttacagaagcagctcaa
15	*clpC* R83A for	cgattcattatactcctgcagctaaaaagtcattgag
16	*clpC* R83A rev	gctcaatgactttttagctgcaggagtataatg
17	HS290 *tapA* operon for	accattcgacatcattctcg
18	HS290 *tapA* operon rev	ctgtttcccagcagtggttc
19	NM391 *tapA* for	ccagtgcgtctcaggtggtatgtttcgattgtttcacaatc
20	XhoI-*tasA* rev	ccgctcgagttaatttttatcctcgcta
21	BamHI-*tasA* for	cgcggatccgcagcagctgattcagcgcctg
22	NcoI-*tasA* rev	catgccatgggctactcactatcagaactagc
23	*tasA* T38A for	cattaaatcaaaggatgctgcatttgcatcaggtacgc

24	*tasA* T38A rev	caagcgtacctgatgcaaatgcagcatcctttgatttaatg
25	*tasA* F39A for	ttaaatcaaaggatgctactgcagcatcaggtacgcttg
26	*tasA* F39A rev	gataaatcaagcgtacctgatgctgcagtagcatcctttga
27	*tasA* ΔA40, S41 for	tcaaaggatgctacttttggtacgcttgatt
28	*tasA* ΔA40, S41 rev	tagcagataaatcaagcgtaccaaaagtagcatcct
29	*tasA* S41A for	atcgaagtcagttggtgcttttggaacaccatcata
30	*tasA* S41A rev	caaaggatgctacttttgcagcaggtacgcttga
31	*tasA* T187A rev	gttccaaaagcaccaactgacttcgatcaggttc
32	*tasA* T187A for	atcgaagtcagttggtgcttttggaacaccatcata
33	*tasA* P188A for	gttccaaaaacagcaactgacttcgatcaggttc
34	*tasA* P188A rev	aacctgatcgatgccagttggtgtttttggaacac
35	*tasA* T189A for	ggtgttccaaaaacaccagcagacttcgatca
36	*tasA* T189A rev	gaacctgatcgaagtctgcttgaacctgatcgaagtc
37	*tasA* D190A for	gtgttccaaaaacaccaactgcattcgatcaggttc
38	*tasA* D190A rev	catttgaacctgatcgaatgcagttggtgtttttgga
39	*tasA* F191A for	gttccaaaaacaccaactgacgcagatcaggttca
40	*tasA* F191A rev	gatttccatttgaacctgatctgcgtcagttggtgt
41	*tasA* D192A for	caccaactgacttcgcacaggttcaaatggaaatc
42	*tasA* D192A rev	ccatttgaacctgtgcgaagtcagttggtgtttttgga
43	NM318 BamHI-*clpC* for	ccccggatccatgatgtttggaagatttacag
44	NM319 NcoI-*clpC* rev	ccccccatggttaattcgttttagcagtcg
45	NM523 *clpC* ΔY670-T679 (Δloop) for	ttcatgtctttatgattttgtttattgcgttttagctcacttg
46	NM522 *clpC* ΔY670-T679 (Δloop) rev	caaaatcataaagacatgaaagataaagtg

Table 4: List of plasmids

Nr	Plasmid	Primer	Description	Reference
1	pDS56 *clpB*, placIq		Production of ClpB in *E. coli* XL1-Blue, amp^R	Provided by Axel Mogk; (Deville et al., 2019)
2	pSUMO *dnaK*		Production of DnaK in *E. coli* BL21 (DE3) pLysS, kan^R	Provided by Axel Mogk; (Deville et al., 2019)
3	pSUMO *dnaJ*		Production of DnaJ in *E. coli* BL21 (DE3) pLysS, kan^R	Provided by Axel Mogk; (Deville et al., 2019)
4	pSUMO *grpE*		Production of GrpE in *E. coli* BL21 (DE3) pLysS, kan^R	Provided by Axel Mogk; (Deville et al., 2019)

5	pET28a *clpC*	1, 2	Production of ClpC in *E. coli* BL21 (DE3) pLysS, kan^R	This work
6	pET28a *mecA*	3, 4	Production of MecA in *E. coli* BL21 (DE3) pLysS, kan^R	This work
7	pCA528 *mcsB*		Production of McsB in *E. coli* BL21 (DE3) pLysS, kan^R	Provided by Noel Molière, unpublished
8	pQE32 *mcsA*		Production of McsA in *E. coli* FI1202	(Kirstein et al., 2005)
9	pET28a *ywlE*	5, 6	Production of YwlE in *E. coli* BL21 (DE3) pLysS, kan^R	This work
10	pCA526 *mcsB* C167S	7, 8	Production of McsB C167S in *E. coli* BL21 (DE3) pLysS, kan^R	This work
11	pET28a *ywlE* C7S	9, 6	Production of YwlE C7S in *E. coli* BL21 (DE3) pLysS, kan^R	This work
12	pET28a *clpC* E280A E618A (DWB)	1, 2	Production of ClpC DWB in *E. coli* BL21 (DE3) pLysS, kan^R	This work
13	pET28a *clpP*	10, 11	Production of ClpP in *E. coli* BL21 (DE3) pLysS, kan^R	This work
14	pQE32 *ctsR*		Production of CtsR in *E. coli* FI1202, amp^R	Provided by Janine Kirstein, unpublished
15	pET28a *clpC* VGF::GGR	1, 2	Production of ClpC VGF::GGR in *E. coli* BL21 (DE3) pLysS, kan^R	This work
16	pET28a *clpC* VGF::IGF	1, 2, 12, 13	Production of ClpC VGF::IGF in *E. coli* BL21 (DE3) pLysS, kan^R	This work
17	pET28a *clpC* R9A	14, 2	Production of ClpC R9A in *E. coli* BL21 (DE3) pLysS, kan^R	This work
18	pET28a *clpC* R83A	1, 2, 15, 16	Production of ClpC R83A in *E. coli* BL21 (DE3) pLysS, kan^R	This work
19	pET28a *clpC* R9A R83A	14, 2, 15, 16	Production of ClpC R9A R83A in *E. coli* BL21 (DE3) pLysS, kan^R	This work
20	pCA528 *tasA* + sigseq		Production of TasA + signal sequence in *E. coli* BL21 (DE3) pLysS, kan^R	Provided by Stephanie Runde, unpublished
21	pCA528 *tasA* - sigseq		Production of TasA - signal sequence in *E. coli* BL21 (DE3) pLysS, kan^R	Provided by Stephanie Runde, unpublished
22	pMAD *tasA* T38A	21, 22, 23, 24	*B. subtilis* markerless point mutation *tasA* T38A in *cis*, ery^R	This work
23	pMAD *tasA* F39A	21, 22, 25, 26	*B. subtilis* markerless point mutation *tasA* F39A in *cis*, ery^R	This work
24	pMAD *tasA* ΔA40, S41	21, 22, 27, 28	*B. subtilis* markerless point mutation *tasA* ΔA40, S41 in *cis*, ery^R	This work
25	pMAD *tasA* S41A	21, 22, 29, 30	*B. subtilis* markerless point mutation *tasA* S41A in *cis*, ery^R	This work
26	pMAD *tasA* T187A	21, 22, 31, 32	*B. subtilis* markerless point mutation *tasA* T187A in *cis*, ery^R	This work

27	pMAD *tasA* P188A	21, 22, 33, 34	*B. subtilis* markerless point mutation *tasA* P188A in *cis*, ery^{R}	This work
28	pMAD *tasA* T189A	21, 22, 35, 36	*B. subtilis* markerless point mutation *tasA* T189A in *cis*, ery^{R}	This work
29	pMAD *tasA* D190A	21, 22, 37, 38	*B. subtilis* markerless point mutation *tasA* D190A in *cis*, ery^{R}	This work
30	pMAD *tasA* F191A	21, 22, 39, 40	*B. subtilis* markerless point mutation *tasA* F191A in *cis*, ery^{R}	This work
31	pMAD *tasA* D192A	21, 22, 41, 42	*B. subtilis* markerless point mutation *tasA* D192A in *cis*, ery^{R}	This work
32	pMAD *clpC* E280A E618A (DWB)		*B. subtilis* markerless point mutation *clpC* E280A E618A (DWB) in *cis*, ery^{R}	(Kirstein et al., 2006)
33	pMAD *clpC* ΔY670-T679 (Δloop)	43, 44, 45, 46	*B. subtilis* markerless mutation *clpC* ΔY670-T679 (Δloop) in *cis*, ery^{R}	This work
34	pMAD *clpC* VGF::IGF	12, 13, 43, 44	*B. subtilis* markerless point mutation *clpC* VGF::IGF in *cis*, ery^{R}	This work

Table 5: List of strains

Strain	Genotype	Reference
Escherichia coli		
DH5α	F^{-} Φ80*lac*ZΔM15 Δ(*lac*ZYA-*arg*F) U169 *rec*A1 *end*A1 *hsd*R17(rk^{-}, mk+) *pho*A *sup*E44 *thi*-1 *gyr*A96 *rel*A1 λ-	Invitrogen™
BL21 (DE3) pLysS	F^{-} ompT hsdSB (rB-mB-) gal dcm (DE3) pLysS (CamR)	(Studier et al., 1990)
XL1-Blue	recA1 endA1 gyrA96 thi-1 hsdR17 supE44 relA1 lac [F´ proAB lacIq ZΔM15 Tn10 (Tetr)]	Agilent
FI1202	lacI q lacL8 gln5::Tn5 l202	(Fiedler and Weiss, 1995)
Bacillus subtilis		
168	trpC2 wild type	(Anagnostopoulos and Spizizen, 1961)
DK 1042	comI Q12L [3610], wild type	(Konkol et al., 2013)
BRK1	DK 1042 Δ*tapAsipWtasA::spec*	This work; 17, 18 PCR product from NM235
BRK2	trpC2 Δ*tapAsipWtasA::spec*	This work; 17, 18 PCR product from NM235
BRK3	DK 1042 Δ*tasA::kan*	This work; 17, 18 PCR product from TB116 (Akos Kovacs)
BRK4	trpC2 Δ*tasA::kan*	This work; 17, 18 PCR product from TB116 (Akos Kovacs)

BRK5	DK 1042 Δ*sipW::ery*	This work; 19, 20 PCR product from TB116 (Akos Kovacs)
BRK6	trpC2 Δ*sipW::ery*	This work; 19, 20 PCR product from TB116 (Akos Kovacs)
BRK7	DK 1042 *tasA* T38A	This work; Plasmid 22
BRK8	DK 1042 *tasA* F39A	This work; Plasmid 23
BRK9	DK 1042 *tasA* ΔA40, S41	This work; Plasmid 24
BRK10	DK 1042 *tasA* S41A	This work; Plasmid 25
BRK11	DK 1042 *tasA* T187A	This work; Plasmid 26
BRK12	DK 1042 *tasA* P188A	This work; Plasmid 27
BRK13	DK 1042 *tasA* T189A	This work; Plasmid 28
BRK14	DK 1042 *tasA* D190A	This work; Plasmid 29
BRK15	DK 1042 *tasA* F191A	This work; Plasmid 30
BRK16	DK 1042 *tasA* D192A	This work; Plasmid 31
BRK17	trpC2 Δ*clpC::tet*	(Molière et al., 2016)
BRK18	DK 1042 Δ*clpC::tet*	Heinrich Schäfer, unpublished
BRK19	trpC2 *clpC* E280A E618A (DWB)	(Kirstein et al., 2006)
BRK20	DK 1042 *clpC* E280A E618A (DWB)	This work; Plasmid 32
BRK21	trpC2 *clpC* VGF::GGR	(Moliere, 2012)
BRK22	trpC2 *clpC* ΔY670-T679 (Δloop)	This work; Plasmid 33
BRK23	trpC2 *clpC* VGF::IGF	This work; Plasmid 34
BRK24	trpC2 Δ*mecA::tet*	Noel Molière, unpublished
BRK25	trpC2 lys-3 Δ*mcsB::kan*	(Krüger et al., 2001)
BRK26	trpC2 Δ*ypbH*::ery	(Koo et al., 2017), BGSC

2.3 Common media and solutions

Luria Bertani (LB) medium

5 g/L	Yeast extract
10 g/L	Tryptone
10 g/L	NaCl

LB agar

5 g/L	Yeast extract
10 g/L	Tryptone
10 g/L	NaCl
15 g/L	Agar

TE buffer

10 mM	Tris-HCl	pH 8.0
1 mM	EDTA	

Table 6: Antibiotics

Antibiotic	**Stock**	**Final concentration**
Ampicillin	100 mg/mL	100 µg/mL
Chloramphenicol	25 mg/mL	10 µg/mL
Erythromycin	1 mg/mL	1 µg/mL
Lincomycin	20 mg/mL	20 µg/mL
Kanamycin	50 mg/mL	50 µg/mL (*E. coli*); 10 µg/mL (*B. subtilis*)
Spectinomycin	100 mg/mL	150 µg/mL
Tetracycline	10 mg/mL	10 µg/mL

2.4 Cloning

Overnight cultures were derived by inoculation of 5 mL LB-medium and agitated incubation at 37 °C. Single colony selection was performed by streaking or plating the culture on agar plates supplemented with antibiotics (Table 6). Plasmid isolation was carried out with the peqGOLD plasmid Miniprep Kit (Peqlab).

Polymerase Chain Reaction (PCR)

To obtain DNA fragments for cloning and transformation, a polymerase chain reaction (PCR) was performed. The primers were obtained from Biomers and the Phusion polymerase with appropriate buffers from New England Biolabs. Denaturation was carried out at 98 °C for 30 sec, annealing at primer-specific temperatures for 30 sec and elongation according to fragment length (~1 kb per min). For *E. coli* colony PCR, to verify successful cloning, the initial denaturation time was set to 3 min.

Restriction enzyme digestion and ligation

For insertion of DNA fragments in plasmids both partners were digested with restrictions enzymes providing specific intersections at which T4 DNA Ligase assembled the desired product. Utilized restriction enzymes are listed with according primers in Table 3.

2.5 *B. subtilis* genomic DNA preparation

The MasterPure Gram positive DNA purification kit was used to isolate genomic DNA from *B. subtilis*. A pellet derived by centrifugation from 1 mL overnight culture was resuspended in 150 µL TE buffer and supplemented with 1 µL Ready-Lyse Lysozyme. After incubation at 37 °C for 30 min 150 µL Proteinase K/Gram Positive Lysis Solution were added and the sample was incubated at 65 °C for 15 min, briefly mixing every 5 min. Cooling down to 37 °C was followed by 5 min on ice. 175 µL MPC Protein Precipitation Reagent were added and mixed with the sample. The supernatant obtained by centrifugation at 4 °C for 10 min at 10000 x g was transferred to a clean tube and 1 µL RNase A was added. After incubation at 37 °C for 30 min 500 µL isopropanol were added and mixed by inverting. The DNA was pelleted by centrifugation, the supernatant was removed, and the pellet was washed with 70 % v/v ethanol. The pellet was resuspended in 35 µL dH_2O and DNA concentration was determined using the Nanodrop.

2.6 Transformation of *E. coli* and *B. subtilis*

E. coli competent cells

To obtain competent *E. coli* cells, able to take up external DNA, 100 mL SOB medium were inoculated to an optical density at 600 nm (OD_{600}) of 0.05 with an overnight culture. After agitated incubation at 37 °C until OD_{600} 0.4 was reached, the cells were chilled on ice for 10 min. The pellet, obtained by centrifugation for 10 min at 5000 xg and 4 °C was resuspended in 32 mL TB buffer and incubated on ice for 10 min. Anew pelleted cells were resuspended in 8 mL TB buffer with dimethyl sulfoxide (DMSO) (final concentration 7 % v/v) and incubated on ice for 10 min. The competent cells were stored in 100 µL aliquots at –80 °C.

SOB medium

2 % w/v	Tryptone
0,5 % w/v	Yeast extract
10 mM	NaCl
2,5 mM	$MnCl_2$
10 mM	$MgCl_2$
10 mM	$MgSO_4$

TB buffer

10 mM	PIPES	pH 6.7
15 mM	$CaCl_2*2H_2O$	
250 mM	KCl	
55 mM	$MnCl_2$	

E. coli transformation

E. coli DH5α was the basic strain used for plasmid generation and *E. coli* BL21 DE3 was utilized for protein overexpression and subsequent purification. For transformation, 100 ng plasmid DNA or 10 µl ligation reaction were added to one aliquot of competent cells. After incubation on ice for 30 min a 45 sec heat shock at 42 °C was performed. Furthermore, 5 min incubation on ice and subsequent addition of 800 µL LB medium were followed by agitated incubation at 37 °C for 45 min. The cell pellet obtained by centrifugation for 1 min at 5000 xg was resuspended in 100 µl remaining supernatant and plated on LB agar plates with appropriate antibiotics.

B. subtilis transformation

To obtain competent *B. subtilis* cells of strains trp(C2) 168 or DK 1042, 5 mL of competence medium were inoculated with 500 µL from an overnight culture. After agitated incubation at 37 °C for 3 h, 5 mL starvation medium were added and further incubated for 2 h. 800 µL of competent cells were supplied with ~1 µg DNA (genomic, PCR fragment, plasmid) and shaken at 37 °C for 45 min. The cell pellet obtained by centrifugation for 1 min at 5000 xg was resuspended in 100 µL of the remaining supernatant and plated on LB agar plates with appropriate antibiotics.

2.7 Thermotolerance experiments

20 mL of LB medium were inoculated with an overnight culture to an OD_{600} of 0.05 and grown in a water bath at 37 °C shaking at 200 rpm. When OD_{600} 0.4 was reached the culture was split and one half was conferred to 48 °C for 15 min for a mild pre-shock and the other half was left at 37 °C. At t_0 both cultures were shifted to 53 °C. Samples were taken at t_0, t_{30}, t_{60} and t_{120}, diluted and plated on LB agar plates for subsequent counting of colony forming units (cfu). By evaluation of cfu over time, the thermoresistance (no pre-shock) and thermotolerance (with pre-shock) of different strains were evaluated.

2.8 Biofilm cultivation

1.4 mL medium (MOLP or Msgg) were inoculated with overnight culture (at a dilution of 1:100) of the corresponding strains in 24-well plates and incubated without agitation at 30 °C. To monitor phenotypical differences in more detail 28 µL Coomassie and Congo Red (CC) dye were added to 1.4 mL medium prior to inoculation (Romero et al., 2010). Pictures of the biofilms were taken every day for two or three days depending on the *B. subtilis* strain and experimental setup.

MOLP medium

30 g/L	Peptone
20 g/L	Saccharose
7 g/L	Yeast extract
1.9 g/L	KH_2PO_4
0.0001 mg/L	$CuSO_4$
0.005 mg/L	$FeCl_3*6H_2O$
0.004 mg/L	Na_2MoO_4
0,002 mg/L	KI
3.6 mg/L	$MnSO_4*H_2O$
0.45 g/L	$MgSO_4$
0.14 mg/L	$ZnSO_4*7H_2O$
0.01 mg/L	H_3BO_3
10 mg/L	$C_6H_8O_7$

adjust to pH 7.0

Msgg medium

5 mM	KH_2PO_4	pH 7.0
100 mM	MOPS	pH 7.0
2 mM	$MgCl_2$	
700 µM	$CaCl_2$	
50 µM	$MnCl_2$	
50 µM	$FeCl_3$	
1 µM	$ZnCl_2$	
2 µM	Thiamine	
0.5 % v/v	Glycerol	
0.5 % w/v	Potassium glutamate	
50 µg/µL	L-Tryptophan	
50 µg/µL	L-Phenylalanine	

Coomassie and Congo Red dye (CC)

2 % w/v	Congo Red
1 % w/v	Coomassie Brilliant Blue G250
70%	Ethanol

2.8.1 Biofilm reconstitution experiments

Experiments were performed for reconstitution of biofilm formation in the *tasA* deletion mutant by addition of purified TasA, according to previous studies (Romero et al., 2010). 60-300 µg of recombinantly produced TasA were added to the cultures 2 hours after inoculation. The cultures were incubated at 30 °C without agitation.

The form of TasA fibrils in native biofilms was assessed in cooperation with Dr. Anne Diehl, Prof. Dr. Hartmut Oschkinat (Leibniz-Forschungsinstitut für Molekulare Pharmakologie), Dr. Yvette Roske (Max-Delbrück-Centrum für Molekulare Medizin) et al. (Diehl et al., 2018). Therefore, recombinantly produced $^{2}H,^{13}C,^{15}N\text{-TasA}_{261}$ (provided by Anne Diehl et al.) was added to reconstitute the biofilm. Matrix harvest for NMR analysis was carried out by circumspect detachment of the pellicle biofilm from the supernatant.

2.8.2 Biofilm sample fractionation and TasA protein level determination

The biofilm samples were fractionated for determination of TasA localization. Therefore, the whole culture including matrix and supernatant was harvested after cultivation for 2 days and centrifuged at 4500 rpm for 20 min. The supernatant was filter sterilized and stored at 4 °C (supernatant fraction). 3.5 mL TE buffer were added to the pellet and treated with mild sonication to disrupt the biofilm structure (2.5 output control, 20 % power, ~25 one-second pulses). Centrifugation was performed for 20 min at 4500 rpm, the supernatant was filter sterilized and stored at 4 °C (matrix fraction). 1 mL TE-buffer and 5 µL Lysozyme were added to the pellet and incubated at 37 °C for 30 min (cell fraction). All collected samples were treated with trichloroacetic acid (TCA) to a final concentration of ~10 % and incubated on ice for 30 min. Centrifugation at 14000 rpm for 15 min and two washing steps with 1 mL cold acetone followed. The precipitated protein pellets were dried under vacuum in a Speed Vac for 30 min and solubilized in 100 µL 1x SDS sample buffer. In each case 10 µL sample were resolved on a 12.5 % polyacrylamide gel and blotted on nitrocellulose membranes. Immunoblotting was performed with α-TasA antibody (1:5000), α -ClpC antibody (1:5000) and α -rabbit horseradish peroxidase conjugate (1:5000). The chemiluminescent signal was visualized with according imagers (INTAS, BioRad).

For TasA protein level determination pellet and supernatant fractions were separated by centrifugation for 10 min at 15000 rpm. The supernatant was transferred to a new tube and 500 µL TE-buffer were added to the pellet. The biofilm was disrupted, and the cells lysed by harsh sonication (2.5 output control, 30 % power, 3x ~25 one-second pulses) or homogenization in FastPrep-24^{TM} 5G (~20 µL 0.1mm glass beads, 3x 30 sec 6 m/sec). The protein concentrations of the samples were determined using a Bradford assay and 5 µg protein were applied on a 12.5 % SDS gel. For evaluation of protein concentration, 0.4 µg TasA were applied on every gel. The band intensity in western blots was determined with ImageJ software and TasA levels in the samples were calculated according to the standard curve obtained with purified TasA (Figure 7) (Schneider et al., 2012).

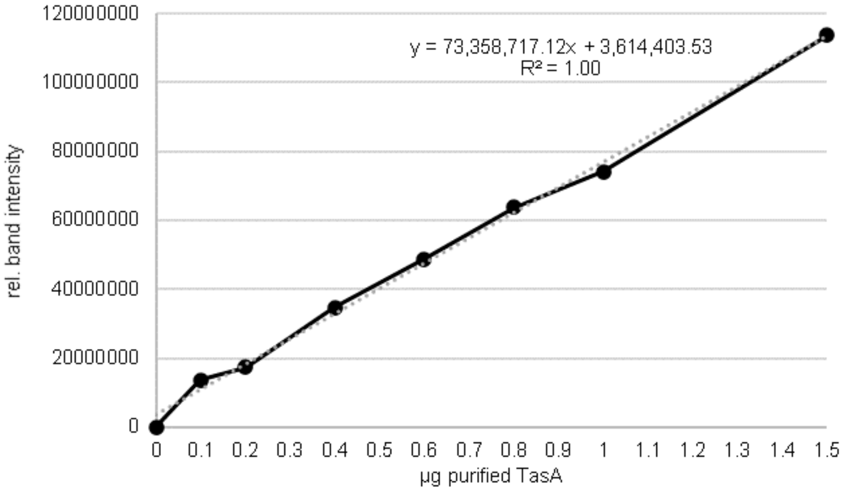

Figure 7 Standard curve for calculation of TasA protein concentration in western blots.

Standard curve for determination of TasA protein level by means of quantitative western blotting. 0 µg – 1.5 µg purified TasA were applied on SDS-PAGE and a western blot with TasA antibody was performed. ImageJ software was used to calculate the band intensities displayed in this plot.

2.9 Protein purification

Recombinant protein production was carried out in *E. coli* BL21 DE3 using different expression vectors (pCA528, pET28a, pRsetA). 1.5 L of LB medium, supplied with corresponding antibiotics, were inoculated 1:100 with an overnight culture and incubated at 37 °C and 170 rpm until OD_{600} 0.4 was reached. After the induction of protein overexpression with 0.1-1 mM IPTG, the cultures were incubated for 1 h at 37 °C and 170 rpm and overnight at 16 °C and 170 rpm. The cell harvest was carried out by centrifugation for 15 min at 7000 rpm and 4 °C. The pellet was stored at -20 °C.

For proper protein purification all following steps were performed at 4 °C. The pellet was resuspended in lysis buffer containing DNase and PMSF (for ClpP purification only Dnase). Cell lysis was performed by french pressing 3x at 1200 psi and the cell debris was removed by centrifugation at 17000 rpm and 4 °C for 20 min. Before application on the FPLC Äkta system, the lysate was sterile filtered (applied for ClpC).

Protein structure models were created with UCSF Chimera, developed by the Resource for Biocomputing, Visualization, and Informatics at the University of California, San Francisco, with support from NIH P41-GM103311 (Pettersen et al., 2004).

2.9.1 His-tagged proteins

Affinity chromatography for His-tagged proteins was carried out with Ni-NTA agarose columns. After equilibration of the column with 3 column volumes (CV) of Lysis buffer, the cell lysate was applied. Washing was performed with at least 3 CV of wash buffer until no more unbound protein was detected in the flow through, checked with a Bradford assay. The protein elution fractions were collected after addition of 3 CV of elution buffer. Protein concentrations were determined with a Bradford assay or Nanodrop analysis and the protein purity was checked with SDS-PAGE.

Lysis Buffer

50 mM	Tris-HCl	pH 7.5
150 mM	NaCl	
5 mM	$MgCl_2$	
10 mM	Imidazole	
5 µg/mL	Dnase	
1 mM	PMSF	

Wash Buffer

50 mM	Tris-HCl	pH 7.5
150 mM	NaCl	
5 mM	$MgCl_2$	
20 mM	Imidazole	

Elution Buffer

50 mM	Tris-HCl	pH 7.5
150 mM	NaCl	
5 mM	$MgCl_2$	
250 mM	Imidazole	

To receive protein in high purity, anion exchange chromatography using a Resource Q 1 mL column (GE Healthcare) was performed (ClpC). After equilibration with 3 CV Aex 1 buffer, 1 mL of protein sample was diluted in 25 mL of Aex 1 buffer and applied on the column. To avoid protein precipitation at extreme low salt concentrations the Aex 1 buffer contained 50 mM KCl. After washing with 3 CV Aex 1 buffer, a gradient with increasing amounts of Aex 2 buffer utilized to elute the target protein according to the isoelectric point. The protein concentration in elution fractions was determined using a Bradford assay or Nanodrop analysis and SDS-PAGE was performed to control protein purity.

Aex 1

20 mM	Bicin	pH 8.0
50 mM	KCl	
5 mM	$MgCl_2$	

Aex 2

20 mM	Bicin	pH 8.0
1 mM	KCl	
5 mM	$MgCl_2$	

2.9.2 SUMO-His-tagged proteins

For McsB and TasA overexpression the vector pCA528 was utilized to produce the protein with a cleavable SUMO-His-tag. Cleavage of SUMO-His is only possible, when the protein is properly folded and the Ulp-protease can detect its target sequence, resulting in purification of correctly folded protein species without attached His-tag.

For production of SUMO-His-tagged proteins, the according strain was inoculated 1:100 in 2x LB and grown at 37 °C and 170 rpm until OD_{600} 0.4 was reached. After induction with 0.1 mM IPTG the temperature was set to 16 °C for overnight incubation. Cell harvest and lysis were carried out according to section 2.9.

After equilibration of the Ni-NTA agarose column with 3 CV of Lysis buffer, the cell lysate was applied. Washing was performed in different steps to achieve a denaturation and subsequent refolding gradient. First, 2 CV of SUMO-Wash 1 buffer were applied, followed by 2 CV of SUMO-Wash 2 buffer and at least 2 CV Wash buffer (without Urea), until all unbound protein was washed away. Elution and desalting were performed as described before.

Furthermore, 1 mL protein sample was incubated in a 1.5 mL reaction tube with 10 % Glycerol, 1 mM DTT and 50 µg/mL Ulp protease slowly rotating over night at 4 °C for cleavage of the SUMO-His-tag. For separation of the His-tagged Ulp protease and the truncated SUMO-His-tag from the target protein, the sample was applied on a Ni-NTA column equilibrated with basic buffer and the flow through, containing the target protein was collected. If necessary, proteins were concentrated using Amicon (Merck) or Vivaspin (GE Healthcare) spin columns. Protein concentrations were determined with a Bradford assay or Nanodrop analysis and the protein purity was checked with SDS-PAGE.

SUMO-Wash 1

50 mM	Tris-HCl	pH 7.5
150 mM	NaCl	
5 mM	$MgCl_2$	
20 mM	Imidazole	
8 M	Urea	

SUMO-Wash 2

50 mM	Tris-HCl	pH 7.5
150 mM	NaCl	
5 mM	$MgCl_2$	
20 mM	Imidazole	
4 M	Urea	

2.9.3 Desalting purified protein

Desalting of protein fractions was performed with a 5 mL Hi-Trap Desalting Column (GE Healthcare). Therefore, the column was equilibrated with target buffer (basic buffer). 1.5 mL of protein sample were applied, the flow through was cast away and the desalted protein eluted in the next 2 mL. For further desalting steps the column was equilibrated anew. If necessary, proteins were concentrated using Amicon (Merck) or Vivaspin (GE Healthcare) spin columns. Purified protein samples were supplemented with 5 % Glycerol and stored in aliquots at -80 °C. The protein concentrations were determined with a Bradford assay or Nanodrop analysis and protein purity was checked with SDS-PAGE.

Basic Buffer

50 mM	Tris-HCl	pH 7.5
150 mM	NaCl	
5 mM	$MgCl_2$	

2.10 SDS-PAGE & Western blotting

SDS-PAGE was performed to determine the purity of recombinantly produced proteins, evaluate degradation assays and pellet-supernatant fractionations. Western blot analysis was utilized for detection of phosphorylated arginine, detection of TasA in different fractions and determination of TasA protein levels.

SDS – gel electrophoresis

12.5 % or 15 % acrylamide SDS-gels were casted according to Table 7. The protein samples were mixed with 2x SDS loading dye, denatured at 95 °C for 10 min and PageRuler™ Plus Prestained Protein Ladder was used to estimate protein sizes. The gels were run in SDS running buffer at 90 V until the sample completely entered the gel and at 120 V until the proteins were separated sufficiently. For staining of proteins, the gel was incubated for 60 min in fixing solution and subsequently in colloidal Coomassie staining solution for at least 60 min.

Table 7: SDS-Gels

1 SDS-gel (5 mL)	12.5 %	15%		stacking gel
40 % v/v acryl amide	1.5 mL	1.85 mL	40 % v/v acryl amide	0.45 mL
1 M Tris-HCl pH 8.8	2.1 mL		1 M Tris-HCl pH 6.8	0.39 mL
H_2O	1.35 mL	0.975 mL	H_2O	2.13 mL
10 % SDS	50 µL		10 % SDS	30 µL
10 % APS	50 µL		10 % APS	31 µL
TEMED	3 µL		TEMED	1.8 µL

2x SDS loading dye

200 mM	Tris-HCl	pH 6.8
10 % w/v	SDS	
50 % w/v	Glycerol	
13 % v/v	DTT	
2.5 mg/L	Bromphenol blue	

SDS running buffer

25 mM	Tris base
192 mM	Glycine
0.1 % w/v	SDS

Fixing solution

40% v/v	Methanol
10% v/v	Acetic acid

Coomassie staining solution

2 % w/v	Orthophosphoric acid
10% w/v	$(NH_4)_2SO_4$
5 % w/v	Coomassie brilliant blue G250

Western blotting

Western blotting was performed semi-dry, to transfer proteins on nitrocellulose membranes for subsequent detection with antibodies. Therefore, the SDS-gel was stacked on a nitrocellulose membrane between Whatman filter paper drenched in Towbin buffer. Blotting was performed in the Fastblot B44 system (Biometra) or according to standard protocols in the Trans-Blot Turbo system (Biorad). After blotting, blocking was performed with 5 % w/v skim milk powder in 1x TBS buffer for 60 min swiveling. Primary antibodies were applied according to Table 8 in 1x TBS buffer after washing thoroughly with 1x TBS buffer. Repeated washing was followed by incubation with the secondary α-rabbit antibody bound to horse radish peroxidase for electro chemical luminescence (ECL) detection with an Intas imager or a Chemidox XRS Imager (Biorad). Samples for α-pArg blotting were stored on ice and directly applied on SDS-gels without denaturation. SDS-gel electrophoresis and western blotting were performed at 4 °C to avoid undesired dephosphorylation.

Table 8: Antibodies

Antibody	Dilution
α-ClpC	1:5000
α-TasA	1:5000
α-pArg	1:3000

Towbin buffer

20 mM	Tris
150 mM	Glycine
20 % v/v	Methanol

TBS buffer

50 mM	Tris-HCl	pH 7.5
150 mM	NaCl	

2.11 *In vitro* assays

For characterization of various properties and activities of the purified proteins and protein systems, different *in vitro* assays were performed.

2.11.1 Bradford assay

To determine the concentration of protein samples, 5 µL sample were mixed with 250 µL 1x Roti Nanoquant Bradford solution in a 96-well plate. The absorption at 595 nm was measured and the protein concentration was calculated according to a standard curve in duplicates.

2.11.2 Malachite Green assay

The Malachite Green assay was performed to determine the ATPase activity of purified proteins. Upon ATP hydrolysis freed phosphate binds to molybdate, which itself forms a complex with malachite green, detectable at A_{640}. By using a potassium phosphate standard between 0 µM and 1000 µM, the release of phosphate by ATP hydrolysis in the samples was determined over time.

The staining solution was prepared and stirred for 1 h in the dark prior to use. If not mentioned otherwise, 1 µM of each protein was utilized, according to experimental setups, in a total of 50 µL with 1x *In vitro* Assay buffer and 4 mM ATP. The assay was started by addition of ATP and transfer to 37 °C. 10 µl sample were taken after 0 min, 5 min, 10 min, 15 min and mixed with 160 µL staining solution, previously prepared in 96-well plates. Subsequent addition of 20 µL sodium citrate (34 % (w/v)) stopped the reaction. The absorption was measured at 640 nm with a Spectramax microplate reader. The ATPase activity was calculated by means of the performed standard curve.

***In vitro* Assay buffer (5x)**

250 mM	Tris-HCl	pH 7.8
750 mM	KCl	
100 mM	MgCl2	
10 mM	DTT	

Staining solution

30 mL	Malachite green hydrochloride (45 mg/L)
10 mL	Ammonium molybdate (4.2 % in 4 M HCl)
40 µL	Triton X 100

2.11.3 Degradation assay

The degradation activity of purified proteins was determined with β-casein as model substrate. 1 µM of each protein was used (except for 0.05 µM YwlE/YwlE C7S), according to the experimental setups, in a total of 100 µL with 1x *In vitro* Assay buffer and 4 mM ATP. The reaction was started by addition of ATP and transfer to 37 °C. Samples were taken after 0 min, 30 min, 60 min and 90 min or 120 min, according to the experimental setup. 15 µL sample were transferred to a new tube and mixed with 2x SDS loading dye to stop the reaction. Denaturation prior to SDS-PAGE was performed for 5 min at 95 °C. The degradation efficiency was calculated using ImageJ software to determine substrate and adaptor protein band intensity over time (Schneider et al., 2012).

2.11.4 Light scattering assay

The *in vitro* disaggregation activity of chaperone systems was determined using light scattering experiments. Therefore, 2 µM of model substrates malate dehydrogenase (Mdh) (Roche) or citrate synthase (Cs) (Sigma-Aldrich) were aggregated and inactivated by incubation at 47 °C for 30 min in *In vitro* assay buffer. The light scattering was monitored at 360 nm excitation and emission wavelength in Jasco FP 6500/FP8500 spectrofluorometers with low sensitivity at 30 °C for 120 min. The *E. coli* chaperone system ClpB, DnaK, DnaJ, GrpE (ClpB/KJE) (1.5 µM/ 1 µM/ 0.2 µM/ 0.1 µM) was utilized as positive control and recombinantly produced *B. subtilis* proteins were applied in concentrations according to Table 9, if not mentioned otherwise.

Table 9: Final protein concentrations applied in the light scattering assay

Protein	Final concentration
ClpC	1.5 µM
ClpC DWB	0.25 µM
ClpC VGF::GGR	1.5 µM
ClpC VGF::IGF	1.5 µM
MecA	1 µM
McsB	1 µM
McsB C167S	1 µM
McsA	1 µM
YwlE	0.05 µM
YwlE C7S	0.05 µM
ClpP	1.5 µM
Mdh	1 µM
Cs	1 µM

2.11.5 Malate dehydrogenase activity assay

Refolding of Mdh during disaggregation experiments was determined by Mdh activity measurements. The enzyme activity was assessed before and after inactivation as well as after 15 min, 30 min, 60 min, 90 min and 120 min during light scattering assays. Therefore, 125 µL Mdh assay buffer were added to 2.5 µL sample containing 1 µM Mdh. The time dependent NADH oxidation by Mdh was monitored at 340 nm and 30 °C in a Spectra Max MP3 microplate reader (Molecular Devices) or a Synergy H1 microplate reader (BioTek).

Mdh activity buffer (5 mL)

750 µL	Potassium phosphate buffer (1 M, pH 7.6)
0.931 mg	NADH
0.33 mg	Oxalacetic acid
ad 5 mL	dH_2O

2.11.6 Citrate synthase activity assay

Refolding of Cs during disaggregation experiments was determined by Cs activity measurements. Cs catalyzes the reaction between oxaloacetic acid and acetyl coenzyme A forming CoA-SH and citric acid. CoA-SH reacts with DTNB and the time dependent formation of TNB, measurable at 412 nm, is proportional to Cs activity. For this experiment, the Cs activity was determined before and after inactivation as well as after 15 min, 30 min, 60 min, 90 min and 120 min during light scattering experiments. Therefore 125 µL Cs assay buffer were added to 2,5 µl sample containing 1 µM Cs. The enzymatic reaction was followed at 25 °C in a Synergy H1 microplate reader (BioTek).

Cs activity buffer

200 mM	Tris-HCl	pH 8.1
0.1 mM	DTNB	
0.047 mM	Acetyl Coenzyme A	
0.23 mM	Oxalacetic acid	

3 Results

3.1 *In vitro* characterization of the ClpC disaggregation activity

The example of the disaggregase ClpB in *E. coli* shows that a successful heat stress response and thermotolerance development can depend on the removal of heat induced aggregates, by disaggregation and refolding of those impaired proteins (Weibezahn et al., 2004). However, the Gram-positive model organism *B. subtilis* lacks an exclusive unfoldase comparable to ClpB, but other chaperone systems are assumed to cover its function. The AAA+/Hsp100 protein ClpC from *B. subtilis*, was shown to dissolve and refold heat aggregated substrate in absence of protease ClpP *in vitro* (Schlothauer et al., 2003). Aided by adaptor proteins MecA or YpbH, ClpC was able to restore up to 20 % of the initial luciferase activity. Nevertheless, no thermosensitive phenotype was observed in strains lacking *mecA* and *ypbH* (Schlothauer, 2004). Subsequent *in vivo* studies proposed that McsB is the main ClpC adaptor protein for removal of heat induced subcellular protein aggregates in *B. subtilis* (Hantke, 2019). McsB has a dual function, as adaptor protein for ClpC and as protein arginine kinase, which can be activated by McsA (McsB/McsA). But the impact of these McsB activities on ClpC disaggregation activity has not been studied *in vitro* yet. Therefore, the first part of this work focused mainly on McsB/McsA mediated ClpC activities and the influence of the McsB kinase activity as well as the phosphatase YwlE, on disaggregation and refolding or degradation activities of the protease complex ClpCP.

To examine the activity of various chaperone systems in disaggregation and refolding of heat aggregated substrate, different assays with purified proteins were performed *in vitro*. Heat inactivated and aggregated malate dehydrogenase (Mdh) and citrate synthase (Cs) served as model substrates. The disaggregation of these aggregates by chaperone systems was followed in light scattering experiments and the substrates enzyme activity was measured to monitor protein refolding over time. Furthermore, samples were taken and divided in pellet- and supernatant fractions to display the shift of aggregated protein in the pellet fraction to solubilized or refolded protein in the supernatant fraction by SDS-PAGE. With these combined assays a rough differentiation between only disaggregated and refolded substrate could be determined. The established disaggregation and refolding system ClpB, DnaK, DnaJ, GrpE (ClpB/KJE) from *E. coli* served as positive control (Glover and Lindquist, 1998; Goloubinoff et al., 1999; Zolkiewski, 1999). This control system dissolved 100 % of Mdh aggregates after 100 min and 30 % of the substrates enzyme activity could be restored (Figure 8).

The influence of the adaptor proteins MecA and McsB/McsA on the ClpC disaggregation and refolding activity was compared (Figure 8). MecA-activated ClpC dissolved 47 % of the aggregates, while only 14 % of Mdh activity was recovered (Figure 8 A, B). The SDS-PAGE analysis of pellet and supernatant fractions revealed no considerable Mdh shift, indicating that not much protein was solubilized (Figure 8 C).

ClpC activated by McsB/McsA dissolved 63 % of the aggregates, while only 6 % of Mdh was successfully refolded (Figure 8 A, B). The pellet-supernatant samples were similar to experiments with MecA (Figure 8 C). Compared to MecA, the light scattering curve of ClpC with McsB/McsA displayed a biphasic kinetic starting with a noticeable peak at t_{15}, suggesting that complex formation might occurred. Consistent with this, a complex of ClpC with ClpP, McsB, McsA and substrate CtsR was observed *in vivo* (Kirstein et al., 2007). Overall, the ClpC disaggregation activity induced by McsB/McsA was more efficient, while the adaptor protein MecA facilitated improved substrate refolding. Unlike MecA, McsB can phosphorylate proteins and these observations were the first hints suggesting that arginine phosphorylation might interfere with successful substrate refolding.

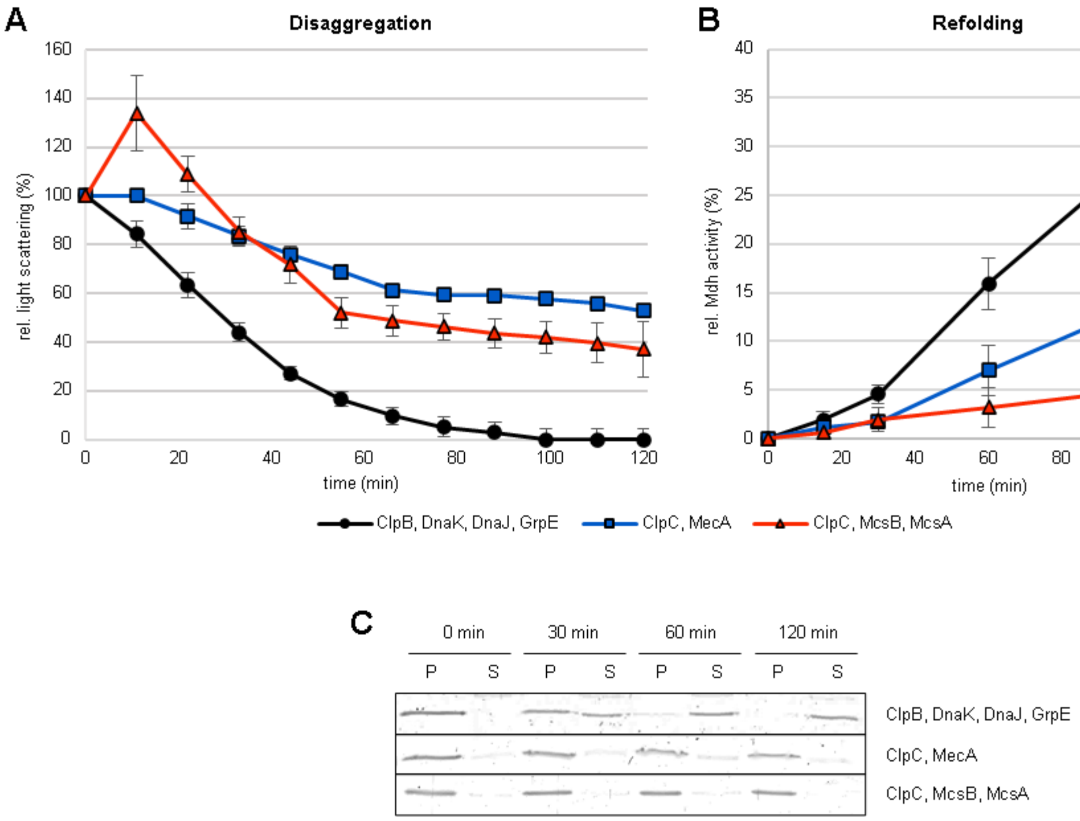

Figure 8 McsB/McsA facilitates moderate ClpC dependent Mdh disaggregation.

(A) Disaggregation of heat aggregated Mdh was monitored with light scattering experiments performed at 30°C for 120 min. ClpB, DnaK, DnaJ, GrpE (●) served as positive control, ClpC, MecA (■) and ClpC, McsB, McsA (▲) were compared. (B) The refolding of Mdh was examined by measuring the enzymatic activity at different time points. Error bars display standard deviations of three replicates. (C) SDS-PAGE of Mdh in pellet (P) and supernatant (S) fractions at indicated time points.

The observed ClpC dependent disaggregation and refolding activities were low compared to the control system ClpB/KJE, suggesting that factors enhancing this protein rescue machinery of *B. subtilis* were possibly missing in this first *in vitro* experiment.

3.1.1 YwlE enhances the McsB-induced ClpC disaggregation and refolding activity

In vivo and *in vitro*, the protein arginine phosphorylation by McsB is counteracted by the phosphatase YwlE (Elsholz et al., 2017; Kirstein et al., 2007). To investigate the influence of YwlE on the McsB-induced ClpC activity, ATPase assays were performed *in vitro*. Remarkably, equimolar concentrations of McsB (1 µM) and YwlE (1 µM) in the reaction led to a strong inhibition of ClpC ATPase activity, consistent with previous studies (Kirstein et al., 2007). Lowering the concentrations of YwlE down to 0.05 µM and 0.01 µM resulted in a recovery of ~80 % of ClpC ATPase activity (Figure 9 D). Based on preliminary disaggregation and refolding experiments that observed low impact of 0.01 µM YwlE, following experiments were carried out with 0.05 µM YwlE (data not shown). This concentration corresponds to physiological YwlE levels (Hantke, 2019; Muntel et al., 2014)

To assess the impact of the phosphatase on the ClpC disaggregation activity. light scattering experiments were performed with low concentrations of YwlE, that no longer inhibited ClpC ATPase activity. With YwlE present, the initial peak of the light scattering curve at t_{15} was smaller than in experiments without YwlE, and 100 % of the heat induced Mdh aggregates were dissolved after 110 min (Figure 9 A). Notably, 50 % of the initial Mdh activity could be recovered with YwlE, which is an even higher refolding efficiency than the control chaperone system ClpB/KJE achieved. The pellet-supernatant experiment was consistent with the light scattering curves, since a removal of aggregates corresponded to Mdh migration from the pellet to the supernatant fraction (Figure 9 C).

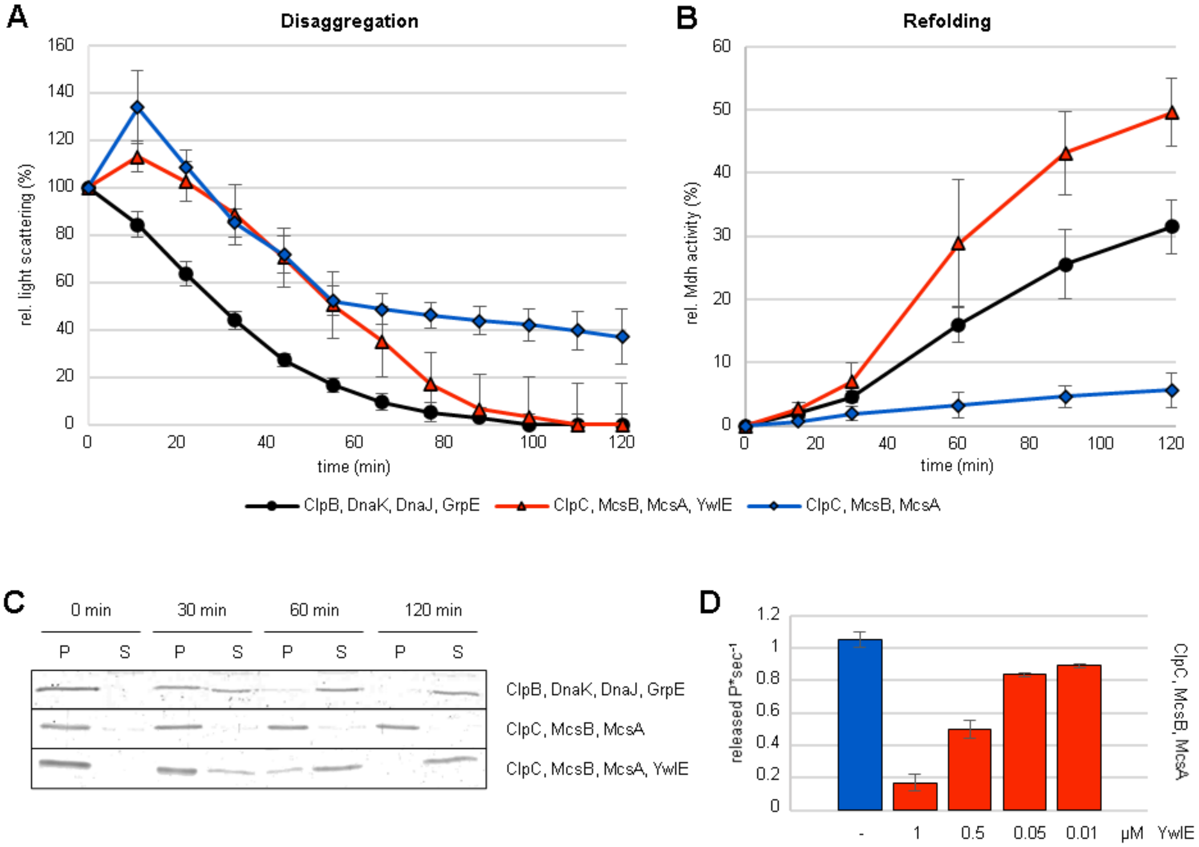

Figure 9 Catalytic amounts of YwlE enhance disaggregation and refolding.

(A) Disaggregation of heat aggregated Mdh was monitored with light scattering experiments performed at 30°C for 120 min. ClpB, DnaK, DnaJ, GrpE (●) served as positive control, ClpC, McsB, McsA, YwlE (▲) and ClpC, McsB, McsA (◆) were compared. (B) The refolding of Mdh was examined by measuring the enzymatic activity at different time points. (C) SDS-PAGE of Mdh in pellet (P) and supernatant (S) fractions at indicated time points. (D) McsB/McsA-induced ClpC ATPase activity in presence of different YwlE concentrations determined in Malachite Green assay. Error bars display standard deviations of three replicates.

The phosphatase YwlE was observed to have potent influence on McsB/McsA induced ClpC disaggregation and refolding activity. Therefore, the interplay of protein arginine phosphorylation and dephosphorylation by McsB and YwlE, respectively, were examined in more detail. With specifically engineered anti-phospho-arginine antibodies (α-pArg) supplied by Fuhrmann *et al.*, the detection of arginine phosphorylated proteins was possible (Fuhrmann et al., 2015b). Samples were taken from disaggregation assays and fractionated for SDS-PAGE and α-pArg western blotting. Since preliminary tests with McsB/McsA-activated ClpC showed that most detectable phosphorylation took place between 0 min and 30 min, samples were taken after 0 min, 15 min, 30 min and 60 min. Autophosphorylated McsB or McsA-activated McsB served as positive controls to monitor successful blotting and detection.

Similar to previous data, a shift of Mdh from the pellet to supernatant fraction was only observable with additional YwlE in the Coomassie stained gel (Figure 9/Figure 10 A, B). The α-pArg blotting revealed phosphorylation of McsB, McsA, Mdh and ClpC in the supernatant and pellet fraction at t_0 without YwlE (Figure 10 A). The phosphorylation signal increased in the supernatant after 15 min of incubation. Here, phosphorylation was detected on all proteins, whereby the McsB signal was especially intense. For ClpC different bands were visible, possibly due to missing denaturation prior to gel application, different charges, conformational states, or high sensitivity of the pArg antibody. The detected protein phosphorylation decreased after 30 min and 60 min in both fractions. Notably, phosphorylation of the substrate Mdh was only detectable in the supernatant fraction, indicating that soluble Mdh is still phosphorylated after disaggregation by ClpC.

The α-pArg blot of McsB/McsA-activated ClpC with YwlE displayed, compared to the McsB control band, only a slight phosphorylation signal for McsB at t_0 (Figure 10 B). The prior observed strong protein phosphorylation was not detected upon incubation with YwlE, indicating a high activity and efficiency of the phosphatase. Even though the YwlE concentration was 20 times lower than the concentration of arginine kinase McsB, no phosphorylation was detected over time. It is known that the McsB kinase activity is inhibited by both ClpC and YwlE *in vivo* (Elsholz et al., 2011a). The *in vitro* experiments with low concentrations of YwlE, resembling physiological levels, suggested that albeit no strong protein arginine phosphorylation by McsB could be detected, ClpC ATPase activity was induced and substrate disaggregation and high refolding efficiencies were achieved (Figure 9, Figure 10).

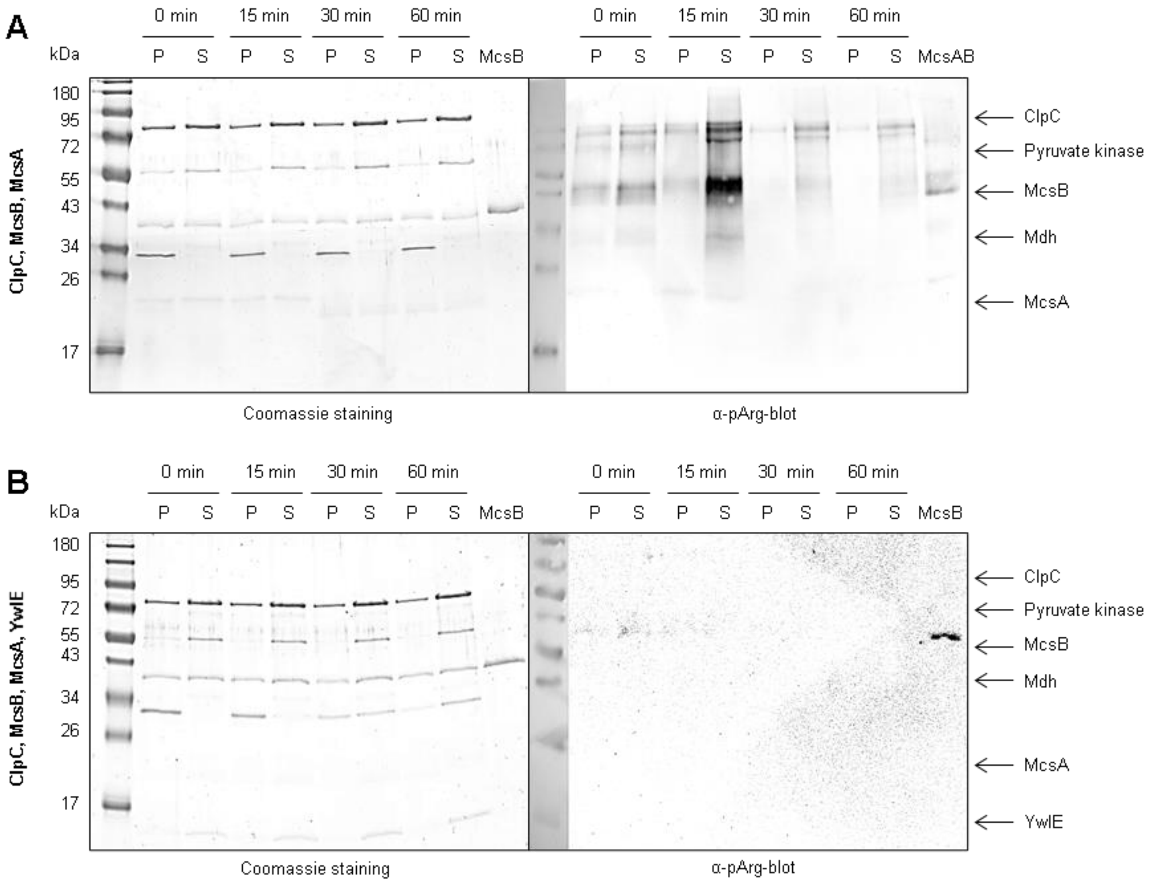
A
B
0 min
15 min
30 min
60 min
P
S
McsB
McsAB
kDa
180
95
72
55
43
34
26
17
ClpC, McsB, McsA
ClpC, McsB, McsA, YwlE
ClpC
Pyruvate kinase
McsB
Mdh
McsA
YwlE
Coomassie staining
α-pArg-blot

Figure 10 Protein phosphorylation by McsB is counteracted by phosphatase YwlE.

Representative SDS-PAGE and western blots of samples from disaggregation experiment taken at indicated time points and divided in pellet (P) and supernatant (S) fractions. On the left, Coomassie staining and on the right western blots with α-pArg antibody (Fuhrman et al) are displayed. ClpC, McsB, McsA (A) and ClpC, McsB, McsA, YwlE (B) were compared with autophosphorylated McsB or McsB/McsA as positive control for pArg western blots.

3.1.2 McsB kinase and YwlE phosphatase activities are essential for efficient refolding

To investigate the impact of arginine phosphorylation and dephosphorylation events as well as possible protein-protein interactions on ClpC activities, a kinase inactive McsB C167S mutant and a phosphatase inactive YwlE C7S mutant were analyzed (Fuhrmann et al., 2013a; Kirstein et al., 2005).

Previous studies observed, that no degradation of the McsB C167S mutant occurs in presence of ClpCP, but the kinase inactive mutant could still inhibit DNA-binding of CtsR (Kirstein et al., 2007, 2005). An ATPase assay was performed to examine whether the McsB C167S mutant can still act as adaptor protein for ClpC. The ClpC ATPase activity induced by the inactive mutant was 55 % lower than with active McsB (Figure 11 D). The addition of active YwlE decreased the ClpC ATPase activity independent of McsB kinase activity. Moreover, the impact of the McsB C167S mutant on disaggregation and refolding of heat aggregated substrate by ClpC was examined. Although the disaggregation rate was lower than with kinase active McsB, 20 % of the initial Mdh activity could be recovered by McsB C167S/McsA-activated ClpC (Figure 11 A, B). Upon addition of YwlE to the reaction with kinase inactive McsB C167S, a peak was observed at t_{15}, suggesting that complex formation occurred, comparable to experiments without YwlE. However, disaggregation or refolding of Mdh was not possible and the pellet-supernatant fractions were consistent with the observed disaggregation curves (Figure 11 A, C).

These observations suggest that McsB could act as an adaptor protein for ClpC independent of the kinase activity and that the arginine phosphorylation by active McsB might interfere with successful refolding. In presence of phosphatase YwlE, kinase active McsB was necessary to facilitate the ClpC dependent disaggregation and refolding activity.

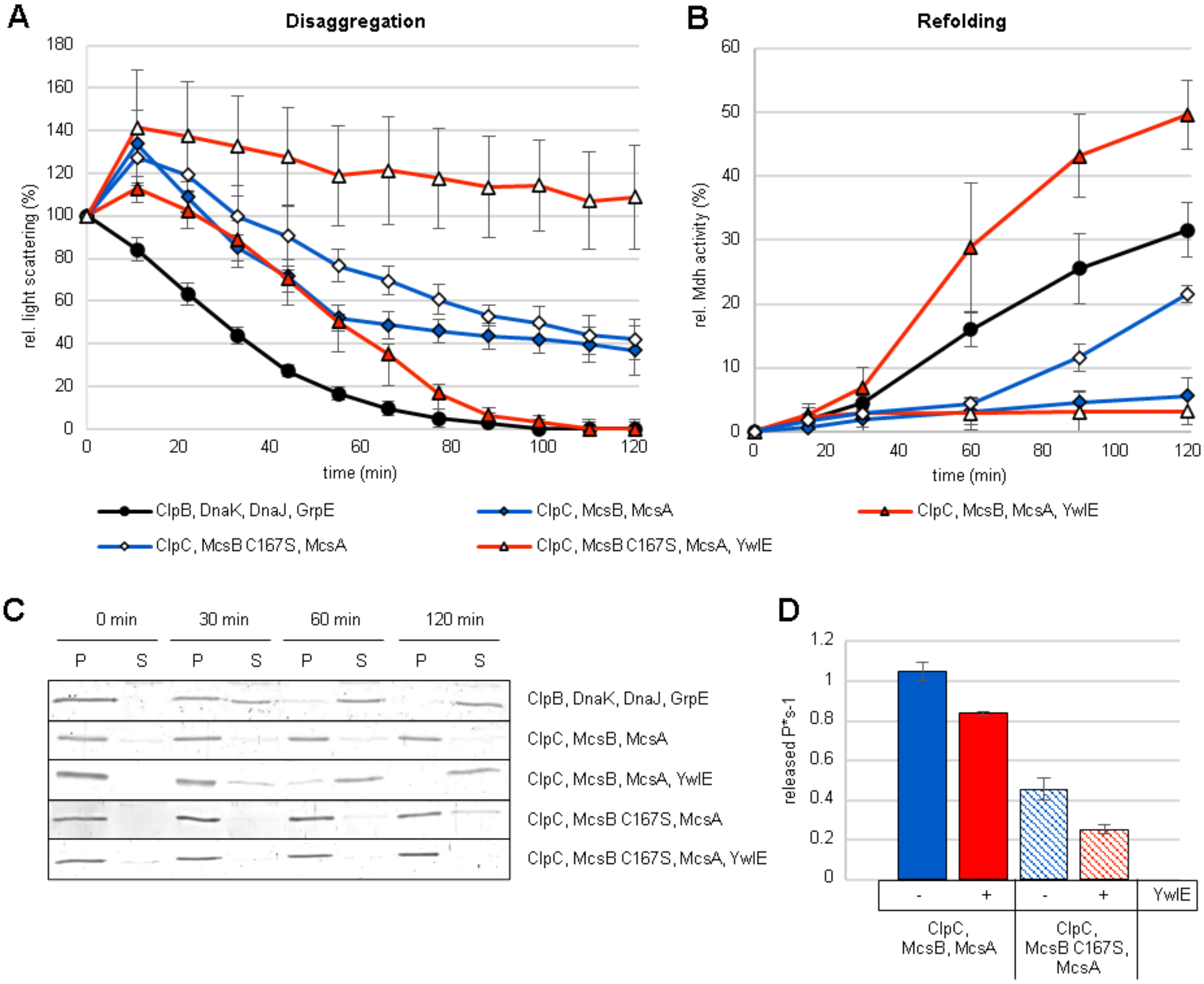

Figure 11 The refolding efficiency increases with kinase inactive McsB C167S/McsA.

(A) Disaggregation of heat aggregated Mdh was monitored with light scattering experiments performed at 30 °C for 120 min. ClpB, DnaK, DnaJ, GrpE (●) served as positive control, ClpC, McsB, McsA (◆), ClpC, McsB C167S, McsA (◇), ClpC, McsB, McsA, YwlE (▲) and ClpC, McsB C167S, McsA, YwlE (△) were compared. (B) The refolding of Mdh was examined by measuring the enzymatic activity at different time points. (C) SDS-PAGE of Mdh in pellet (P) and supernatant (S) fractions at indicated time points. (D) McsB/McsA- and McsB C167S/McsA-induced ClpC ATPase activity in absence (blue) and presence (red) of YwlE determined with Malachite Green assays. Error bars display standard deviations of three replicates.

The activator protein McsA is important for full activation of McsB and subsequent substrate phosphorylation, as well as effective induction of ClpC ATPase or ClpCP degradation activities (Kirstein et al., 2007, 2005). After demonstrating that both, the arginine kinase, and adaptor protein function of McsB are associated to ClpC disaggregation activity, the role of McsA for McsB activation was investigated. Disaggregation and refolding as well as pellet-supernatant experiments revealed that the disaggregation efficiency was highest in the reaction with McsB/McsA-activated ClpC but only 10 % lower without McsA (Figure 12 A, C). Likewise, presence of McsA barely altered the disaggregation efficiency of McsB C167S-activated ClpC (Figure 12 A). However, the previously observed refolding activity of McsB C167S/McsA-activated ClpC was decreased in the absence of McsA, presumably due to the reduced induction of ClpC ATPase activity without McsA (Figure 12 B, D). These experiments indicated that McsA enhanced the McsB-induced ClpC activities, independent of the kinase activity and thus, suggested that besides kinase activation, protein-protein interaction between McsB and McsA might be important for an efficient activation of ClpC.

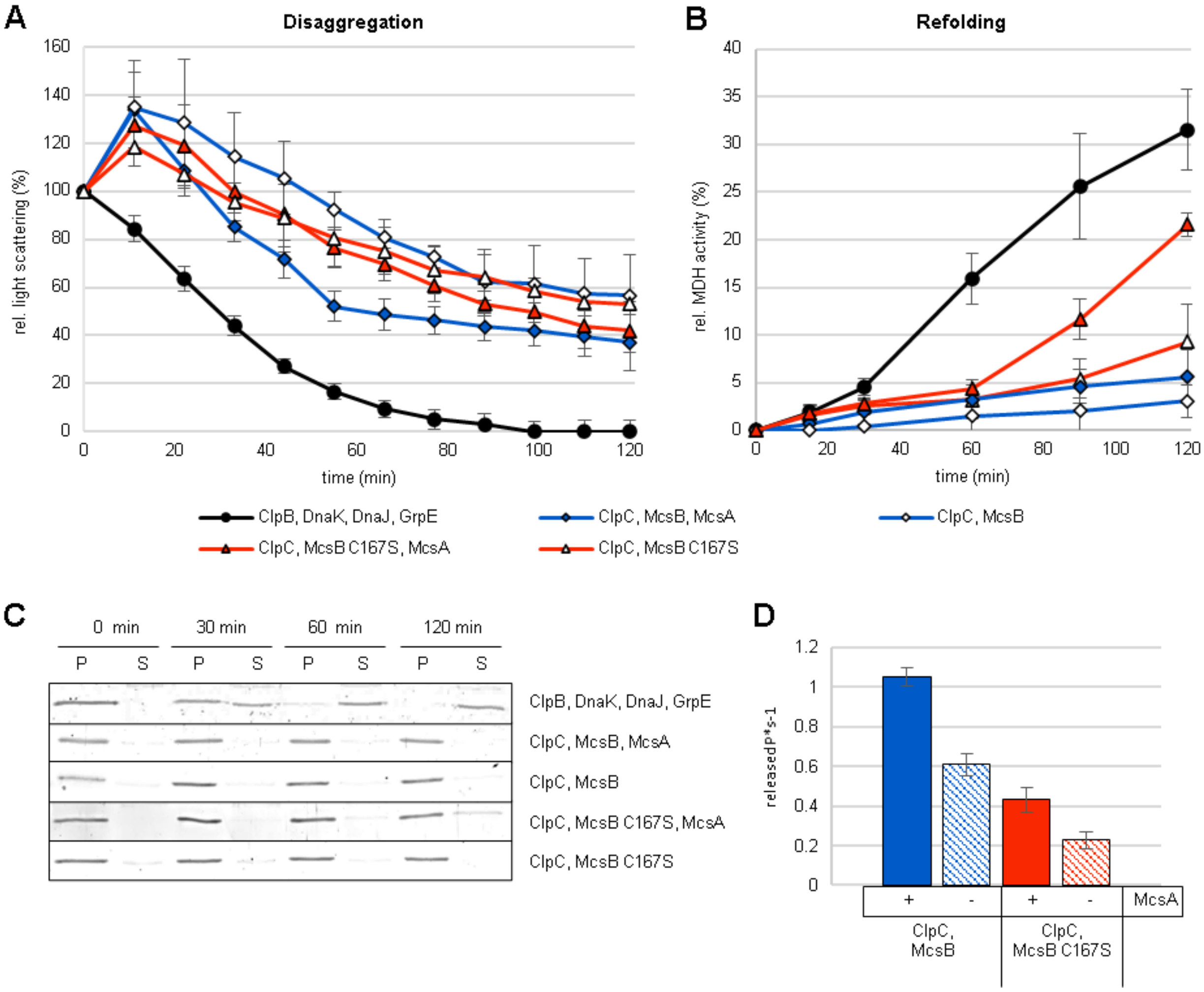

Figure 12 McsA enhances McsB dependent ClpC activities.

(A) Disaggregation of heat aggregated Mdh was monitored with light scattering experiments performed at 30°C for 120 min. ClpB, DnaK, DnaJ, GrpE (●) served as positive control, ClpC, McsB, McsA (◆), ClpC, McsB (◇), ClpC, McsB C167S, McsA (▲) and ClpC, McsB C167S (△) were compared. (B) The refolding of Mdh was examined by measuring the enzymatic activity at different time points. (C) SDS-PAGE of Mdh in pellet (P) and supernatant (S) fractions at indicated time points. (D) McsB- and McsB C167S-induced ClpC ATPase activity in absence and presence of McsA determined in Malachite Green assay. Error bars display standard deviations of three replicates.

After examination of McsB functions, the influence of phosphatase YwlE on ClpC activities was investigated. ClpC ATPase assays revealed that low concentrations of inactive YwlE C7S did not considerably decrease the ClpC activity, compared to active YwlE (Figure 13 D). Addition of the YwlE C7S mutant to McsB/McsA-activated ClpC in the disaggregation assay resulted in a high initial peak, suggesting strong protein complex formation at t_{15} (Figure 13 A). After 120 min 36 % of the Mdh aggregates were dissolved and only 3 % of Mdh were refolded (Figure 13 A, B). Consistently, a notable Mdh shift from pellet to supernatant was only detected in reactions with high disaggregation and refolding efficiencies (Figure 13 C). Since active YwlE was observed to facilitate high refolding activity, these results suggest that the YwlE phosphatase activity is necessary for successful disaggregation and refolding. Additionally, protein-protein interactions might affect the initial complex formation and ClpC dependent disaggregation.

Combination of both inactive mutants McsB C167S and YwlE C7S resulted in a delayed peak in light scattering. After 120 min 44 % of aggregated Mdh was unfolded and 18 % of the initial Mdh activity were recovered (Figure 13 A, B). These observations correspond to prior experiments, suggesting that the kinase activity of McsB interferes with successful substrate refolding and demonstrate that the YwlE phosphatase activity is probably required for efficient disaggregation and refolding, especially in presence of active McsB.

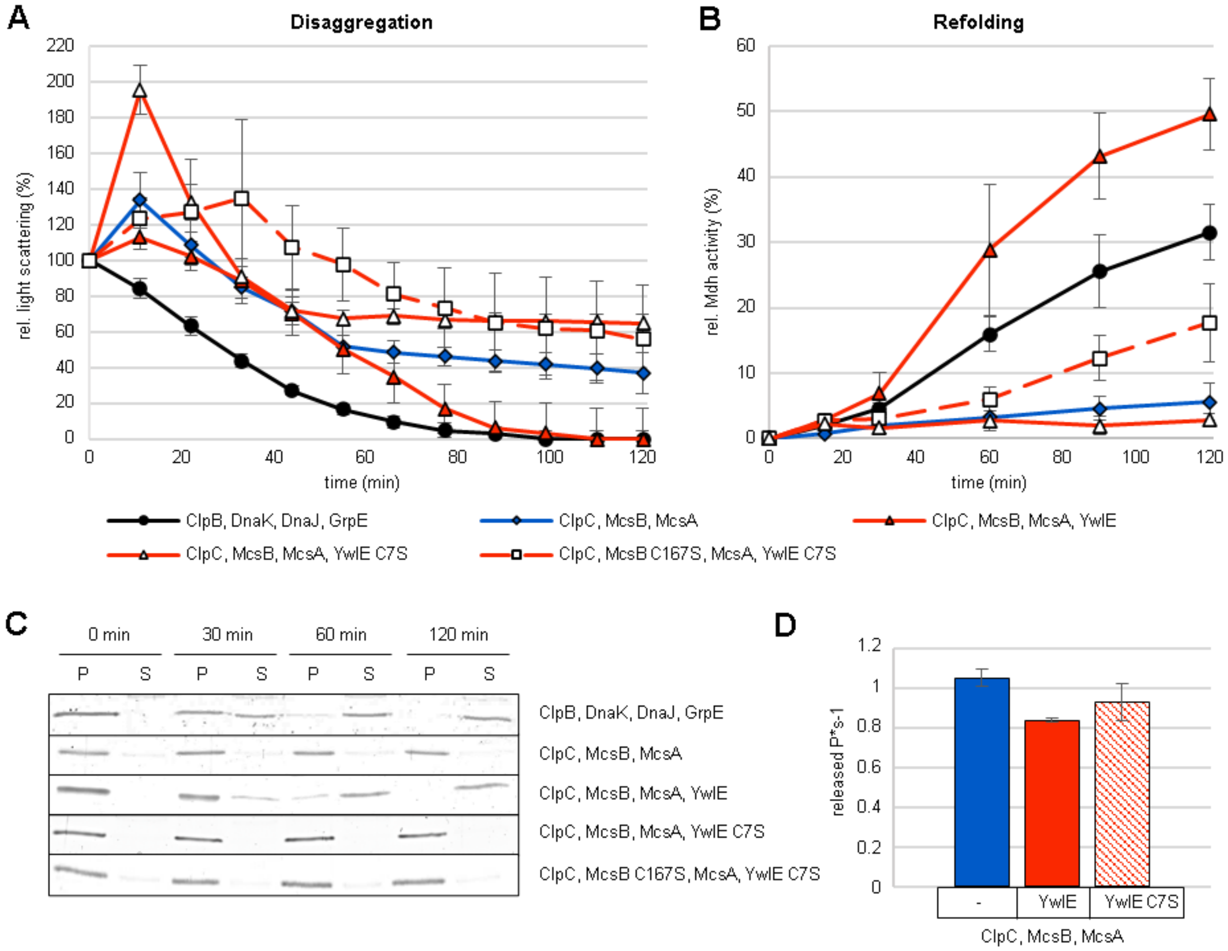

Figure 13 YwlE phosphatase activity is important in presence of active McsB.

(A) Disaggregation of heat aggregated Mdh was monitored with light scattering experiments performed at 30°C for 120 min. ClpB, DnaK, DnaJ, GrpE (●) served as positive control, ClpC, McsB, McsA (◆), ClpC, McsB, McsA, YwlE (▲), ClpC, McsB, McsA, YwlE C7S (△) and ClpC, McsB C167S, McsA, YwlE C7S (□) were compared. (B) The refolding of Mdh was examined by measuring the enzymatic activity at different time points. (C) SDS-PAGE of Mdh in pellet (P) and supernatant (S) fractions at indicated time points. (D) McsB/McsA-induced ClpC ATPase activity with and without YwlE/YwlE C7S determined in Malachite Green assay. Error bars display standard deviations of three replicates.

Protein arginine phosphorylation in the experiments with kinase inactive McsB C167S and phosphatase inactive YwlE C7S was monitored with α-pArg blots (Fuhrmann et al., 2013a; Kirstein et al., 2005). As expected, no phosphorylation was detected in samples with McsB C167S, neither of McsB C167S itself nor of other proteins present in this reaction (Figure 14 A). In contrast to this, strong phosphorylation signals of ClpC, McsB, Mdh and McsA were detected at several time points with YwlE C7S (Figure 14 B). The decrease of detected phosphorylation with incubation time was comparable to the α-pArg blot without YwlE, suggesting that the YwlE C7S mutant did not actively dephosphorylate the substrate, as expected (Figure 10 A).

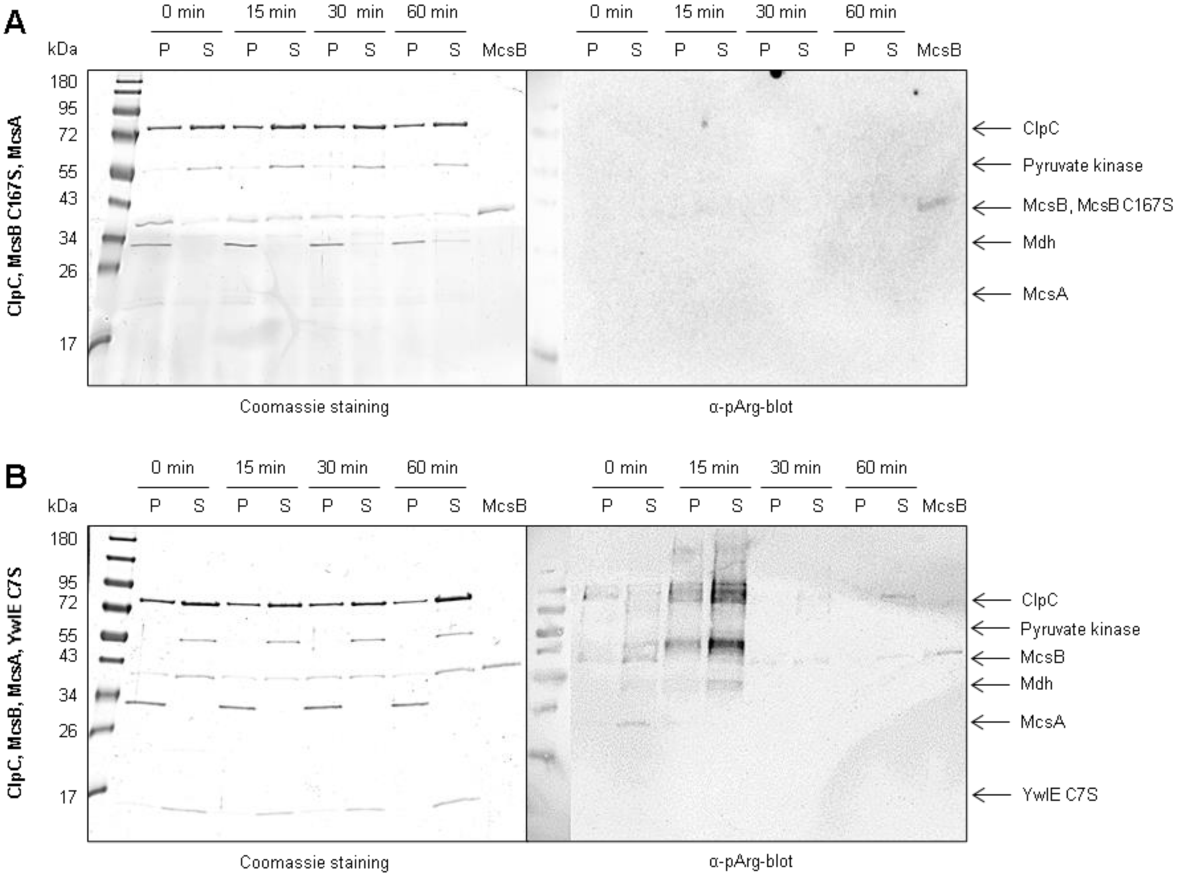
A
0 min
15 min
30 min
60 min
kDa
P S P S P S P S McsB
180
95
72
55
43
34
26
17
ClpC, McsB C167S, McsA
ClpC
Pyruvate kinase
McsB, McsB C167S
Mdh
McsA
Coomassie staining
α-pArg-blot
B
0 min
15 min
30 min
60 min
kDa
P S P S P S P S McsB
180
95
72
55
43
34
26
17
ClpC, McsB, McsA, YwlE C7S
ClpC
Pyruvate kinase
McsB
Mdh
McsA
YwlE C7S
Coomassie staining
α-pArg-blot

Figure 14 Inactive McsB cannot phosphorylate and inactive YwlE cannot dephosphorylate proteins.

Representative SDS-PAGE and western blots of samples from disaggregation experiment taken at indicated time points and divided in pellet (P) and supernatant (S) fractions. On the left, Coomassie staining and on the right western blots with α-pArg antibody (Fuhrman et al) are displayed. ClpC, McsB C167S, McsA (A) and ClpC, McsB, McsA, YwlE C7S (B) were compared with autophosphorylated McsB as positive control for pArg western blots.

3.1.3 Disaggregation and refolding are triggered by McsA activation of McsB kinase

Previous experiments observed that both, the arginine kinase activity of McsB and the phosphatase activity of YwlE are important for successful ClpC dependent disaggregation and refolding of heat induced aggregates. To examine the role of McsB activator McsA in more detail, order-of-addition experiments were performed. Without McsA, only slight disaggregation (12 %) and refolding activity (3 %) was observed in the reaction with ClpC, McsB and YwlE. Subsequently, McsA was added 15 min, 30 min and 60 min after assay start (Figure 15). 15 min after each McsA addition a corresponding peak occurred, suggesting initial protein complex formation (Figure 15 A). The recovery of Mdh activity started approximately 15 min after McsA addition and the refolding kinetics of experiments with McsA addition at different time points were comparable (Figure 15 B). Pre-incubation of ClpC, McsB and YwlE with subsequent addition of McsA was observed to cause steeper disaggregation slopes and facilitated an accelerated start of Mdh recovery. Pellet-supernatant fractionations of these samples were consistent with the light scattering experiments, suggesting that with addition of McsA, the ClpC dependent disaggregation was triggered and Mdh was solubilized (Figure 15 C). This data implies that the ClpC disaggregation and refolding activity is highly dependent on McsA activating the McsB kinase and that addition of McsA can trigger the McsB and YwlE dependent ClpC disaggregation and refolding activity at any time.

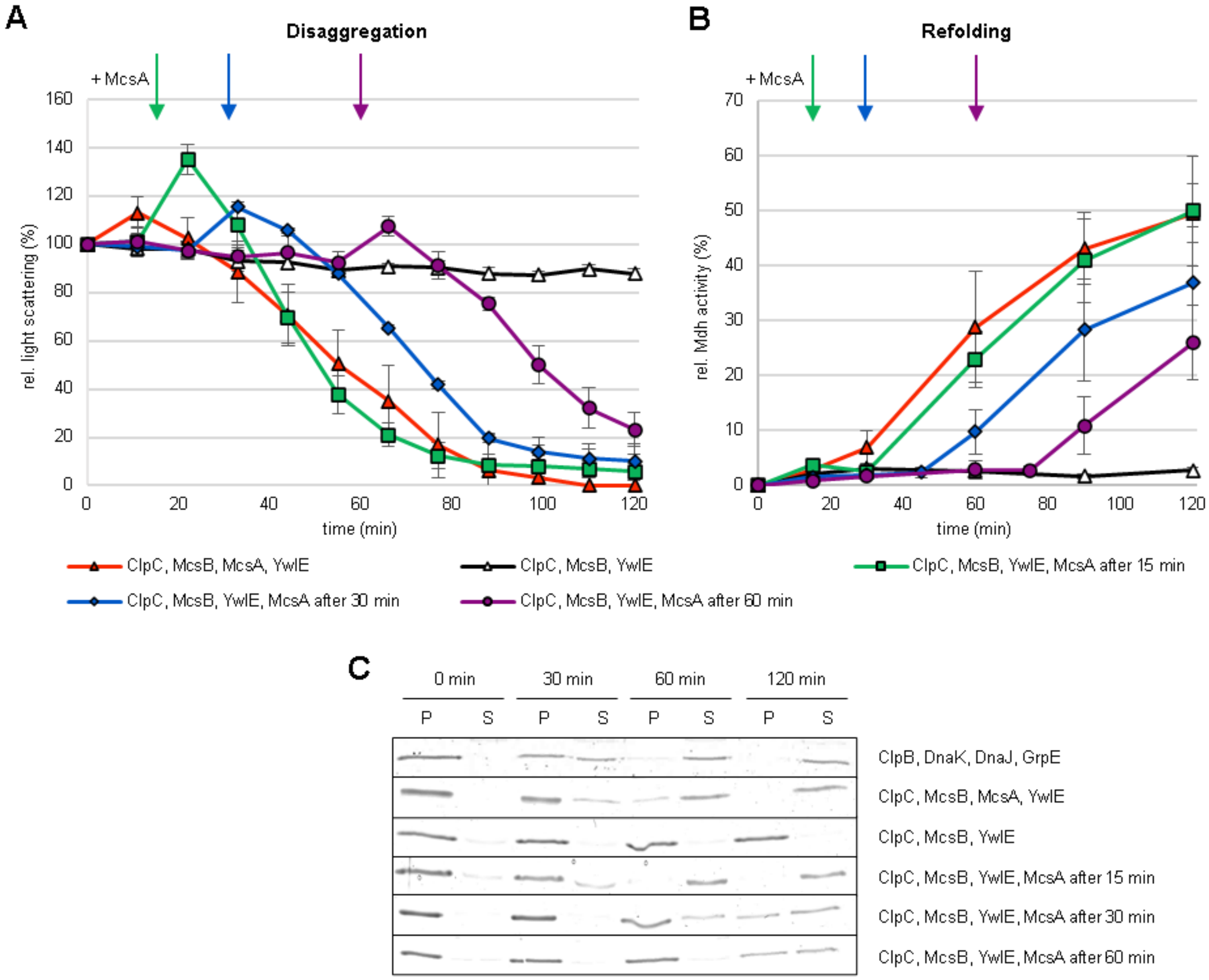

Figure 15 Addition of McsA triggers McsB mediated ClpC disaggregation activity.

Order-of-addition disaggregation and refolding experiment with McsA. (A) Disaggregation of heat aggregated Mdh was monitored with light scattering experiments performed at 30°C for 120 min. ClpC, McsB, YwlE reaction without McsA (△) or with addition of McsA after 0 min (▲), 15 min (■), 30 min (◆), 60 min (●). (B) The refolding of Mdh was examined by measuring the enzymatic activity at different time points. Error bars display standard deviations of three replicates. (C) SDS-PAGE of Mdh in pellet (P) and supernatant (S) fractions at indicated time points.

To examine the arginine phosphorylation status in the McsA order-of-addition experiment, α-pArg blots were performed. Since YwlE was already demonstrated to be a potent phosphatase, samples were taken before and 5 min after addition of McsA (Figure 10/Figure 16). In all experiments no phosphorylation signal was observed before addition of McsA, suggesting that in presence of YwlE the autophosphorylation activity of McsB was not sufficient to obtain detection of phosphorylation (Figure 16 A, B, C). Upon addition of McsA at t_{15}, the McsB kinase was activated and after 5 min ClpC, McsB and McsA were phosphorylated, but after 60 min no phosphorylation signal was visible anymore (Figure 16 A). A similar pattern was observed upon addition of McsA at t_{30} and t_{60}, since phosphorylation of ClpC, McsB and McsA was detected after 5 min (Figure 16 B, C). However, YwlE did not dephosphorylate all protein as rapidly as observed in previous experiments and with McsA addition at t_{30} the phosphorylation signal was still visible after 60 min of incubation (Figure 10). It is possible that due to long incubation without McsA activating McsB, the YwlE phosphatase activity was hindered and weak oligomerizations leading to inactivation took place, as already described for YwlE and other cognate phosphatases (Blobel et al., 2009). In contrast to previous experiments without YwlE, phosphorylation of the substrate Mdh could not be observed in any reaction (Figure 10/Figure 14). This might be an indication that the earlier detected McsB dependent phosphorylation of soluble Mdh is quickly dephosphorylated in presence of YwlE phosphatase and may enable the observed refolding activity.

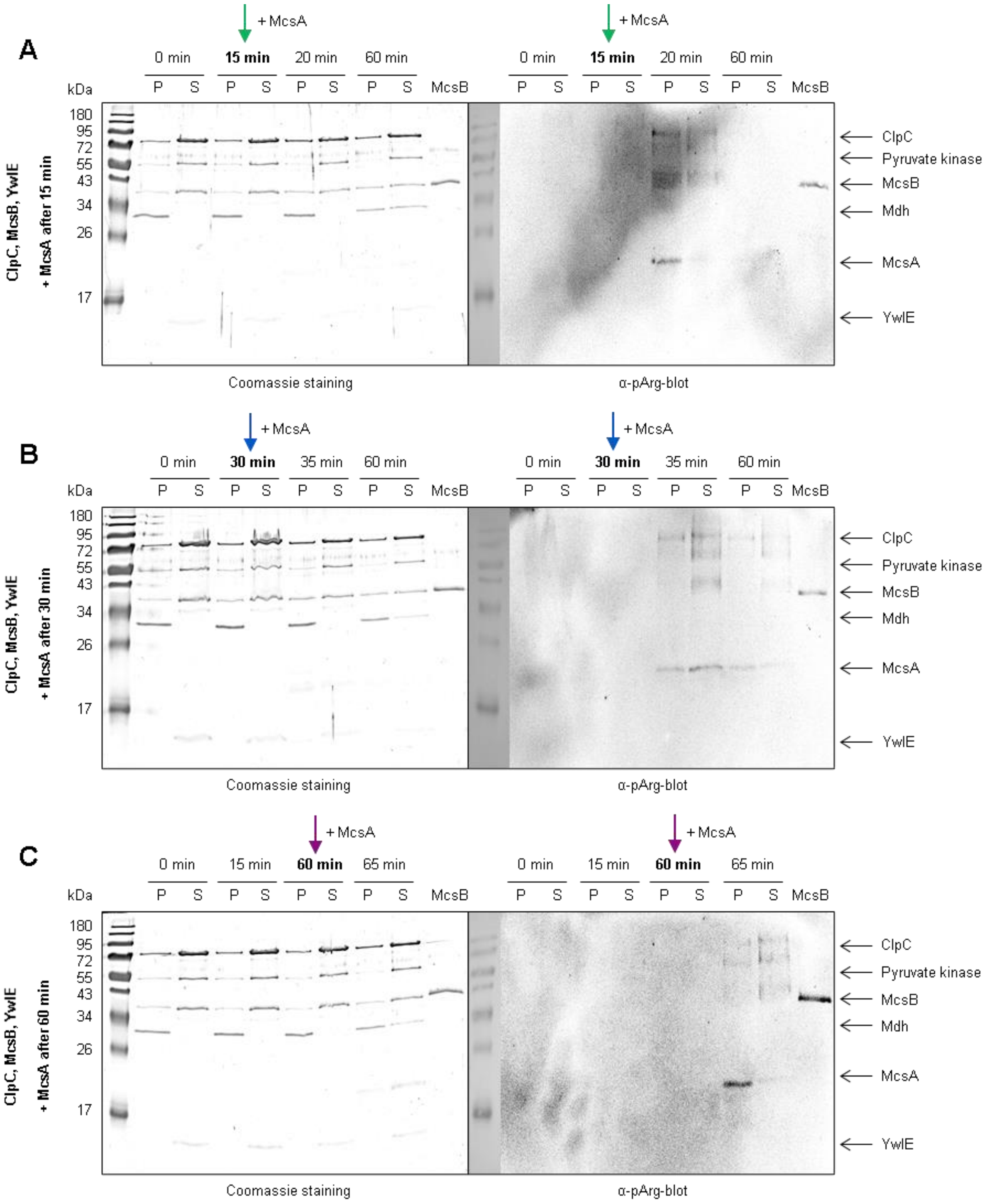
A
+ McsA
0 min
15 min
20 min
60 min
P S P S P S P S McsB
kDa
180
95
72
55
43
34
26
17
ClpC, McsB, YwlE
+ McsA after 15 min
Coomassie staining
α-pArg-blot
ClpC
Pyruvate kinase
McsB
Mdh
McsA
YwlE
B
+ McsA
0 min
30 min
35 min
60 min
P S P S P S P S McsB
ClpC, McsB, YwlE
+ McsA after 30 min
Coomassie staining
α-pArg-blot
C
+ McsA
0 min
15 min
60 min
65 min
P S P S P S P S McsB
ClpC, McsB, YwlE
+ McsA after 60 min
Coomassie staining
α-pArg-blot

Figure 16 McsA addition activates McsB kinase at various time points.

Representative SDS-PAGE and western blots of samples from McsA order-of-addition experiment taken at indicated time points and divided in pellet (P) and supernatant (S) fractions. On the left, Coomassie staining and on the right western blots with α-pArg antibody are displayed (Fuhrman et al). ClpC, McsB, YwlE with McsA addition after 15 min (A), 30 min (B) and 60 min (C). Autophosphorylated McsB served as positive control for pArg western blots.

3.1.4 The influence of YwlE depends on protein dephosphorylation

Knowing, that addition of McsA could trigger the ClpC disaggregation and refolding activity at any point of time, comparable order-of-addition experiments were performed with YwlE. Consistent with previous observations, a high peak occurred after 15 min, indicating possible protein accumulation in absence of YwlE (Figure 9/Figure 17 A). Notably, full aggregate removal was only possible in the reaction with YwlE initially present. Delayed addition of YwlE at t_{15}, t_{30} or t_{60} led to a decrease in disaggregation efficiency from 76 % to 46 % or 44 %, respectively (Figure 17 A). The refolding efficiency was observed to be related to the disaggregation activity and highest Mdh recovery occurred in the reaction with YwlE present from the beginning (Figure 17 B). With decreasing disaggregation activity upon late addition of YwlE, the Mdh recovery was reduced. The pellet-supernatant fractionation was consistent with these observations, since absence or late addition of YwlE did not result in a shift of aggregated Mdh from the pellet to the supernatant fraction (Figure 17 C). Thus, compared to experiments with McsA, addition of the phosphatase YwlE did not trigger full ClpC dependent disaggregation and refolding activity at any point of time (Figure 16). On the contrary, initial presence of YwlE in the reaction was observed to be necessary for efficient aggregate removal and substrate recovery.

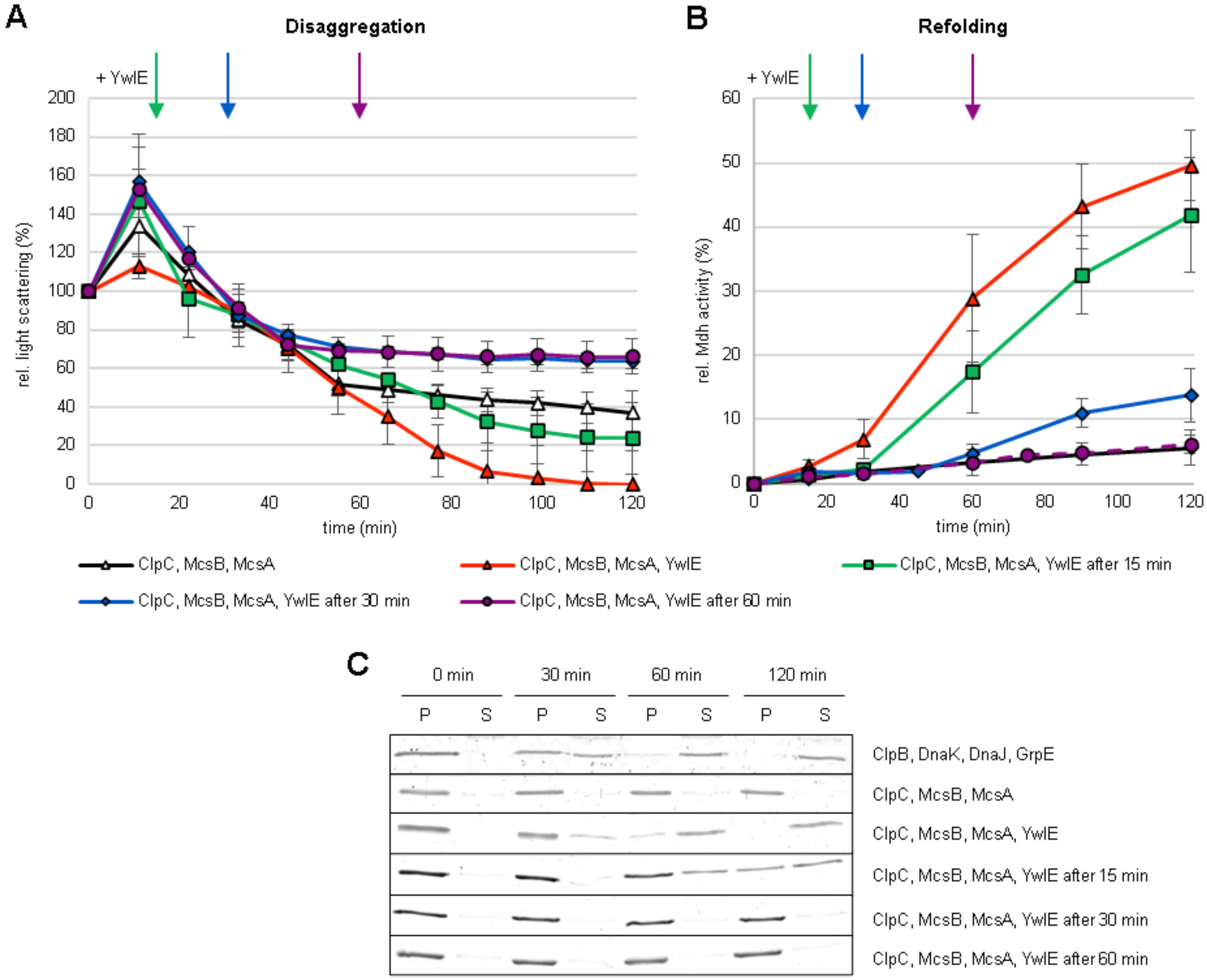

Figure 17 Early presence of YwlE is important for ClpC mediated disaggregation and refolding.

Order-of-addition disaggregation and refolding experiment with YwlE. (A) Disaggregation of heat aggregated Mdh was monitored with light scattering experiments performed at 30°C for 120 min. ClpC, McsB, McsA reaction without YwlE (△) or with addition of YwlE after 0 min (▲), 15 min (🟩), 30 min (◆), 60 min (●). (B) The refolding of Mdh was examined by measuring the enzymatic activity at different time points. Error bars display standard deviations of three replicates. (C) SDS-PAGE of Mdh in pellet (P) and supernatant (S) fractions at indicated time points.

To examine, whether the observed effects are connected to arginine phosphorylation and subsequent dephosphorylation events, α-pArg blots of the order-of-addition experiments were performed. Similar to previous experiments, phosphorylation signals of ClpC, McsB, Mdh and McsA were detected after 0 min and 15 min for all samples, whereas signals after 15 min were notably stronger in the supernatant fractions (Figure 10/Figure 18 A, B, C). As expected, addition of YwlE at t_{15} resulted in vanishing of every signal except for a slight ClpC phosphorylation band in the pellet fraction after 20 min (Figure 18 A). Phosphorylation of McsB and ClpC was observed 30 min after assay start, but with addition of YwlE no more bands were detectable (Figure 18 B). The initial signal of ClpC and McsB phosphorylation after 60 min was lower than after 30 min and disappeared completely after YwlE addition (Figure 18 C).

These experiments suggest that YwlE is a potent phosphatase, since even low concentrations could dephosphorylate nearly every detectable phosphorylation in 5 min. Comparison of the disaggregation and refolding experiments with the α-pArg blots revealed a possible connection between the efficiency of refolding upon YwlE addition and the level of initial arginine phosphorylation in the sample (Figure 17, Figure 18). These observations imply that a successful disaggregation and refolding might be directly related to the dephosphorylation of proteins by YwlE.

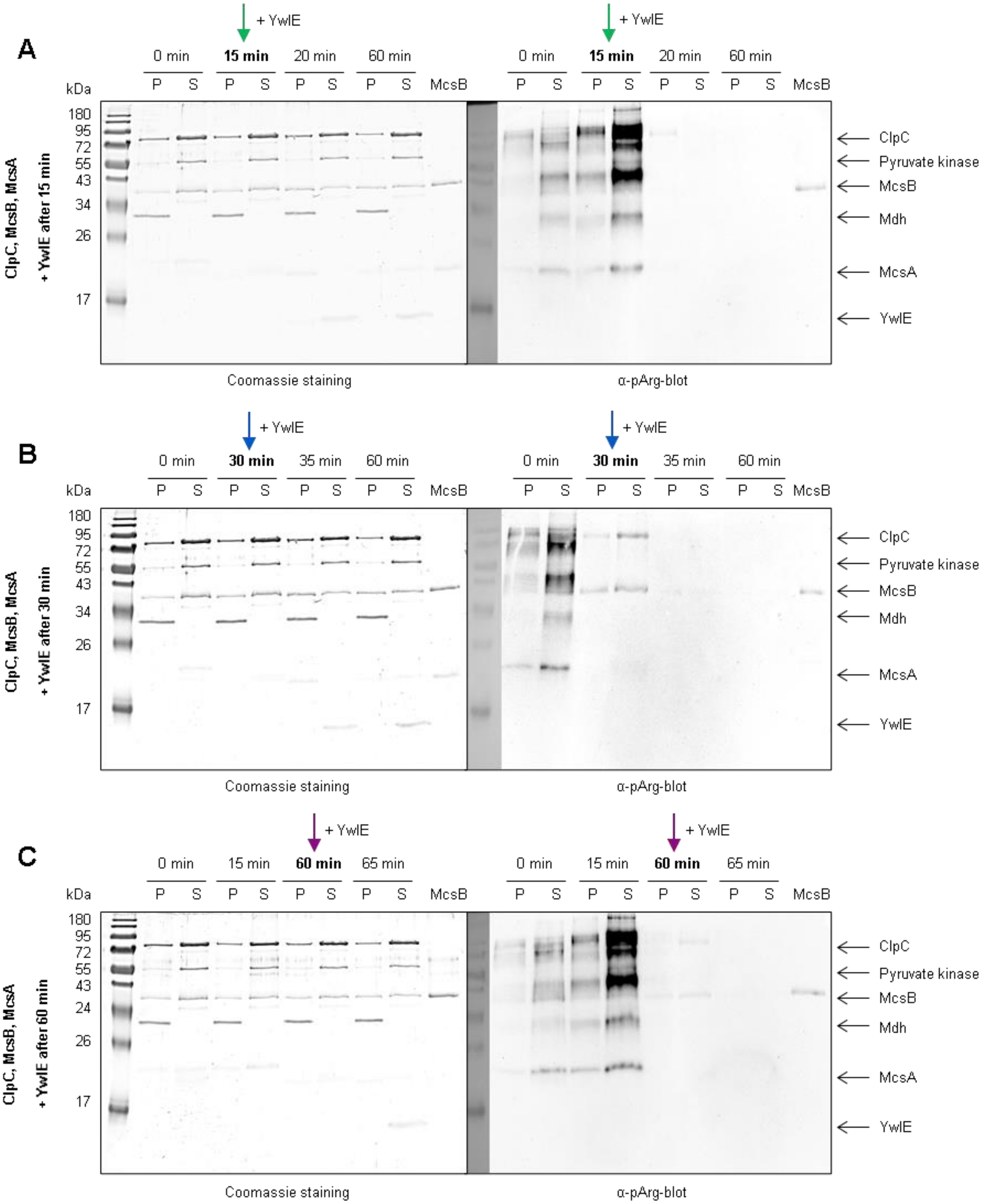
A
+ YwlE
0 min
15 min
20 min
60 min
P S P S P S P S McsB
kDa
180
95
72
55
43
34
26
17
ClpC, McsB, McsA
+ YwlE after 15 min
Coomassie staining
α-pArg-blot
ClpC
Pyruvate kinase
McsB
Mdh
McsA
YwlE
B
+ YwlE
0 min
30 min
35 min
60 min
ClpC, McsB, McsA
+ YwlE after 30 min
C
+ YwlE
0 min
15 min
60 min
65 min
24
ClpC, McsB, McsA
+ YwlE after 60 min

Figure 18 Addition of YwlE dephosphorylates proteins at various time points.

Representative SDS-PAGE and western blots of samples from YwlE order-of-addition experiment taken at indicated time points and divided in pellet (P) and supernatant (S) fractions. On the left, Coomassie staining and on the right western blots with α-pArg antibody are displayed (Fuhrman et al). ClpC, McsB, McsA with YwlE addition after 15 min (A), 30 min (B) and 60 min (C). Autophosphorylated McsB served as positive control for pArg western blots.

3.1.5 The phosphatase YwlE assists protein refolding

Disaggregation and refolding of heat induced aggregates by chaperones is often achieved by several binding, pulling and release cycles, only partially unfolding the substrate, as described for the *E. coli* ClpB/KJE system (Haslberger et al., 2008; Li et al., 2015). However, characterization of the ClpC based system indicated a unique operation principle, dependent on McsB kinase and YwlE phosphatase activities. It was assumed that McsB phosphorylates and targets substrate for ClpC dependent disaggregation and consistent with this, the highest substrate phosphorylation was observed after disaggregation (Figure 10). Since the reaction without YwlE led to poor refolding activities and application of a kinase inactive McsB mutant could trigger moderate refolding, it was hypothesized that arginine phosphorylation might prevent successful refolding of the disaggregated substrate. In the proposed model YwlE serves as refolding assistant, possibly facilitating refolding events by controlled dephosphorylation of unfolded substrate.

To test this hypothesis, a special disaggregation and refolding experiment was set up. The idea was to first allow phosphorylation and targeting of Mdh by McsB/McsA for ClpC dependent disaggregation. It was presumed that after 15 min ample amounts of substrate protein were unfolded and phosphorylated. Then, the ClpC DWB trap mutant, with impaired ATPase activity, was added to halt ClpC disaggregation by formation of inactive, mixed oligomers, comparably described for a ClpB mutant in *E. coli* (Kirstein et al., 2006; Mogk et al., 2003c; Weibezahn et al., 2003). Subsequent addition of YwlE was assumed to trigger refolding by dephosphorylation of the previously disaggregated, phosphorylated substrate.

To ensure that the concentration of added ClpC DWB was high enough to prevent further disaggregation, the ClpC ATPase activity was measured without YwlE, with YwlE and with inactive YwlE C7S. ClpC DWB was added in concentrations from 1.5 µM to 0.1 µM to the reaction (Figure 19). Notably, even the addition of 1.5 µM ClpC DWB resulted in 28 % of remaining activity and no complete inhibition of the ClpC ATPase activity was achieved. The presence of both ClpC DWB and YwlE strongly restricted the ClpC ATPase activity, dependent on the YwlE phosphatase activity.

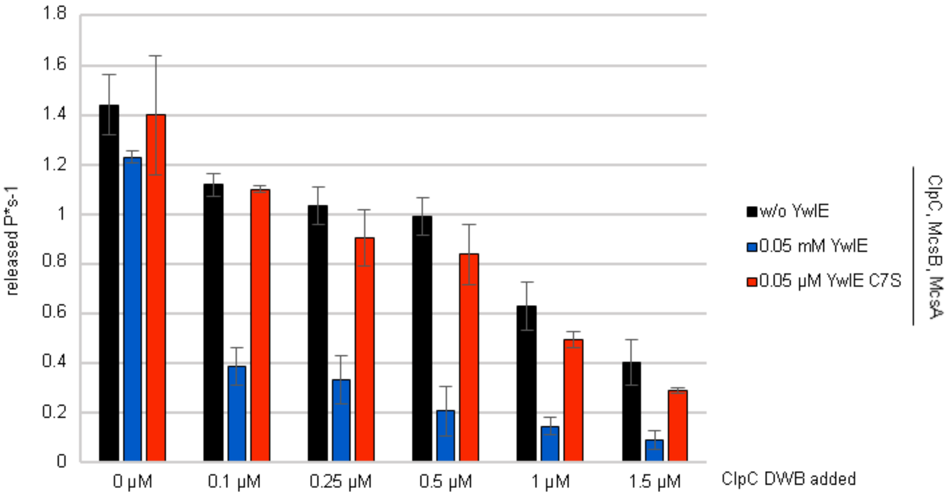

Figure 19 Addition of ClpC DWB decreases the ATPase activity.

ClpC (1.5 µM) ATPase activity with McsB (1 µM), McsA (1 µM) without YwlE (black), with 0.05 µM YwlE (red) and 0.05 µM YwlE C7S (blue) determined with Malachite Green assay. The ClpC DWB trap mutant was added in indicated concentrations. Error bars display standard deviations of three replicates.

The addition of 0.25 µM ClpC DWB to the light scattering and refolding experiment at t_{15} resulted in an extended initial peak, suggesting only slowly dispersing complex formation with mixed ClpC oligomers (Figure 20 A). The curve stayed stable after 55 min with 22 % of aggregates dissolved. Furthermore, no refolding of Mdh occurred, comparably observed in the reaction with simultaneous addition of ClpC DWB and inactive YwlE C7S (Figure 20 A, B). Addition of ClpC DWB and active YwlE at t_{15} or t_{20} led to a quick disruption of the initial protein accumulation, implying that active YwlE might disturb the stable complex formation of the substrate and McsB/McsA-activated ClpC. Remarkably, addition of active YwlE at t_{15} led to a rescue of 15 % Mdh activity. The decreased Mdh recovery upon late YwlE addition at t_{20} might be due to the decreasing phosphorylation levels with extended incubation time and thus, possibly less substrate for YwlE to act on. The pellet-supernatant fractionations displayed no evident Mdh shift from pellet to supernatant, consistent with the observed low disaggregation and refolding activity (Figure 20 C). Hence, this data supports the suggested model in that controlled YwlE dependent dephosphorylation might facilitate refolding of previously phosphorylated and unfolded substrate proteins.

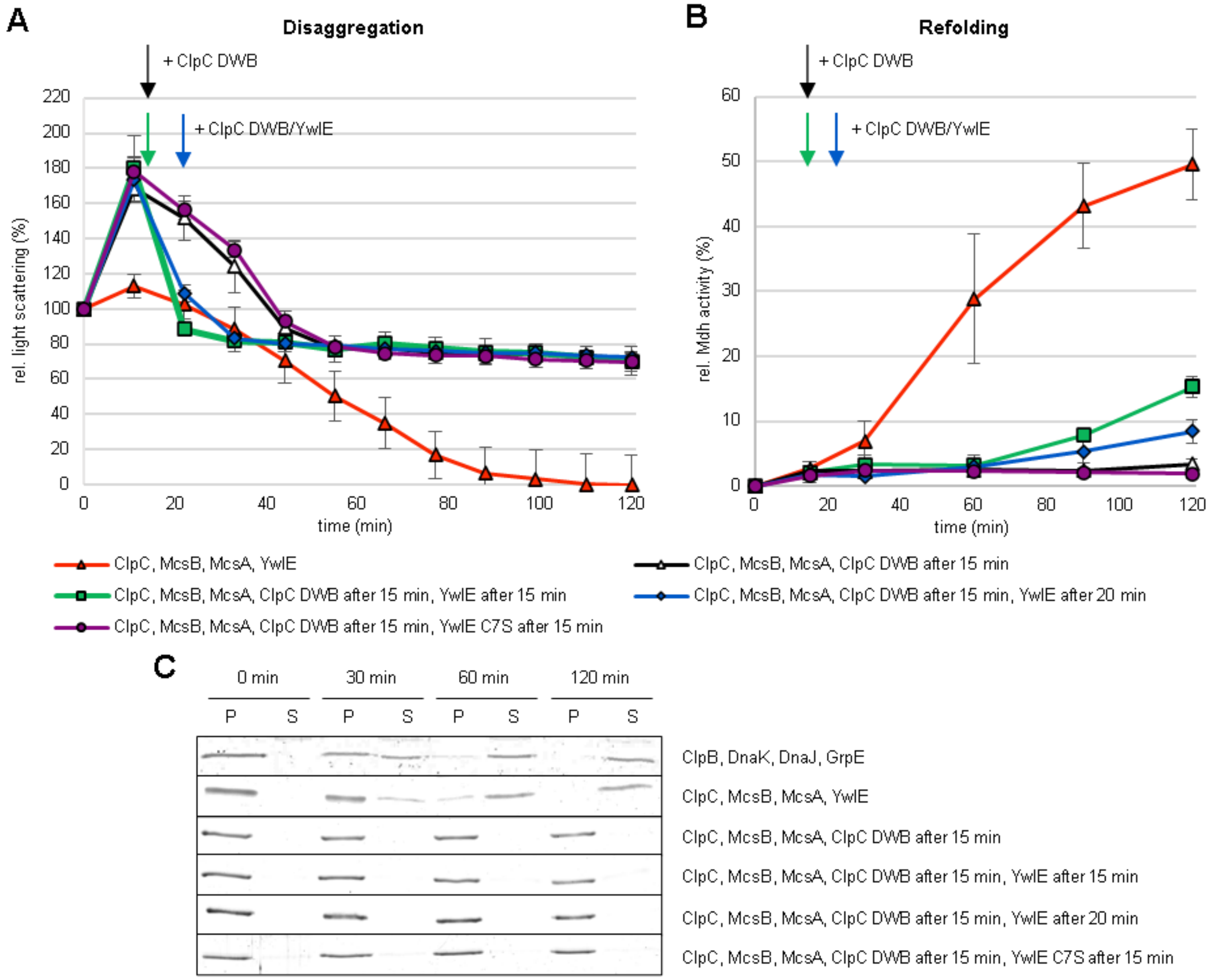

Figure 20 Addition of ClpC DWB stops disaggregation and YwlE assists substrate refolding.

(A) Disaggregation of heat aggregated Mdh was monitored with light scattering experiments performed at 30°C for 120 min. ClpC, McsB, McsA reactions with addition of ClpC DWB after 15 min (△) and YwlE after 15 min (■), after 20 min (◆) or YwlE C7S after 15 min (●) were compared to positive control ClpC, McsB, McsA, YwlE (▲). (B) The refolding of Mdh was examined by measuring the enzymatic activity at different time points. Error bars display standard deviations of three replicates. (C) SDS-PAGE of Mdh in pellet (P) and supernatant (S) fractions at indicated time points.

3.2 Protein refolding or degradation with the protease complex ClpCP

B. subtilis ClpC can form a protease complex with ClpP (ClpCP) and unfolded substrate proteins are transferred to the associated protease for degradation. Therefore, ClpC can contribute to both, substrate rescue and degradation. Experiments including the protease ClpP were performed to assess how these at first glance opposing activities are compatible with each other.

Upon addition of ClpP to McsB/McsA-activated ClpC, the expected ClpCP protease complex formed and the substrate Mdh was disaggregated and mostly degraded (Figure 21). The SDS-

PAGE analysis of the pellet-supernatant fractions supported this, because only a slight Mdh band remained in the supernatant fraction after 120 min (Figure 21 C). Notably, not all disaggregated substrate was degraded but 13 % of Mdh activity were recovered (Figure 21 B). Hence, while disaggregation took place, a fraction of substrate protein escaped the transfer to ClpP for degradation and was refolded instead. This might be facilitated by specific properties of the ClpCP interaction and the observed increased disaggregation rate allowing full aggregate removal in presence of ClpP.

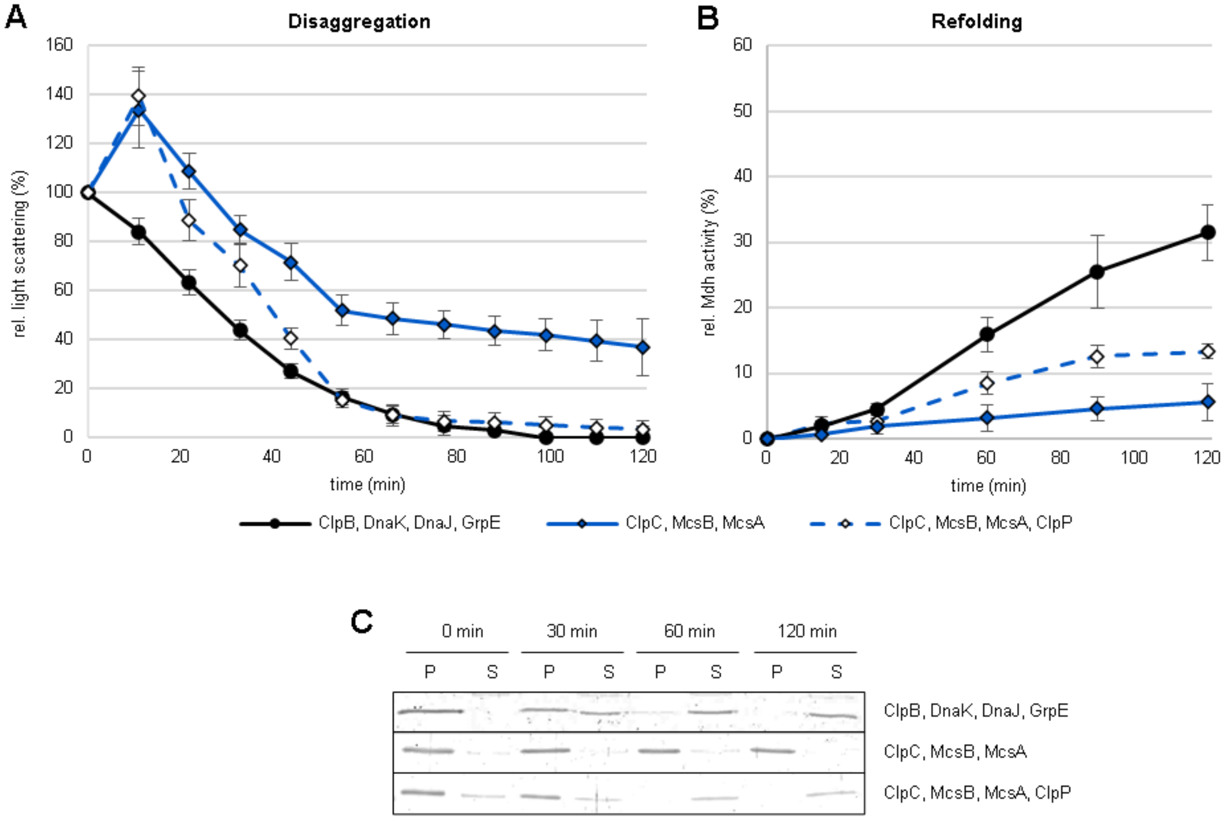

Figure 21 ClpP improves the refolding efficiency of McsB/McsA-activated ClpC.

(A) Disaggregation of heat aggregated Mdh was monitored with light scattering experiments performed at 30°C for 120 min. ClpB, DnaK, DnaJ, GrpE (●) served as positive control, ClpC, McsB, McsA (◆) and ClpC, McsB, McsA, ClpP (◇) were compared. (B) The refolding of Mdh was examined by measuring the enzymatic activity at different time points. Error bars display standard deviations of three replicates. (C) SDS-PAGE of Mdh in pellet (P) and supernatant (S) fractions at indicated time points.

3.2.1 Active YwlE enables substrate refolding rather than degradation by ClpCP

To study the impact of YwlE on ClpCP degradation activity, experiments with addition of the phosphatase were performed. The disaggregation kinetics of McsB/McsA-activated ClpCP without and with YwlE were similar, but a high Mdh refolding activity was observed with YwlE present.

Here, 44 % of the initial Mdh activity were recovered, which was comparable to the efficiency of the experiment without ClpP (Figure 22 A, B). The pellet-supernatant fractionation displayed a Mdh shift from pellet to supernatant, consistent with the disaggregation curves. Notably, with YwlE and ClpP present, substrate disaggregation and refolding were favored instead of substrate degradation (Figure 22 B, C). These experiments suggest that the phosphatase YwlE facilitated refolding even in presence of ClpP and the ClpCP degradation activity appeared to be impaired.

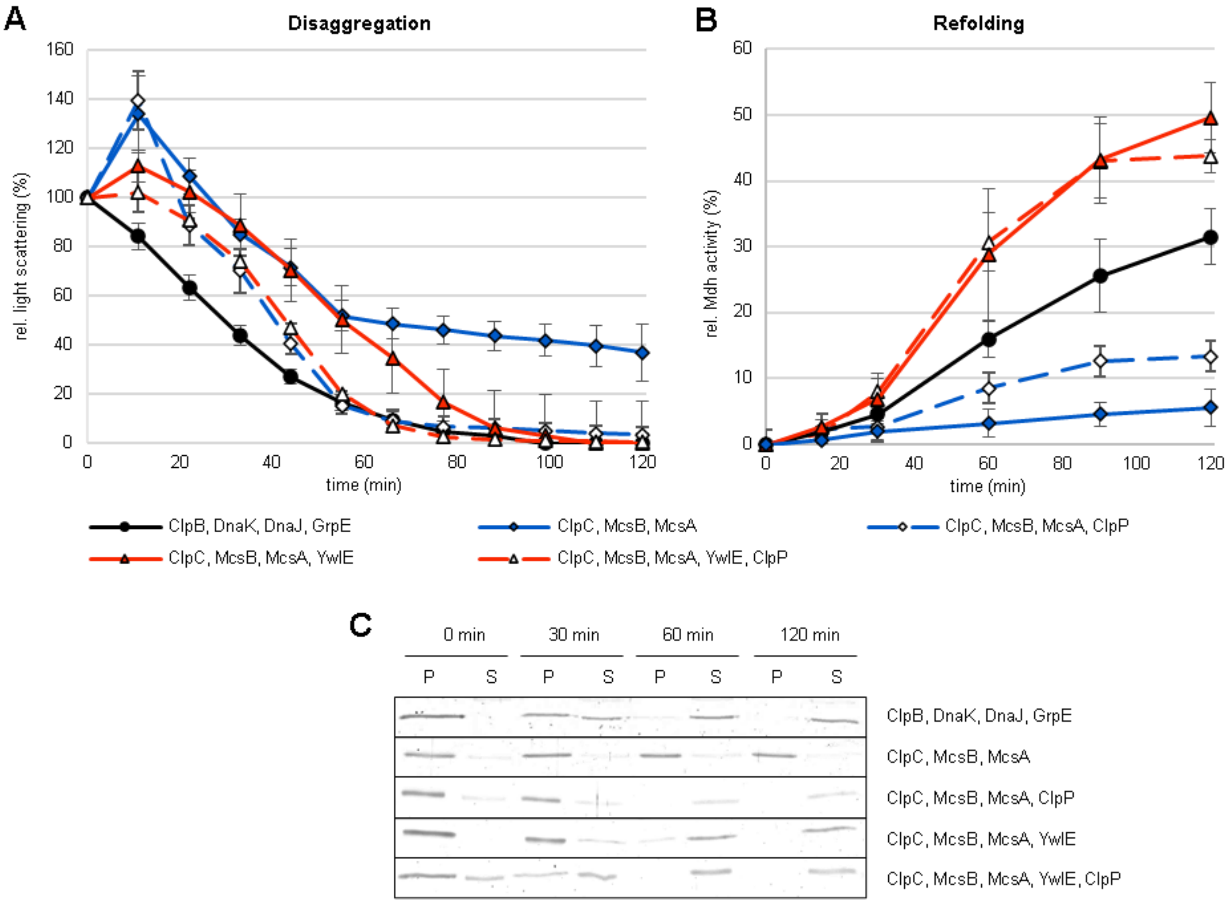

Figure 22 YwlE facilitates refolding despite presence of protease ClpP.

(A) Disaggregation of heat aggregated Mdh was monitored with light scattering experiments performed at 30°C for 120 min. ClpB, DnaK, DnaJ, GrpE (●) served as positive control, ClpC, McsB, McsA (◆), ClpC, McsB, McsA, ClpP (◇), ClpC, McsB, McsA, YwlE (▲) and ClpC, McsB, McsA, YwlE, ClpP (△) were compared. (B) The refolding of Mdh was examined by measuring the enzymatic activity at different time points. Error bars display standard deviations of three replicates. (C) SDS-PAGE of Mdh in pellet (P) and supernatant (S) fractions at indicated time points.

The inactive mutant YwlE C7S was utilized to examine, whether the observed refolding activity in presence of ClpP is connected to the YwlE phosphatase activity. Consistent with previous experiments, an increased initial complex formation was observed in presence of YwlE C7S, with and without ClpP (Figure 13 A/Figure 23 A). Although the ClpP addition slightly increased the disaggregation efficiency, no complete aggregate removal was possible in presence of the phosphatase inactive YwlE C7S mutant. The refolding activity of McsB/McsA-activated ClpCP was not affected by addition of YwlE C7S, suggesting that the phosphatase inactive mutant only affected the disaggregation activity (Figure 23 B). As anticipated, the only partial Mdh degradation and a slight shift to the supernatant occurred (Figure 23 C).

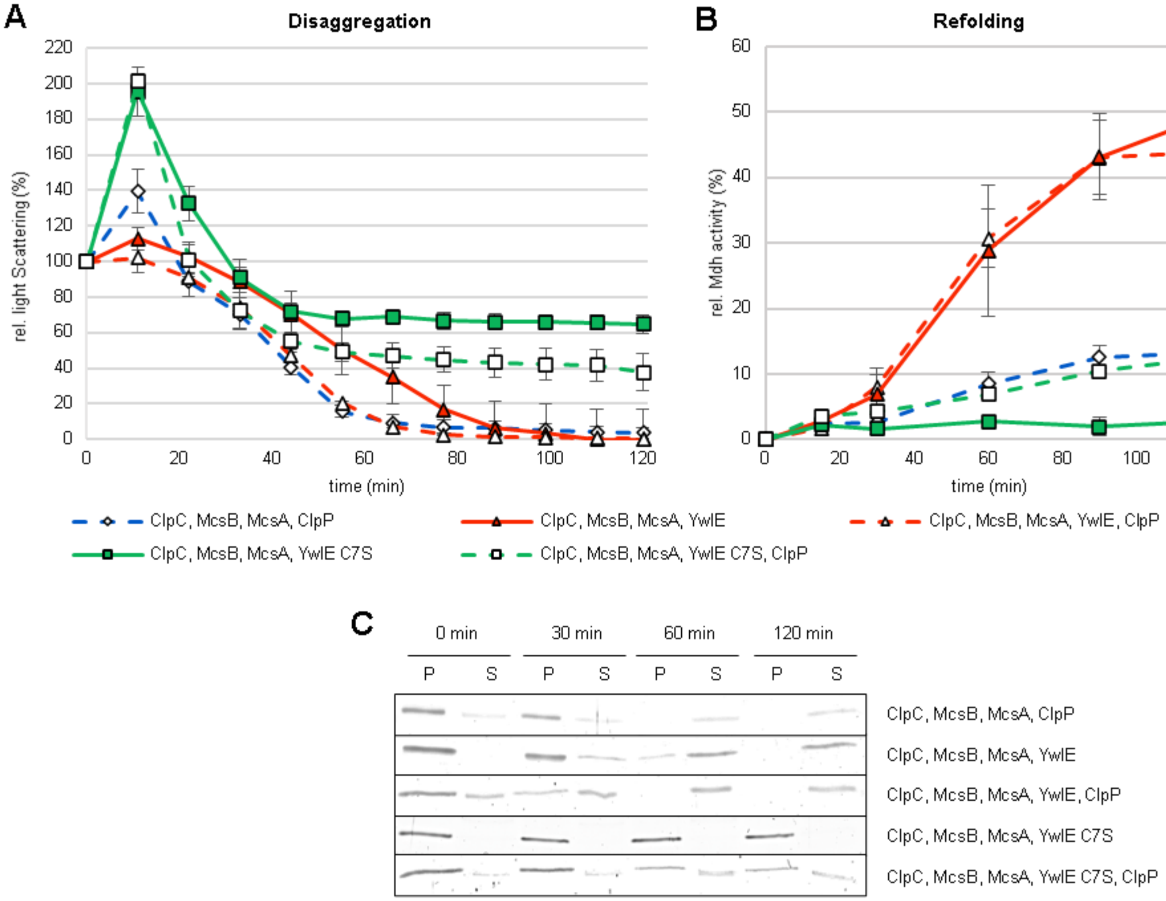

Figure 23 YwlE C7S affects substrate disaggregation.

(A) Disaggregation of heat aggregated Mdh was monitored with light scattering experiments performed at 30°C for 120 min. ClpC, McsB, McsA, ClpP (◇), ClpC, McsB, McsA, YwlE (▲), ClpC, McsB, McsA, YwlE, ClpP (△), ClpC, McsB, McsA, YwlE C7S (🟩) and ClpC, McsB, McsA, YwlE C7S, ClpP (□) were compared. (B) The refolding of Mdh was examined by measuring the enzymatic activity at different time points. Error bars display standard deviations of three replicates. (C) SDS-PAGE of Mdh in pellet (P) and supernatant (S) fractions at indicated time points.

It is known that high ATPase rates and fast substrate translocation can promote an efficient substrate degradation by AAA+ proteases, like ClpXP from *E. coli* (Martin et al., 2008). Therefore, the impact of ClpP on the ClpC ATPase activity was determined and degradation assays were performed to monitor the exact influence of YwlE on ClpCP degradation activity. α-pArg blots with YwlE and inactive YwlE C7S monitored the protein arginine phosphorylation during the degradation reactions.

The presence of ClpP increased the ATPase activity of McsB/McsA-activated ClpC, with and without YwlE, as indicated by previous studies (Figure 24 A) (Turgay et al., 1998). This enhanced activity might be linked to the observed improved disaggregation and refolding activity (Figure 22). Furthermore, the degradation of β-casein by ClpCP was examined with different adaptor proteins and with addition of YwlE or phosphatase inactive YwlE C7S (Figure 24 B). The MecA-induced ClpCP degradation efficiency was not affected by presence of active or inactive YwlE. However, with adaptor protein McsB/McsA a total of 82.3 % β-casein were degraded by ClpCP. In presence of active YwlE, the ClpCP activity was strongly decreased and only 42.7 % β-casein were degraded. This constraining impact was relieved with phosphatase inactive YwlE C7S and 71.5 % β-casein were degraded, suggesting that the influence of YwlE on McsB/McsA-induced ClpCP degradation activity mainly depends on the phosphatase activity. Consistent with this, previous studies demonstrated that high concentrations of active YwlE exceedingly impair McsB/McsA-induced ClpC ATPase activity and stabilize McsB in a degradation assay (Kirstein et al., 2007). The data obtained in this work indicates that low concentrations of YwlE relieve most of the inhibitory impact on McsB/McsA-induced ClpC ATPase activity but still interfere with degradation of substrates by ClpCP (Figure 9/Figure 24). These observations suggest that YwlE might play a role in the decision between substrate refolding or degradation by McsB/McsA-activated ClpCP.

As expected, no phosphorylation signal was detected in presence of active YwlE in the α-pArg blots (Figure 24 C). With the phosphatase inactive mutant YwlE C7S a phosphorylation signal was detected at every sampled time point, comparable to the experiment without YwlE (Figure 10). At t_0 all proteins in the reaction, except for YwlE C7S, were phosphorylated. The signal intensity increased after incubation for 15 min, whereat the strongest phosphorylation signals were observed for ClpC and McsB. The phosphorylation signals in the supernatant fractions of all samples were stronger than in the pellet fractions, consistent with previous results (Figure 10). Notably, the phosphorylation signal of Mdh was again more abundant in the t_0 and t_{15} supernatant fractions, indicating that even in presence of ClpP most of the detectable phosphorylation occurred on disaggregated, soluble substrate (Figure 10/Figure 14/Figure 24).

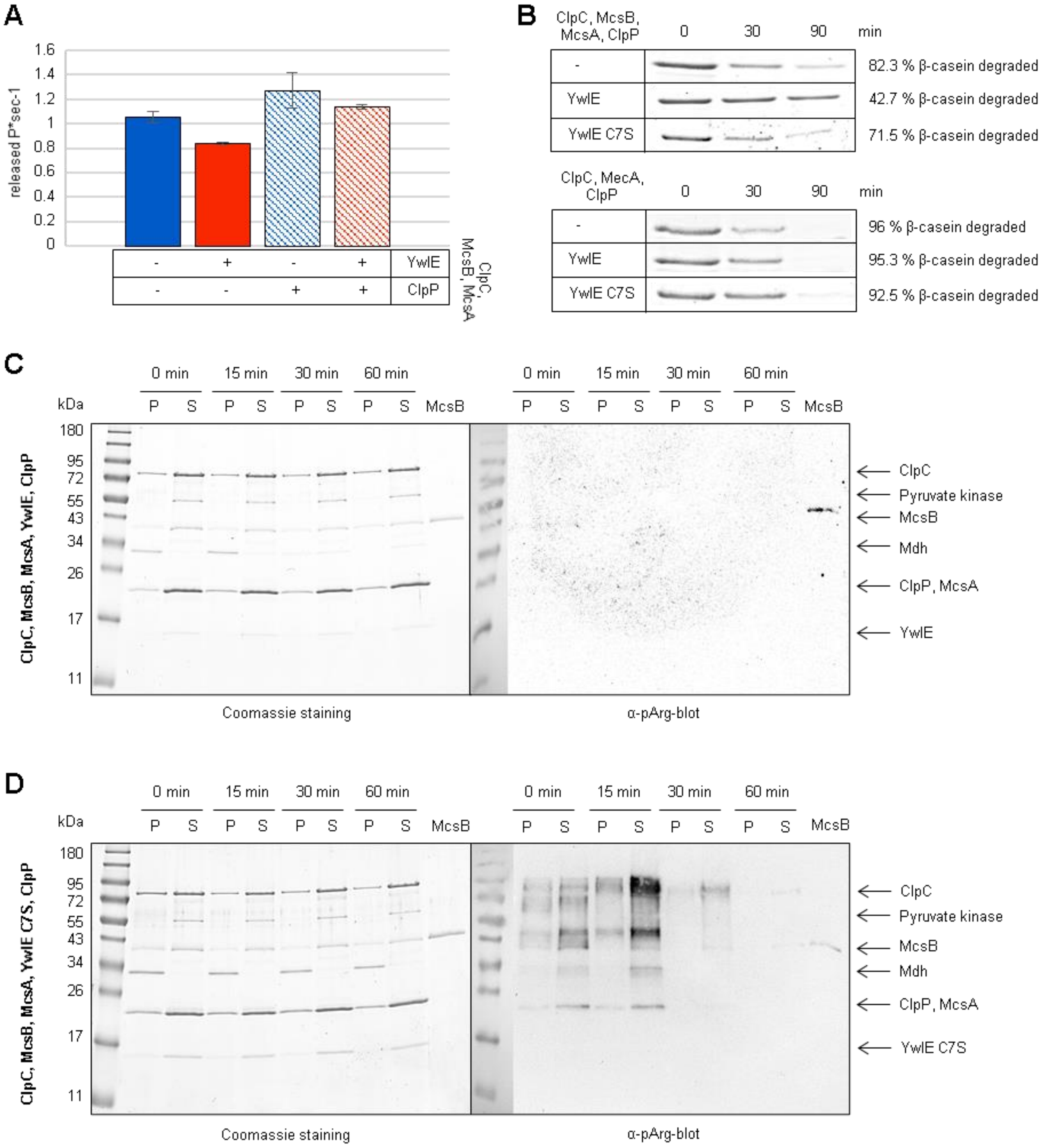

Figure 24 ClpP stimulates ATPase activity and YwlE impairs ClpCP degradation activity.

(A) McsB/McsA-induced ClpC ATPase activity was determined in Malachite Green assay, ± YwlE and ± ClpP. Error bars display standard deviations of three replicates. (B) SDS-PAGE analysis of β-casein degradation over 90 min by ClpC, McsB, McsA, ClpP ± YwlE/YwlE C7S and ClpC, MecA, ClpP ± YwlE/YwlE C7S. (C,D) Representative SDS-PAGE and western blots of samples from disaggregation assay with ClpC, McsB, McsA, ClpP, YwlE (C)/YwlE C7S (D) taken at indicated time points and divided in pellet (P) and supernatant (S) fractions. On the left, Coomassie staining and on the right western blots with α-pArg antibody are displayed (Fuhrman et al). Autophosphorylated McsB served as positive control for pArg western blots.

The phosphorylation of disaggregated model substrate Mdh was observed repeatedly, with McsB/McsA-activated ClpC (Figure 10) and ClpCP (Figure 24). To monitor the protein phosphorylation in presence of different substrates, degradation assays and α-pArg blots with β-casein and CtsR as substrates were performed. Both substrates are already known to be phosphorylated by McsB/McsA and targeted for ClpCP degradation (Elsholz et al., 2010; Kirstein et al., 2007, 2005; Trentini et al., 2016). At t_0, several phosphorylation signals were detected in the degradation reaction with β-casein, including ClpC, McsB and ClpP/McsA (Figure 25 A). The substrate only displayed phosphorylation at t_{15}, indicating that β-casein was phosphorylated prior to degradation. As expected, the McsB substrate CtsR was also phosphorylated before ClpCP dependent degradation, consistent with previous studies (Figure 25 B) (Kirstein et al., 2007, 2005). Most of the phosphorylation signal was visible at early time points in both α-pArg blots. This indicates, consistent with previous studies, that the kinase activity of McsB might play a role in substrate targeting for ClpCP degradation (Kirstein et al., 2007; Trentini et al., 2016).

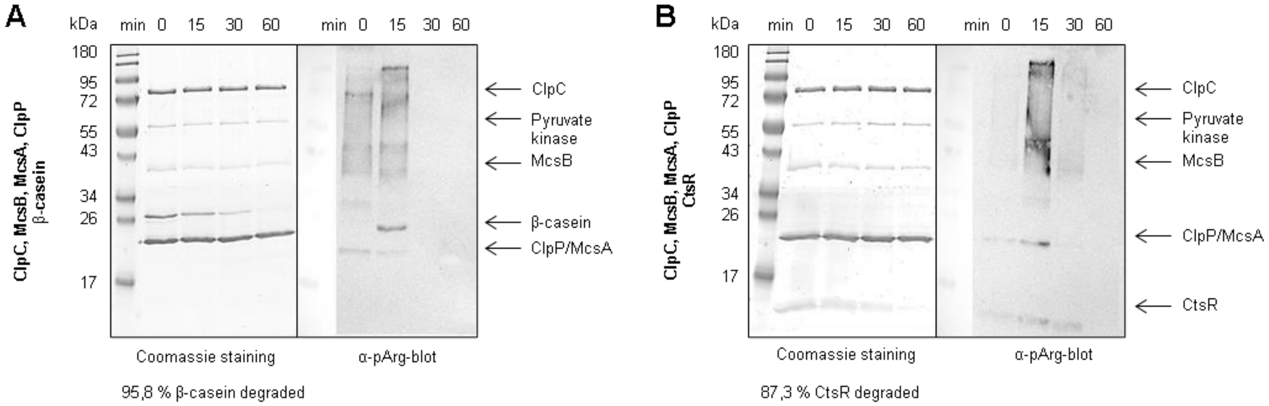
A
kDa
min 0 15 30 60
min 0 15 30 60
180
95
72
55
43
34
26
17
ClpC, McsB, McsA, ClpP
β-casein
ClpC
Pyruvate kinase
McsB
β-casein
ClpP/McsA
Coomassie staining
α-pArg-blot
95,8 % β-casein degraded
B
kDa
min 0 15 30 60
min 0 15 30 60
180
95
72
55
43
34
26
17
ClpC, McsB, McsA, ClpP
CtsR
ClpC
Pyruvate kinase
McsB
ClpP/McsA
CtsR
Coomassie staining
α-pArg-blot
87,3 % CtsR degraded

Figure 25 McsB phosphorylates ClpCP substrates β-casein and CtsR prior to degradation.

Representative SDS-PAGE and western blots of samples from degradation assay with ClpC, McsB, McsA, ClpP and substrates β-casein (A) or CtsR (B)taken at indicated time points. On the left, Coomassie stained SDS-gels and on the right western blots with α-pArg antibody are displayed (Fuhrman et al) are displayed.

3.2.2 McsB C167S can act as adaptor protein for ClpCP

ClpC was observed to specifically recognize phosphorylated arginine residues, enabling degradation of phosphorylated substrates by ClpCP in absence of adaptor proteins (Trentini et al., 2016). To analyze the impact of McsB in its function as adaptor protein or as arginine kinase on ClpCP, different assays were performed with the kinase inactive mutant McsB C167S. Previous experiments demonstrated that the kinase inactive McsB C167S mutant facilitated a lowered ClpC ATPase activity and disaggregation by ClpC, by acting as adaptor protein (Figure 12). Addition of ClpP to McsB C167S/McsA-activated ClpC resulted in removal of nearly 100 % of Mdh aggregates after 120 min and 12 % of Mdh activity were recovered (Figure 26 A, B). The pellet-supernatant fractionation displayed that besides a slight Mdh shift to the supernatant, degradation of the substrate occurred (Figure 26 C). This indicates that substrate degradation, facilitated by kinase inactive McsB C167S, could still be possible. It was demonstrated previously that a low refolding activity can be triggered by presence of ClpP in reactions without YwlE (Figure 21). Here, addition of ClpP reduced the Mdh recovery with kinase inactive McsB C167S, probably due to degradation of the unfolded substrate (Figure 26 B).These observations indicate that the adaptor protein McsB can facilitate substrate degradation, independent of the kinase activity. However, efficient ClpC ATPase induction and associated ClpCP dependent substrate degradation depends on both McsB functions, as adaptor protein and arginine kinase.

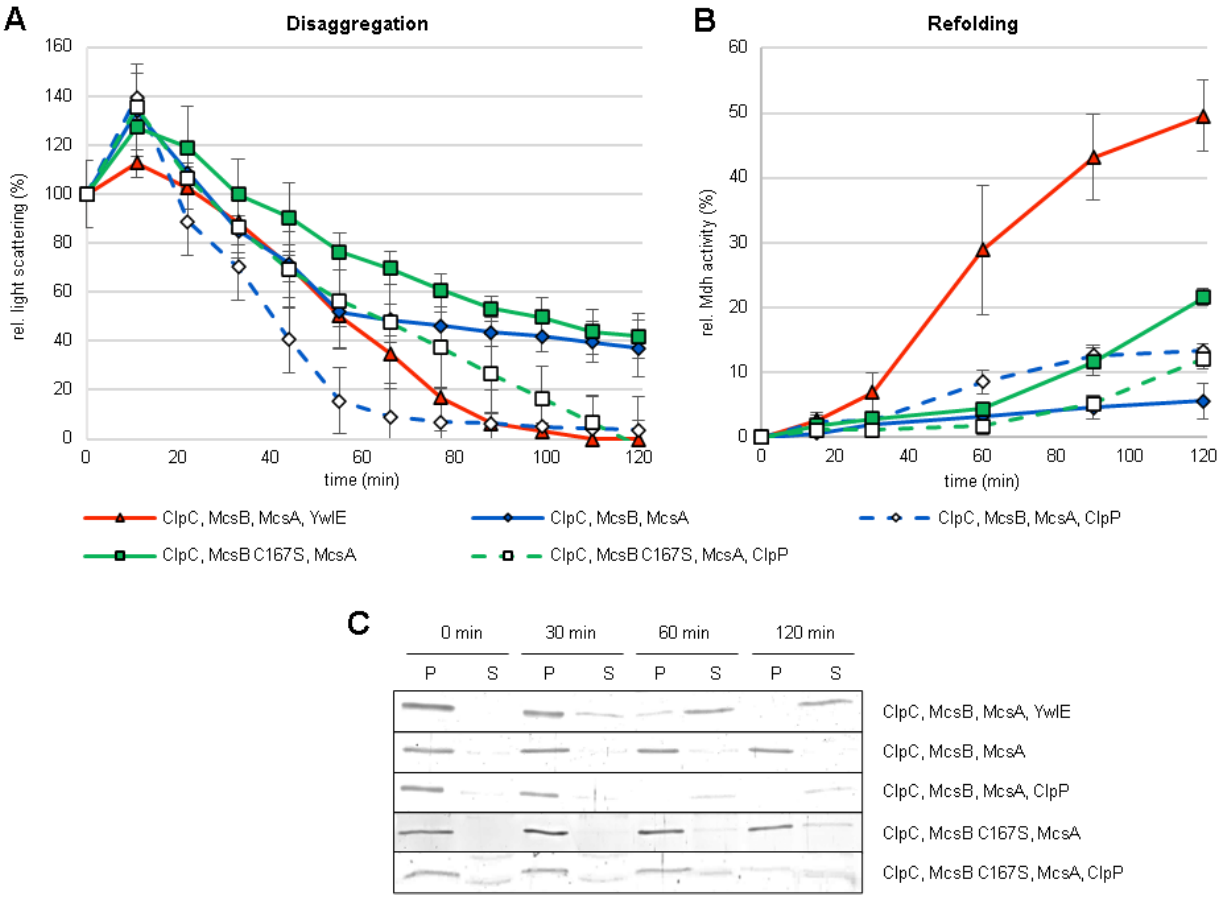

Figure 26 Kinase inactive McsB C167S/McsA still enables ClpCP degradation activity.

(A) Disaggregation of heat aggregated Mdh was monitored with light scattering experiments performed at 30°C for 120 min., ClpC, McsB, McsA, YwlE (▲), ClpC, McsB, McsA (◆), ClpC, McsB, McsA, ClpP (◇) ClpC, McsB C167S, McsA (🟩) and ClpC, McsB C167S, McsA, ClpP (□) were compared. (B) The refolding of Mdh was examined by measuring the enzymatic activity at different time points. Error bars display standard deviations of three replicates. (C) SDS-PAGE of Mdh in pellet (P) and supernatant (S) fractions at indicated time points.

YwlE was observed to promote the disaggregation and refolding of substrates instead of degradation in presence of ClpP (Figure 22). To elucidate whether the influence of active YwlE on degradation by ClpCP is related to McsB dependent protein phosphorylation, experiments with kinase inactive McsB C167S were performed. The addition of ClpP to McsB C167S/McsA-activated ClpC with YwlE only led to a slightly steeper disaggregation curve, while no refolding activity was detectable (Figure 27 A, B). This result was expected, because previous experiments without ClpP already indicated that kinase active McsB is necessary for the YwlE impact on the disaggregation system (Figure 11/Figure 18).The pellet-supernatant fractionation validated that no notable disaggregation occurred (Figure 27 C). Furthermore, degradation assays were performed to monitor the exact ClpCP degradation activity, induced by kinase inactive McsB C167S, with and without YwlE (Figure 27 D). Consistent with earlier experiments, the substrate degradation was decreased but still possible with McsB C167S/McsA-activated ClpCP (Figure 26). Addition of YwlE decreased the ClpCP degradation activity independent of McsB kinase activity, presumably due to lowered ClpC ATPase rates or possible protein-protein interactions (Figure 9 D/Figure 11 D). Although McsB can function as adaptor protein for ClpC and ClpCP independent of its kinase activity, the phosphorylation of proteins was observed to be necessary for the regulatory interplay with YwlE and efficient disaggregation and refolding.

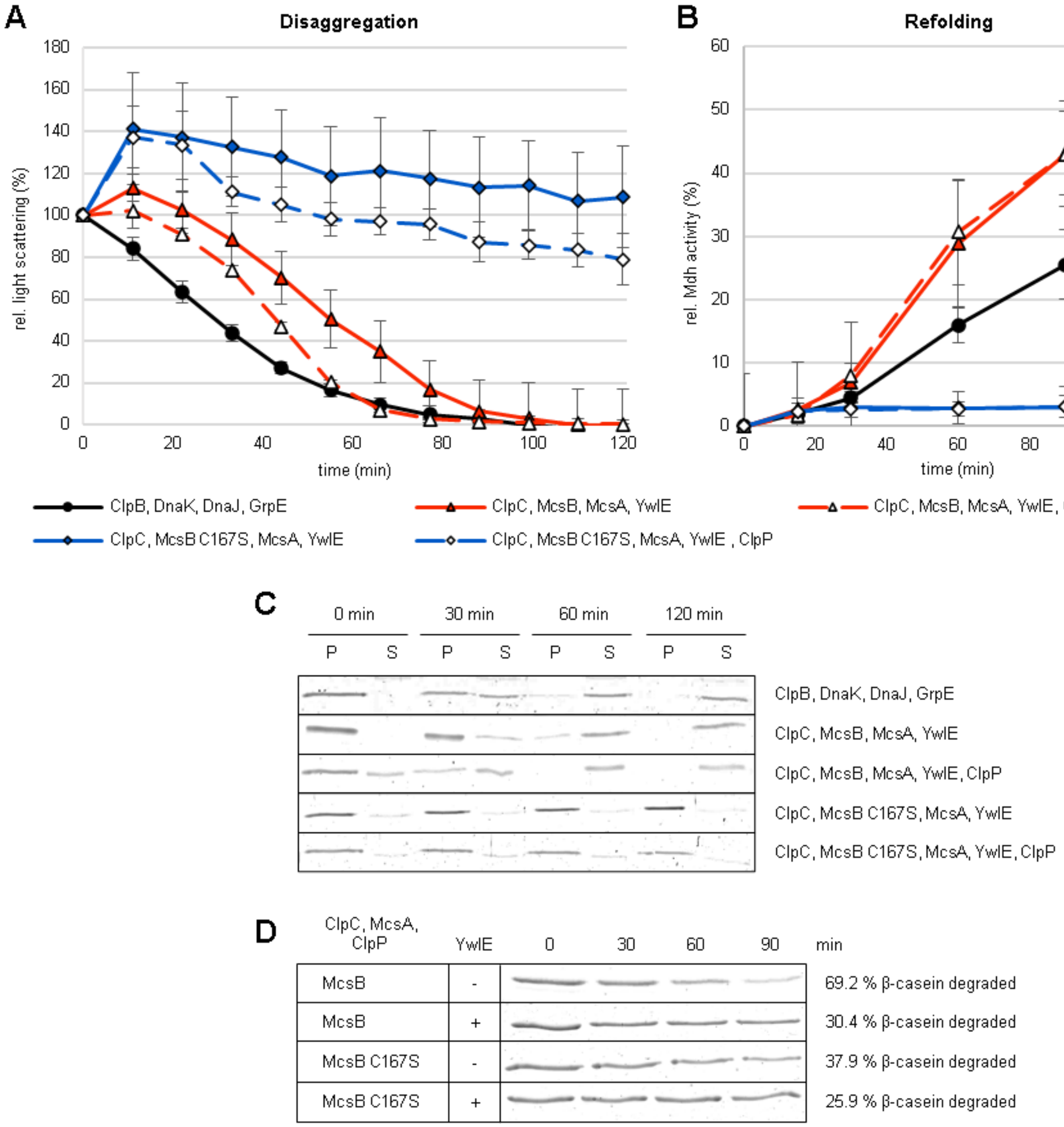

Figure 27 The McsB C167S function as ClpCP adaptor protein is still affected by YwlE.

(A) Disaggregation of heat aggregated Mdh was monitored with light scattering experiments performed at 30°C for 120 min., ClpB, DnaK, DnaJ, GrpE (●) served as positive control. ClpC, McsB, McsA, YwlE (▲), ClpC, McsB, McsA YwlE, ClpP (△), ClpC, McsB C167S, McsA, YwlE (◆) and ClpC, McsB C167S, McsA, YwlE, ClpP (◇) were compared. (B) The refolding of Mdh was examined by measuring the enzymatic activity at different time points. Error bars display standard deviations of three replicates. (C) SDS-PAGE of Mdh in pellet (P) and supernatant (S) fractions at indicated time points. (D) SDS-PAGE analysis of β-casein degradation over 90 min by ClpC, McsB/McsB C167S, McsA, ClpP ± YwlE.

3.2.3 ClpC P-loop mutations affect the ClpCP degradation activity

Mutations in the ClpC-ClpP interaction loop (P-loop) were utilized to examine the influence of altered ClpP interactions with ClpC on several chaperone activities *in vitro*. One substitution mutation in the conserved tripeptide of the ClpC P-loop, VGF::GGR, was introduced to abolish the association, as previously demonstrated for ClpXP (Martin et al., 2007; Moliere, 2012).

ClpC ATPase and degradation assays were performed to monitor the influence of the ClpC VGF::GGR loop mutation on ClpC activities *in vitro*. The MecA- or McsB/McsA-induced ATPase activity of the ClpC VGF::GGR mutant was only slightly decreased compared to wild type ClpC (Figure 28 A). Degradation of model substrate β-casein was not observed with the ClpC VGF::GGR P-loop mutant (Figure 28 B). However, the ClpC VGF::GGR mutant was suggested to recognize and translocate substrate, while only the interaction with ClpP and the protein degradation is prevented (Moliere, 2012).

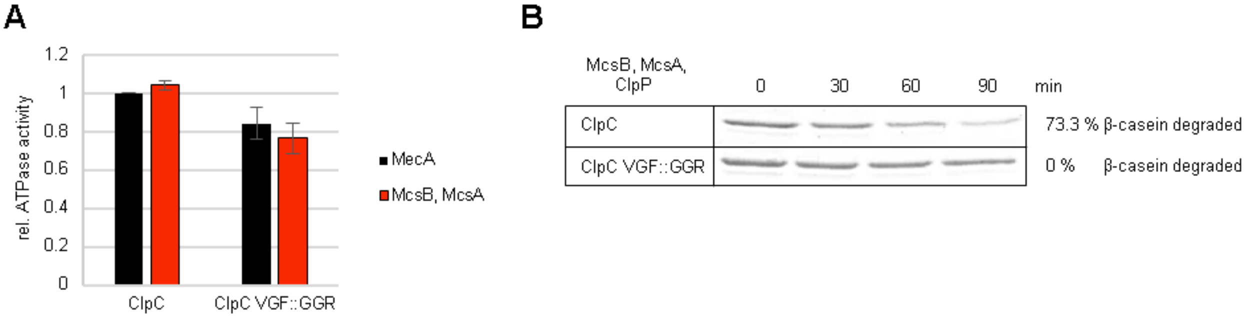

Figure 28 ClpC VGF::GGR mutant displays no degradation activity with ClpP.

(A) ClpC and ClpC VGF::GGR mutant ATPase activity with adaptor proteins MecA (black) and McsB/McsA (red) was determined using Malachite Green assay. Error bars display standard deviations of three replicates. (B) SDS-PAGE analysis of β-casein degradation over 90 min by ClpC/ClpC VGF::GGR, McsB, McsA, ClpP.

Light scattering and refolding experiments were performed to examine, whether the ClpC P-loop plays a role in disaggregation and refolding activities and if the ability to degrade substrates is linked to disaggregation. Only a slight decrease in the disaggregation and refolding efficiencies of the McsB/McsA-activated ClpC VGF::GGR mutant was observed, when compared to wild type ClpC (Figure 29 A, B). As expected, the mutant was able to dissolve 100 % of protein aggregates with YwlE and the refolding activity was comparable to the control ClpB/KJE (Figure 29 A, B). Consistent with these observations, the Mdh shift from pellet to supernatant was slower in the reaction with McsB/McsA-activated ClpC VGF::GGR and YwlE (Figure 29 C). The slight reduction in disaggregation and refolding activities of the ClpC VGF::GGR mutant was probably caused by the lowered ATPase activity (Figure 28 A).

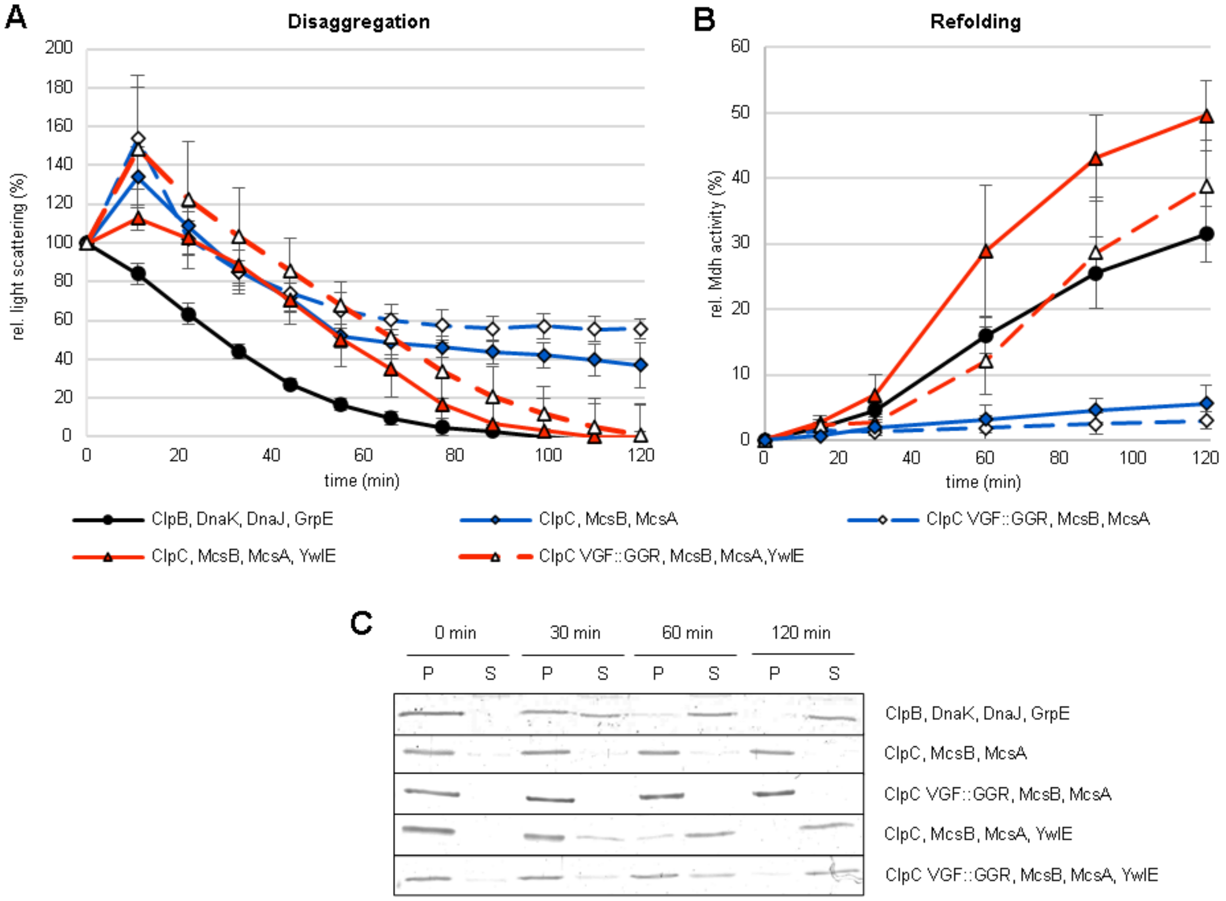

Figure 29 ClpC VGF::GGR mutant still disaggregates and refolds substrate.

(A) Disaggregation of heat aggregated Mdh was monitored with light scattering experiments performed at 30°C for 120 min., ClpB, DnaK, DnaJ, GrpE (●) served as positive control. ClpC, McsB, McsA (◆) ClpC VGF::GGR, McsB, McsA (◇), ClpC, McsB, McsA, YwlE (▲) and ClpC VGF::GGR, McsB, McsA YwlE (△) were compared. (B) The refolding of Mdh was examined by measuring the enzymatic activity at different time points. Error bars display standard deviations of three replicates. (C) SDS-PAGE of Mdh in pellet (P) and supernatant (S) fractions at indicated time points.

The YwlE phosphatase activity was proposed to affect the decision between degradation and refolding. This raised the question, whether a comparable impact could still be observed with the ClpC mutant, which was no longer able to transfer substrate to ClpP for degradation. Notably, McsB/McsA-activated ClpC VGF::GGR with ClpP was able to disaggregate 59 % of aggregates, slightly more than without ClpP (55 %), but no complete aggregate removal was possible without YwlE (Figure 29 A, Figure 30 A). Compared to wild type ClpC, addition of ClpP did not improve the substrate refolding with ClpC VGF::GGR in absence of YwlE (Figure 30 B). However, addition of ClpP and YwlE to ClpC VGF::GGR affected the substrate disaggregation and decreased the refolding activity, even though pellet-supernatant fractionations suggested that no degradation took place (Figure 30 C).

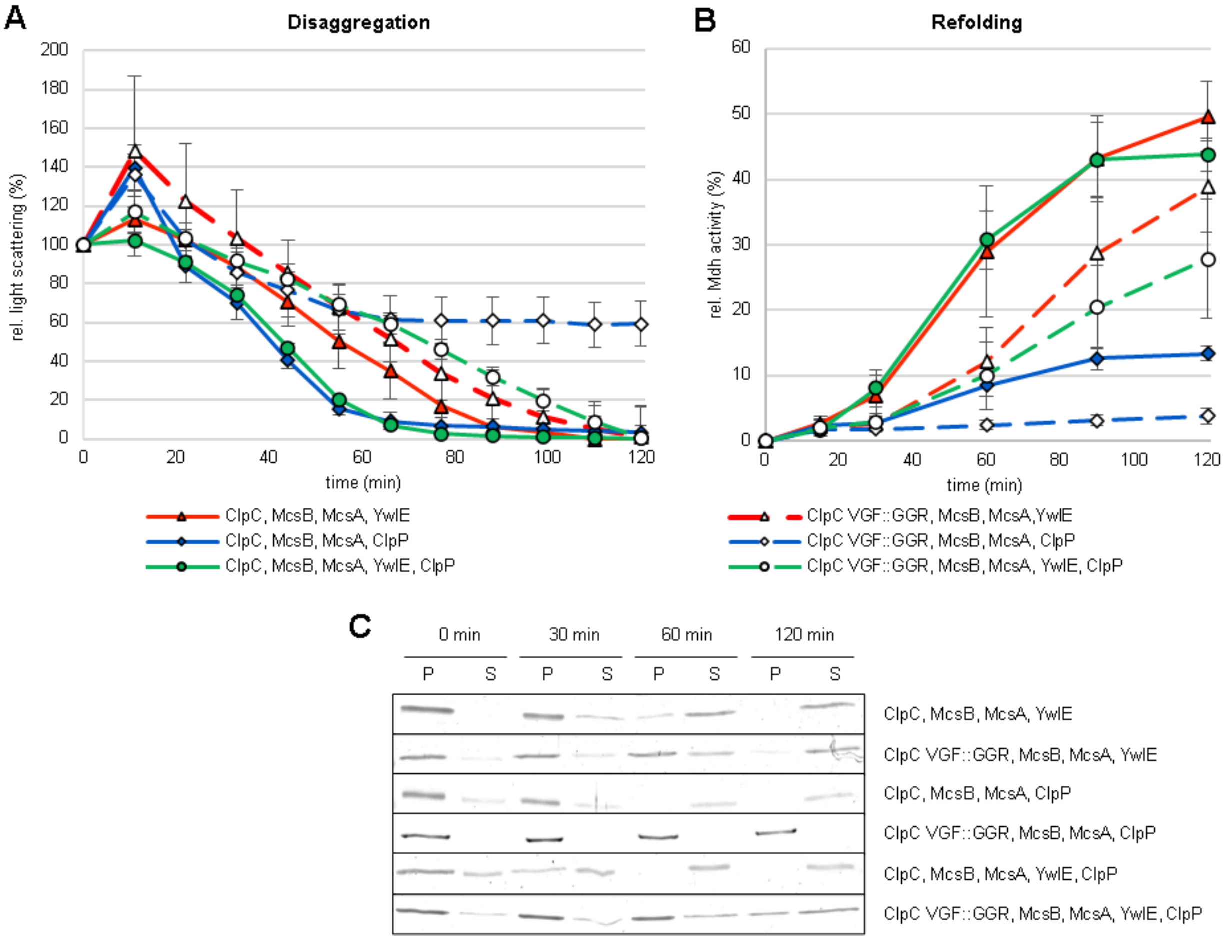

Figure 30 ClpP has no positive influence on ClpC VGF::GGR refolding activity.

(A) Disaggregation of heat aggregated Mdh was monitored with light scattering experiments performed at 30°C for 120 min., ClpC, McsB, McsA, YwlE (▲), ClpC VGF::GGR, McsB, McsA YwlE (△), ClpC, McsB, McsA, ClpP (◆) ClpC VGF::GGR, McsB, McsA, ClpP (◇) ClpC, McsB, McsA, YwlE, ClpP (●) and ClpC VGF::GGR, McsB, McsA, YwlE, ClpP (○) were compared. (B) The refolding of Mdh was examined by measuring the enzymatic activity at different time points. Error bars display standard deviations of three replicates. (C) SDS-PAGE of Mdh in pellet (P) and supernatant (S) fractions at indicated time points.

Many AAA+ Clp proteins, like *B. subtilis* ClpX, possess an IGF tripeptide in the ClpP interaction loop (Kim et al., 2001). Therefore, the impact of a mutation, substituting the ClpC VGF tripeptide with IGF, was examined. ClpC ATPase and degradation assays were performed to characterize basic ClpC functions. The ATPase activity of ClpC VGF::IGF was slightly decreased with adaptor proteins MecA and McsB/McsA (Figure 31 A). It was expected that this mutant was still able to form the protease complex with ClpP and degrade substrate, because other Clp proteins containing this loop, e.g. ClpX, also interact with the same protease. Notably, the ClpC VGF::IGF mutant displayed accelerated degradation activity with ClpP, compared to wild type ClpCP (Figure 31 B). Addition of YwlE only slightly affected the substrate degradation by ClpC VGF::IGF-ClpP, compared to the strong inhibition of substrate degradation by wild type ClpCP. Thus, the inhibitory impact of YwlE on the degradation activity of wild type ClpCP was observed to be relieved with the ClpC VGF::IGF mutant.

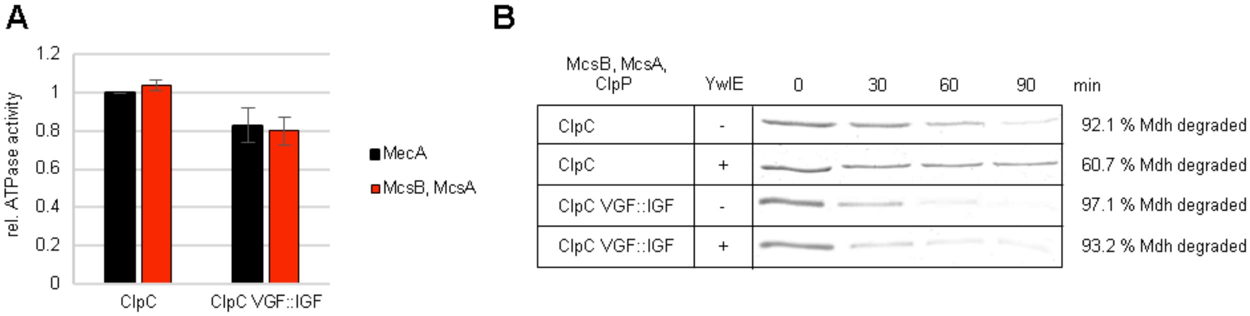

Figure 31 ClpC VGF::IGF-ClpP displays increased degradation activity despite presence of YwlE.

(A) ClpC and ClpC VGF::IGF mutant ATPase activity with adaptor proteins MecA (black) and McsB/McsA (red) was determined using Malachite Green assay. Error bars display standard deviations of three replicates. (B) SDS-PAGE analysis of β-casein degradation over 90 min by ClpC/ClpC VGF::IGF, McsB, McsA, ClpP ± YwlE.

Knowing, that the ClpC VGF::IGF mutation could increase the degradation activity with ClpP, disaggregation and refolding experiments were performed. Besides an high initial peak at t_{15}, suggesting increased complex formation, the ClpC VGF::IGF mutant displayed the same disaggregation and refolding activities as McsB/McsA-activated wild type ClpC (Figure 32 A, B). Consistent with the pellet-supernatant fractionation experiments, no increase in disaggregation efficiency was observed (Figure 32 C). Addition of YwlE led to a notably higher refolding activity with ClpC VGF::IGF (74 %) compared to wild type ClpC (50 %). Thus, the ClpC VGF::IGF mutation improved the refolding efficiency, despite lowered ATPase activity and comparable disaggregation activity in presence of YwlE.

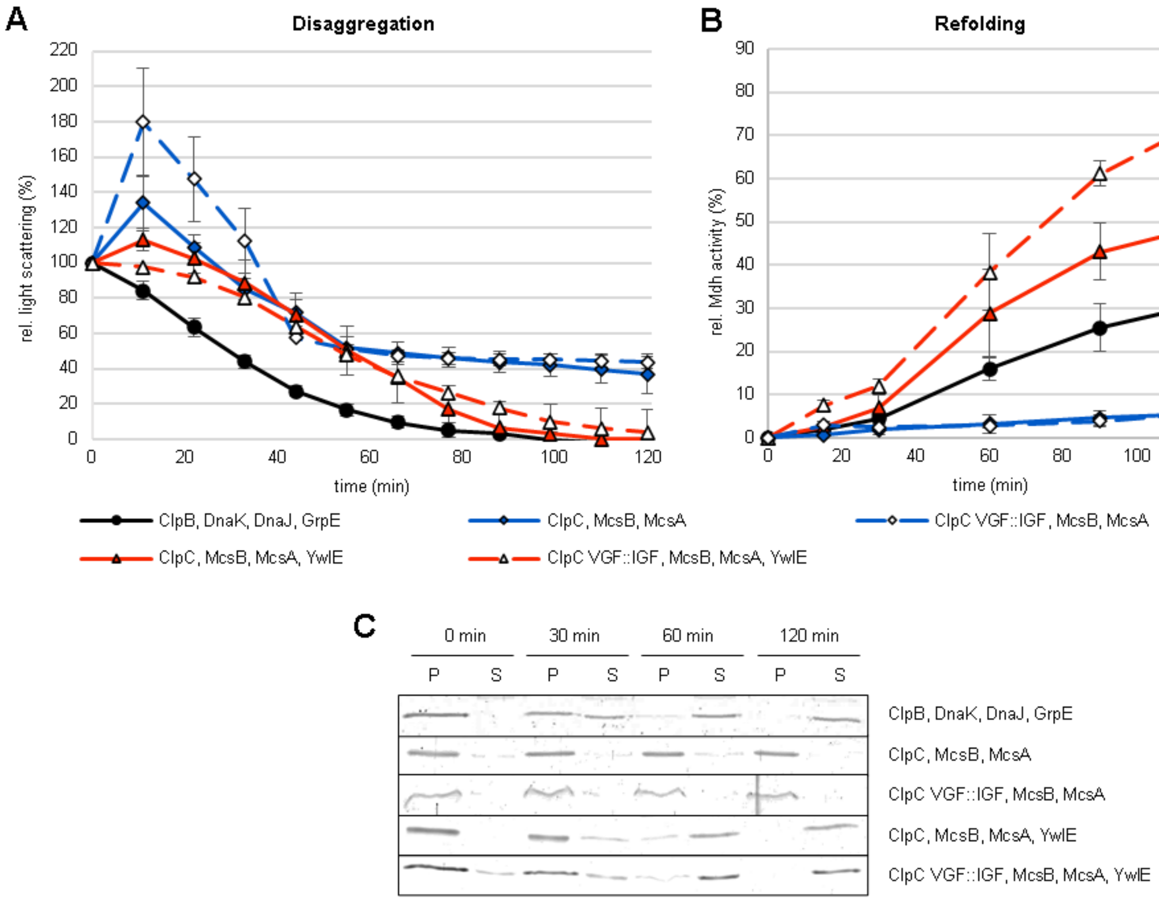

Figure 32 The refolding efficiency is increased with the ClpC VGF::IGF mutant.

(A) Disaggregation of heat aggregated Mdh was monitored with light scattering experiments performed at 30°C for 120 min., ClpB, DnaK, DnaJ, GrpE (●) served as positive control. ClpC, McsB, McsA (◆) ClpC VGF::IGF, McsB, McsA (◇), ClpC, McsB, McsA, YwlE (▲) and ClpC VGF::IGF, McsB, McsA YwlE (△),were compared. (B) The refolding of Mdh was examined by measuring the enzymatic activity at different time points. Error bars display standard deviations of three replicates. (C) SDS-PAGE of Mdh in pellet (P) and supernatant (S) fractions at indicated time points.

ClpP was added to the disaggregation and refolding experiments to monitor the influence of the protease on ClpC VGF::IGF activity. Consistent with previously observed enhanced degradation activity of the ClpC VGF:IGF mutant, addition of ClpP resulted in a steep disaggregation curve and 100 % of aggregates were dissolved after 70 min, while nearly no Mdh activity could be recovered (Figure 31 B/Figure 33 A, B). Addition of YwlE further increased the disaggregation rate and as expected, no considerable refolding took place, because the substrate was degraded. The pellet-supernatant fractionation experiment was consistent with these observations and illustrated the improved degradation activity of this ClpC VGF::IGF mutant (Figure 33 C). To sum up, the mutation altering the ClpC P-loop VGF tripeptide to IGF resulted in an enhanced degradation activity, even circumventing the inhibitory influence of active YwlE on the degradation activity of wild type ClpCP.

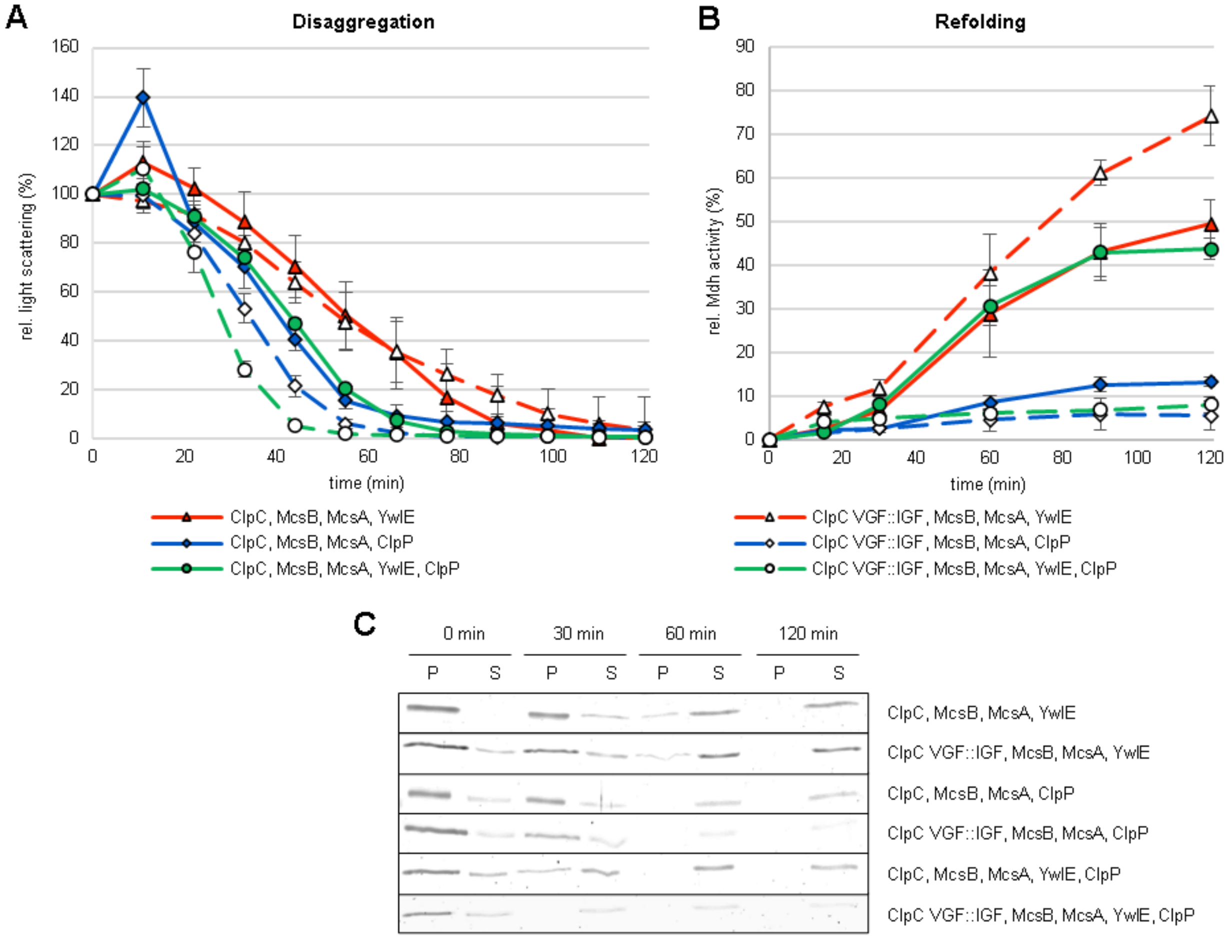

Figure 33 ClpC VGF::IGF overcomes the inhibitory effect of YwlE on degradation.

(A) Disaggregation of heat aggregated Mdh was monitored with light scattering experiments performed at 30°C for 120 min., ClpC, McsB, McsA, YwlE (▲), ClpC VGF::IGF, McsB, McsA YwlE (△), ClpC, McsB, McsA, ClpP (◆) ClpC VGF::IGF, McsB, McsA, ClpP (◇) ClpC, McsB, McsA, YwlE, ClpP (●) and ClpC VGF::IGF, McsB, McsA, YwlE, ClpP (○) were compared. (B) The refolding of Mdh was examined by measuring the enzymatic activity at different time points. Error bars display standard deviations of three replicates. (C) SDS-PAGE of Mdh in pellet (P) and supernatant (S) fractions at indicated time points.

ClpC VGF::IGF does not interfere with thermotolerance development *in vivo*

The deletion of *clpC* has severe influence on thermotolerance development in *B. subtilis* (Krüger et al., 2000, 1994). This impact relies mainly on its disaggregase function, since thermotolerance is restored in a ClpC VGF::GGR mutant (Moliere, 2012). In order to examine, whether the *in vitro* enhanced degradation activity of ClpC VGF::IGF could influence the heat stress response *in vivo*, experiments with respective mutant strains were performed. Thermotolerance experiments analyze both, the thermoresistance of a strain, while counting formed colonies after a severe, lethal heat shock (53 °C) and the thermotolerance, describing the ability of a strain to adapt to heat with a mild pre-shock at 48 °C for 15 min allowing survival at 53 °C.

The Δ*clpC* strain was less thermoresistant upon severe heat exposure and was not able to develop thermotolerance, confirming previous studies (Figure 34 A) (Krüger et al., 2000, 1994). In contrast to this, the *clpC* VGF::GGR mutant, lacking the ClpCP dependent degradation activity, displayed comparable thermoresistance and thermotolerance to the wild type, as described before (Figure 34 B) (Moliere, 2012). When examining the *clpC* VGF::IGF mutant only marginal improvement of both, thermoresistance and thermotolerance were observed (Figure 34 C). Nevertheless, future studies need to evaluate, whether this mutant leads to enhanced degradation activity *in vivo*.

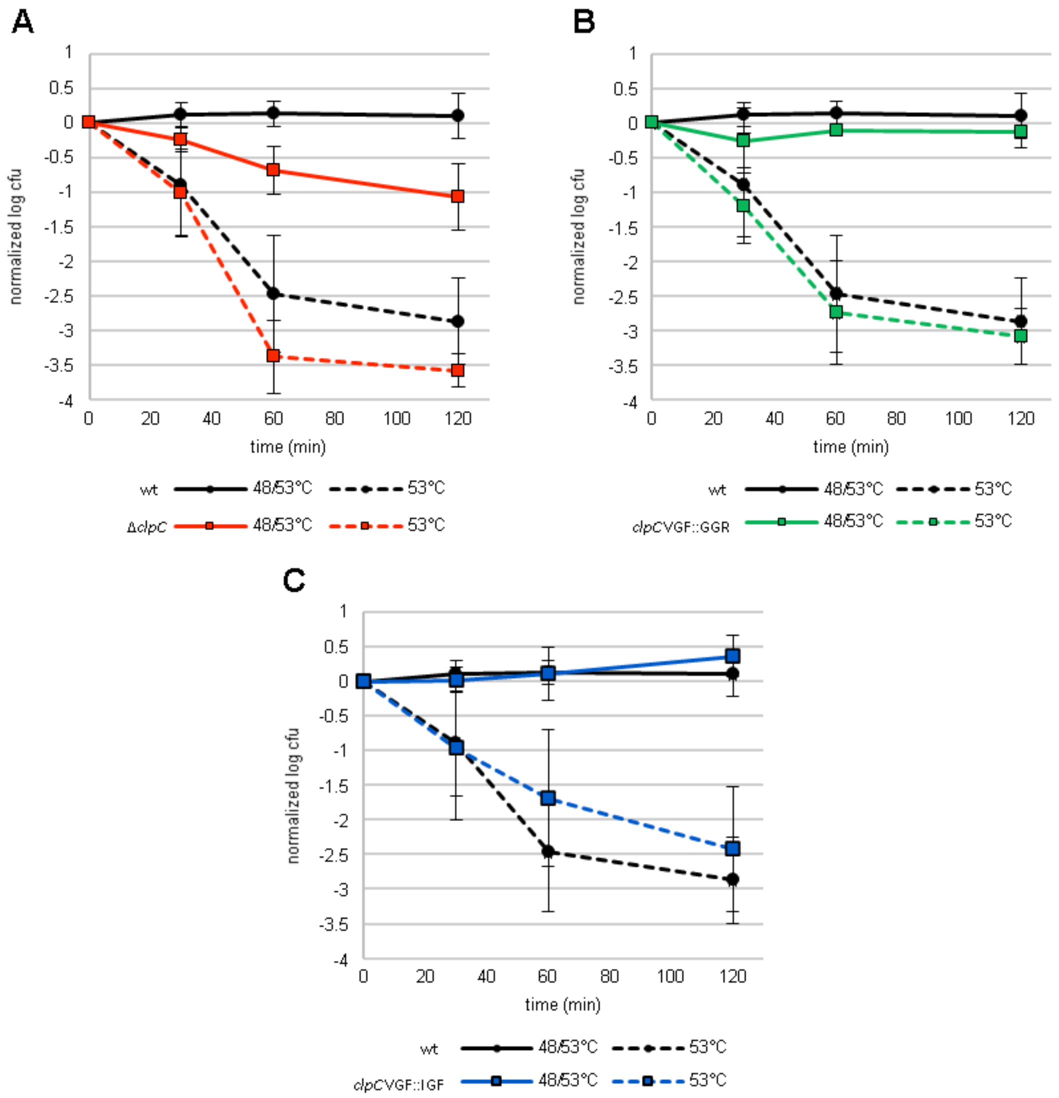

Figure 34 ClpC P-loop mutations do not impair thermotolerance.

In vivo thermotolerance experiments comparing wt strain 168 (●) with (A) Δ*clpC* (🟥 BRK17), (B) *clpC* VGF::GGR (🟩 BRK21) and (C) *clpC* VGF::IGF (🟦 BRK23). The strains were either treated with a mild preshock for 15 min at 48 °C (solid line) or directly shifted from 37 °C to 53 °C (dotted line) and survival was determined by counting of cfu over time.

3.2.4 Native Mdh is not significantly affected by the chaperone system components

In order to verify, whether the *in vitro* described chaperone system or single proteins have impact on the activity and stability of native Mdh, control experiments were performed. Active Mdh was incubated with indicated proteins under assay conditions and the Mdh activity was monitored over time. Neither McsB/McsA nor ClpC did significantly affect the Mdh activity (Figure 35). Only incubation with ClpC, McsB/McsA and protease ClpP resulted in slight loss of Mdh activity after 120 min, while no degradation occurred (Figure 35 B). Notably, the α-pArg blotting displayed a strong phosphorylation signal for McsB, while nearly no phosphorylation of active Mdh was detectable (Figure 35 C). This is consistent with the assumption that McsB only recognizes specific substrates, like CtsR, or misfolded and unfolded as well as aggregated proteins.

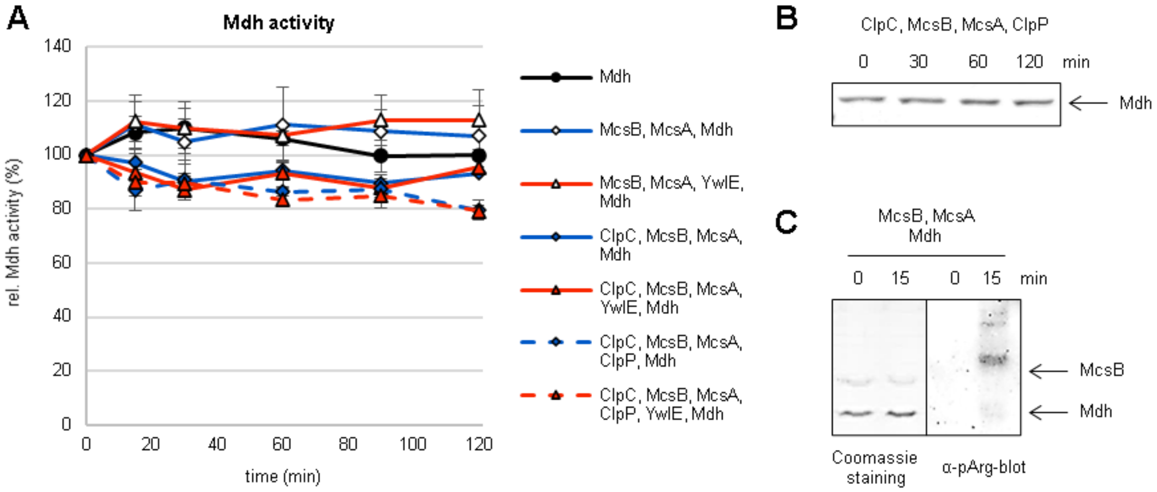

Figure 35 Chaperone system components with active Mdh.

(A) Active Mdh was incubated in presence of different proteins at 30°C for 120 min and the Mdh activity was measured at different time points. Mdh (●) was compared with McsB, McsA, Mdh (◇), McsB, McsA, YwlE, Mdh (△), ClpC McsB, McsA, Mdh (◆), ClpC McsB, McsA, YwlE, Mdh (▲), ClpC McsB, McsA, ClpP, Mdh (◆, dotted line) and ClpC McsB, McsA, ClpP, YwlE, Mdh (▲, dotted line). (B) SDS-gel analysis of a degradation assay with active Mdh as substrate was performed, with samples taken at indicated time points. (C) A representative Coomassie stained SDS-gel (left hand side) and a western blot with α-pArg antibody (right hand side) of the McsB, McsA, Mdh sample at t_0 and t_{15} are displayed.

3.2.5 Disaggregation and refolding of the model substrate citrate synthase

Disaggregation and refolding experiments with the model substrate Citrate synthase (Cs) were performed to assess, whether the characterized chaperone system, comprising ClpC, McsB, McsA and YwlE, is also active with another *in vitro* model substrate. In contrast to model substrate Mdh no complete removal of heat induced Cs aggregates was possible, even for the control system ClpB/KJE (Figure 36). A high peak in light scattering was observed for McsB/McsA-activated ClpC with Cs at t_{15}, suggesting that complex formation occurred. Since this high peak was absent in the reaction with kinase inactive McsB C167S/McsA, it was considered that the complex formation might be connected to the phosphorylation of proteins by active McsB. The ClpC dependent disaggregation efficiency with both, McsB/McsA and McsB C167S/McsA, was observed to be slightly higher than disaggregation facilitated by ClpC/MecA or ClpB/KJE. However, ClpC/MecA and ClpC/McsB/McsA were able to induce refolding of up to 32 % of the initial Cs activity, comparable to control system ClpB/KJE. The previously observed positive impact of kinase inactive McsB C167S on refolding of Mdh could be confirmed with Cs here, suggesting that protein phosphorylation by McsB could also affect refolding of Cs (Figure 11, Figure 36 B).

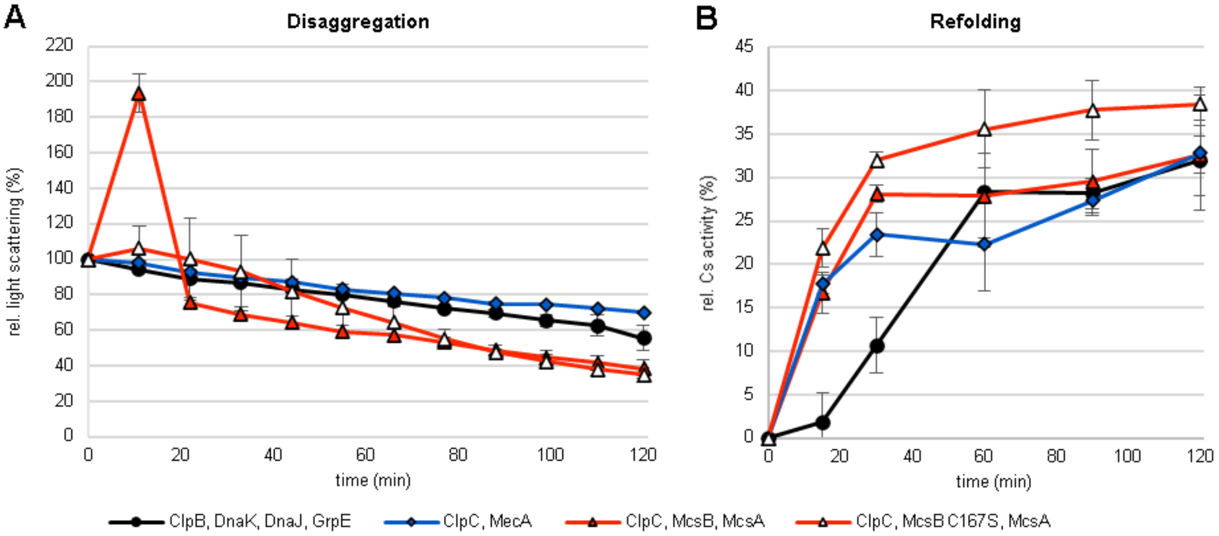

Figure 36 The refolding efficiency of Cs is increased with McsB C167S.

(A) Disaggregation of heat aggregated Cs was monitored with light scattering experiments performed at 30°C for 120 min. ClpB, DnaK, DnaJ, GrpE (●) served as positive control, ClpC, MecA (◆), ClpC, McsB, McsA (▲) and ClpC, McsB C167S, McsA, (△) were compared. (B) The refolding of Cs was examined by measuring the enzymatic activity at different time points. Error bars display standard deviations of three replicates.

Addition of the phosphatase YwlE resulted in small changes of the disaggregation curve (Figure 37 A). A lower protein accumulation peak in the beginning and a second small peak after 30 min incubation time were observed. This illustrates the biphasic disaggregation kinetic of ClpC, McsB, McsA, YwlE, which was less visible with model substrate Mdh (Figure 8). Consistent with the observed positive effect of YwlE on refolding of Mdh, an increased refolding of Cs was detected (Figure 37 B). Addition of ClpP to McsB/McsA-activated ClpC resulted in slightly enhanced disaggregation of Cs. The positive impact of ClpP, improving refolding of substrate Mdh, could be confirmed for Cs and addition of YwlE significantly increased the refolding activity (Figure 21/Figure 37 B). ATPase assays revealed that in presence of Cs, the inhibitory effect of YwlE on ClpC ATPase activity was enhanced, with and without ClpP (Figure 37 C). Furthermore, heat aggregated Cs did not serve as substrate for degradation by McsB/McsA-activated ClpCP and the adaptor protein McsB was observed to be stabilized (Figure 37 D).

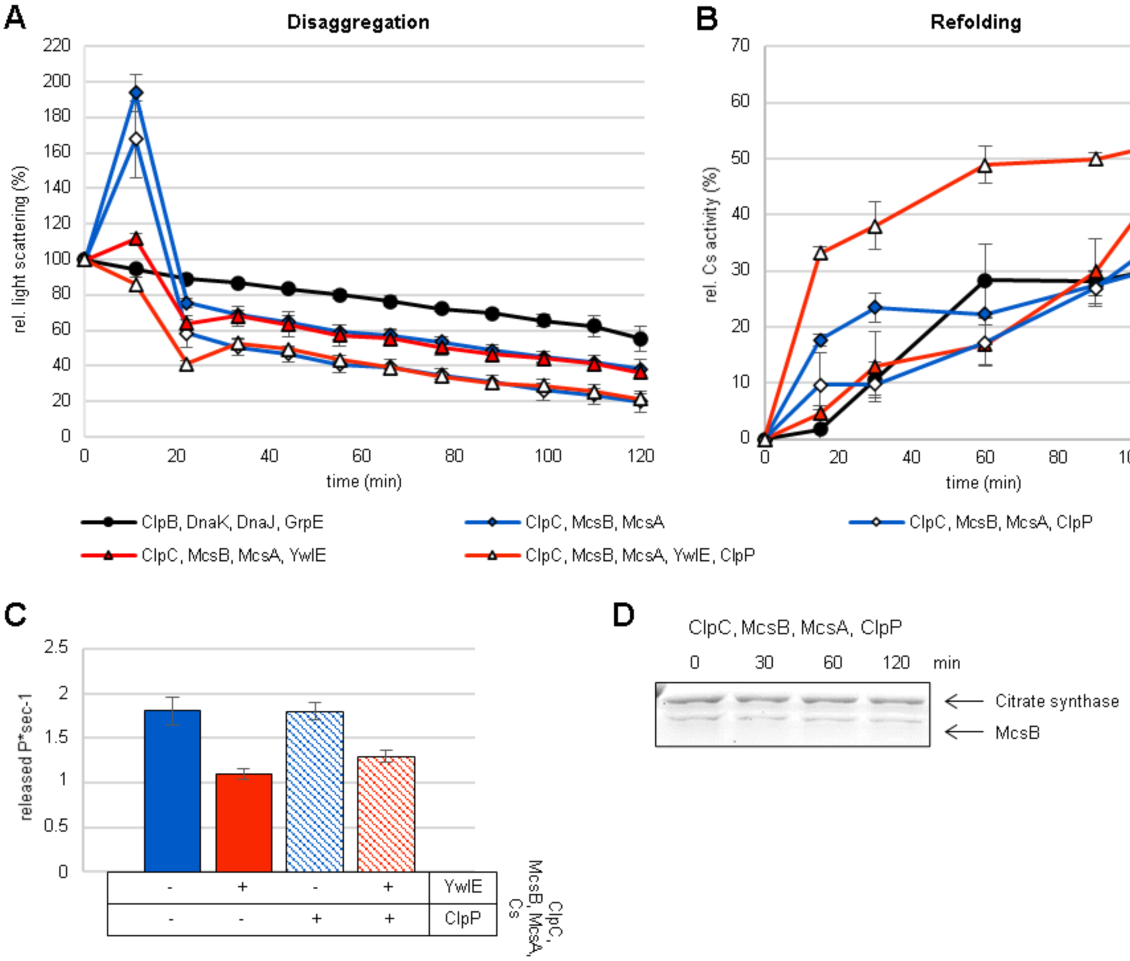

Figure 37 Cs is no substrate for degradation by ClpCP but YwlE increases the refolding efficiency.

(A) Disaggregation of heat aggregated Cs was monitored with light scattering experiments performed at 30°C for 120 min. ClpB, DnaK, DnaJ, GrpE (●) served as positive control, ClpC, McsB, McsA (◆), ClpC, McsB, McsA, ClpP (◇), ClpC, McsB, McsA, YwlE (▲) and ClpC, McsB, McsA, YwlE, ClpP (△) were compared. (B The refolding of Cs was examined by measuring the enzymatic activity at different time points. Error bars display standard deviations of three replicates. (C) McsB/McsA-induced ClpC ATPase activity in presence of Cs was determined with Malachite Green assay, ± YwlE and ± ClpP. Error bars display standard deviations of three replicates. (D) SDS-gel analysis of a degradation assay with Cs as substrate was performed, with samples taken at indicated time points.

The experiments with model substrate Cs indicate that the chaperone system based on ClpC, McsB, McsA and YwlE could facilitate disaggregation and refolding of different substrate proteins. Since addition of YwlE improved the refolding efficiency, it is likely that the refolding mechanism based on substrate phosphorylation by McsB and dephosphorylation by YwlE was applicable on model substrate Cs. Even though Cs appeared to be no substrate for degradation by ClpCP, McsB targeted the aggregated protein for ClpC dependent disaggregation and refolding. This observation suggests that this chaperone system might detect and refold various unfolded, misfolded, and aggregated proteins *in vivo*.

3.3 ClpC activation by adaptor proteins MecA and McsB

Activation of ClpC in *B. subtilis* is facilitated by interaction with the known adaptor proteins MecA, YpbH and McsB (Kirstein et al., 2006). These interactions take place at the N-terminal domain and the linker domain of ClpC leading to oligomerization and formation of the active hexameric barrel structure (Kirstein et al., 2006). So far, different ClpC mutations were described, allowing either activation via MecA (ClpC R5A, ClpC R254A), activation via McsB or prevent recognition of phosphorylated substrates (ClpC F436A, ClpC E32A/E106A) (Carroni et al., 2017; Elsholz et al., 2012; Hantke, 2019). This indicates that not only the substrate selection by adaptor proteins, but also distinct ClpC activation mechanisms could be relevant for ClpC functions in *B. subtilis*.

3.3.1 N-terminal ClpC mutations affect adaptor protein mediated activities

Mutations in the ClpC N-terminal region were introduced, to gain more insight into possible adaptor protein dependent activation mechanisms. The crystal structure of MecA bound to ClpC depicts two arginines, R9 and R83, on the interaction sites (Figure 38 A) (Liu et al., 2013). Albeit they were not annotated as phosphorylation sites for McsB so far, it was assumed that they could take part in adaptor protein dependent activation of ClpC (Elsholz et al., 2012; Schmidt et al., 2014; Trentini et al., 2014). Substituting these arginines with alanines separately and in a double substitution mutant resulted in changes of the ATPase and the degradation activity of ClpC *in vitro* (Figure 38 B, C). The ClpC R9A mutant did not impair MecA-dependent activation but decreased McsB/McsA-induced ClpC ATPase and ClpCP degradation activity. Replacing the arginine on the other side of the binding pocket, R83A, affected the ClpC ATPase and the ClpCP degradation activity, independent of the utilized adaptor protein. Notably, a double mutation of R9A and R83A completely impaired ClpC activities. These different activation patterns of ClpC R9A and R83A mutants, suggested that variations in ClpC activation by several adaptor proteins could facilitate specific ClpC substrate recognition and translocation activities as well as influences on ClpCP dependent degradation activity.

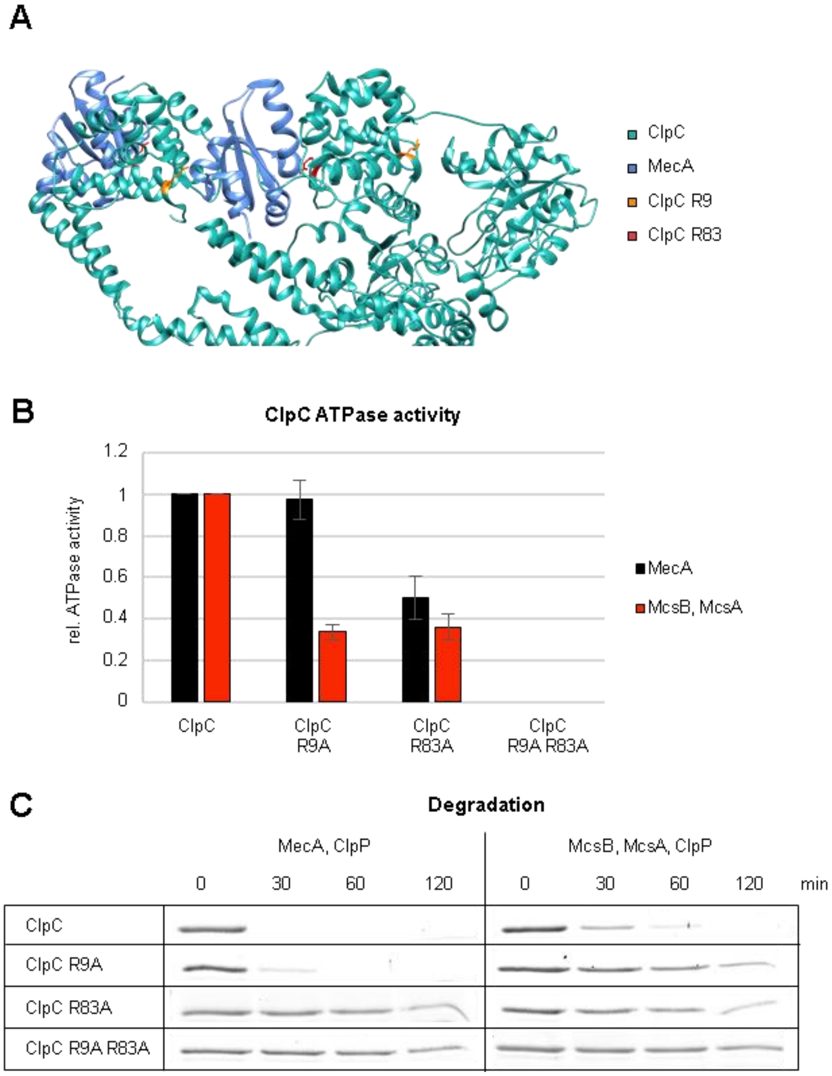

Figure 38 ATPase and degradation activities are affected by N-terminal ClpC mutations.

(A) Chimera model of ClpC N-terminal bound MecA (PDB ID 3J3S) with highlighted R9 (orange) and R83 (red). (B) Malachite Green assay was performed to determine ATPase activity of ClpC, ClpC R9A, ClpC R83A and ClpC R9A R83A with adaptor proteins MecA (black) and McsB/McsA (red). Error bars display standard deviations of three replicates. (C) SDS-PAGE analysis of β-casein degradation over 120 min by indicated ClpC mutants with ClpP and adaptor proteins MecA and McsB/McsA.

3.3.2 MecA and McsB facilitate distinct ClpCP activation

To analyze the differences in degradation kinetics of the MecA- and the McsB/McsA-activated ClpCP protease complexes, *in vitro* degradation assays were performed with β-casein as model substrate. Furthermore, the P-loop mutant ClpC VGF::IGF was characterized in more detail. Therefore, the amount of degraded β-casein or respective adaptor protein was determined in presence of different concentrations of the protease ClpP after 60 min (Figure 39). The proportion of degraded protein was assessed with SDS-PAGE analysis and subsequent calculation of band intensities using ImageJ software.

Complete degradation of β-casein by MecA-activated ClpCP was only observed with a 2:1 ratio of ClpP to ClpC. In a ClpCP protease complex, two hexameric ClpC barrels are flanking two stacked heptameric ClpP rings and it might be possible that higher ClpP concentrations facilitated the formation of this protease complex (Frees et al., 2007; Kirstein et al., 2009b; Lee et al., 2011; Wang et al., 1997). While comparing degradation patterns, it is noteworthy that degradation of the adaptor protein MecA only started, when approximately 80 % of the substrate were already degraded, as observed before (Figure 39 A) (Schlothauer et al., 2003; Turgay et al., 1998). In contrast to this, ClpCP activated by McsB/McsA degraded the substrate and adaptor protein at the same time (Figure 32 B). This leads to the assumption, that MecA might release the substrate and can re-target new substrate, whereas McsB may possibly bind stronger to the substrate and is transmitted through the ClpC pore and also transferred to ClpP for degradation. Nevertheless, *in vivo* different substrates are targeted specifically by adaptor proteins to ClpCP, such as ComK targeting by MecA or CtsR targeting by McsB (Kirstein et al., 2005; Turgay et al., 1998). It was already observed that MecA is stabilized in presence of substrates, such as ComK or β-casein, but especially the phosphorylation of proteins by adaptor protein McsB might lead to different ClpCP degradation activities than observed for β-casein (Schlothauer et al., 2003; Turgay et al., 1998).

However, comparing these substrate and adaptor protein degradation patterns with the experiments utilizing ClpC VGF::IGF, a similar impact was visible. The degradation of MecA started only, when the majority of β-casein was already degraded and the degradation of McsB and β-casein were nearly simultaneous until 70 % of the substrate were removed (Figure 39 C, D). Furthermore, ClpC VGF:IGF-ClpP displayed enhanced degradation activity regardless of the utilized adaptor protein, since 100 % of the substrate were already degraded with 1 µM ClpP compared to 2 µM ClpP for MecA-activated ClpC (Figure 39 C). The same impact was observed for McsB/McsA-activated ClpCP, only degrading 75 % of β-casein with 5 µM ClpP present and ClpC VGF::IGF-ClpP degrading all substrate with only 2 µM ClpP present (Figure 39 D). Overall, the adaptor protein MecA facilitated an accelerated ClpCP degradation activity when compared to McsB/McsA.

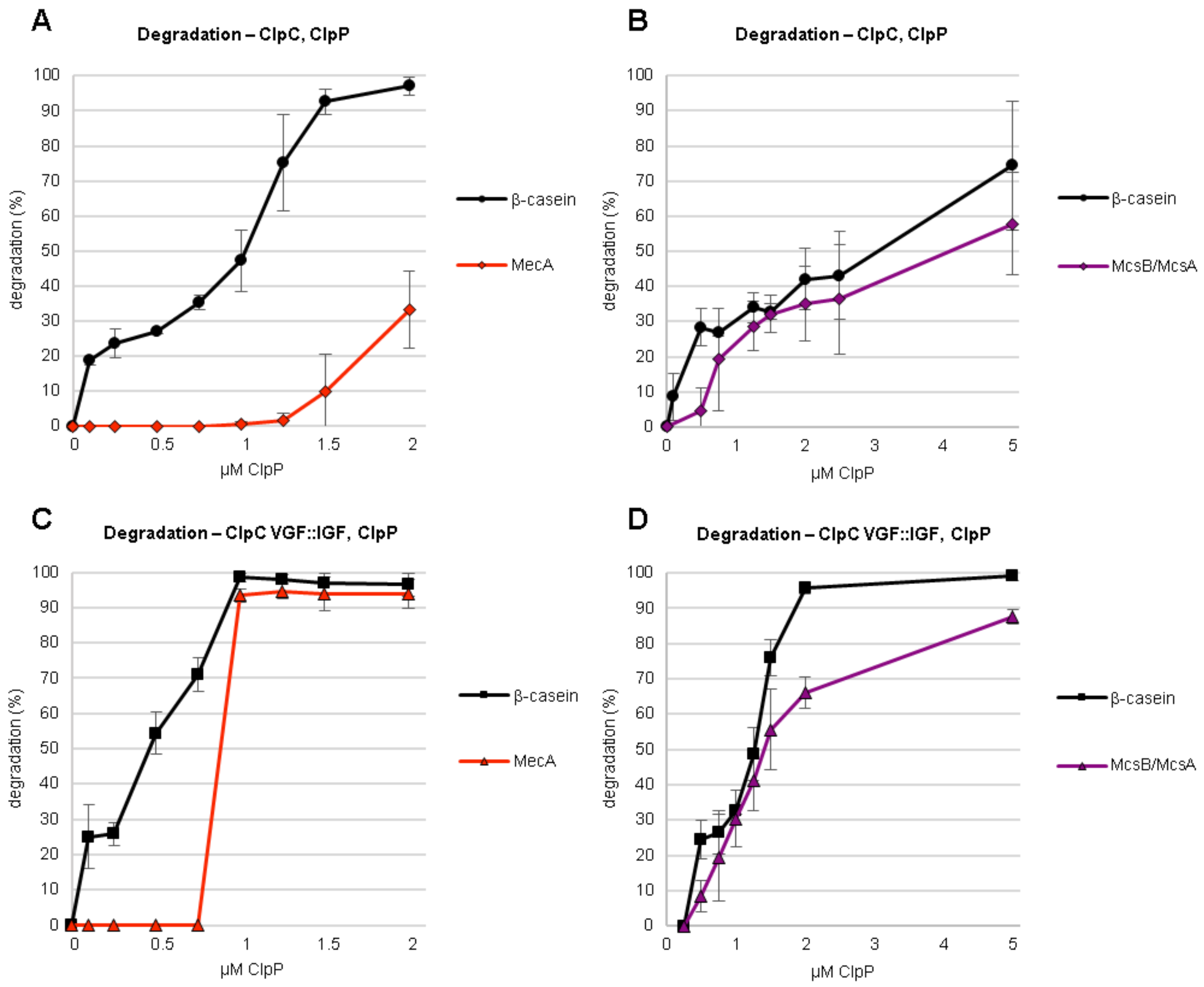

Figure 39 ClpCP degradation activity is altered with adaptor proteins MecA or McsB/McsA.

Degradation of β-casein or adaptor proteins 1 µM MecA (A, C) and 1 µM McsB (B, D) after 60 min was calculated by determining SDS-PAGE band intensity using ImageJ software. 1 µM ClpC (A, B) and 1 µM ClpC VGF::IGF (C, D) degradation patterns were compared in presence of different concentrations of ClpP. Error bars display standard deviations of three replicates.

The results obtained by these experiments suggest that although both adaptor proteins seem to share some interaction sides on ClpC, distinct modes of activation might take place. While MecA and McsB are known to target different substrates specifically, they could possibly facilitate distinct ClpC activities, e.g. degradation, disaggregation, and refolding, in varying levels. Moreover, the ClpC VGF::IGF mutant displayed an enhanced degradation activity and the experiments with increasing concentrations of ClpP suggested that the ClpC-ClpP interaction might be more stable with an IGF tripeptide in the interaction loop. Consistent with this, a mutation in *E. coli* ClpX, substituting the IGF with a VGF, was observed to decrease the degradation activity (Amor et al., 2019). Moreover, the regulatory effect of active YwlE, assisting refolding while preventing degradation, was not observed with ClpC VGF::IGF. This indicates that wild type ClpC with the VGF tripeptide might be well equipped for protein refolding with McsB/McsA and YwlE as well as protein degradation in association with ClpP, under different conditions.

During the first part of this work *in vitro* experiments were performed to characterize a system for disaggregation and refolding of heat aggregated substrates in *B. subtilis*. While disaggregation was performed by the AAA+ protein ClpC, the refolding mechanism was observed to depend on substrate phosphorylation by adaptor protein and arginine kinase McsB as well as dephosphorylation by catalytic amounts of phosphatase YwlE (Figure 9/Figure 20). Experiments with the protease ClpP indicated that active YwlE could prevent substrate degradation, while supporting the rescue of substrates (Figure 22). Mutations in the ClpC P-loop, for interaction with ClpP, suggested that the VGF tripeptide might be well-suited to enable both, substrate rescue and removal mechanisms (Figure 29/Figure 33). These ClpC functions could be additionally influenced by distinct activation modes by adaptor proteins MecA and McsB (Figure 38/Figure 39).

3.4 The role of ClpC and TasA in biofilm formation

Bacterial biofilm formation can promote a higher tolerance against external influences, such as host immune responses or antibiotics and occurs under various conditions (Donlan, 2002; Hunter, 2008; Mah, 2012; Olsen, 2015). Understanding the mechanisms of biofilm regulation and matrix formation is relevant for research in medicine or agriculture (Davies, 2003; Ramakrishna et al., 2019). The soil-dwelling bacterium *B. subtilis* is a well-established model organism for studies of the biofilm matrix composition and the regulation of biofilm formation (Hashem et al., 2019; Vlamakis et al., 2013). One essential component of the biofilm is the protein TasA, which forms amyloid-like fibrils, stabilizing the matrix (Branda et al., 2006; Romero et al., 2010). Since functional amyloid fibrils were also observed to be involved in reproduction and virulence of bacteria, protein folding and secretion mechanisms are of special interest (Chapman, 2002; Claessen, 2003; Dueholm et al., 2010; Oh et al., 2007). However, *in vitro* the form of TasA fibrils changes under different pH and surface conditions and in many bacteria the folding of functional amyloids is assisted by various proteins or chaperones (Cámara-Almirón et al., 2018; Chai et al., 2013; Nenninger et al., 2009; Romero et al., 2010; Shu et al., 2016). Therefore, different experiments were performed to examine the TasA fibril form *in vivo* as well as influences of structural characteristics of TasA and the chaperone ClpC on successful pellicle biofilm formation.

For evaluation of pellicle biofilm formation, pictures of cultures showing representative, replicable phenotypes were taken over time. To begin with, two commonly in biofilm research utilized media, MOLP and Msgg, were compared. The *B. subtilis* DK 1042 wild type strain and a Δ*tapA-sipW-tasA* mutant were grown in both media to evaluate differences in the pellicle phenotypes. *TapA, sipW* and *tasA* are required for robust biofilm formation in *B. subtilis*, since TapA supports TasA fibril formation and anchors those fibrils to the cell wall and SipW is the signal peptidase necessary for processing and thus, secretion of TapA and TasA (Branda et al., 2006; Chu et al., 2006; Romero et al., 2014; Stöver and Driks, 1999a; Terra et al., 2012; Tjalsma et al., 1998). The wild type strain developed a wrinkly biofilm in MOLP medium, while the mutant was not able to build matrix, consistent with previous studies (Figure 40) (Stöver and Driks, 1999b). In Msgg medium only a flat, slightly fluffy biofilm was formed by the wild type on day one and two, whereas the mutant probe stayed coating free. Hence, further experiments were carried out in MOLP medium because differences in pellicle phenotypes were better visible.

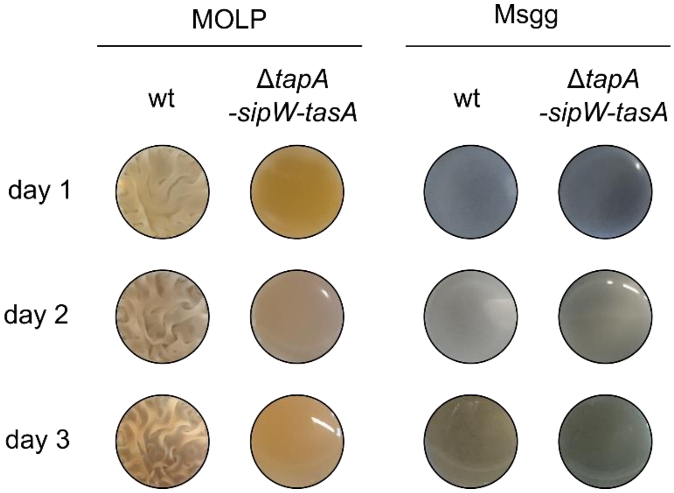

Figure 40 Distinct pellicle morphologies are better visible in MOLP than in Msgg medium.

Pellicle biofilm formation of *B. subtilis* DK 1042 wt and Δ*tapA-sipW-tasA* (BRK1) in MOLP and Msgg media over 3 days.

Furthermore, mutants of two *B. subtilis* strains, DK 1042 and the more domesticated 168, were compared in order to elucidate which strain depicted more distinct phenotypes for further analysis. In general, the observed phenotypes of *B. subtilis* in MOLP medium could be classified in three different categories (Figure 41). The first category, including the wild type of both strains, developed strong wrinkly bulges on the biofilm surface. The second class, including the DK 1042 Δ*tasA* and Δ*sipW* mutants, displayed a flat biofilm without wrinkle formation. Moreover, no, or only submerged biofilm formation was categorized as third phenotype and was observed in the mutant strains Δ*tasA* (168), Δ*sipW* (168) and Δ*tapA-sipW-tasA* (168/DK1042). The domesticated strain 168 comprises different mutations, altering the biofilm formation less robust, and therefore, it was expected that matrix growth and wrinkle formation were affected (see section 1.4.2). Consistent with this, wrinkle formation started earlier in strain DK 1042 (day one), compared to strain 168 (day two), while on day three DK 1042 had most probably surpassed stationary phase and the matrix began to decompose. (Figure 41). Additionally, pellicle biofilms were grown in media supplemented with Coomassie and Congo Red dye (CC) to stain the matrix and visualize further characteristics. With this dye amyloid curli fibers were detected in *E. coli* biofilms and binding of Congo Red to amyloid-like TasA fibrils was reported (Chapman, 2002; Romero et al., 2010). As expected, the biofilm of the DK 1042 wild type stained red with CC dye present, but the cultures stayed blue when no TasA was expressed (Δ*tapA-sipW-tasA,* Δ*tasA*) or exported (Δ*sipW*) (Figure 41). The cultures of strains 168 wild type and Δ*tasA* stayed blue, while the Δ*sipW* and Δ*tapA-sipW-tasA* cultures turned brown, most probably due to low TasA levels in the wild type and unspecific interactions in the mutant cultures.

Further experiments examining different *tasA* mutants were carried out using the DK 1042 strain, because it displayed more distinct biofilm characteristics, produces a robust biofilm matrix, and does not comprise mutations that alter biofilm formation.

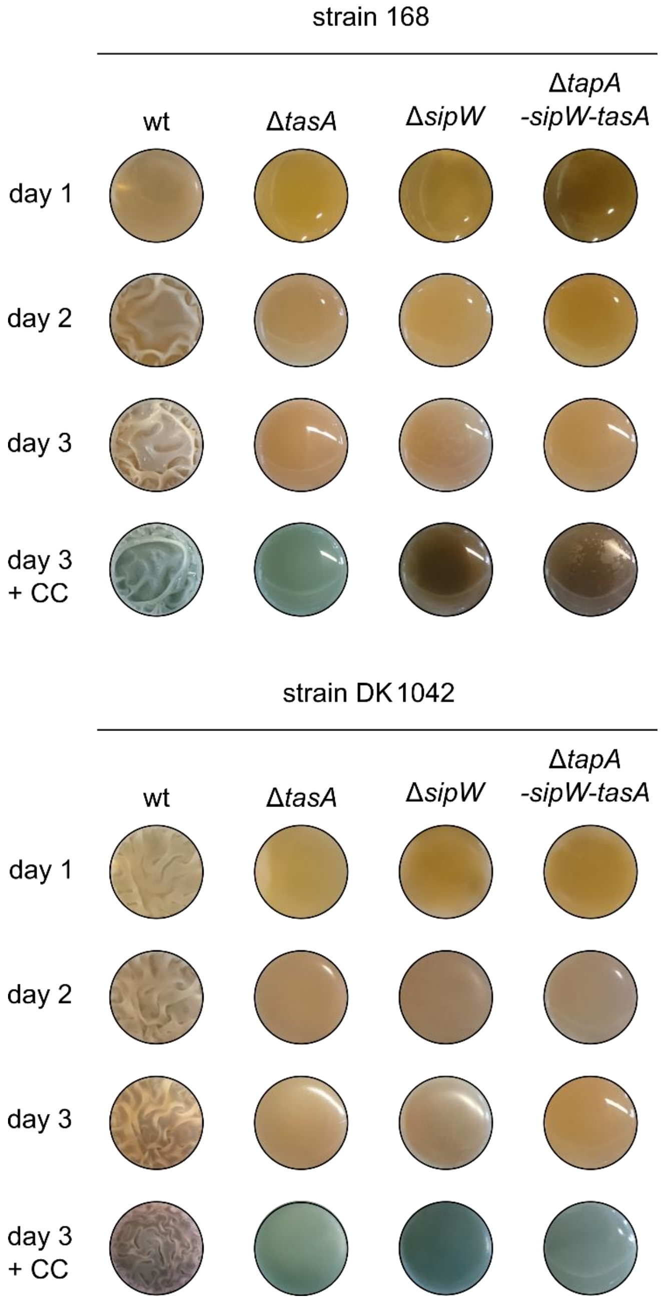
strain 168
wt
Δ*tasA*
Δ*sipW*
Δ*tapA*
-*sipW*-*tasA*
day 1
day 2
day 3
day 3
+ CC
strain DK 1042
wt
Δ*tasA*
Δ*sipW*
Δ*tapA*
-*sipW*-*tasA*
day 1
day 2
day 3
day 3
+ CC

Figure 41 Strains 168 and DK 1042 display different biofilm phenotypes.

Pellicle biofilm formation of *B. subtilis* wt 168 and wt DK 1042 as well as mutant strains Δ*tasA* (BRK4), Δ*sipW* (BRK6), Δ*tapA-sipW-tasA* (BRK1) in strain 168 and mutant strains Δ*tasA* (BRK3), Δ*sipW* (BRK5) and Δ*tapA-sipW-tasA* (BRK2) in strain DK 1042 in MOLP media were compared over 3 days and pellicle biofilms of these strains in MOLP with CC dye after 3 days are displayed.

Additional experiments were conducted to monitor the TasA protein levels in the samples and to determine TasA localization. For examination of TasA protein levels, the whole culture was separated in supernatant and pellet fraction by centrifugation. Therefore, the pellet fraction contained bacterial cells as well as the biofilm matrix (biofilm & cell fraction) and the supernatant fraction contained the culture medium and soluble, secreted proteins (supernatant fraction). The TasA protein levels in both fractions were analyzed using quantitative western blotting (see section 2.8.2).

In the biofilm and cell fraction of the wild type nearly 4 % of the protein was TasA, whereas the supernatant contained 2.5 % TasA (Figure 42). The mutants Δ*tasA* and Δ*tapA-sipW-tasA* did not contain TasA, as expected. However, the Δ*sipW* strain displayed low amounts of TasA in the biofilm and cell fraction. Consistent with previous studies, the deletion of *sipW* was expected to prevent TasA export and it was assumed that the observed protein was intracellular (Stöver and Driks, 1999b). To confirm this hypothesis more precise fractionation experiments to determine the exact TasA localization were performed.

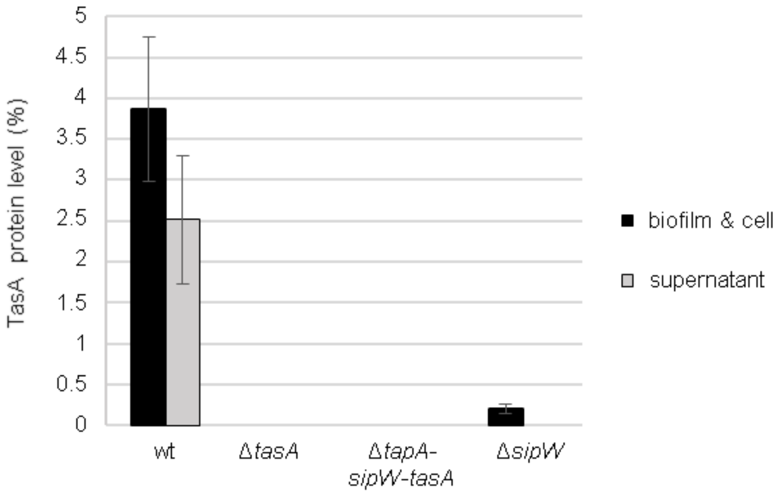

Figure 42 TasA protein is absent or not exported in *tasA*-operon mutants of strain DK 1042.

For determination of TasA protein levels samples of *B. subtilis* DK 1042 strains wt, Δ*tasA* (BRK3), Δ*tapA-sipW-tasA* (BRK2) and Δ*sipW* (BRK5) were harvested after 2 days and divided in supernatant and biofilm & cell fractions by centrifugation. SDS-PAGE with these samples and subsequent western blotting were performed. Protein levels were calculated with ImageJ band quantification and a standard curve. Error bars display standard deviations of three biological samples.

The impact of different mutants on *tasA* gene expression, signal peptide cleavage, TasA export and maturation of the biofilm was investigated by separation of the cultures in supernatant (S), matrix (M) and cell (C) fractions for western blot analysis (see section 2.8.2). To verify, that the separation of cells from supernatant and matrix was successful, α-ClpC western blotting was performed. It is important to mention, that the data of these TasA localization experiments is not comparable to the results of the previous TasA level determination, since exact protein concentrations were determined for TasA levels and protein precipitation was performed to examine the TasA localization in detail. Additionally, different methods for sample fractionation were applied.

The localization of TasA in the cultures of wild type DK 1042, Δ*tasA*, Δ*tapA-sipW-tasA* and Δ*sipW* mutants was compared (Figure 43). The wild type sample displayed no TasA in the supernatant fraction and two bands in the matrix fraction (Figure 43 A). As expected, one band was detected on the same height as purified TasA, while one band was lower, probably a degradation product. The wild type cell fraction was expected to contain TasA + SigSeq and displayed only one signal on the height of TasA without signal sequence. Nevertheless, two signals were observed for purified TasA + SigSeq, one on the height of mature TasA and the other slightly higher. Since the TasA signal sequence only consists of 27 amino acids, it is not assured that a significant upshift on the SDS-gel compared to processed TasA is visible. Thus, suggesting that during purification of TasA + SigSeq possibly conformational changes occurred, resulting in observed band patterns. As expected, Δ*tasA* and Δ*tapA-sipW-tasA* mutants no longer produced TasA (Figure 43 B, C). Furthermore, the Δ*sipW* mutant displayed a TasA signal inside the cell but no export and matrix insertion were observed (Figure 43 D). One TasA band in the cell fraction was on the height of purified TasA without SigSeq. But the abundant two bands were lower, comparable to the second, lower band in wild type matrix fraction. This observation indicates that probably conformational changes or degradation of TasA occurred when no regular signal peptide cleavage and export were possible. Detection of a light signal in the supernatant fraction suggested either export of TasA degradation products or unspecific binding of the antibody.

In conclusion, precise culture fractionation revealed that TasA is present in the matrix and cell fractions of the wild type strain, as expected. The Δ*tasA*, Δ*tapA-sipW-tasA* mutants did not produce TasA and the Δ*sipW* mutant was not able to export mature TasA and develop a wrinkly biofilm, consistent with previous studies (Stöver and Driks, 1999a).

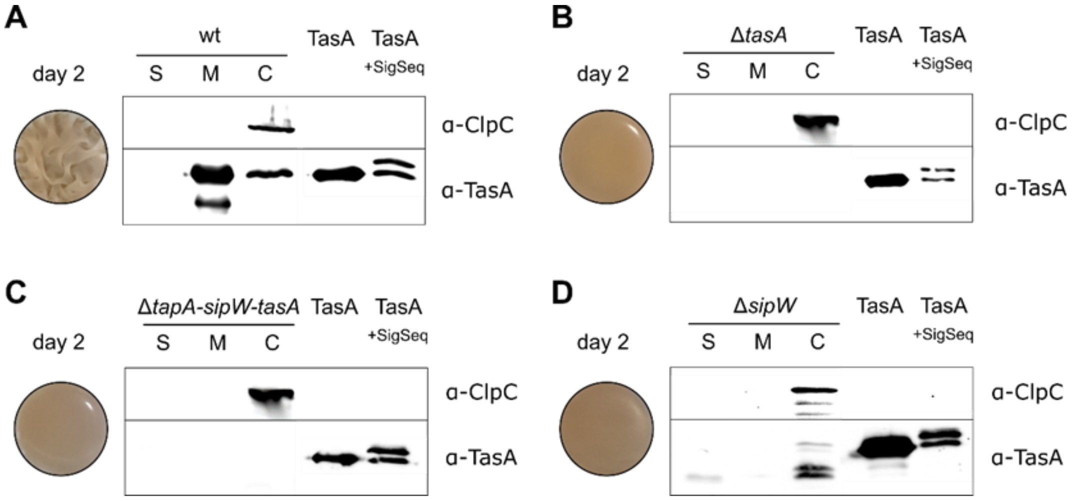

Figure 43 TasA localizes in the cells and matrix of the wt and is not exported in the Δ*sipW* strain.

Harvest and fractionation of pellicle biofilm samples was performed as described previously. *B. subtilis* DK 1042 strains (A) wt, (B) Δ*tasA* (BRK3), (C) Δ*tapA-sipW-tasA* (BRK2) and (D) Δ*sipW* (BRK5) were fractionated in supernatant (S), matrix (M) and cell (C) samples. Subsequent SDS-PAGE and western blotting with ClpC and TasA antibody were performed with purified TasA and TasA with signal sequence (+SigSeq) as control. Pellicle biofilms of these strains after 2 days are displayed.

3.4.1 The structure of TasA comprises two PPII helices

Addition of purified TasA to the culture of a Δ*tasA* mutant restores the wrinkly biofilm phenotype of the wild type (Romero et al., 2010). Consistent with this, experiments were performed with addition of different concentrations of recombinantly produced TasA to Δ*tasA* mutant cultures and even 60 µg TasA were sufficient to promote wrinkle formation (Figure 44). Increasing the amount of supplied TasA to 150 µg or 300 µg did not result in significant changes in the biofilm phenotype. Moreover, addition of TasA could not restore the wrinkly phenotype in a Δ*tapA-sipW-tasA* mutant, most probably since *tapA* and *sipW* are also essential for robust biofilm formation (Chu et al., 2006).

Previous studies observed that *in vitro* TasA fibrils can undergo structural changes under different conditions (Chai et al., 2013). In order to better understand the assembly and function of these amyloid-like fibrils in the matrix *in vivo*, the fibril form of TasA in native biofilms was investigated in cooperation with Dr. Anne Diehl, Dr. Yvette Roske, Prof. Dr. Hartmut Oschkinat et al. (Diehl et al., 2018). Recombinantly produced ^{2}H,^{13}C,^{15}N-TasA$_{261}$ (supplied by Diehl et al. and referred to as TasA$_{261}$) was added to the culture of the Δ*tasA* mutant and the wrinkly phenotype was restored (Figure 44). These biofilms, which included over 90 % of the supplied protein, were harvested and subsequent in situ solid-state MAS NMR experiments were performed (Diehl et al., 2018).

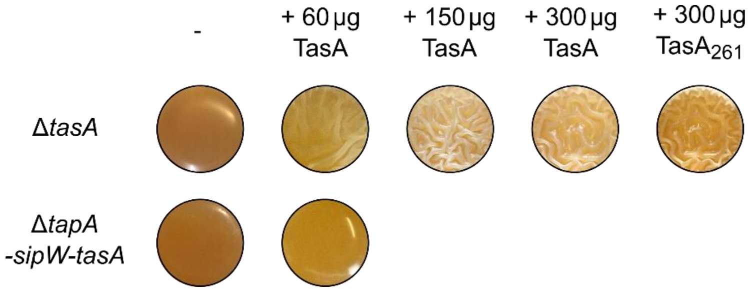

Figure 44 Biofilms are reconstructed by TasA addition.

Pellicle biofilm formation of *B. subtilis* DK 1042 strains Δ*tasA* (BRK3) and Δ*tapA-sipW-tasA* (BRK1) after incubation for 2 days at 30 °C. Addition of different concentration of purified TasA restored biofilm formation. $TasA_{261}$ was provided by Anne Diehl et al. and the restored biofilm was harvested for NMR-studies.

Characterization of the purified recombinant protein showed that TasA can assume different structural forms *in vitro* dependent on pH, temperature, and incubation time, whereby a rapid shift in pH was observed to promote formation of heterogeneous TasA fibrils with high β-sheet-content (Chai et al., 2013; Diehl et al., 2018). Comparison of NMR spectra of TasA monomers and two high-molecular-weight aggregate forms with the matrix incorporated $TasA_{261}$ indicated that in native biofilms predominantly homogenous, β-sheet-rich TasA fibrils occur, which are resistant to *B. subtilis* proteases (Diehl et al., 2018).

The crystal structure of monomeric TasA depicts two PPII helices in the dynamic sections of the protein (Diehl et al., 2018). The identified PPII helix 1 comprises amino acids A40, S41, G42, whereas PPII helix 2 includes T187, P188, T189, A190, P191 and A192 (Figure 45). These flexible segments were proposed to facilitate structural changes and fibril formation of TasA.

To analyze the influence of the identified dynamic PPII helices on TasA secretion, biofilm formation and maturation, several *tasA* mutant strains were established and examined for biofilm formation and pellicle phenotype, as well as TasA levels and localization in different fractions.

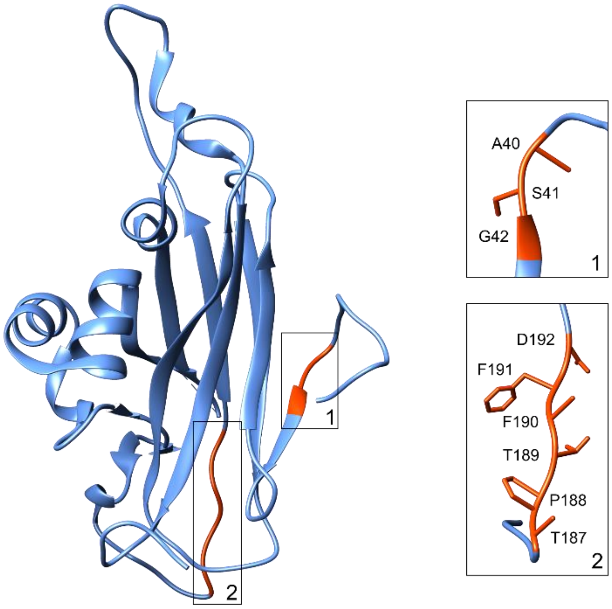

Figure 45 PPII helices in the TasA crystal structure.

Chimera model of the crystal structure of monomeric TasA (PDB ID 5OF2) with red highlighted PPII helices 1 and 2 (Diehl et al., 2018). Detailed view on structure model of amino acid residues in PPII helices 1 and 2.

3.4.2 The intact PPII helix 1 is important for proper TasA export

The relevance of certain amino acids in the TasA PPII helix 1 for biofilm formation was examined with the *tasA* ΔA40, S41 and *tasA* S41A mutants. Furthermore, substitution mutations to alanine of helix adjacent F39 and T38 and were established and analyzed. All strains were constructed using the pMAD plasmid, to achieve marker-less replacement.

The matrix and wrinkle formation of *tasA* T38A and *tasA* F39A mutant strains was slightly slower than in the wild type strain and addition of CC resulted in less red staining of the biofilm (Figure 46). The *tasA* ΔA40, S41 mutant strain developed no wrinkles at any time and only a flat biofilm was formed. The culture stayed blue upon addition of CC dye, comparable to the Δ*tasA* mutant. In contrast to this, a wrinkly phenotype similar to the wild type was observed in the *tasA* S41A mutant, but additive CC dye caused an intensive red staining. Taken together, the observed enhanced and impaired wrinkle formation in the distinct PPII helix 1 mutants, indicated that the amino acids A40 and S41 are crucial for TasA dependent biofilm formation.

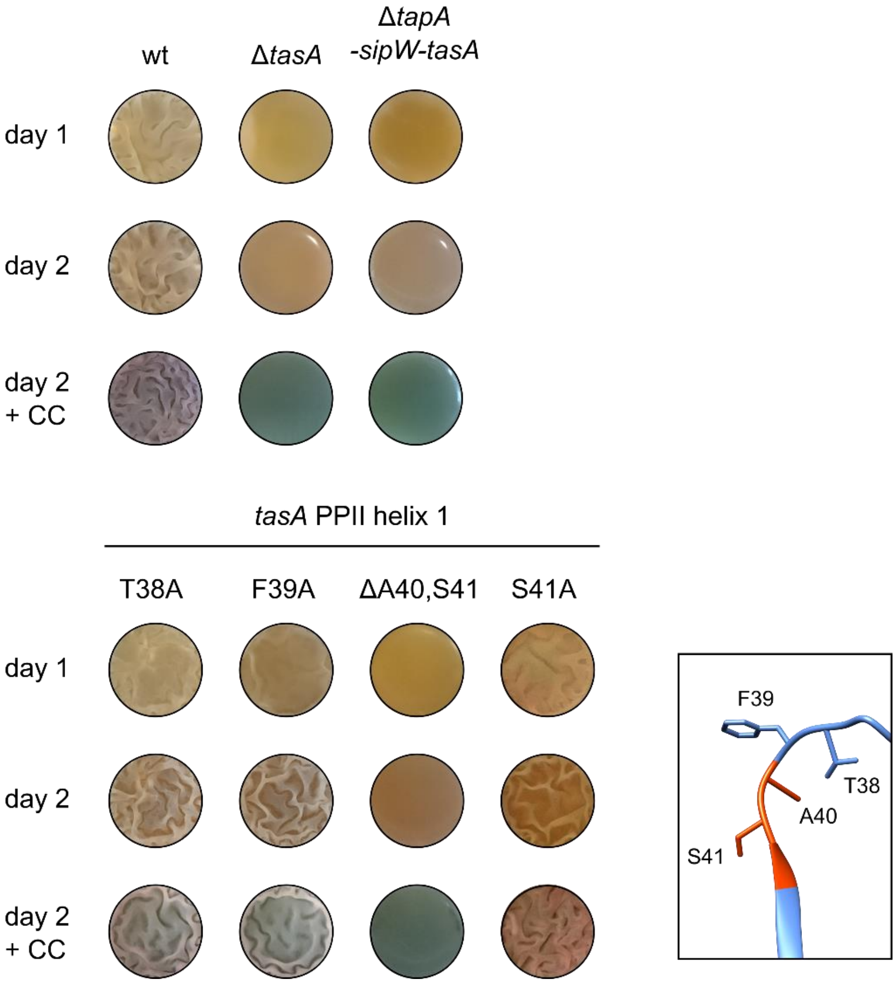

Figure 46 Mutations in the *tasA* PPII helix 1 lead to distinct phenotypes.

Pellicle biofilm formation of *B. subtilis* DK 1042 strains wt, Δ*tasA* (BRK3) and Δ*tapA*-*sipW*-*tasA* (BRK1) in MOLP media were compared with mutants of TasA PPII helix 1; *tasA* T38A (BRK7), *tasA* F39A (BRK8), *tasA* ΔA41, S41 (BRK9) and *tasA* S41A (BRK10) over 2 days and pellicle biofilm formation of these strains in MOLP with CC dye after 2 days is displayed. Detailed view on the model of substituted amino acid residues in PPII helix 1.

The TasA protein levels in fractions of PPII helix 1 mutants were determined using quantitative western blot analysis (Figure 47). The *tasA* T38A and *tasA* F39A mutants contained less TasA in the biofilm and cell fraction than the wild type. No TasA was detected in the supernatant fractions of these mutants, indicating that in total less TasA was produced but the secreted protein was fully incorporated in the matrix. Moreover, the *tasA* F39A and the *tasA* ΔA41, S41 mutants contained comparably low amounts of TasA, even though the deletion mutant was not able to form wrinkly biofilm. Since TasA secretion was observed to be necessary for the wrinkly phenotype, these results suggested that the TasA export was affected in the *tasA* ΔA41, S41 mutant (Figure 43). In contrast to this, the *tasA* S41A mutant strain contained 2-fold higher TasA levels in the biofilm and cell fraction than the wild type and less TasA in the supernatant. Consistent with previous studies, the high TasA levels might relate to the observed intensive red coloration of the wrinkly matrix, suggesting an enhanced TasA export in the *tasA* S41A mutant (Romero et al., 2010).

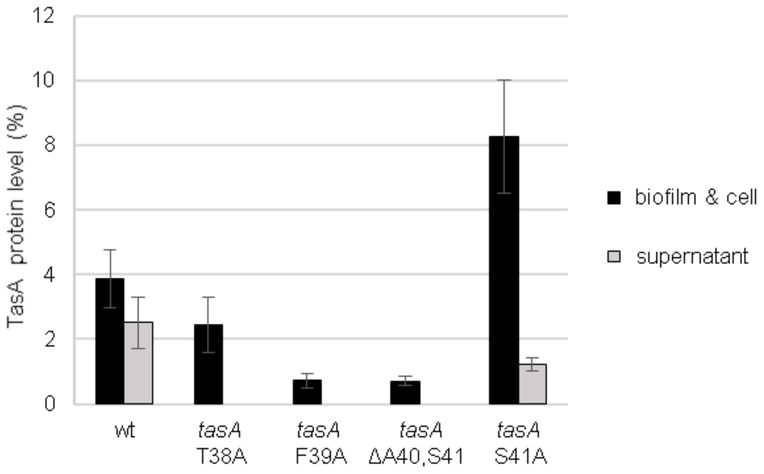

Figure 47 TasA protein levels differ in PPII helix 1 mutant strains.

For determination of TasA protein levels samples of *B. subtilis* DK 1042 strains wt, *tasA* T38A (BRK7), *tasA* F39A (BRK8), *tasA* ΔA41, S41 (BRK9) and *tasA* S41A (BRK10) were harvested after 2 days and divided in supernatant and biofilm & cell fractions by centrifugation. SDS-PAGE with these samples and subsequent western blotting were performed. Protein levels were calculated with ImageJ band quantification and a standard curve. Error bars display standard deviations of three biological samples.

After determination of the protein levels, the exact TasA localization was examined. Therefore, the PPII helix 1 mutant samples were separated in supernatant, matrix and cell fractions for western blot analysis (Figure 48). The mutants that developed wrinkly biofilms (*tasA* T38A, *tasA* F39A, *tasA* S41A) displayed the same TasA localization pattern as the wild type. The *tasA* S41A mutant strain, with reinforced biofilm growth, revealed an additional lower band in the cell fraction. However, due to the separation protocol it could not be completely excluded that matrix protein remained in this fraction. Furthermore, an impaired wrinkle formation was observed in the *tasA* ΔA41, S41 mutant and remarkably, the TasA localization resembled the pattern of the Δ*sipW* mutant (Figure 43). This result strongly indicates that deletion of these two amino acids of the PPII helix 1, at the N-terminus of TasA, might disturb the process of signal peptide cleavage by SipW and thus, impaired successful TasA export.

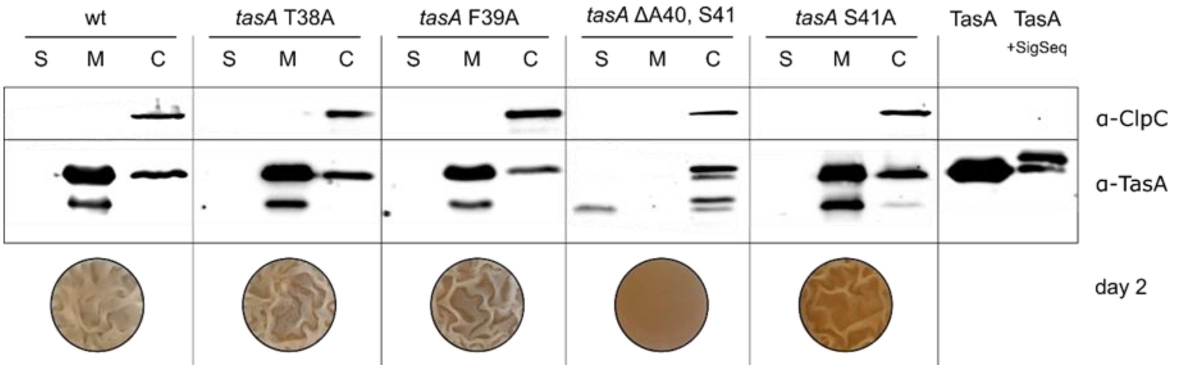

Figure 48 A deletion in *tasA* PPII 1 helix prevents TasA export.

B. subtilis DK 1042 strains wt and PPII helix 1 mutants *tasA* T38A (BRK7), *tasA* F39A (BRK8), *tasA* ΔA41, S41 (BRK9) and *tasA* S41A (BRK10) were fractionated in supernatant (S), matrix (M) and cell (C) samples. Subsequent SDS-PAGE and western blotting with ClpC and TasA antibody were performed with purified TasA and TasA with signal sequence (+SigSeq) as control. Pellicle biofilms of these strains after 2 days are displayed.

3.4.3 Mutations in *tasA* PPII helix 2 impair biofilm formation

Single marker-less substitution mutations to alanine were established to analyze the influence of single amino acid changes in the *tasA* PPII helix 2 on the biofilm phenotype. The point mutations *tasA* T187A, *tasA* P188A, *tasA* T89A, *tasA* D190A, *tasA* F191A and *tasA* D192A were introduced in strain DK 1042.

The wrinkle formation of the *tasA* T187A mutant was slowed on day one, but red staining with CC dye and biofilm morphology on day two were similar to the wild type (Figure 49). The *tasA* T189A and *tasA* F191A mutants displayed the same wrinkle phenotype as the wild type, albeit red staining with CC dye was slightly decreased. An affected biofilm formation was observed in the *tasA* P188A mutant, since first bulges were formed on day two and the approach supplemented with CC dye barely stained red. No bulges and no red staining were observed in *tasA* D190A and *tasA* D192A mutant strains, comparable to the phenotype of the Δ*tasA* mutant.

These observations indicate that in PPII helix 2 the amino acids P188, D190 and D192 might be important for TasA fibril formation and matrix maturation.

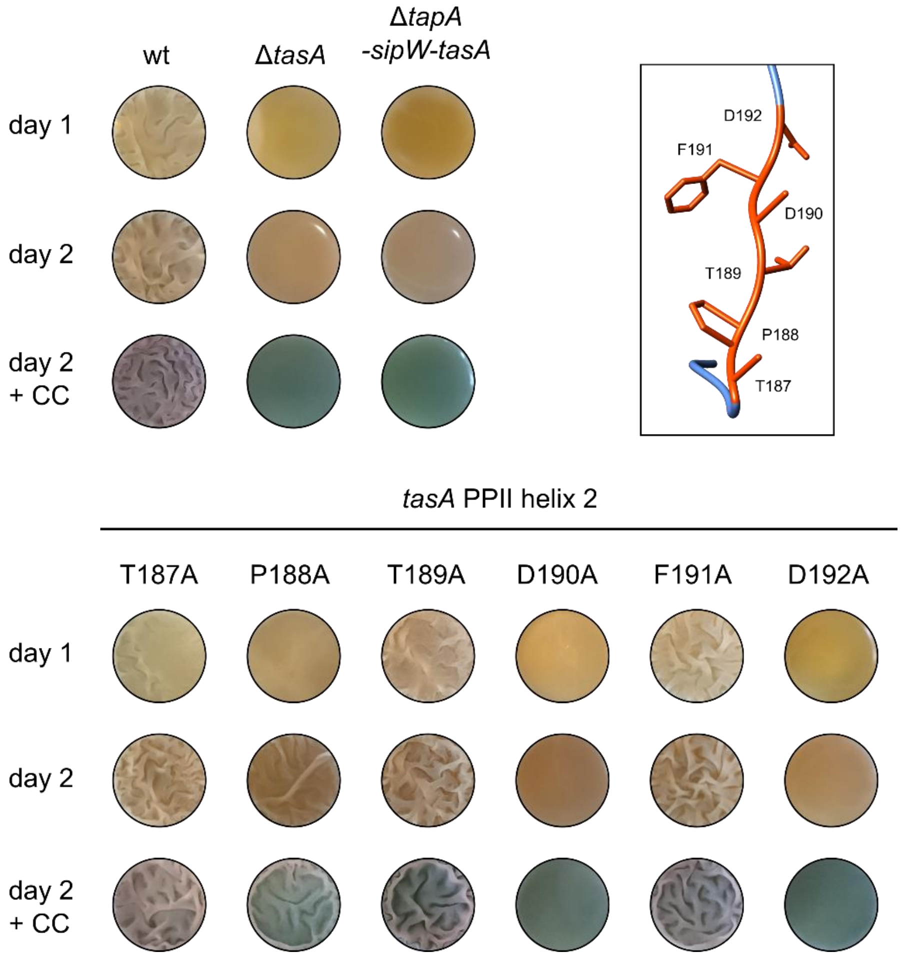

Figure 49 Several PPII helix 2 mutations affect the biofilm phenotype.

Pellicle biofilm formation of *B. subtilis* DK 1042 strains wt, Δ*tasA* (BRK3) and Δ*tapA*-*sipW*-*tasA* (BRK1) in MOLP media were compared with mutants of TasA PPII helix 2; *tasA* T187A (BRK11), *tasA* P188A (BRK12), *tasA* T189A (BRK13), *tasA* D190A (BRK14), *tasA* F191A (BRK15) and *tasA* D192A (BRK16) over 2 days and pellicle biofilms of these strains in MOLP with CC dye after 2 days are displayed. Detailed view on model of substituted amino acid residues in PPII helix 2.

Quantitative western blots of supernatant and pellet fractions were performed to determine the TasA levels in different mutant strains. The biofilm and cell fractions of mutant strains *tasA* T187A, *tasA* F191A and *tasA* T189A exhibited higher TasA levels than the wild type (Figure 50). These strains still formed wrinkles comparable to the wild type control, but *tasA* T189A and *tasA* F191A strains did not display equal red staining suggesting that the TasA structure and thus dye binding were affected (Figure 49). In all mutants with less or no wrinkle formation (*tasA* P188A, *tasA* D190A, *tasA* D192A) low TasA protein levels in the biofilm and cell fraction were observed, consistent with absence of red coloration. Higher TasA levels in the supernatant than in the biofilm and cell fraction were detected for the *tasA* D192A mutant indicating that TasA was exported, but fibril formation and matrix maturation were impaired.

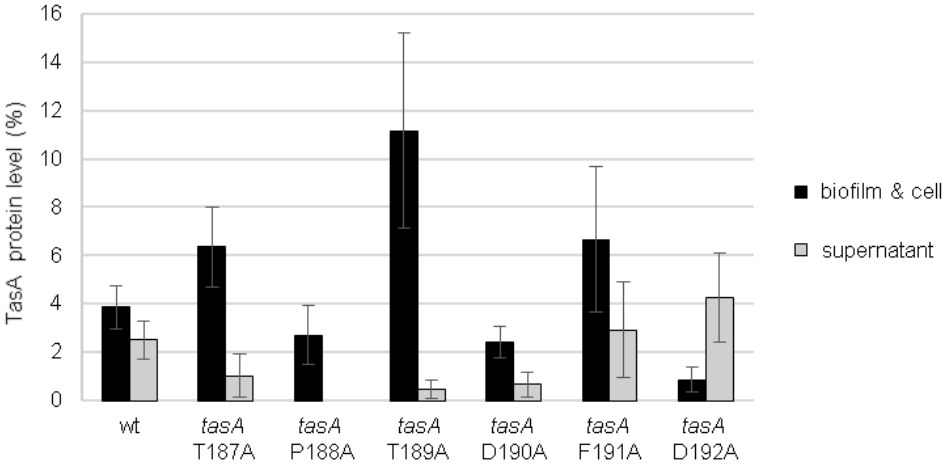

Figure 50 Distinct TasA protein levels in PPII helix 2 mutants.

For determination of TasA protein levels samples of *B. subtilis* DK 1042 strains wt, *tasA* T187A (BRK11), *tasA* P188A (BRK12), *tasA* T189A (BRK13), *tasA* D190A (BRK14), *tasA* F191A (BRK15) and *tasA* D192A (BRK16) were harvested after 2 days and divided in supernatant and biofilm& cell fractions by centrifugation. SDS-PAGE with these samples and subsequent western blotting were performed. Protein levels were calculated with ImageJ band quantification and a standard curve. Error bars display standard deviations of three biological samples.

Furthermore, the localization of TasA in supernatant, matrix or cell fraction was examined in the PPII helix 2 mutant strains. The strains forming wrinkly biofilm (*tasA* T187A, *tasA* P188A, *tasA* T189A, *tasA* F191A) displayed TasA localization in matrix and cell fractions similar to the wild type. A slight, lower band in the cell fraction was detected in *tasA* T187A and *tasA* T189A strains, but due to the fractionation protocol it is possible that matrix protein remained in the cell sample (Figure 51 A, B). The *tasA* P188A, *tasA* D190A and *tasA* D192A strains displayed TasA signal in the supernatant fraction suggesting that TasA was presumably processed and exported but not entirely included into the biofilm. Notably, all TasA signals in these mutants were slightly lower than in the wild type. This might be explained with conformational changes that possibly prevented successful TasA fibril formation and biofilm maturation. The alanine substitution of asparagine in the PPII helix completely abolished wrinkle formation and appeared to have more impact than alanine substitution of proline, because wrinkle formation was completely abolished and not only slowed.

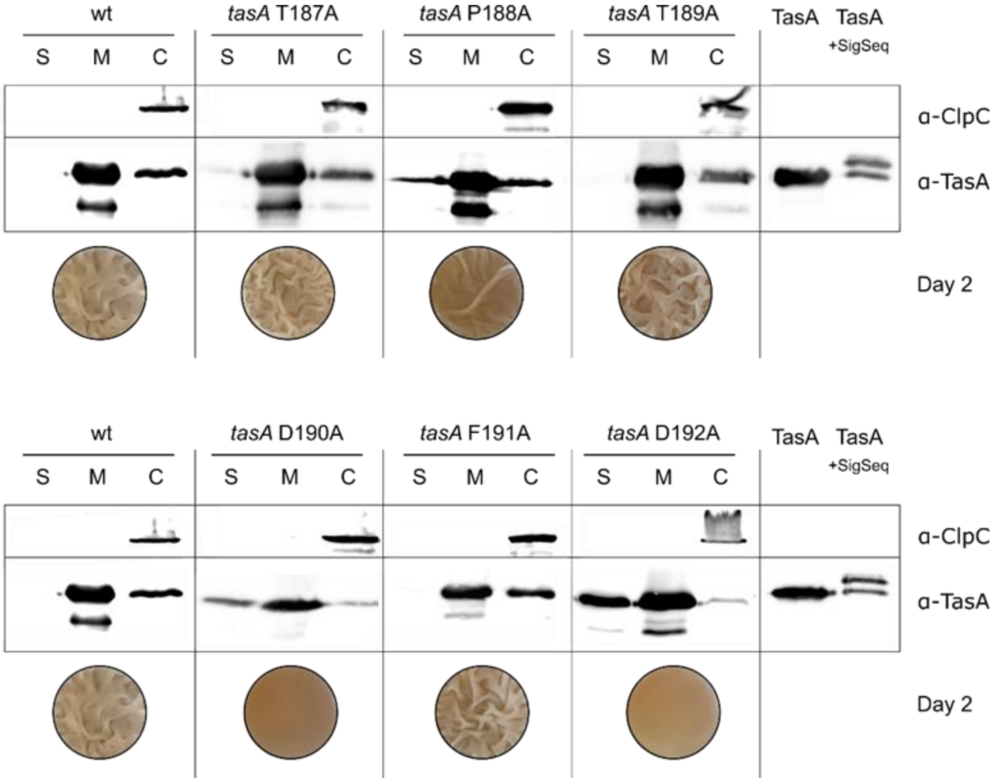

Figure 51 TasA localizes in the supernatant of several PPII helix 2 mutant strains.

B. subtilis DK 1042 strains wt and PPII helix 2 mutants *tasA* T187A (BRK11), *tasA* P188A (BRK12), *tasA* T189A (BRK13), *tasA* D190A (BRK14), *tasA* F191A (BRK15) and *tasA* D192A (BRK16) were fractionated in supernatant (S), matrix (M) and cell (C) samples. Subsequent SDS-PAGE and western blotting with ClpC and TasA antibody were performed with purified TasA and TasA with signal sequence (+SigSeq) as control. Pellicle biofilms of these strains after 2 days are displayed.

To sum up, NMR experiments with TasA$_{261}$ from native, reconstituted biofilms demonstrated, that *in vivo* probably homogenous, β-sheet-rich TasA fibrils occur (Diehl et al., 2018). The crystal structure of monomeric TasA displayed two PPII helices. These possibly flexible segments were analyzed to reveal the function of the TasA PPII helices in export, fibril formation and thus, matrix composition. Examination of *tasA* PPII helix 1 mutants suggested that this flexible structure near the N-terminus could play a role in SipW recognition and processing mechanisms. The *tasA* PPII helix 2 might be involved in fibril folding and matrix maturation, as the distinct phenotypes of the mutants indicated. Nevertheless, further experiments are required to completely characterize the mechanics of TasA export, fibril formation and the interactions of TasA with other matrix components.

3.4.4 Biofilm formation is affected in *clpC* mutants

The AAA+ protein ClpC is involved in regulation of biofilm formation in *B. subtilis* (see section 1.4.2). Together with the adaptor protein MecA, ClpC controls the activity of the key regulator Spo0A-P and the protease complex ClpCP influences expression of e.g. *eps*- and *tapA*-operons by proteolysis of key regulators (Chai et al., 2010a; Ogura and Tsukahara, 2010; Prepiak et al., 2011). Furthermore, the matrix protein TasA, which forms amyloid-like fibrils, was observed to be a possible interaction partner for ClpC *in vitro* (unpublished, Janine Kirstein) (Romero et al., 2010). Previous studies demonstrated that the folding of functional amyloids is often assisted by different proteins or chaperones in bacteria and prion propagation of yeast protein was observed to be facilitated by the Hsp104 chaperone system in *S. cerevisiae* and the ClpB chaperone system in *E. coli* (Cámara-Almirón et al., 2018; Chernoff et al., 1995; Nenninger et al., 2009; Shu et al., 2016; Yuan et al., 2014). Therefore, the influence of the chaperone ClpC on pellicle formation was examined with special regard to TasA.

To monitor whether the strain DK 1042 or the more domesticated strain 168 were better suited to analyze phenotypes of *clpC* mutants, a Δ*clpC* mutant and a *clpC* DWB mutant were assessed in these strains under biofilm conditions. The Δ*clpC* mutants of both strains displayed slowed wrinkle formation and the biofilm matrix in the Δ*clpC* (DK 1042) mutant did not decompose after 3 days (Figure 52). The ClpC DWB mutation prevents ATP hydrolysis, so that adaptor protein and substrate binding but no translocation can take place (Kirstein et al., 2006). The phenotype of the *clpC* DWB (DK 1042) mutant resembled the wild type, but significant differences were observed in strain 168. Already on day one strong wrinkle formation occurred and addition of CC dye resulted in red coloring of the biofilm, whereas the wild type (168) stayed blue. Since *clpC* mutants in the domesticated strain 168 displayed more severe, distinguishable pellicle phenotypes, this strain was utilized for further examination of ClpC and its adaptor proteins in biofilm formation.

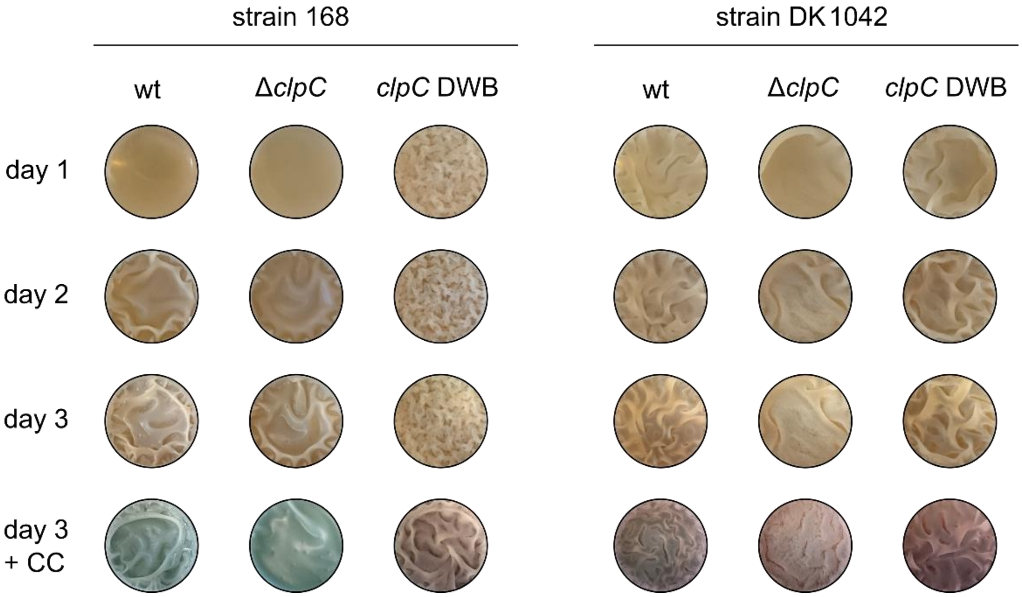

Figure 52 Pellicle formation is affected in *clpC* mutants in strain 168 and DK 1042.

Pellicle biofilms of *B. subtilis* strains wt 168, Δ*clpC* 168 (BRK17), *clpC* DWB 168 (BRK19), wt DK 1042, Δ*clpC* 1042 (BRK18) and *clpC* DWB DK 1042 (BRK20) in MOLP media were compared over 3 days and pellicle biofilms of these strains in MOLP with CC dye after 3 days are displayed.

The TasA protein levels in strains 168 and DK 1042 wild type, Δ*clpC* mutants and *clpC* DWB mutants were determined using quantitative western blot analysis. The *clpC* (168) mutants contained higher TasA levels in the biofilm and cell fractions than the wild type (168) and no TasA in the supernatant fractions (Figure 53). Likewise, no TasA was present in the supernatant fractions of *clpC* (DK 1042) mutants, but a lower TasA level was observed in the biofilm and cell fraction of the *clpC* DWB (DK 1042) mutant compared to the wild type (DK 1042). Consistent with previous observations, high TasA levels in the biofilm and cell fraction of *clpC* DWB (168) were probably linked to red coloration of the wrinkly biofilm in presence of amyloid binding CC dye (Figure 41) (Romero et al., 2010). However, the Δ*clpC* (168) mutant did only form light bulges and stayed blue, despite high TasA concentrations. This observation suggests that TasA integration in the matrix is affected, possibly due to impaired expression of other matrix compounds and altered regulation of cellular development, as suggested by previous studies (Chai et al., 2010a; Ogura and Tsukahara, 2010; Prepiak et al., 2011).

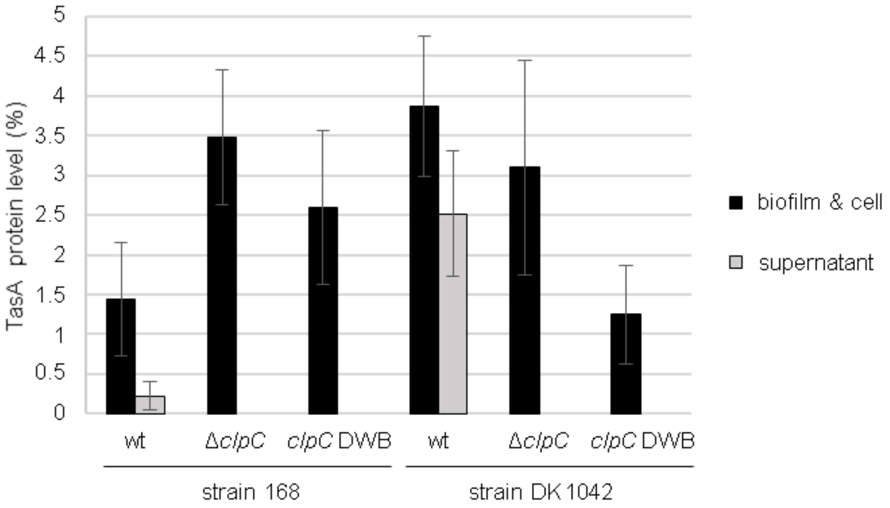

Figure 53 TasA protein levels vary in *clpC* mutants of strains 168 and DK 1042.

For determination of TasA protein levels samples of *B. subtilis* strains wt 168, Δ*clpC* 168 (BRK17), *clpC* DWB 168 (BRK19), wt DK 1042, Δ*clpC* DK 1042 (BRK18) and *clpC* DWB DK 1042 (BRK20) were harvested after 2 days and divided in supernatant and biofilm & cell fractions by centrifugation. SDS-PAGE with these samples and subsequent western blotting were performed. Protein levels were calculated with ImageJ band quantification and a standard curve. Error bars display standard deviations of three biological samples.

3.4.5 ClpCP dependent degradation is involved in pellicle formation

The regulatory degradation of different key players, such as transcriptional regulator SlrR or two-component regulator DegU-P, by the ClpCP protease complex can affect biofilm formation in *B. subtilis* (Chai et al., 2010a; Ogura and Tsukahara, 2010). To gain further insight into this regulatory involvement in pellicle biofilm formation and possible influences on biofilm component TasA, different *clpC* mutants with altered P-loops for ClpP interaction were examined (see section 3.2.3).

Previous experiments already indicated that the Δ*clpC* mutant developed less wrinkles than the wild type and that the *clpC* DWB mutant displayed enhanced wrinkle formation and red staining with additional CC dye (Figure 52). Mutations in of the *clpC* P-loop, preventing ClpCP degradation activity (*clpC* VGF::GGR, *clpC* Δloop) resulted in increased wrinkle formation and red staining, when compared to the wild type (Figure 28/Figure 54). Consistent with earlier studies, this observation suggests that the ClpCP degradation activity might be involved in down-regulation of biofilm formation (Chai et al., 2010a; Ogura and Tsukahara, 2010). Compared to the wild type, no differences in pellicle phenotype were observed for the *clpC* VGF::IGF mutant. ClpC VGF::IGF displayed enhanced degradation activity with ClpP *in vitro*, but since the substrate selection was still dependent on adaptor proteins, the mutant probably processed the same substrates as wild type ClpC and no changes in biofilm formation could be observed (Figure 31).

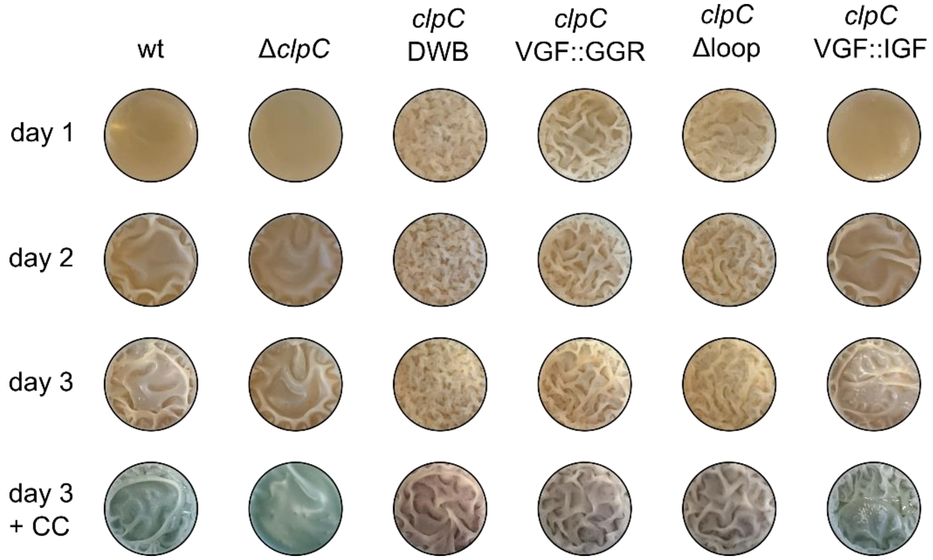

Figure 54 Wrinkle formation is enhanced when ClpCP degradation is prevented.

Pellicle biofilm formation of *B. subtilis* 168 strains wt, Δ*clpC* (BRK17), *clpC* DWB (BRK19), *clpC* VGF::GGR (BRK21), *clpC* Δloop (BRK22) and *clpC* VGF::IGF (BRK23) in MOLP media were compared over 3 days and pellicle biofilms of these strains in MOLP with CC dye after 3 days are displayed.

The TasA levels in fractions of the different *clpC* mutant strains were determined with quantitative western blotting (Figure 55). The Δ*clpC* mutant contained high TasA levels, but no red coloration with CC dye and slowed wrinkle formation were observed, most probably due to affected expression of different matrix compounds and impaired incorporation of TasA in the biofilm. Mutations in *clpC*, preventing ClpCP degradation activity (*clpC* DWB. *clpC* VGF::GGR, *clpC* Δloop), resulted in increased levels of TasA in the biofilm and cell fraction, when compared to the wild type. This result is consistent with previously observed enhanced wrinkle formation and red coloration with CC dye. The *clpC* VGF::IGF mutant also contained high TasA levels, while displaying the same phenotype as the wild type. Moreover, increased TasA levels in the supernatant fraction were observed in all strains with mutations in the ClpC P-loop (*clpC* VGF::GGR, *clpC* Δloop, *clpC* VGF::IGF), which might be due to affected TasA incorporation into the matrix and disturbed regulations altering the matrix composition.

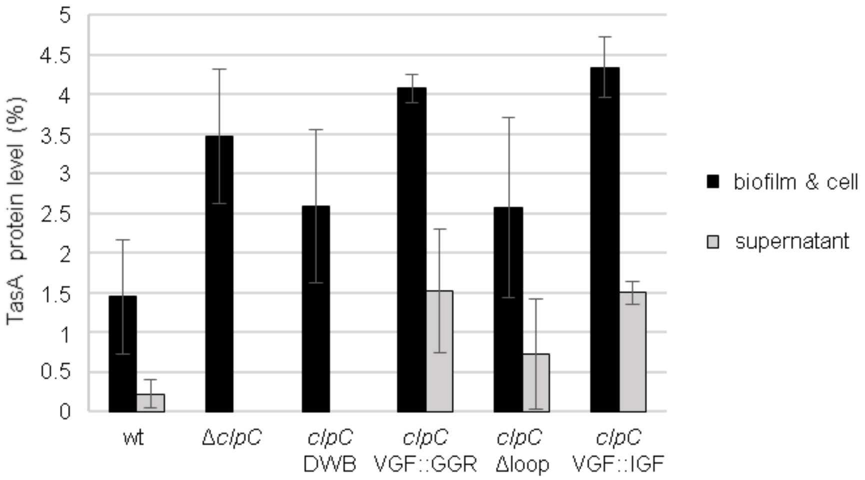

Figure 55 TasA protein levels are increased in *clpC* mutants.

For determination of TasA protein levels samples of *B. subtilis* 168 strains wt, Δ*clpC* (BRK17), *clpC* DWB (BRK19), *clpC* VGF::GGR (BRK21), *clpC* Δloop (BRK22) and *clpC* VGF::IGF (BRK23) were harvested after 2 days and divided in supernatant and biofilm & cell fractions by centrifugation. SDS-PAGE with these samples and subsequent western blotting were performed. Protein levels were calculated with ImageJ band quantification and a standard curve. Error bars display standard deviations of three biological samples.

To further examine the influence of ClpC on TasA localization under biofilm conditions, more precise sample fractionation and western blot analysis were performed. The TasA localization pattern of the *clpC* DWB mutant strain resembled the wild type, despite significant differences in phenotypes (Figure 56). Unfortunately, no fractionation of the Δ*clpC* mutant sample was possible, which might be due to decreased cell stability in this strain. The different *clpC* loop mutants (*clpC* VGF::GGR, *clpC* Δloop, *clpC* VGF::IGF) displayed a TasA localization comparable to the wild type.

These observations are consistent with previous studies showing that degradation of key regulators by ClpCP influence biofilm formation in *B. subtilis* and that for typical pellicle and wrinkle formation the presence of functional ClpC is necessary.

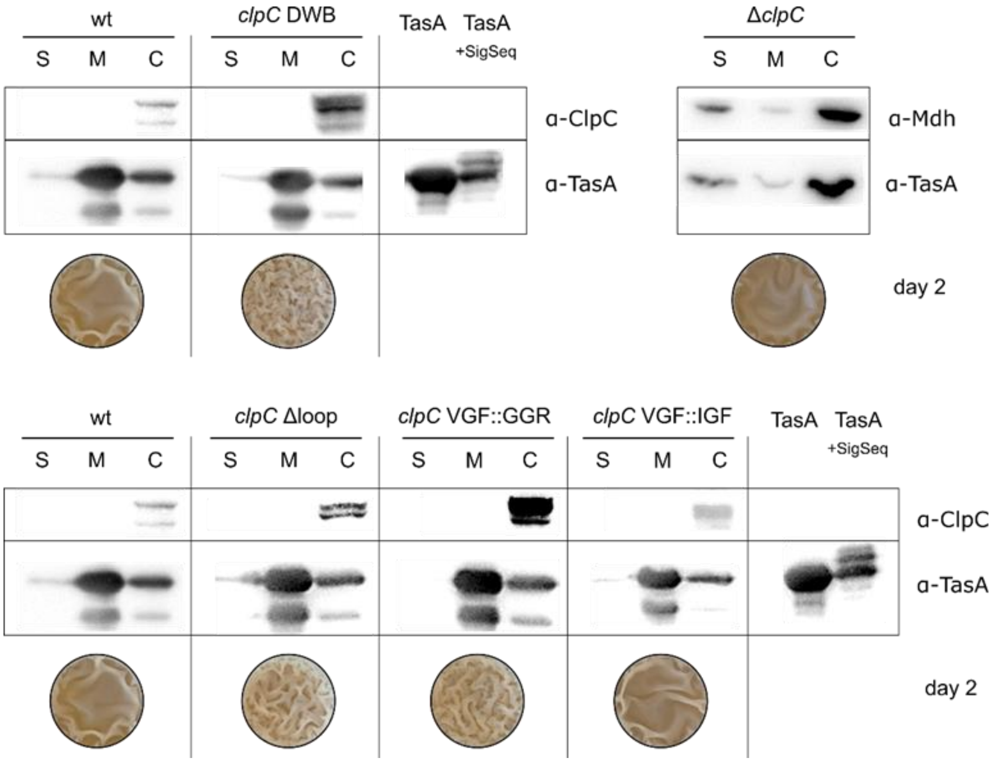

Figure 56 TasA localization is not disturbed in *clpC* mutant strains.

Harvest and fractionation of pellicle biofilm samples was performed as described previously. *B. subtilis* 168 strains wt, Δ*clpC* (BRK17), *clpC* DWB (BRK19), *clpC* VGF::GGR (BRK21), *clpC* Δloop (BRK22) and *clpC* VGF::IGF (BRK23) were fractionated in supernatant (S), matrix (M) and cell (C) samples. Subsequent SDS-PAGE and western blotting with ClpC and TasA antibody were performed with purified TasA and TasA with signal sequence (+SigSeq) as control. Pellicle biofilms of these strains after 2 days are displayed.

3.4.6 Adaptor protein YpbH could be involved in regulations via ClpCP

Until now, three adaptor proteins for ClpC, facilitating substrate specificity and ClpC activity are known, namely MecA, McsB and YpbH (Kirstein et al., 2007; Persuh et al., 2002; Turgay et al., 1998). To evaluate differences between these adaptor proteins in biofilm formation, pellicle phenotypes of mutant strains (Δ*mecA*, Δ*mcsB*, Δ*ypbH)* were analyzed.

A highly pleiotropic phenotype was observed in the Δ*mecA* mutant strain (Figure 57). On the one hand biofilm growth and wrinkle formation were impaired on day one. On the other hand, distinct wrinkles developed until day three and strong red staining with CC dye was observed. This phenotype appeared to be consistent with the already described influence of MecA on biofilm regulation by targeting of key regulator Spo0A (Prepiak et al., 2011). The Δ*mcsB* mutant strain also displayed impaired initiation of biofilm formation since no matrix was visible on day one and wrinkle formation only started at day three. Deletion of *ypbH* led to enhanced wrinkle formation even starting on day one. A strong wrinkly phenotype was visible on day three, which was comparable to *clpC* mutants preventing substrate degradation by ClpCP (*clpC* DWB, *clpC* VGF::GGR, *clpC* Δloop). These observations suggest that YpbH, besides its role in competence and sporulation, could influence ClpCP activities in biofilm formation (Persuh et al., 2002).

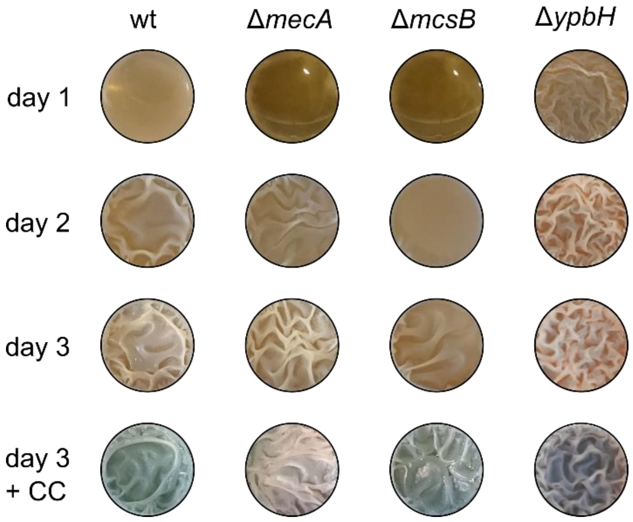

Figure 57 Deletion of ClpC adaptor proteins affects pellicle formation.

Pellicle biofilm formation of *B. subtilis* 168 strains wt, Δ*mecA* (BRK24), Δ*mcsB* (BRK25) and Δ*ypbH* (BRK26) in MOLP media were compared over 3 days and pellicle biofilms of these strains in MOLP with CC dye after 3 days are displayed.

The TasA concentrations in the different adaptor protein deletion strains were analyzed using quantitative western blots (Figure 58). The Δ*mcsB* and Δ*mecA* mutants contained higher TasA concentrations in biofilm and cell as well as supernatant fractions than the wild type, but only Δ*mecA* stained red with CC dye present (Figure 57). Though, the Δ*mcsB* and Δ*clpC* mutants display a comparable decrease in wrinkle formation despite high TasA levels. This might indicate that McsB, together with ClpC, could be involved in expression of other biofilm compounds and thus, matrix formation and TasA incorporation is affected in the deletion mutants. The TasA levels of the Δ*ypbH* strain were comparable to the wild type, while an enhanced wrinkle formation was observed in the mutant. These results are consistent with the slight red coloration of the matrix with CC dye and suggest further reasons for the hyper-wrinkly phenotype, than enhanced TasA expression.

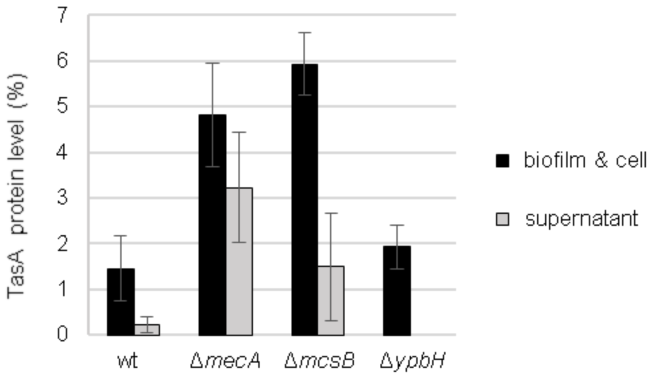

Figure 58 TasA protein levels differ in adaptor protein deletion mutants.

For determination of TasA protein levels samples of strains wt 168, ΔmecA (BRK24), ΔmcsB (BRK25) and ΔypbH (BRK26) were harvested after 2 days and divided in supernatant and biofilm& cell fractions by centrifugation. SDS-PAGE with these samples and subsequent western blotting were performed. Protein levels were calculated with ImageJ band quantification and a standard curve. Error bars display standard deviations of three biological samples.

Precise sample fractionation of ClpC adaptor protein mutants was performed to analyze the TasA localization pattern (Figure 59). The TasA distribution in all mutants was comparable to the wild type, despite the significant differences in the pellicle morphology (Figure 57). This indicated that the observed phenotypes were probably not caused by defects in TasA export.

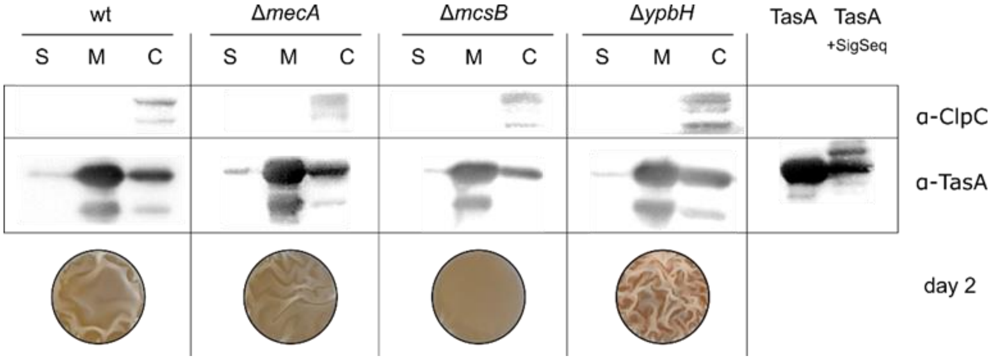

Figure 59 TasA localization is not affected in ClpC adaptor protein mutant strains.

B. subtilis strains wt 168, ΔmecA (BRK24), ΔmcsB (BRK25) and ΔypbH (BRK26) were fractionated in supernatant (S), matrix (M) and cell (C) samples. Subsequent SDS-PAGE and western blotting with ClpC and TasA antibody were performed with purified TasA and TasA with signal sequence (+SigSeq) as control. Pellicle biofilms of these strains after 2 days are displayed.

Consistent with previous studies, ClpC was observed to be involved in pellicle biofilm formation of *B. subtilis*, albeit no clear role for the chaperone in TasA folding could be determined (Chai et al., 2010a; Ogura and Tsukahara, 2010; Prepiak et al., 2011). Deletion of *clpC* probably affected matrix maturation, whereas *clpC* mutants with impaired ClpCP degradation activity contained elevated TasA levels and thus, displayed enhanced wrinkle formation. A comparable phenotype was observed in the Δ*ypbH* mutant, suggesting that this adaptor protein might be involved in regulatory proteolysis by ClpCP. Nevertheless, future experiments need to identify possible substrates for YpbH dependent ClpCP activities and evaluate the exact involvement of the adaptor protein in biofilm formation.

4 Discussion

4.1 McsB facilitates diverse ClpC dependent activities

In *B. subtilis* the AAA+ chaperone ClpC is involved in many cellular processes, such as competence development, sporulation and stress response (Krüger et al., 1994; Pan et al., 2001; Turgay et al., 1998). The influence of ClpC and protease complex ClpCP on heat stress response is linked to regulatory mechanisms, like expression of class III heat shock genes, as well as general protein quality control and removal of misfolded proteins (Kirstein et al., 2007, 2005; Krüger et al., 2000; Krüger and Hecker, 1998). In *E. coli* it was observed that a successful thermotolerance development depends on disaggregation and refolding of heat induced subcellular protein aggregates (Weibezahn et al., 2004). Since disaggregases like ClpB or ClpG, that perform this task in various Gram-negative bacteria, are absent in *B. subtilis*, ClpC has been considered to accomplish this function (Katikaridis et al., 2019; Lee et al., 2018; Schlothauer et al., 2003; Weibezahn et al., 2004). *In vitro* studies confirmed that adaptor proteins MecA and YpbH can enable ClpC dependent disaggregation and refolding of heat aggregated substrate in the absence of the protease ClpP (Schlothauer et al., 2003). However, deletion of *mecA* and *ypbH* did not result in thermosensitivity.

Besides adaptor proteins MecA and YpbH, McsB is known to facilitate ClpC dependent activities in *B. subtilis* (Kirstein et al., 2005). The adaptor protein McsB is a protein arginine kinase that is activated by McsA, and is involved in post-translational regulation and targeting of proteins to PQC systems (Elsholz et al., 2012; Kirstein et al., 2007; Macek et al., 2019; Trentini et al., 2016). In addition to high expression and activation of the arginine kinase activity under heat stress, McsB colocalizes with subcellular protein aggregates at the cell poles (Kirstein et al., 2008). The chaperones ClpC and ClpX, as well as the protease ClpP are recruited to those aggregates and it was suggested that McsB might also function as adaptor protein for ClpX (Lilge et al., 2020). Moreover, McsB is able to outcompete MecA for binding to ClpC *in vitro* (Kirstein et al., 2007). Latest *in vivo* studies confirmed that the clearance of aggregates by ClpC and associated recovery from heat shock is only possible in presence of adaptor protein McsB (Hantke, 2019). Nevertheless, the exact mechanism for removal of heat induced aggregates by either disaggregation and refolding or degradation involving McsB in *B. subtilis* has not been described yet.

4.1 Discussion

4.1.1 Adaptor protein and arginine kinase activities of McsB

In this work, the ClpC dependent disaggregation and refolding of heat induced aggregates was characterized *in vitro*. Consistent with previous studies, the adaptor protein MecA facilitated moderate ClpC dependent disaggregation and refolding of protein aggregates (Figure 8) (Schlothauer et al., 2003). With McsB/McsA activating ClpC, a slightly enhanced disaggregation activity, albeit no efficient refolding was observed (Figure 8). In contrast to adaptor protein MecA, McsB possesses arginine kinase activity, which was suggested to interfere with effective substrate refolding in this system.

In general, phosphorylation of amino acid residues can alter the properties of proteins, often resulting in activation or inhibition of enzymes as well as influencing their interaction capacity and thereby affecting many regulatory processes, as reviewed extensively (Garcia-Garcia et al., 2016; Kobir et al., 2011; Olsen et al., 2006; Soufi et al., 2008). Arginine residues are especially important for protein-protein, protein-small molecule or protein-nucleic acid interactions and phosphorylation by McsB kinase modifies the charge from positive to negative, whereby these interactions can be substantially influenced (Fuhrmann et al., 2016, 2015a, 2009; Lancelot et al., 1979; Luscombe, 2001; Schmidt et al., 2014). One example is the phosphorylation of the heat shock regulator CtsR by McsB, resulting in impaired DNA binding of the repressor (Fuhrmann et al., 2009). Furthermore, McsB dependent phosphorylation was observed to influence degradation of transcriptional modulator MgsR, which is part of the σ^B regulon (Lilge et al., 2020).

The impact of arginine phosphorylation on McsB-dependent ClpC activities was examined utilizing the kinase inactive McsB C167S mutant (Kirstein et al., 2005). The ClpC ATPase induction was reduced with McsB C167S/McsA, when compared to kinase active McsB (Figure 11 D). This is consistent with the observed decrease in ClpC disaggregation activity *in vitro* (Figure 11 A/Figure 36). Nevertheless, McsB C167S displayed a kinase independent adaptor protein function. Previous studies showed that the kinase inactive McsB C167S mutant still interferes with DNA-binding of repressor CtsR *in vitro* and functions as adaptor protein targeting transcriptional regulator MgsR for degradation *in vivo* (Kirstein et al., 2005; Lilge et al., 2020). Furthermore, a reduced aggregate removal capacity of the *mcsB* C167S mutant strain was observed under heat stress conditions *in vivo* (Hantke, 2019). Notably, McsB C167S/McsA-activated ClpC displayed improved refolding efficiency *in vitro*, compared to kinase active McsB (Figure 11 B/Figure 36). This enhanced substrate recovery with kinase inactive McsB C167S reinforces the hypothesis that arginine phosphorylation by McsB could interfere with successful substrate refolding. Moreover, the substrate recovery was dependent on the presence of McsA, even though α-pArg blots confirmed the kinase inactivity of the McsB C167S mutant (Figure 12 A, B/Figure 14 A). These observations, combined with an improved ClpC ATPase induction by McsB C167S in presence of McsA, indicate that a protein-protein interaction of McsB with McsA is important for efficient ClpC functions, independent of kinase activation (Figure 12 D).

Taken together, McsB, activated by McsA, facilitated moderate ClpC dependent disaggregation of heat induced aggregates, whereby the McsB kinase activity appeared to interfere with substrate refolding *in vitro* (Figure 8/Figure 11). Though, *in vivo* there are many factors that could influence this disaggregation and refolding process and it was assumed that an important part of the active system was missing in the initial disaggregation and refolding *in vitro* experiments.

4.1.2 A refolding system based on arginine phosphorylation and dephosphorylation

Protein arginine phosphorylation by McsB serves as reversible post-translational modification in *B. subtilis* and many regulatory factors are targets of the kinase *in vivo* (Elsholz et al., 2012; Schmidt et al., 2014). However, detection of phosphorylation on arginine residues was only possible in a strain lacking the phosphatase YwlE or in presence of phosphatase inhibitors. Because of the sequence homology, YwlE was first annotated as a tyrosine phosphatase, but later described to specifically dephosphorylate arginine residues *in vivo* and *in vitro* (Elsholz et al., 2012; Fuhrmann et al., 2013a; Kirstein et al., 2005; Musumeci et al., 2005). In *B. subtilis*, YwlE is the only arginine phosphatase and is considered to play a major role in stress sensing (Elsholz et al., 2012, 2011a; Fuhrmann et al., 2013a; Kirstein et al., 2008, 2006).

Phosphatase YwlE enables efficient disaggregation and refolding

It is known that equal amounts of YwlE and McsB/McsA inhibit the ClpC ATPase and ClpCP degradation activities *in vitro* (Kirstein et al., 2007). The inhibitory influence of YwlE on McsB activities was proposed to be independent of protein-protein interactions, since YwlE and McsB do not form a stable complex (Fuhrmann et al., 2016). Experiments with decreasing YwlE concentrations revealed that the inhibitory impact on the McsB/McsA-induced ClpC ATPase activity is relieved in presence of lowered concentrations of YwlE (Figure 9 D). These low YwlE concentrations are consistent with physiological YwlE levels (Hantke, 2019; Muntel et al., 2014). Moreover, presence of these catalytic amounts of YwlE substantially increased the disaggregation and refolding efficiency of heat induced aggregates by McsB/McsA-activated ClpC *in vitro* (Figure

9 A, B). With both, activated McsB kinase and phosphatase YwlE present, all protein aggregates were dissolved, and successful reactivation of the substrate was observed. These results imply that YwlE could also support removal of heat induced aggregates *in vivo*. Consistent with this, altered levels of YwlE can have drastic impact on aggregate removal capacities, thermotolerance and thermoresistance in *B. subtilis* (Hantke, 2019).

Specifically engineered anti-phospho-arginine antibodies (α-pArg), kindly provided by Fuhrmann et al., were utilized to monitor phosphorylation and dephosphorylation events during the disaggregation and refolding process (Fuhrmann et al., 2015b). Western blots of the *in vitro* disaggregation samples revealed arginine phosphorylation of ClpC, McsB, McsA and soluble Mdh (Figure 10 A). Remarkably, low concentrations YwlE, which no longer inhibited McsB/McsA-induced ClpC ATPase activity, catalyzed the dephosphorylation of all previously detected phosphorylated proteins, thus verifying the potent activity of this phosphatase (Figure 9 D/Figure 10 B). It is important to mention, that successful refolding was only achieved in presence of catalytic amounts of YwlE. This supports the previous suggestion, that arginine phosphorylation interfered with substrate refolding. Based on these observations, it is likely to speculate that the success of ClpC dependent disaggregation and refolding is connected to a well-balanced interplay of McsB kinase and YwlE phosphatase activities.

Notably, two cysteine residues are located in the active-site pocket of YwlE and are crucial for the phosphatase activity (Fuhrmann et al., 2013a, 2013b). Under oxidative stress conditions YwlE is inactivated by formation of a disulfide bridge between these cysteine residues (Fuhrmann et al., 2016). Experiments with a phosphatase inactive YwlE C7S mutant demonstrated that the efficient disaggregation and refolding of heat induced aggregates by ClpC depends on the phosphatase activity of YwlE (Figure 13 A, B/Figure 14 B). Nevertheless, in presence of active YwlE, the phosphorylation of proteins by McsB is necessary for disaggregation and refolding, as observed with the kinase inactive McsB C167S mutant (Figure 11 B). Furthermore, active YwlE reduced the ClpC ATPase activity, regardless of McsB kinase activity, and the inactive YwlE C7S largely decreased ClpC disaggregation activity in presence of McsB C167S/McsA (Figure 11 D/Figure 13 A). These observations imply that in addition to McsB kinase and YwlE phosphatase activities, protein-protein interactions between YwlE and other components could influence this disaggregation system.

Summarizing, both McsB kinase and YwlE phosphatase activities are required for efficient aggregate removal and refolding by ClpC *in vitro*. Other *in vivo* studies demonstrated that active McsB and YwlE are involved in thermotolerance development and aggregate clearance in *B. subtilis* (Hantke, 2019; Moliere, 2012). The data obtained in this study suggests that McsB is not only involved in CtsR regulation, but might also facilitate the ClpC dependent removal of possibly toxic protein aggregates by disaggregation and refolding under heat stress conditions, which was already shown to be important for heat tolerance in *E. coli* (Weibezahn et al., 2004).

Factors regulating McsB- and YwlE-dependent refolding

The presence of well-functioning PQC machineries is essential for the bacterial cell. This is emphasized by the severe phenotypes of *mcsB*, *clpC* or *clpP* mutants and the toxic impact of antibiotic compounds, like ADEP, resulting in unrestrained proteolysis by ClpP (Brötz-Oesterhelt et al., 2005; Elsholz et al., 2012; Kirstein et al., 2009a; Kock et al., 2004; Krüger et al., 1994; Msadek et al., 1994). Furthermore, the control over arginine phosphorylation levels in the cell is of importance, since a deletion of *ywlE* resulted in global transcriptomic changes (Elsholz et al., 2012). Under normal conditions, the arginine kinase activity of McsB is inhibited by binding to ClpC and counteracted by YwlE *in vivo* and *in vitro* (Elsholz et al., 2011b; Kirstein et al., 2007). Upon heat shock, the expression of class III heat shock genes rises, including the repressor *ctsR*, as well as *mcsB*, *mcsA* and *clpC* (Krüger and Hecker, 1998). The inhibitory ClpC interaction with McsB is decreased, which leaves place for kinase activation by McsA and phosphorylation of substrates (Elsholz et al., 2011b).

To gain more insight into the possible function of the disaggregation and refolding system, *in vitro* order-of-addition experiments were performed with McsB kinase activator McsA and phosphatase YwlE. These experiments indicated that addition of McsA activated McsB kinase and facilitated ClpC dependent disaggregation and refolding at any point of time in presence of YwlE (Figure 15/Figure 16). In contrast to previous experiments, YwlE did not quickly dephosphorylate proteins and phosphorylation was even detected in the presence of YwlE, suggesting that the phosphatase might be inactivated by incubation without activated McsB. Consistent with this, weak oligomerization was proposed to inactivate YwlE and cognate tyrosine phosphatases in the absence of phosphorylated substrate and with increasing substrate concentrations the phosphatase is reactivated (Blobel et al., 2009). Furthermore, order-of-addition experiments with YwlE revealed that successful disaggregation and refolding upon phosphatase addition was only possible when phosphorylated proteins were still detected in the sample (Figure 17/Figure 18). This agrees with previous observations, that the positive impact of YwlE on disaggregation and refolding is directly linked to its phosphatase activity (Figure 13).

The described protein quality control system characterized in this thesis, consists of AAA+ protein ClpC, arginine kinase McsB, its activator McsA and phosphatase YwlE. Both McsA and YwlE are redox-sensing proteins and take part in heat- and oxidative stress response systems in *B. subtilis* (Elsholz et al., 2011b; Fuhrmann et al., 2016). These stress response systems are intricately interwoven, since the expression of class III heat shock genes, under control of repressor CtsR is also induced during oxidative stress (Leichert et al., 2003; Mostertz et al., 2004). In contrast to CtsR inactivation by an intrinsic thermosensor upon heat stress, McsA serves as redox sensor enabling McsB dependent CtsR de-repression under oxidative stress conditions (Elsholz et al., 2011b, 2010). It is tempting to speculate, that the redox sensitivity of McsA and YwlE could influence the here described ClpC dependent disaggregation and refolding machinery under different stress conditions. Upon oxidative or severe heat stress, YwlE and McsA might be inhibited and the protein control machinery, formerly refolding substrates could be switched to degradation of proteins irreversibly damaged by these severe conditions. Consistent with this hypothesis, *in vivo* studies observed that the ClpCP degradation activity is important for the removal of puromycin induced aggregates, containing truncated and misfolded proteins, that cannot be refolded (Hantke, 2019).

The mechanism of McsB and YwlE dependent refolding

McsB kinase and YwlE phosphatase were observed to be necessary for an efficient ClpC dependent disaggregation and refolding system. Therefore, the detailed operating principle of this mechanism was further characterized. Previous experiments suggested that protein arginine phosphorylation by McsB interferes with efficient substrate refolding *in vitro* (Figure 8/Figure 11). Notably, arginine phosphorylation of model substrate Mdh could only be observed in the soluble fractions *in vitro*, indicating that substrate proteins are most probably still phosphorylated after ClpC translocation and disaggregation (Figure 10 A/Figure 14 B). This McsB dependent phosphorylation might stabilize the unfolded and soluble state of substrate proteins. The phosphorylation of highly disordered proteins containing serine-arginine rich regions was already shown to increase their solubility, as well as phosphorylation of yeast or soybean proteins used in food production (Campbell et al., 1992; Huang and Kinsella, 1986; Nikolakaki et al., 2008). In the case of this refolding system. it was hypothesized that substrate phosphorylation by McsB could stabilize the unfolded state of the substrate after disaggregation by ClpC. Subsequent dephosphorylation of the soluble proteins by catalytic amounts of YwlE might then enable controlled refolding and substrate recovery.

To test this hypothesis, a special disaggregation and refolding experiment was set up. The McsB/McsA induced ClpC disaggregation of phosphorylated substrate was stopped after 15 min by addition of a ClpC trap mutant (ClpC DWB). This ClpC DWB trap mutant binds adaptor proteins and forms a hexameric barrel, but ATP hydrolysis and thus, substrate processing is not feasible in this mutant (Kirstein et al., 2006). As expected, an extended complex formation peak was observed upon addition of ClpC DWB, since the substrate translocation was stopped, similar to experiments with a ClpB trap mutant from *E. coli* (Figure 20 A) (Weibezahn et al., 2003). Furthermore, no relevant Mdh activity could be recovered, supporting the first part of the hypothesis, that arginine phosphorylation interferes with successful refolding. Addition of YwlE, simultaneous with ClpC DWB, enabled recovery of Mdh activity in the extent of previously disaggregated substrate (Figure 20 A, B). Thus, endorsing the second part of the hypothesis, that dephosphorylation of the disaggregated substrate by YwlE could assist substrate refolding. These observations strongly indicate that the mechanism for protein recovery depends on phosphorylation of substrates by activated McsB, disaggregation by ClpC and subsequent dephosphorylation by YwlE, supporting refolding of substrate proteins.

Comparable protein folding systems based on phosphorylation and dephosphorylation of the substrate are not described until now. However, in eukaryotes different post-translational modifications (PTM) are supporting protein maturation in the endoplasmatic reticulum (ER). Protein glycosylation is known to improve the stability and solubility of unfolded proteins, whereat protein folding depends on coordinated trimming of the PTM as well as interaction with chaperones of the protein quality control system (Jayaprakash and Surolia, 2017; Xu and Ng, 2015). Furthermore, a site-specific ubiquitination and deubiquitination cycle at the ER membrane is involved in chaperone assisted protein folding of a signaling coreceptor (Perrody et al., 2016). In prokaryotes many chaperone-dependent protein folding systems are described so far. They are highly diverse and can function via, e. g. ATP-dependent substrate binding and release (DnaK, DnaJ, GrpE) (Szabo et al., 1994), ATP-dependent substrate binding, encapsulation and release (GroELS) (Chen et al., 2013; Hayer-Hartl et al., 2016) or by ATP-independent substrate encapsulation and release (trigger factor) (Singhal et al., 2015). However, the exact processes promoting protein folding are often not completely understood and the data obtained in this work indicates that PTM based folding mechanisms also occur in bacteria and need to be further investigated.

4.1.3 Aggregate removal by protein rescue or degradation

The hexameric AAA+ protein ClpC can associate with heptameric ClpP to form a protease complex and ClpC adaptor proteins target substrates for degradation (Kirstein et al., 2007; Schlothauer et al., 2003; Turgay et al., 1998). Recent studies observed, that proteins phosphorylated by McsB can be recognized by the N-terminal domain of ClpC and are thus targeted to ClpCP for degradation in absence of adaptor proteins (Trentini et al., 2016). However, the targeting of heat shock regulator CtsR by McsB to protease complex ClpCP does not depend on phosphorylation of the substrate, but on McsB as adaptor protein *in vivo* (Elsholz et al., 2010). Furthermore, McsB is degraded by ClpCP, but under heat shock conditions YwlE prevents rapid degradation of McsB *in vivo* (Elsholz et al., 2010; Kirstein et al., 2005). Therefore, experiments with ClpP were performed to assess the involvement of ClpC in disaggregation and ClpCP in degradation as well as possible influences on the McsB and YwlE dependent refolding *in vitro*.

The addition of ClpP to the disaggregation experiment did not only result in complete aggregate removal and substrate degradation, but moderate protein refolding occurred with McsB/McsA-activated ClpCP (Figure 21/Figure 29). As observed before, the ClpC ATPase activity was increased in presence of ClpP (Figure 24 A) (Turgay et al., 1998). These results are consistent with studies showing that high ATPase rates and fast substrate translocation support the ClpXP degradation activity (Martin et al., 2008). Furthermore, interactions between chaperone and protease via highly conserved loops were observed to contribute to their activity (Kim et al., 2001). In *E. coli* the ClpX P-loop stabilizes the ClpX-ClpP interaction, and further dynamic contacts between ClpX pore-2-loops and N-terminal loops of ClpP can regulate ATPase rates for efficient activities (Martin et al., 2007). Thus, the efficacies of substrate degradation by AAA+ proteases or disaggregation by AAA+ chaperones are dependent on a specific interplay between ATPase- and translocation rate, unfolding force of the chaperone, interaction with the protease, as well as properties of the substrate itself (Martin et al., 2008). The results of this work suggest that a dynamic interaction between ClpC and ClpP might allow a small substrate fraction to escape from full degradation. Consistent with this, the substrate transition between Clp chaperones and ClpP was considered to be facilitated by ATP dependent conformational changes, resulting in rotation-like movements of the chaperone on the protease (Beuron et al., 1998; Lopez et al., 2020; Ripstein et al., 2020).

Remarkably, addition of protease ClpP to the complete refolding system, including YwlE, did not result in the expected substrate degradation. In presence of both, YwlE and ClpP, substrate disaggregation and refolding activities were favored (Figure 22). This impact of YwlE, interfering with substrate degradation and promoting recovery, was observed to be mainly connected to the phosphatase activity (Figure 24 B). Application of the phosphatase inactive YwlE C7S mutant did not affect the low refolding activity in presence of ClpP, but impaired ClpC dependent aggregate removal (Figure 23). It is tempting to speculate, that YwlE C7S interaction with compounds of this system could occur via pArg residues, thus altering ClpC and ClpCP activities (Fuhrmann et al., 2013a). Thereby it is unlikely, that direct protein-protein interaction of YwlE with ClpCP result in conformational changes affecting the induced degradation efficiency, because YwlE had no impact on MecA dependent substrate degradation by ClpCP (Figure 24 B). Since most phosphorylated substrate was detected in the soluble fraction, it is also possible that the translocated substrate is not always directly handed over to ClpP for degradation, but highly active YwlE has the opportunity to dephosphorylate, thus facilitating refolding instead of degradation of substrates (Figure 10 A/Figure 14 B).

Different models describe the unfolding of proteins by barrel shaped AAA+ chaperones and protease complexes. Mechanical pulling of the substrate through the axial pore can unfold proteins and either direct full translocation of the substrate or several binding, pulling and release cycles could be performed (Cordova et al., 2014; Kenniston et al., 2005; Li et al., 2015). However, the substrate properties might contribute to the applied unfolding mechanism, since even highly knotted polypeptide chains can enter the flexible ClpXP pore for degradation, while other stable, native proteins require repeated binding and pulling by ClpXP in *E. coli* (Kenniston et al., 2005; Lee et al., 2001; Sivertsson et al., 2019). The disaggregation and unfolding of protein aggregates by the ClpB/KJE system depends on partial threading, without unfolding of native protein domains, which suffices for reactivation of heat aggregated substrates (Haslberger et al., 2008). Nevertheless, ClpB does not interact with a protease and is less stable than ClpC. Notably, MecA-activated ClpC disaggregates the whole substrate, regardless of domain structure, transferring it directly to ClpP for degradation (Haslberger et al., 2008). Taking this in account, the results of this work might indicate that McsB and YwlE could destabilize the interaction between ClpC and ClpP, thus allowing refolding of substrates in presence of the protease. Since both ClpC and ClpP are phosphorylated by McsB, dephosphorylation by YwlE could possibly alter protein-protein interactions and threading mechanics in this system (Figure 24) (Elsholz et al., 2012; Schmidt et al., 2014).

Different studies suggested a connection between the McsB kinase activity and ClpCP dependent substrate degradation. Apparently, the kinase inactive McsB C167S mutant is not degraded by ClpCP *in vitro* and CtsR is stabilized in a *mcsB* C167S mutant strain under heat shock conditions *in vivo* (Elsholz et al., 2010; Kirstein et al., 2007). Nevertheless, β-casein was still degraded by McsB C167S/McsA-activated ClpCP, but not as efficient as with kinase active McsB/McsA (Figure 27 D). This reduced degradation activity was further decreased in presence of active YwlE, suggesting that not only McsB kinase and YwlE phosphatase activities but also interactions between YwlE and ClpC or ClpP might play a role in this system (Figure 27 D). These experiments are consistent with previous observations, that McsB C167S can act as adaptor protein for ClpC and enables decreased aggregate clearance *in vivo* (Figure 11) (Hantke, 2019). However, an efficient ClpCP substrate degradation facilitated by McsB appeared to depend on both, the adaptor protein function, as well as the arginine kinase activity.

Disaggregation and refolding of model substrate Citrate synthase

In vivo a big variety of substrate proteins are processed by the bacterial protein quality control system. Therefore, different model substrates are utilized for *in vitro* examination of chaperone and protease systems, such as heat inactivated Mdh, luciferase, α-Glucosidase or citrate synthase (Cs) for investigation of the *E.coli* ClpB/KJE system (Katikaridis et al., 2019; Mogk et al., 2003b, 2003a; Schlieker et al., 2004; Weibezahn et al., 2004). In addition to model substrate Mdh, the ClpC dependent disaggregation and refolding of heat aggregated citrate synthase (Cs) was examined in this work. The complete removal of aggregates was not achieved, consistent with other studies utilizing this substrate (Figure 36 A/Figure 37 A) (Katikaridis et al., 2019). In contrast to experiments with the model substrate Mdh, McsB/McsA-activated ClpC facilitated ample refolding of Cs even in the absence of YwlE (Figure 36 B/Figure 8 B). Nevertheless, application of kinase inactive McsB C167S or addition of YwlE again improved the refolding efficiency, consistent with the experiments utilizing Mdh (Figure 36 B/Figure 37 B). Furthermore, presence of ClpP also enhanced refolding of Cs, although Cs did not appear to be a substrate for degradation by McsB/McsA-activated ClpCP (Figure 37 D). Notably, the ClpC ATPase activity was not increased in presence of ClpP and Cs, consistent with studies observing a reduced ClpXP ATPase activity in presence of stable substrates (Figure 37 C) (Burton, 2001). However, the experiments with Cs as model substrate indicate that the ClpC dependent disaggregation and refolding system, based on substrate phosphorylation by McsB and dephosphorylation by YwlE, enhanced the refolding efficiency with different substrates and may also improve aggregate clearance and protein rescue *in vivo*.

Model of ClpC dependent disaggregation and refolding *in vivo*

In particular, the disaggregation and refolding of heat impaired proteins is an efficient system for removal of subcellular protein aggregates and occurs among many species, implying that the characterized protein rescue systems may fulfill this task in *B. subtilis* (Mogk et al., 2018; Wallace et al., 2015; Weibezahn et al., 2004). Here, a model is proposed for ClpC dependent disaggregation and refolding of possibly toxic heat induced aggregates *in vivo,* based on results of experiments in this work as well as previous studies. Under non-heat shock conditions, the adaptor protein and arginine kinase McsB is mostly inactivated by ClpC and YwlE, leaving place for e.g. MecA-dependent ClpC activity (Figure 60) (Elsholz et al., 2011a; Kirstein et al., 2007). Upon heat shock, the repressor of class III heat shock genes, CtsR, is inactivated by an intrinsic thermosensor and expression of the *clpC*-operon, including *mcsB* and *mcsA*, rises, whereas transcription levels of *ywlE* only increase slightly (Maaβ et al., 2014; Nicolas et al., 2012). At the same time, the McsB interaction with ClpC is decreased, allowing McsB kinase activation by McsA, and rapid degradation of McsB is prevented by YwlE (Elsholz et al., 2011a, 2010). During heat stress the components of the here described disaggregation and refolding system localize at subcellular protein aggregates and could facilitate their removal (Kirstein et al., 2008). The misfolded and aggregated proteins are probably targeted for ClpC dependent disaggregation by McsA-activated McsB (Hantke, 2019). Arginine phosphorylation could stabilize the unfolded substrate and subsequent dephosphorylation by YwlE might assist correct refolding and substrate recovery instead of degradation, thus supporting protein homeostasis in *B. subtilis*.

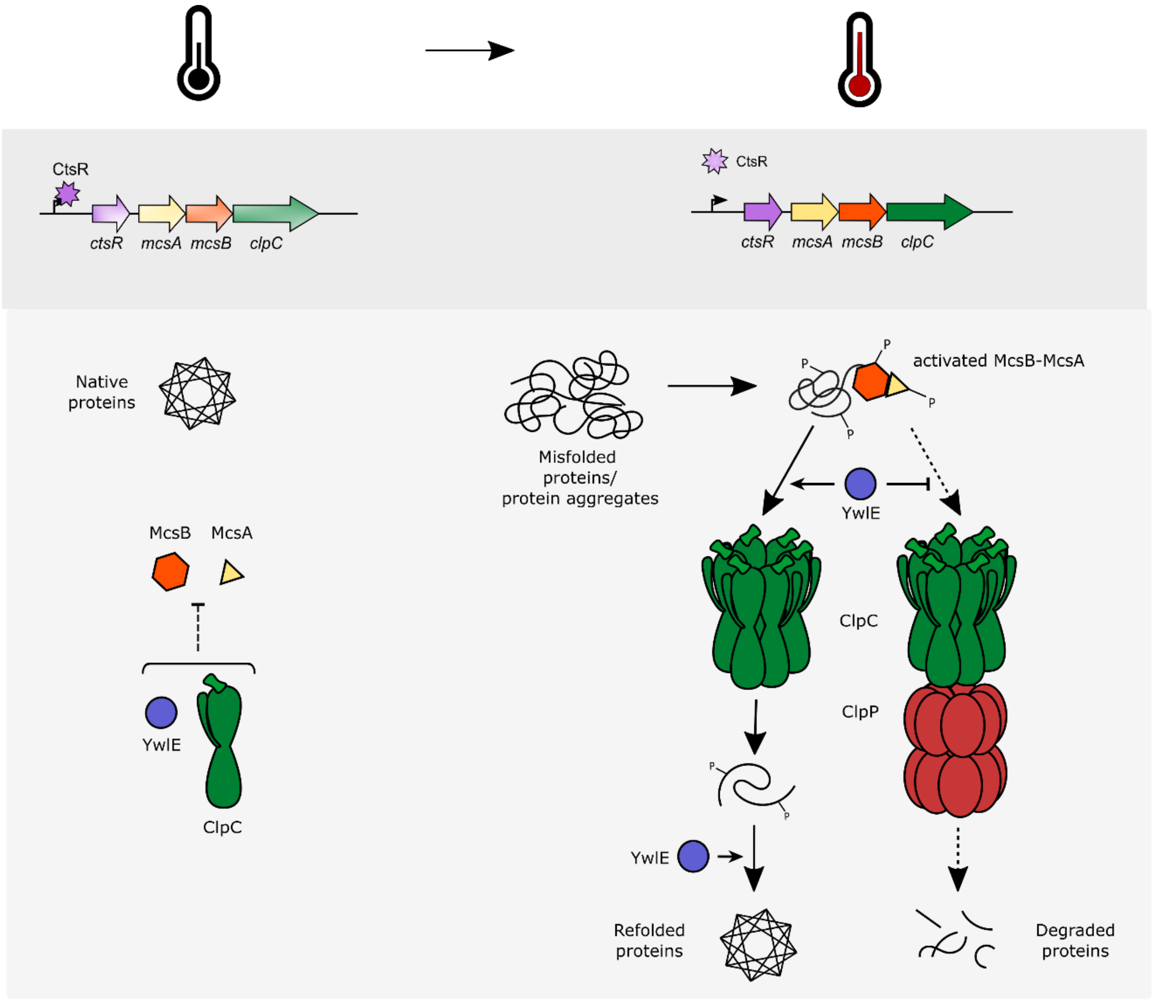
CtsR
ctsR
mcsA
mcsB
clpC
CtsR
ctsR
mcsA
mcsB
clpC
Native proteins
Misfolded proteins/ protein aggregates
activated McsB-McsA
P
P
P
P
YwlE
McsB
McsA
ClpC
ClpP
YwlE
ClpC
P
P
YwlE
Refolded proteins
Degraded proteins

Figure 60 Schematic model of ClpC, McsB, McsA, YwlE roles in the PQC system.

Under normal conditions transcription of the *clpC* operon is repressed by CtsR and both ClpC and YwlE interfere with kinase activation of McsB (Elsholz et al., 2011a; Kirstein et al., 2007). Upon heat shock, CtsR is inactivated by an intrinsic thermosensor and the *clpC* operon is highly expressed (Elsholz et al., 2010). McsA can activate McsB, which targets protein aggregates and promotes ClpC- and YwlE-dependent disaggregation and refolding rather than ClpCP-dependent degradation.

4.1.4 The properties of the ClpCP interaction enable degradation and refolding

In *B. subtilis*, disaggregation and refolding of heat impaired substrates is dependent on AAA+ chaperone ClpC, as indicated by observations of this thesis and previous studies (Hantke, 2019). Nevertheless, ClpC possesses a P-loop, containing a highly conserved tripeptide (VGF), which facilitates the interaction with hydrophobic pockets on the surface of protease ClpP (Kim et al., 2001). *In vivo*, the thermosensitive phenotype of a Δ*clpC* mutant was already observed to be restored in a *clpC* mutant with altered P-loop (VGF::GGR) in *B. subtilis* (Figure 34 A, B) (Moliere, 2012). This ClpC VGF::GGR mutant facilitated substrate disaggregation and refolding *in vitro*, while no substrate degradation could take place, due to impaired ClpC-ClpP interaction (Figure 28 B/Figure 29). *In vivo* studies demonstrated, that the disaggregation activity of this ClpC VGF::GGR mutant is sufficient for aggregate clearance (Hantke, 2019). Thus, the ClpCP degradation activity was dispensable for thermotolerance development and recovery from heat shock in *B. subtilis*. However, ClpC can fulfil both activities, disaggregation and refolding of substrates as well as degradation in complex with ClpP and the question remains, if one activity could be favored under heat stress conditions *in vivo* or if a special set of proteins is refolded while others are degraded. This could be resolved in future experiments with mass spectrometric approaches and pulse-chase analysis to examine protein levels in different mutant strains under various conditions.

In this study, the ClpC VGF tripeptide on the P-loop tip was substituted by an IGF, present in e.g. ClpX or *E. coli* ClpA. The amino acids valine and isoleucine differ only in one methyl group, but this change was already observed to influence the ligand selectivity a protein (Yuan et al., 2010). Notably, a substitution of the *E. coli* ClpX IGF tripeptide with VGF largely decreased the ClpXP degradation efficiency *in vitro* (Amor et al., 2019). Consistent with this, a ClpC VGF::IGF substitution mutation substantially increased degradation rates of MecA- and McsB/McsA-activated ClpCP, while the ATPase activity was comparable to wild type ClpC (Figure 31). This impact is probably caused by an improved association between ClpC and ClpP as suggested by titration experiments (Figure 39). But neither surface plasmon resonance (SPR) spectroscopy experiments by Jolene Pörschke (Master´s thesis, Institute for Microbiology, LUH) nor Microscale thermophoresis (MST) experiments were able to support this yet. Especially the multiple protein interactions between adaptor proteins facilitating ClpC oligomerization and subsequent ClpP binding, complicate the intricate setup. In the future, isothermal titration calorimetry (ITC), specific pull-down experiments or additional buffer and adaptor protein systems for MST could be investigated. Nevertheless, application of the ClpC VGF::IGF mutant in the disaggregation and refolding assay revealed remarkable results. While ClpC VGF::IGF was able to refold substrate in presence of YwlE more effectively than wild type ClpC, addition of ClpP resulted in substrate degradation (Figure 32/Figure 33). Thus, compared to wild type ClpCP, the degradation activity was not affected by the phosphatase YwlE (Figure 22). These observations suggest that the ClpC VGF::IGF mutant overcame the inhibitory impact of YwlE in presence of ClpP, most probably due to the proposed increased ClpC-ClpP affinity. In conclusion, *B. subtilis* ClpC with the VGF tripeptide for ClpP interaction might be perfectly equipped for degradation as well as reactivation of substrates under distinct conditions.

The *clpC* VGF::IGF mutant *in vivo*

Since ClpC is highly involved in thermotolerance development, a *clpC* VGF::IGF mutant strain was characterized regarding heat stress phenotypes *in vivo*. Only marginal improvements in thermotolerance and thermoresistance were observed compared to the wild type (Figure 34 C). This ClpC mutant may enable enhanced degradation of damaged proteins *in vivo*, resulting in the slight advantage under heat stress conditions. However, ClpC activity and substrate recognition still depend on adaptor proteins (Battesti and Gottesman, 2013; Kirstein et al., 2009b, 2006). Therefore, ClpC VGF::IGF-ClpP probably processed the same substrates as wild type ClpCP, but it still needs to be evaluated whether the mutant could interfere with protein rescue *in vivo*.

In vivo studies focusing on transcriptomic changes in *clpC* P-loop mutant strains, revealed further insight into the involvement of ClpCP in many regulatory pathways (Jolene Pörschke, Master´s thesis, Institute for Microbiology, LUH). A loss of ClpCP degradation activity in the *clpC* VGF::GGR mutant strain affected transcription of key regulators in competence development, possibly due to missing degradation of ComK/ComS, as well as several heat stress and oxidative stress related regulators. A *clpC* VGF::IGF mutant strain displayed no significant changes compared to the wild type strain, probably because of already discussed control over substrate selection by adaptor proteins. However, it needs to be assessed in future experiments if the enhanced degradation activity of the ClpC VGF::IGF mutant in complex with protease ClpP can also be observed *in vivo*.

Moreover, it would be interesting to have a closer look on ClpE and its special features. This AAA+ Hsp100 consists of a hybrid structure, with the N-terminal domain of ClpX and linker-domain, double Walker B domains and VGF tripeptide in the P-loop comparable to ClpC. Under severe heat stress conditions ClpE is highly expressed and was shown to take part in CtsR regulation and presumably disaggregation of substrates (Derre et al., 1999; Derré et al., 1999; Gerth et al., 2004; Miethke et al., 2006). ClpE can be activated without help of adaptor proteins dependent on the N-terminal zinc finger, but nevertheless interacts with McsB, which was recently proposed to be also an adaptor protein for ClpX (Elsholz et al., 2011a; Lilge et al., 2020; Miethke et al., 2006). So far, not much is known about the exact disaggregation and degradation mechanics of ClpE. In its role as supporter of protein quality control under severe stress conditions, it might be possible that ClpE could possess an even higher disaggregation activity than ClpC with a broader substrate spectrum acquired by the distinct N-terminal domain. Recently, the disaggregase ClpG was shown to be the dominant disaggregase with higher unfolding force than the established ClpB/KJE system, in various bacteria (Katikaridis et al., 2019).

4.1.5 Differences in adaptor protein dependent ClpC activation

Activation of AAA+ protein ClpC can be facilitated by N-terminal and linker domain interaction with adaptor proteins in *B. subtilis* (Kirstein et al., 2006). These adaptor proteins select substrates and target them to ClpC for disaggregation or degradation by the ClpCP complex. The adaptor protein MecA contains a N-terminal domain (NTD) and a C-terminal domain (CTD) (Kirstein et al., 2006; F. Wang et al., 2009). The NTD recruits and binds substrate proteins and the CTD facilitates ClpC oligomer formation and activation. Deletion of the ClpC NTD or linker domain results in strongly reduced MecA binding (Kirstein et al., 2006). Furthermore, a mutation on the tip of the linker domain, *clpC* F436A, severely affected *S. aureus* and *B. subtilis* ClpC activities (Carroni et al., 2017). Activation of this ClpC F436A mutant is still possible with McsB, but not with adaptor protein MecA *in vitro* (Hantke, 2019). Other mutations in the NTD of ClpC were shown to affect only the activation by McsB. The protein arginine kinase McsB phosphorylates different residues of ClpC *in vivo* and *in vitro* and phosphorylation of ClpC R5 and ClpC R254 were observed to be substantial for McsB dependent but not for MecA dependent ClpC activation (Elsholz et al., 2012). Likewise, substitution mutations of E32 and E106 in the NTD of ClpC prevent recognition of phosphorylated substrate, while activation via adaptor protein MecA is still possible (Trentini et al., 2016).

In this study, additional substitution mutations in the N-terminal adaptor protein interaction site of ClpC were identified to alter ClpC ATPase and ClpCP degradation activities (Figure 38). Different activation patterns of the ClpC R9A mutant by MecA or McsB/McsA were observed. MecA facilitates full activation of ClpC R9A, whereas the McsB/McsA dependent activation was affected. Furthermore, activation of the ClpC R83A mutant was impaired with both adaptor proteins and the ClpC R9A R83A double mutant could not be activated at all. In addition to this, variances in protein degradation by either MecA- or McsB/McsA-activated ClpCP were observed. Notably, MecA facilitated accelerated substrate degradation by ClpCP, when compared to McsB/McsA (Figure 39). Degradation of the adaptor protein MecA only started after approximately 80 % of substrate was degraded, while McsB degradation occurred simultaneous with the substrate. These results imply that MecA can be “reused” as adaptor protein for degradation, while McsB might be degraded attached to the substrate. These observations strongly suggest that different ClpC activation mechanisms occur, facilitated by adaptor proteins MecA and McsB. The distinct properties of these adaptor proteins, such as the arginine kinase activity of McsB, could result in alterations of substrate degradation by ClpCP.

In conclusion, this work presents that the AAA+ protein ClpC from *B. subtilis* can fulfil various functions, whereby different activation mechanisms by adaptor proteins MecA or McsB could alter affiliated ClpC activities. Moreover, a ClpC dependent disaggregation and refolding system for removal of heat induced aggregates was characterized *in vitro*. The refolding mechanism was proposed to depend on a well concerted interplay of both McsB kinase and YwlE phosphatase activities.

4.2 TasA and ClpC are important for pellicle biofilm formation

In the second part of this thesis biofilm formation of Gram-positive model organism *B. subtilis* was examined. In general, biofilm formation is the most abundant lifestyle of bacterial communities and relevant for several domains of research in medicine or agriculture (Hunter, 2008). A broad knowledge of biofilm formation is crucial for treatment of different diseases caused by pathogenic bacteria, since these biofilm communities exhibit a higher tolerance against external influences, such as host immune responses or antibiotics (Donlan, 2002; Mah, 2012; Olsen, 2015). However, these advantages are also shared by bacterial biofilms formed on plants (Danhorn and Fuqua, 2007). Soil-dwelling *B. subtilis* as well as many other bacteria colonize plant roots, acting as phytopathogen or forming a symbiotic relationship, which can enhance plant growth and thereby even improve crop yield (Bogino et al., 2013; Hashem et al., 2019; Ramakrishna et al., 2019). Because of this wide-ranging significance of biofilms, a detailed insight into regulation of biofilm formation and matrix composition is essential.

In this study structural characteristics of TasA, one of the most abundant biofilm matrix components, were investigated in *B. subtilis* (Branda et al., 2006; Romero et al., 2010). This protein was first described to be associated with spore formation and to possess antimicrobial properties (Stöver and Driks, 1999b). Processing by signal peptidase SipW is essential for TasA secretion and assisted by TapA, TasA forms extracellular amyloid-like fibrils (Romero et al., 2011, 2010; Stöver and Driks, 1999b, 1999a). *In vitro* studies observed that specific pH and surface conditions can promote TasA fibril formation, comparable to the self-assembly of other bacterial amyloids, e.g. chaplins from *S. coelicolor* (Bokhove et al., 2013; Chai et al., 2013; Diehl et al., 2018; Ekkers et al., 2014; Keller et al., 2011; Moores et al., 2011). So far, only the bacteriotoxin Mcc from *K. pneumoniea* and the transcription termination factor Rho from *C. botulinum* have been proposed to share functions of fungal prion proteins, which can self-propagate amyloid formation (Liebman and Chernoff, 2012; Shahnawaz et al., 2017; Wickner et al., 2007; Yuan and Hochschild, 2017). The prion propagation of yeast protein is supported by the Hsp104 chaperone system in *S. cerevisiae* and the ClpB chaperone system in *E. coli* (Chernoff et al., 1995; Yuan et al., 2014).

In bacteria, the assembly of functional amyloids is often facilitated by various protein interactions, e. g. chaperones supporting formation of curli amyloid fibrils in *E. coli* (Cámara-Almirón et al., 2018; Nenninger et al., 2009; Shu et al., 2016). These functional amyloids were observed to have different roles in virulence, reproduction and especially in biofilm formation (Chapman, 2002; Claessen, 2003; Dueholm et al., 2010; Oh et al., 2007; Romero et al., 2010). In *B. subtilis* amyloid-like TasA fibrils stabilize the extracellular biofilm matrix and deletion of *tasA* severely impairs biofilm formation (Romero et al., 2010).

Pellicle biofilms of *B. subtilis* were examined regarding the essential functions of the *tapA-sipW-tasA* operon and TasA localization in matrix formation. The laboratory *B. subtilis* strains wild type DK 1042 and the more domesticated strain wild type 168 were utilized to examine the phenotypes of different mutants in pellicle formation (see section 1.4.2) (Konkol et al., 2013; Zeigler et al., 2008). Comparison of both strains revealed more distinct wrinkle formation and accelerated biofilm growth in strain DK 1042 (Figure 41). As expected, deletion of *tasA* affected the biofilm formation and strain DK 1042 developed a flat biofilm, whereas no matrix formation was observed in strain 168. Deletion mutants of signal peptidase W (*sipW*) or the whole *tapA-sipW-tasA* operon fully impaired biofilm formation in both strains, consistent with previous studies (Branda et al., 2006; Hamon et al., 2004; Romero et al., 2010). TapA was described to support TasA fibril formation and facilitates attachment of these fibrils to the cell surface (Romero et al., 2011). Since TapA and TasA export depends on SipW, which processes the N-terminal signal sequence of these proteins, it was expected that no functional TasA could be secreted in absence of SipW (Figure 43 D) (Stöver and Driks, 1999b, 1999a). The differences in biofilm formation between the *B. subtilis* strains were probably caused by various mutations in strain 168, which influence biofilm associated regulations and alter the pellicle matrix less robust (see section 1.4.2) (McLoon et al., 2011). Nevertheless, it needs to be kept in mind, that distinct laboratory stocks of strain 168 are used in different research groups. The ability of these 168 strains to form complex colonies and pellicles was observed to vary (Gallegos-Monterrosa et al., 2016). Since these variations can complicate comparison between different studies, many mutants were compared in strain 168 and DK 1042, during this work. The strain DK 1042 is closely related to the “wild ancestor” NCIB 3610 and only comprises one mutation facilitating genetic studies (Konkol et al., 2013). Therefore, different aspects of biofilm formation are often examined in strain DK 1042 (Dragoš et al., 2018; Earl et al., 2019; Gallegos-Monterrosa et al., 2016; Otto et al., 2019; Richter et al., 2018).

4.2.1 PPII helices contribute to the structural integrity of TasA

In vitro, TasA was already described to form fibrils, which can undergo structural changes in different pH and surface conditions (Chai et al., 2013; Romero et al., 2010). During this work, the form of TasA fibrils in the biofilm matrix *in vivo* was resolved in cooperation with Dr. Anne Diehl, Dr. Yvette Roske, Prof. Dr. Hartmut Oschkinat et al. (Diehl et al., 2018). It was observed that addition of recombinantly produced TasA to a Δ*tasA* mutant restored the wrinkly biofilm phenotype in *B. subtilis* DK 1042, consistent with previous studies (Figure 44) (Romero et al., 2010). Biofilms were then reconstructed with ^{2}H,^{13}C,^{15}N-TasA$_{261}$ and harvested for NMR studies (Diehl et al., 2018). Examination of recombinantly produced TasA in NMR experiments revealed that three distinct structural forms could occur, the monomeric form and two aggregated high-molecular-weight forms, one with high helical or loop structure content and the other with high β-structure-content. Comparison with the matrix incorporated TasA demonstrated that *in vivo* probably β-sheet-rich, homogenous fibrils occur, which are resistant against extracellular proteases.

The resolved crystal structure of monomeric TasA displayed two dynamic sections with polyproline II (PPII) helical structure (Figure 45) (Diehl et al., 2018). PPII helices are, besides commonly occurring α-helices and β-sheets, an important conformation in folded polypeptide chains (Adzhubei and Sternberg, 1993). These structures can provide elasticity, support protein-protein interactions and were observed to be involved in self-assembly of fibril and prion proteins (Adzhubei et al., 2013; Camilloni et al., 2012; Gill, 2000). Therefore, the importance of the PPII helices in the structure of *B. subtilis* TasA for biofilm formation was investigated by examination of strains with *tasA* alanine substitution and deletion mutations in PPII helix 1 and 2.

TasA PPII helix 1 supports SipW dependent processing and export

The described PPII helix 1 is located near the N-Terminus of TasA and comprises amino acids A40, S41 and G42. Mutant strains *tasA* T38A and *tasA* F39A did not exhibit apparent differences in pellicle phenotypes or TasA export patterns, as expected, because the substituted amino acids are not directly located in the anticipated flexible region (Figure 46/Figure 48). However, a non-wrinkly phenotype was observed in the *tasA* ΔA40, S41 mutant, similar to the Δ*tasA* mutant (Figure 46). Fractionation of the sample revealed, that TasA ΔA40, S41 was expressed but not exported, comparable to TasA in a Δ*sipW* mutant (Figure 48/Figure 43). The results suggested that this deletion in the PPII helix 1, near the N-terminus of TasA, probably disturbed the recognition and processing of the N-terminal signal sequence by SipW, necessary for successful TasA export (Branda et al., 2006; Serrano et al., 1999; Stöver and Driks, 1999b). Consistent with this, several studies reported that PPII helices have properties enabling protein recognition and protein-protein interactions, which might be important for the SipW dependent processing of TasA (Adzhubei et al., 2013; Bochicchio and Tamburro, 2002; Siligardi and Drake, 1995).

Moreover, the substitution mutation *tasA* S41A displayed opposite phenotypical characteristics (Figure 46). While biofilm growth in this mutant strain was comparable to the wild type DK 1042, an enhanced wrinkle formation could be observed. The wrinkly morphology of *B. subtilis* biofilms was considered to facilitate liquid transport and was proposed to be promoted by localized cell death, which enables mechanical forces to build 3-dimensional structures depending on stiffness of the matrix (Asally et al., 2012; Wilking et al., 2013). Even though no direct correlation between complexity of wrinkle formation and expression levels of *epsA-O* and *tapA-sipW-tasA* operons in different strains was observed, both operons are essential for sound matrix formation and mutant strains with affected biofilm regulation, overproducing Eps and TasA, were described to develop more wrinkles (Chu et al., 2006; Gallegos-Monterrosa et al., 2016; Kearns et al., 2005; Richter et al., 2018; Seminara et al., 2012). Therefore, the observed increased TasA levels in the matrix fraction of the *tasA* S41A mutant strain, might suggest that in this case enhanced TasA production and export could be responsible for the hyper-wrinkly phenotype (Figure 47) (Kearns et al., 2005; Seminara et al., 2012; Trejo et al., 2013). The high TasA levels indicated that the PPII helix S41A mutation might facilitate fibril formation and/or enhanced SipW recognition, processing and thus, TasA export (Adzhubei et al., 2013; Rath et al., 2005).

TasA PPII helix 2 might be involved in fibril formation

The crystal structure of monomeric TasA predicted that the PPII helix 2 includes amino acids T187, P188, T189, D190, F191 and D192. Examination of the *tasA* PPII helix 2 in pellicle morphology revealed different phenotypes in the individual substitution mutant strains (Figure 49). The pellicle biofilms of *tasA* T187A, T189A and F191A mutant strains were similar to the wild type strain DK 1042. A decreased or no wrinkle formation was observed in the *tasA* P188A, D190A and D192A mutant strains. Notably, unlike the wild type, TasA localized in the supernatant fraction of these three mutants and the TasA protein band in all fractions was slightly lower than wild type TasA (Figure 51).

Previous studies examined the amino acid propensity in PPII structures and observed preferences for specific amino acids on distinct helical positions (Kumar and Bansal, 2016). The observations of this work suggest that the three amino acids, P188, D190 and D192, might be involved in building the characteristic PPII helix structure in TasA and substitutions with alanine disrupted this pattern. Moreover, the results indicate that disturbance of the PPII helix 2 could affect TasA fibril formation and thus matrix incorporation, resulting in the observed decrease of wrinkle formation (Figure 49). This is consistent with studies showing that fibril formation and assembly can be supported by PPII helical structures, as already stated for e.g. elastin, abductin and lamprin (Bochicchio and Tamburro, 2002).

The results of this study reinforce the relevance of amyloid-like TasA fibrils in matrix formation of *B. subtilis*. By investigation of TasA incorporated in pellicle biofilms, it was observed that *in vivo* predominantly β-sheet rich, homogenous TasA fibrils occur and analysis of the TasA crystal structure predicted two PPII helices (Diehl et al., 2018). Examination of strains with mutations in the *tasA* PPII helix 1 revealed that this dynamic segment near the N-terminus could facilitate signal peptide processing and secretion of TasA (Figure 46/Figure 48). Mutations in the TasA PPII helix 2 suggested that this flexible region could be important for fibril folding and thus, matrix maturation (Figure 49/Figure 51). These observations indicate that the PPII helices in TasA might play a vital role in TasA export and biofilm formation.

4.2.2 ClpC activities regulate biofilm formation

The regulation of biofilm formation and expression of the *eps*-operon and *tapA*-operon depend on a sophisticated network with different key regulators in *B. subtilis* (see section 1.4.2). The Hsp100/AAA+ protein ClpC, together with associated protease ClpP (ClpCP), is involved in this intricate system by e. g. regulatory degradation of SlrR (Chai et al., 2010a). SlrR is essential in the early stages of biofilm formation and promotes matrix production by complex formation with SinR, the repressor of the *eps*-operon and *tapA*-operon (Chai et al., 2010a; Kobayashi, 2008). ClpCP dependent degradation or autocleavage of SlrR was described to relieve the influence of the key regulator. Moreover, the phosphorylated two-component response regulator DegU (DegU-P) is targeted to ClpCP for degradation (Molière et al., 2016; Ogura and Tsukahara, 2010). Various cellular processes underly the control of DegU-P in a concentration-dependent manner, whereby low levels can promote complex colony development and BslA expression (Kobayashi, 2007b; Verhamme et al., 2007). Furthermore, activity of the key regulator Spo0A-P is influenced by MecA-ClpC, independent of ClpCP dependent degradation (Prepiak et al., 2011). In addition to this regulatory involvement, *in vitro* studies observed ClpC interaction with the biofilm protein TasA, which forms amyloid-like fibrils stabilizing the matrix in *B. subtilis* (Janine Kirstein, unpublished) (Romero et al., 2010). This observation suggests that ClpC could influence TasA folding inside the cell and may promote successful export and formation of amyloid-like fibrils, comparable to other chaperones in bacteria that interact with amyloid proteins and Hsp104 in *S. cerevisiae* and ClpB in *E. coli*, which influence propagation of yeast prion proteins (Cámara-Almirón et al., 2018; Chernoff et al., 1995; Nenninger et al., 2009; Serio and Lindquist, 2001). Therefore, the impact of ClpC on pellicle biofilm formation, with special regard to matrix component TasA, was investigated utilizing different *clpC* and ClpC adaptor protein mutants.

In order to identify variations in *B. subtilis* strains regarding ClpC dependent biofilm formation, *clpC* mutants were examined in strains 168 and DK 1042. Previous studies observing slowed decomposition of the matrix in a Δ*clpC* mutant could be confirmed in strain DK 1042, albeit wrinkle formation was decreased compared to the wild type in both strains (Figure 52) (Chai et al., 2010a). The *clpC* DWB mutant strains, expressing a ClpC trap mutant that cannot hydrolyze ATP and process bound substrate, displayed enhanced biofilm formation in both examined *B. subtilis* strains (Figure 52) (Kirstein et al., 2006). Especially the *clpC* DWB (168) mutant was observed to develop extensive wrinkles and red coloration upon addition of Congo Red (CC) dye. This CC dye was described to bind to TasA amyloid-like fibrils, resulting in red coloration of the matrix (Figure 52) (Romero et al., 2010). The wild type (168) did not exhibit this red coloration upon addition of CC, probably due to lower TasA levels (Figure 53). However, the Δ*clpC* (168) mutant contained elevated TasA levels, but no red coloration of the matrix with CC dye was observed. These results indicate that TasA maturation and incorporation in the matrix could be disturbed in absence of ClpC. An altered expression of matrix compounds, such as Eps, in Δ*clpC* mutants was already described to affect matrix composition and may also explain the observed decrease in wrinkle formation (Chai et al., 2010a; Ogura and Tsukahara, 2010; Prepiak et al., 2011). The enhanced wrinkle formation in the *clpC* DWB trap mutant suggested that active ClpC, which processes substrates and can transfer them to ClpP for degradation, might be necessary for well-adjusted biofilm formation (Figure 53). Overall, comparison of both *B. subtilis* strains revealed that the observed influences of the *clpC* mutants were especially severe in strain 168. The domesticated strain 168 was described to form less robust pellicle biofilms due to alterations in different genes associated to biofilm formation (McLoon et al., 2011). The results imply that the *clpC* mutations further perturbed this already affected regulation in strain 168. These evident changes of morphology facilitated examination of biofilm formation in *clpC* (168) mutants.

The involvement of ClpC in biofilm regulation is related to ClpCP regulatory proteolysis and therefore, pellicle biofilm formation was examined with different *clpC* (168) mutants affecting this protease complex. The interaction between ClpC and protease ClpP depends on the VGF tripeptide on the tip of the P-loop (Kim et al., 2001). A ClpC VGF::GGR mutation or deletion of this interaction loop (ClpC Δloop) resulted in loss of degradation activity, while the substrate was still translocated and disaggregated by ClpC *in vitro* (Figure 28 B/Figure 29). The ClpC VGF::IGF mutation was observed to increase the degradation activity of the ClpCP complex *in vitro* (Figure 31 B).

In vivo, the *clpC* VGF::IGF mutant strain displayed no phenotypical impact on pellicle biofilm formation, when compared to the wild type strain, suggesting that a possible increased degradation activity does not influence biofilm morphology (Figure 54). Impaired ClpCP degradation activity in mutant strains *clpC* VGF::GGR and *clpC* Δloop resulted in accelerated biofilm growth and wrinkle formation, similar to strain *clpC* DWB (Figure 54). Since these mutations did not influence TasA export and localization, the altered morphology was probably caused by missing ClpCP degradation activity, most likely on a regulatory level (Figure 55/Figure 56). Consistent with these observations, other biofilm studies in *S. aureus* described a decreased matrix formation in *clpC* and *clpX* deletion mutants and increased biofilm formation in *clpP* mutants (Frees et al., 2004). This impact of *clpP* (and *clpX*) in *S. aureus* is linked to control over the repressor of biofilm formation Agr (“accessory gene regulator”) and cell wall hydrolase Sle1 (Boles and Horswill, 2008; Frees et al., 2003; Liu et al., 2017).

The results from experiments in this work suggest a connection of increased pellicle biofilm formation in *B. subtilis* with ClpC dependent substrate degradation by ClpP (Figure 54). Further experiments need to evaluate in more detail whether the observed impact could depend on impaired degradation of key regulators like SlrR or DegU-P and if other unknown factors play a role in this network.

ClpC adaptor proteins involved in regulation of biofilm formation

The adaptor proteins MecA, McsB and YpbH facilitate substrate selection and activation of ClpC in *B. subtilis* (Kirstein et al., 2009b, 2007; Persuh et al., 2002; Turgay et al., 1998). Influences of respective adaptor proteins on biofilm formation were assessed by examination of deletion mutants. Initiation of biofilm formation was delayed in a Δ*mecA* strain, but in later growth states enhanced matrix development and high TasA expression were observed (Figure 57/Figure 58). MecA as adaptor protein for ClpC is known to be involved in competence development by targeting of ComK for ClpCP dependent degradation as well as in biofilm formation and sporulation by altering Spo0A-P transcriptional activity (Prepiak et al., 2011; Turgay et al., 1998). This regulatory impact of MecA on Spo0A-P is ClpC dependent, while here, compared to inactivation of ComK, no degradation of the regulator occurs (Prepiak et al., 2011). It was proposed, that the MecA-ClpC complex targets Spo0A-P bound to promotors and interferes with transcription, which results in e.g. downregulation of *eps* genes (Tanner et al., 2018). De-repression of Spo0A-P repressed promotors by MecA was not reported. This involvement of MecA in Spo0A-P regulation is consistent with the observations of this work. Biofilm formation is, among others, initiated by rising levels of Spo0A-P, which lead to expression of *sinI*, and overexpression of MecA was described to downregulate the expression of *sinI* (Bai et al., 1993; Kearns et al., 2004; Prepiak et al., 2011; Shafikhani et al., 2002). High concentrations of Spo0A-P again repress *sinI* and thus, the deletion of *mecA* might result in affected initiation of biofilm formation by missing control over Spo0A-P regulation (Chai et al., 2011). Furthermore, the observed enhanced matrix formation and increased TasA levels in later growth phases might be linked to increased expression of *eps* and *tapA-sipW-tasA* operons due to relieved Spo0A-P repression by ClpC-MecA (Prepiak et al., 2011; Tanner et al., 2018). Nevertheless, regulation of biofilm formation is highly complex and the deletion of *mecA* probably affected many aspects of this network.

Furthermore, the influence of ClpC adaptor protein and arginine kinase McsB on biofilm formation was examined with a deletion mutant. Similar to the Δ*mecA* strain, initiation of biofilm formation was delayed in the Δ*mcsB* strain, but wrinkle formation was still decreased in later growth states compared to the wild type strain (Figure 57). This phenotype resembled the Δ*clpC* strain, since reduced wrinkle formation and no red coloration were observed despite high TasA levels (Figure 52/Figure 53/Figure 58). No involvement of McsB, in its role as adaptor protein for ClpC, in biofilm formation was reported yet. However, the observations of this work indicate that McsB might be involved in ClpC dependent expression of various biofilm compounds and thus, matrix formation and TasA incorporation were affected in the deletion mutant. Moreover, several substrates for the protein arginine kinase McsB were identified in *B. subtilis* (Elsholz et al., 2012). Transcriptional analyses revealed a connection between the McsB kinase activity and many developmental processes, including biofilm formation and the key regulator Spo0A was found to be a target for McsB kinase activity (Schmidt et al., 2014). Therefore, McsB might participate in regulation of biofilm formation in its role as adaptor protein for ClpC and as protein arginine kinase, influencing key regulators.

Compared to MecA and McsB not much is known about ClpC adaptor protein YpbH, so far. This paralogue of MecA was observed to be involved in the same cellular processes, such as sporulation and competence development, and it was proposed that YpbH also participates in Spo0A-P regulation (Persuh et al., 2002; F. Wang et al., 2009). Deletion of *ypbH* resulted in accelerated biofilm growth and enhanced wrinkle formation compared to the wild type strain (Figure 57). These observations do not correspond to the Δ*mecA* phenotype and suggest that MecA and YpbH could participate in diverse regulatory networks. Moreover, it is to mention that despite enhanced wrinkle formation, the TasA levels were not increased in the Δ*ypbH* mutant strain and the phenotypic pattern was similar to *clpC* mutants which were no longer able to transfer substrate to ClpP for degradation (*clpC* DWB, *clpC* VGF::GGR, *clpC* Δloop) (Figure 54/Figure 58). These results suggest that YpbH might be the adaptor protein responsible for targeting of essential key players towards ClpCP for regulatory degradation in biofilm formation. In future experiments, combined pull-down assays with YpbH under biofilm conditions and mass spectrometric approaches may help to find substrates targeted by this adaptor protein and experiments with strains overexpressing *ypbH* might support characterization of the regulatory mechanisms defining biofilm formation.

Examination of *clpC* in pellicle formation of *B. subtilis* could neither demonstrate nor exclude a possible role of ClpC in assistance of TasA folding, but was consistent with previous studies, reporting participation of the AAA+ chaperone in regulatory processes (Ogura and Tsukahara, 2010; Prepiak et al., 2011; Tanner et al., 2018). Since the network controlling biofilm formation is highly complex, not all aspects of ClpC involvement in biofilm regulation are understood so far. Results presented in this work imply distinct functions of ClpC adaptor proteins and suggest that YpbH might facilitate regulatory degradation by ClpCP and thus influences biofilm formation in *B. subtilis*.

4.3 Summary and Conclusion

Protein homeostasis entails the removal of misfolded and aggregated protein species by either refolding or degradation and is crucial for cellular survival. This work characterizes a system from *B. subtilis* for disaggregation and refolding of heat induced protein aggregates *in vitro*. While disaggregation was carried out by the AAA+ chaperone ClpC, protein arginine phosphorylation by the kinase and adaptor protein McsB as well as dephosphorylation by the phosphatase YwlE were observed to be essential for the refolding process. Therefore, arginine phosphorylation is a post-translational modification not only involved in adjustments of cellular regulatory networks, but might also play a role in protein rescue mechanisms *in vivo* (Elsholz et al., 2012; Schmidt et al., 2014). The finding that post-translational modifications could be involved in protein folding in bacteria may help to understand protein maturation and refolding processes in prokaryotes.

One important aspect of PQC systems is the distinction between protein rescue and degradation. The examined chaperone ClpC can form a protease complex with ClpP (ClpCP) for degradation of substrate proteins. In presence of active McsB and YwlE not degradation, but substrate refolding was observed to be the preferred activity. This might represent a possible regulation for substrate rescue or removal mechanisms. Consistently, the ClpC P-loop, with the conserved VGF tripeptide for interaction with ClpP, was demonstrated to be perfectly fitted to enable a switch between ClpC chaperone and ClpCP protease functions. This characterization of ClpCP activities provides detailed insights into bacterial AAA+ protease complexes, that are involved in general as well as regulatory degradation processes and were recently found to be an effective target for different antimicrobial compounds.

Functional amyloid proteins fulfill distinct tasks in signal transduction, cell regulation and scaffolding in eukaryotes and prokaryotes. In *B. subtilis*, the biofilm protein TasA forms amyloid-like fibrils, stabilizing the extracellular matrix (Romero et al., 2010). Mutations in flexible regions of *tasA* revealed the significance of PPII helices for export and folding of the fibril protein, while activities of the chaperone ClpC could not be linked to fibril maturation. These insights into amyloid secretion and assembly in bacteria may help to understand regulations of functional amyloids and folding mechanisms of pathogenic amyloids, which are associated to many human diseases (Loquet et al., 2018).

List of Figures

Figure 1 Model of Quorum sensing and σ^B regulation. 2

Figure 2 McsB is an arginine kinase and ClpC adaptor protein. 5

Figure 3 Schematic overview of PQC systems in aggregate removal and prevention. 7

Figure 4 Schematic model example of AAA+ protein structure. 9

Figure 5 Involvement of selected Clp proteins in regulatory pathways. 13

Figure 6 Regulation model of biofilm matrix production under control of Spo0A-P and DegU-P. 19

Figure 7 Standard curve for calculation TasA protein concentration in western blots. 34

Figure 8 McsB/McsA facilitates moderate ClpC dependent Mdh disaggregation. 46

Figure 9 Catalytic amounts of YwlE enhance disaggregation and refolding. 48

Figure 10 Protein phosphorylation by McsB is counteracted by phosphatase YwlE. 50

Figure 11 The refolding efficiency increases with kinase inactive McsB C167S/McsA. 52

Figure 12 McsA enhances McsB dependent ClpC activities. 53

Figure 13 YwlE phosphatase activity is important in presence of active McsB. 55

Figure 14 Inactive McsB cannot phosphorylate and inactive YwlE cannot dephosphorylate proteins. 56

Figure 15 Addition of McsA triggers McsB mediated ClpC disaggregation activity. 58

Figure 16 McsA addition activates McsB kinase at various time points. 60

Figure 17 Early presence of YwlE is important for ClpC mediated disaggregation and refolding. 62

Figure 18 Addition of YwlE dephosphorylates proteins at various time points. 64

Figure 19 Addition of ClpC DWB decreases the ATPase activity. 66

Figure 20 Addition of ClpC DWB stops disaggregation and YwlE assists substrate refolding. 67

Figure 21 ClpP improves the refolding efficiency of McsB/McsA-activated ClpC. 68

Figure 22 YwlE facilitates refolding despite presence of protease ClpP. 69

Figure 23 YwlE C7S affects substrate disaggregation. 70

Figure 24 ClpP stimulates ATPase activity and YwlE impairs ClpCP degradation activity. 72

Figure 25 McsB phosphorylates ClpCP substrates β-casein and CtsR prior to degradation. 73

Figure 26 Kinase inactive McsB C167S/McsA still enables ClpCP degradation activity. 75

Figure 27 The McsB C167S function as ClpCP adaptor protein is still affected by YwlE. 77

Figure 28 ClpC VGF::GGR mutant displays no degradation activity with ClpP. 78

Figure 29 ClpC VGF::GGR mutant still disaggregates and refolds substrate. 79

Figure 30 ClpP has no positive influence on ClpC VGF::GGR refolding activity. 80

Figure 31 ClpC VGF::IGF-ClpP displays increased degradation activity despite presence of YwlE. 81

Figure 32 The refolding efficiency is increased with the ClpC VGF::IGF mutant. 82

Figure 33 ClpC VGF::IGF overcomes the inhibitory effect of YwlE on degradation. 83

Figure 34 ClpC P-loop mutations do not impair thermotolerance. 85

Figure 35 Chaperone system components with active Mdh. 86

Figure 36 The refolding efficiency of Cs is increased with McsB C167S. 87

Figure 37 Cs is no substrate for degradation by ClpCP but YwlE increases the refolding efficiency. ... 88

Figure 38 ATPase and degradation activities are affected by N-terminal ClpC mutations. 90

Figure 39 ClpCP degradation activity is altered with adaptor proteins MecA or McsB/McsA. 92

Figure 40 Distinct pellicle morphologies are better visible in MOLP than in Msgg medium. 94

Figure 41 Strains 168 and DK 1042 display different biofilm phenotypes. 96

Figure 42 TasA protein is absent or not exported in *tasA*-operon mutants of strain DK 1042. 97

Figure 43 TasA localizes in the cells and matrix of the wt and is not exported in the Δ*sipW* strain. 99

Figure 44 Biofilms are reconstructed by TasA addition. 100

Figure 45 PPII helices in the TasA crystal structure. 101

Figure 46 Mutations in the *tasA* PPII helix 1 lead to distinct phenotypes. 102

Figure 47 TasA protein levels differ in PPII helix 1 mutant strains. 103

Figure 48 A deletion in *tasA* PPII 1 helix prevents TasA export. 104

Figure 49 Several PPII helix 2 mutations affect the biofilm phenotype. 105

Figure 50 Distinct TasA protein levels in PPII helix 2 mutants. 106

Figure 51 TasA localizes in the supernatant of several PPII helix 2 mutant strains. 107

Figure 52 Pellicle formation is affected in *clpC* mutants in strain 168 and DK 1042. 109

Figure 53 TasA protein levels vary in *clpC* mutants of strains 168 and DK 1042. 110

Figure 54 Wrinkle formation is enhanced when ClpCP degradation is prevented. 111

Figure 55 TasA protein levels are increased in *clpC* mutants... 112

Figure 56 TasA localization is not disturbed in *clpC* mutant strains. 113

Figure 57 Deletion of ClpC adaptor proteins affects pellicle formation... 114

Figure 58 TasA protein levels differ in adaptor protein deletion mutants. 115

Figure 59 TasA localization is not affected in ClpC adaptor protein mutant strains. 115

Figure 60 Schematic model of ClpC, McsB, McsA, YwlE roles in the PQC system........................... 128

List of Tables

Table 1: List of devices 22

Table 2: List of chemicals and reagents 23

Table 3: List of primers 23

Table 4: List of plasmids 24

Table 5: List of strains 26

Table 6: Antibiotics 28

Table 7: SDS-Gels 38

Table 8: Antibodies 39

Table 9: Final protein concentrations applied in the light scattering assay 42

References

Adzhubei, A.A., Sternberg, M.J.E., 1993. Left-handed Polyproline II Helices Commonly Occur in Globular Proteins. Journal of Molecular Biology 229, 472–493. https://doi.org/10.1006/jmbi.1993.1047

Adzhubei, A.A., Sternberg, M.J.E., Makarov, A.A., 2013. Polyproline-II Helix in Proteins: Structure and Function. Journal of Molecular Biology 425, 2100–2132. https://doi.org/10.1016/j.jmb.2013.03.018

Amor, A.J., Schmitz, K.R., Baker, T.A., Sauer, R.T., 2019. Roles of the ClpX IGF loops in ClpP association, dissociation, and protein degradation. Protein Science 28, 756–765. https://doi.org/10.1002/pro.3590

Anagnostopoulos, C., Spizizen, J., 1961. REQUIREMENTS FOR TRANSFORMATION IN BACILLUS SUBTILIS. J. Bacteriol. 81, 741–746.

Arkhipova, T.N., Veselov, S.U., Melentiev, A.I., Martynenko, E.V., Kudoyarova, G.R., 2005. Ability of bacterium Bacillus subtilis to produce cytokinins and to influence the growth and endogenous hormone content of lettuce plants. Plant Soil 272, 201–209. https://doi.org/10.1007/s11104-004-5047-x

Asally, M., Kittisopikul, M., Rue, P., Du, Y., Hu, Z., Cagatay, T., Robinson, A.B., Lu, H., Garcia-Ojalvo, J., Suel, G.M., 2012. Localized cell death focuses mechanical forces during 3D patterning in a biofilm. Proceedings of the National Academy of Sciences 109, 18891–18896. https://doi.org/10.1073/pnas.1212429109

Bai, U., Mandic-Mulec, I., Smith, I., 1993. SinI modulates the activity of SinR, a developmental switch protein of Bacillus subtilis, by protein-protein interaction. Genes & Development 7, 139–148. https://doi.org/10.1101/gad.7.1.139

Baker, T.A., Sauer, R.T., 2006. ATP-dependent proteases of bacteria: recognition logic and operating principles. Trends in Biochemical Sciences 31, 647–653. https://doi.org/10.1016/j.tibs.2006.10.006

Battesti, A., Gottesman, S., 2013. Roles of adaptor proteins in regulation of bacterial proteolysis. Current Opinion in Microbiology 16, 140–147. https://doi.org/10.1016/j.mib.2013.01.002

Beauregard, P.B., Chai, Y., Vlamakis, H., Losick, R., Kolter, R., 2013. Bacillus subtilis biofilm induction by plant polysaccharides. Proceedings of the National Academy of Sciences 110, E1621–E1630. https://doi.org/10.1073/pnas.1218984110

Beltrao, P., Bork, P., Krogan, N.J., Noort, V., 2013. Evolution and functional cross-talk of protein post-translational modifications. Mol Syst Biol 9, 714. https://doi.org/10.1002/msb.201304521

Benson, A.K., Haldenwang, W.G., 1993. Bacillus subtilis sigma B is regulated by a binding protein (RsbW) that blocks its association with core RNA polymerase. Proceedings of the National Academy of Sciences 90, 2330–2334. https://doi.org/10.1073/pnas.90.6.2330

Beuron, F., Maurizi, M.R., Belnap, D.M., Kocsis, E., Booy, F.P., Kessel, M., Steven, A.C., 1998. At Sixes and Sevens: Characterization of the Symmetry Mismatch of the ClpAP Chaperone-Assisted Protease. Journal of Structural Biology 123, 248–259. https://doi.org/10.1006/jsbi.1998.4039

Blair, K.M., Turner, L., Winkelman, J.T., Berg, H.C., Kearns, D.B., 2008. A molecular clutch disables flagella in the Bacillus subtilis biofilm. Science 320, 1636–1638. https://doi.org/10.1126/science.1157877

Blobel, J., Bernadó, P., Xu, H., Jin, C., Pons, M., 2009. Weak oligomerization of low-molecular-weight protein tyrosine phosphatase is conserved from mammals to bacteria. FEBS Journal 276, 4346–4357. https://doi.org/10.1111/j.1742-4658.2009.07139.x

Bochicchio, B., Tamburro, A.M., 2002. Polyproline II structure in proteins: Identification by chiroptical spectroscopies, stability, and functions. Chirality 14, 782–792. https://doi.org/10.1002/chir.10153

Bogino, P., Oliva, M., Sorroche, F., Giordano, W., 2013. The Role of Bacterial Biofilms and Surface Components in Plant-Bacterial Associations. IJMS 14, 15838–15859. https://doi.org/10.3390/ijms140815838

Bojer, M.S., Struve, C., Ingmer, H., Hansen, D.S., Krogfelt, K.A., 2010. Heat Resistance Mediated by a New Plasmid Encoded Clp ATPase, ClpK, as a Possible Novel Mechanism for Nosocomial Persistence of Klebsiella pneumoniae. PLoS ONE 5, e15467. https://doi.org/10.1371/journal.pone.0015467

Bojer, M.S., Struve, C., Ingmer, H., Krogfelt, K.A., 2013. ClpP-dependent and -independent activities encoded by the polycistronic clpK-encoding locus contribute to heat shock survival in Klebsiella pneumoniae. Research in Microbiology 164, 205–210. https://doi.org/10.1016/j.resmic.2012.11.005

Bokhove, M., Claessen, D., de Jong, W., Dijkhuizen, L., Boekema, E.J., Oostergetel, G.T., 2013. Chaplins of Streptomyces coelicolor self-assemble into two distinct functional amyloids. Journal of Structural Biology 184, 301–309. https://doi.org/10.1016/j.jsb.2013.08.013

Boles, B.R., Horswill, A.R., 2008. agr-Mediated Dispersal of Staphylococcus aureus Biofilms. PLoS Pathog 4, e1000052. https://doi.org/10.1371/journal.ppat.1000052

Branda, S.S., Chu, F., Kearns, D.B., Losick, R., Kolter, R., 2006. A major protein component of the Bacillus subtilis biofilm matrix. Mol. Microbiol. 59, 1229–1238. https://doi.org/10.1111/j.1365-2958.2005.05020.x

Brigulla, M., Hoffmann, T., Krisp, A., Volker, A., Bremer, E., Volker, U., 2003. Chill Induction of the SigB-Dependent General Stress Response in Bacillus subtilis and Its Contribution to Low-Temperature Adaptation. Journal of Bacteriology 185, 4305–4314. https://doi.org/10.1128/JB.185.15.4305-4314.2003

Brötz-Oesterhelt, H., Beyer, D., Kroll, H.-P., Endermann, R., Ladel, C., Schroeder, W., Hinzen, B., Raddatz, S., Paulsen, H., Henninger, K., Bandow, J.E., Sahl, H.-G., Labischinski, H., 2005. Dysregulation of bacterial proteolytic machinery by a new class of antibiotics. Nat. Med. 11, 1082–1087. https://doi.org/10.1038/nm1306

Burbulys, D., Trach, K.A., Hoch, J.A., 1991. Initiation of sporulation in B. subtilis is controlled by a multicomponent phosphorelay. Cell 64, 545–552. https://doi.org/10.1016/0092-8674(91)90238-T

Burkholder, W.F., Kurtser, I., Grossman, A.D., 2001. Replication initiation proteins regulate a developmental checkpoint in Bacillus subtilis. Cell 104, 269–279. https://doi.org/10.1016/s0092-8674(01)00211-2

Burton, R.E., 2001. Effects of protein stability and structure on substrate processing by the ClpXP unfolding and degradation machine. The EMBO Journal 20, 3092–3100. https://doi.org/10.1093/emboj/20.12.3092

Butcher, R.A., Schroeder, F.C., Fischbach, M.A., Straight, P.D., Kolter, R., Walsh, C.T., Clardy, J., 2007. The identification of bacillaene, the product of the PksX megacomplex in Bacillus subtilis. Proceedings of the National Academy of Sciences 104, 1506–1509. https://doi.org/10.1073/pnas.0610503104

Cámara-Almirón, J., Caro-Astorga, J., de Vicente, A., Romero, D., 2018. Beyond the expected: the structural and functional diversity of bacterial amyloids. Critical Reviews in Microbiology 44, 653–666. https://doi.org/10.1080/1040841X.2018.1491527

Cámara-Almirón, J., Navarro, Y., Díaz-Martínez, L., Magno-Pérez-Bryan, M.C., Molina-Santiago, C., Pearson, J.R., de Vicente, A., Pérez-García, A., Romero, D., 2020. Dual functionality of the amyloid protein TasA in Bacillus physiology and fitness on the phylloplane. Nat Commun 11, 1859. https://doi.org/10.1038/s41467-020-15758-z

Camilloni, C., De Simone, A., Vranken, W.F., Vendruscolo, M., 2012. Determination of Secondary Structure Populations in Disordered States of Proteins Using Nuclear Magnetic Resonance Chemical Shifts. Biochemistry 51, 2224–2231. https://doi.org/10.1021/bi3001825

Campbell, N.F., Shih, F.F., Marshall, W.E., 1992. Enzymic phosphorylation of soy protein isolate for improved functional properties. J. Agric. Food Chem. 40, 403–406. https://doi.org/10.1021/jf00015a008

Carroni, M., Franke, K.B., Maurer, M., Jäger, J., Hantke, I., Gloge, F., Linder, D., Gremer, S., Turgay, K., Bukau, B., Mogk, A., 2017. Regulatory coiled-coil domains promote head-to-head assemblies of AAA+ chaperones essential for tunable activity control. eLife 6. https://doi.org/10.7554/eLife.30120

Ceri, H., Olson, M.E., Stremick, C., Read, R.R., Morck, D., Buret, A., 1999. The Calgary Biofilm Device: new technology for rapid determination of antibiotic susceptibilities of bacterial biofilms. J. Clin. Microbiol. 37, 1771–1776.

Chai, L., Romero, D., Kayatekin, C., Akabayov, B., Vlamakis, H., Losick, R., Kolter, R., 2013. Isolation, Characterization, and Aggregation of a Structured Bacterial Matrix Precursor. J. Biol. Chem. 288, 17559–17568. https://doi.org/10.1074/jbc.M113.453605

Chai, Y., Kolter, R., Losick, R., 2010a. Reversal of an epigenetic switch governing cell chaining in Bacillus subtilis by protein instability: Reversal of an epigenetic switch. Molecular Microbiology no-no. https://doi.org/10.1111/j.1365-2958.2010.07335.x

Chai, Y., Kolter, R., Losick, R., 2009. Paralogous antirepressors acting on the master regulator for biofilm formation in Bacillus subtilis. Mol. Microbiol. 74, 876–887. https://doi.org/10.1111/j.1365-2958.2009.06900.x

Chai, Y., Norman, T., Kolter, R., Losick, R., 2011. Evidence that metabolism and chromosome copy number control mutually exclusive cell fates in Bacillus subtilis. EMBO J. 30, 1402–1413. https://doi.org/10.1038/emboj.2011.36

Chai, Y., Norman, T., Kolter, R., Losick, R., 2010b. An epigenetic switch governing daughter cell separation in Bacillus subtilis. Genes Dev. 24, 754–765. https://doi.org/10.1101/gad.1915010

Chapman, M.R., 2002. Role of Escherichia coli Curli Operons in Directing Amyloid Fiber Formation. Science 295, 851–855. https://doi.org/10.1126/science.1067484

Chen, D.-H., Madan, D., Weaver, J., Lin, Z., Schröder, G.F., Chiu, W., Rye, H.S., 2013. Visualizing GroEL/ES in the Act of Encapsulating a Folding Protein. Cell 153, 1354–1365. https://doi.org/10.1016/j.cell.2013.04.052

Chen, I., 2005. The Ins and Outs of DNA Transfer in Bacteria. Science 310, 1456–1460. https://doi.org/10.1126/science.1114021

Chernoff, Y., Lindquist, S., Ono, B., Inge-Vechtomov, S., Liebman, S., 1995. Role of the chaperone protein Hsp104 in propagation of the yeast prion-like factor [psi+]. Science 268, 880–884. https://doi.org/10.1126/science.7754373

Choudhary, C., Mann, M., 2010. Decoding signalling networks by mass spectrometry-based proteomics. Nat Rev Mol Cell Biol 11, 427–439. https://doi.org/10.1038/nrm2900

Choudhary, D.K., Johri, B.N., 2009. Interactions of Bacillus spp. and plants – With special reference to induced systemic resistance (ISR). Microbiological Research 164, 493–513. https://doi.org/10.1016/j.micres.2008.08.007

Chu, F., Kearns, D.B., Branda, S.S., Kolter, R., Losick, R., 2006. Targets of the master regulator of biofilm formation in Bacillus subtilis. Mol Microbiol 59, 1216–1228. https://doi.org/10.1111/j.1365-2958.2005.05019.x

Chu, F., Kearns, D.B., McLoon, A., Chai, Y., Kolter, R., Losick, R., 2008. A novel regulatory protein governing biofilm formation in Bacillus subtilis. Mol. Microbiol. 68, 1117–1127. https://doi.org/10.1111/j.1365-2958.2008.06201.x

Claessen, D., 2003. A novel class of secreted hydrophobic proteins is involved in aerial hyphae formation in Streptomyces coelicolor by forming amyloid-like fibrils. Genes & Development 17, 1714–1726. https://doi.org/10.1101/gad.264303

Clare, D.K., Vasishtan, D., Stagg, S., Quispe, J., Farr, G.W., Topf, M., Horwich, A.L., Saibil, H.R., 2012. ATP-triggered conformational changes delineate substrate-binding and -folding mechanics of the GroEL chaperonin. Cell 149, 113–123. https://doi.org/10.1016/j.cell.2012.02.047

Cordova, J.C., Olivares, A.O., Shin, Y., Stinson, B.M., Calmat, S., Schmitz, K.R., Aubin-Tam, M.-E., Baker, T.A., Lang, M.J., Sauer, R.T., 2014. Stochastic but Highly Coordinated Protein Unfolding and Translocation by the ClpXP Proteolytic Machine. Cell 158, 647–658. https://doi.org/10.1016/j.cell.2014.05.043

Danhorn, T., Fuqua, C., 2007. Biofilm Formation by Plant-Associated Bacteria. Annu. Rev. Microbiol. 61, 401–422. https://doi.org/10.1146/annurev.micro.61.080706.093316

Davey, M.E., O'Toole, G.A., 2000. Microbial Biofilms: from Ecology to Molecular Genetics. Microbiology and Molecular Biology Reviews 64, 847–867. https://doi.org/10.1128/MMBR.64.4.847-867.2000

Davies, D., 2003. Understanding biofilm resistance to antibacterial agents. Nat Rev Drug Discov 2, 114–122. https://doi.org/10.1038/nrd1008

Davies, D.G., 1998. The Involvement of Cell-to-Cell Signals in the Development of a Bacterial Biofilm. Science 280, 295–298. https://doi.org/10.1126/science.280.5361.295

Derre, I., Rapoport, G., Devine, K., Rose, M., Msadek, T., 1999. ClpE, a novel type of HSP100 ATPase, is part of the CtsR heat shock regulon of Bacillus subtilis. Mol Microbiol 32, 581–593. https://doi.org/10.1046/j.1365-2958.1999.01374.x

Derré, I., Rapoport, G., Msadek, T., 2000. The CtsR regulator of stress response is active as a dimer and specifically degraded in vivo at 37 degrees C. Mol. Microbiol. 38, 335–347.

Derré, I., Rapoport, G., Msadek, T., 1999. CtsR, a novel regulator of stress and heat shock response, controls clp and molecular chaperone gene expression in gram-positive bacteria. Mol. Microbiol. 31, 117–131.

Deville, C., Franke, K., Mogk, A., Bukau, B., Saibil, H.R., 2019. Two-Step Activation Mechanism of the ClpB Disaggregase for Sequential Substrate Threading by the Main ATPase Motor. Cell Reports 27, 3433-3446.e4. https://doi.org/10.1016/j.celrep.2019.05.075

Diamant, S., Ben-Zvi, A.P., Bukau, B., Goloubinoff, P., 2000. Size-dependent Disaggregation of Stable Protein Aggregates by the DnaK Chaperone Machinery. J. Biol. Chem. 275, 21107–21113. https://doi.org/10.1074/jbc.M001293200

Diehl, A., Roske, Y., Ball, L., Chowdhury, A., Hiller, M., Molière, N., Kramer, R., Stöppler, D., Worth, C.L., Schlegel, B., Leidert, M., Cremer, N., Erdmann, N., Lopez, D., Stephanowitz, H., Krause, E., van Rossum, B.-J., Schmieder, P., Heinemann, U., Turgay, K., Akbey, Ü., Oschkinat, H., 2018. Structural changes of TasA in biofilm formation of *Bacillus subtilis*. Proceedings of the National Academy of Sciences 115, 3237–3242. https://doi.org/10.1073/pnas.1718102115

Donlan, R.M., 2002. Biofilms: Microbial Life on Surfaces. Emerg. Infect. Dis. 8, 881–890. https://doi.org/10.3201/eid0809.020063

Dougan, D.A., Hantke, I., Turgay, K., 2018. Dysregulating ClpP: From Antibiotics to Anticancer? Cell Chem Biol 25, 929–930. https://doi.org/10.1016/j.chembiol.2018.08.002

Dougan, D.A., Mogk, A., Zeth, K., Turgay, K., Bukau, B., 2002. AAA+ proteins and substrate recognition, it all depends on their partner in crime. FEBS Lett. 529, 6–10.

Dragoš, A., Kiesewalter, H., Martin, M., Hsu, C.-Y., Hartmann, R., Wechsler, T., Eriksen, C., Brix, S., Drescher, K., Stanley-Wall, N., Kümmerli, R., Kovács, Á.T., 2018. Division of Labor during Biofilm Matrix Production. Current Biology 28, 1903-1913.e5. https://doi.org/10.1016/j.cub.2018.04.046

D’Souza, C., Nakano, M.M., Zuber, P., 1994. Identification of comS, a gene of the srfA operon that regulates the establishment of genetic competence in Bacillus subtilis. Proc. Natl. Acad. Sci. U.S.A. 91, 9397–9401. https://doi.org/10.1073/pnas.91.20.9397

Dueholm, M.S., Petersen, S.V., Sønderkaer, M., Larsen, P., Christiansen, G., Hein, K.L., Enghild, J.J., Nielsen, J.L., Nielsen, K.L., Nielsen, P.H., Otzen, D.E., 2010. Functional amyloid in Pseudomonas: Functional amyloid in Pseudomonas. Molecular Microbiology no-no. https://doi.org/10.1111/j.1365-2958.2010.07269.x

Dufour, A., Haldenwang, W.G., 1994. Interactions between a Bacillus subtilis anti-sigma factor (RsbW) and its antagonist (RsbV). J. Bacteriol. 176, 1813–1820. https://doi.org/10.1128/jb.176.7.1813-1820.1994

Earl, C., Arnaouteli, S., Sukhodub, T., MacPhee, C.E., Stanley-Wall, N.R., 2019. The majority of the matrix protein TapA is dispensable for biofilm formation by *Bacillus subtilis* (preprint). Microbiology. https://doi.org/10.1101/794164

Eiamphungporn, W., Helmann, J.D., 2008. The Bacillus subtilis sigma(M) regulon and its contribution to cell envelope stress responses. Mol. Microbiol. 67, 830–848. https://doi.org/10.1111/j.1365-2958.2007.06090.x

Eichler, J., Koomey, M., 2017. Sweet New Roles for Protein Glycosylation in Prokaryotes. Trends in Microbiology 25, 662–672. https://doi.org/10.1016/j.tim.2017.03.001

Ekkers, D.M., Claessen, D., Galli, F., Stamhuis, E., 2014. Surface modification using interfacial assembly of the Streptomyces chaplin proteins. Appl Microbiol Biotechnol 98, 4491–4501. https://doi.org/10.1007/s00253-013-5463-z

Elsholz, A.K.W., Birk, M.S., Charpentier, E., Turgay, K., 2017. Functional Diversity of AAA+ Protease Complexes in Bacillus subtilis. Front Mol Biosci 4, 44. https://doi.org/10.3389/fmolb.2017.00044

Elsholz, A.K.W., Hempel, K., Michalik, S., Gronau, K., Becher, D., Hecker, M., Gerth, U., 2011a. Activity Control of the ClpC Adaptor McsB in Bacillus subtilis. Journal of Bacteriology 193, 3887–3893. https://doi.org/10.1128/JB.00079-11

Elsholz, A.K.W., Hempel, K., Pöther, D.-C., Becher, D., Hecker, M., Gerth, U., 2011b. CtsR inactivation during thiol-specific stress in low GC, Gram+ bacteria: Dual activity control of CtsR. Molecular Microbiology 79, 772–785. https://doi.org/10.1111/j.1365-2958.2010.07489.x

Elsholz, A.K.W., Michalik, S., Zühlke, D., Hecker, M., Gerth, U., 2010. CtsR, the Gram-positive master regulator of protein quality control, feels the heat. EMBO J 29, 3621–3629. https://doi.org/10.1038/emboj.2010.228

Elsholz, A.K.W., Turgay, K., Michalik, S., Hessling, B., Gronau, K., Oertel, D., Mäder, U., Bernhardt, J., Becher, D., Hecker, M., Gerth, U., 2012. Global impact of protein arginine phosphorylation on the physiology of Bacillus subtilis. Proc. Natl. Acad. Sci. U.S.A. 109, 7451–7456. https://doi.org/10.1073/pnas.1117483109

Erbse, A., Schmidt, R., Bornemann, T., Schneider-Mergener, J., Mogk, A., Zahn, R., Dougan, D.A., Bukau, B., 2006. ClpS is an essential component of the N-end rule pathway in Escherichia coli. Nature 439, 753–756. https://doi.org/10.1038/nature04412

Fabret, C., Feher, V.A., Hoch, J.A., 1999. Two-component signal transduction in Bacillus subtilis: how one organism sees its world. J. Bacteriol. 181, 1975–1983.

Farr, G.W., Furtak, K., Rowland, M.B., Ranson, N.A., Saibil, H.R., Kirchhausen, T., Horwich, A.L., 2000. Multivalent Binding of Nonnative Substrate Proteins by the Chaperonin GroEL. Cell 100, 561–573. https://doi.org/10.1016/S0092-8674(00)80692-3

Fiedler, U., Weiss, V., 1995. A common switch in activation of the response regulators NtrC and PhoB: phosphorylation induces dimerization of the receiver modules. EMBO J. 14, 3696–3705.

Finkel, S.E., Kolter, R., 2001. DNA as a Nutrient: Novel Role for Bacterial Competence Gene Homologs. Journal of Bacteriology 183, 6288–6293. https://doi.org/10.1128/JB.183.21.6288-6293.2001

Flynn, J.M., Neher, S.B., Kim, Y.I., Sauer, R.T., Baker, T.A., 2003. Proteomic discovery of cellular substrates of the ClpXP protease reveals five classes of ClpX-recognition signals. Mol. Cell 11, 671–683.

Fort, P., Kajava, A.V., Delsuc, F., Coux, O., 2015. Evolution of Proteasome Regulators in Eukaryotes. Genome Biology and Evolution 7, 1363–1379. https://doi.org/10.1093/gbe/evv068

Frees, D., Chastanet, A., Qazi, S., Sørensen, K., Hill, P., Msadek, T., Ingmer, H., 2004. Clp ATPases are required for stress tolerance, intracellular replication and biofilm formation in Staphylococcus aureus: Clp ATPases in S. aureus. Molecular Microbiology 54, 1445–1462. https://doi.org/10.1111/j.1365-2958.2004.04368.x

Frees, D., Qazi, S.N.A., Hill, P.J., Ingmer, H., 2003. Alternative roles of ClpX and ClpP in Staphylococcus aureus stress tolerance and virulence: ClpX and ClpP in S. aureus stress tolerance and virulence. Molecular Microbiology 48, 1565–1578. https://doi.org/10.1046/j.1365-2958.2003.03524.x

Frees, D., Savijoki, K., Varmanen, P., Ingmer, H., 2007. Clp ATPases and ClpP proteolytic complexes regulate vital biological processes in low GC, Gram-positive bacteria. Mol. Microbiol. 63, 1285–1295. https://doi.org/10.1111/j.1365-2958.2007.05598.x

Fricke, B., Drößler, K., Willhardt, I., Schierhorn, A., Menge, S., Rücknagel, P., 2001. The cell envelope-bound metalloprotease (camelysin) from Bacillus cereus is a possible pathogenic factor. Biochimica et Biophysica Acta (BBA) - Molecular Basis of Disease 1537, 132–146. https://doi.org/10.1016/S0925-4439(01)00066-7

Fuhrmann, J., Clancy, K.W., Thompson, P.R., 2015a. Chemical Biology of Protein Arginine Modifications in Epigenetic Regulation. Chem. Rev. 115, 5413–5461. https://doi.org/10.1021/acs.chemrev.5b00003

Fuhrmann, J., Mierzwa, B., Trentini, D.B., Spiess, S., Lehner, A., Charpentier, E., Clausen, T., 2013a. Structural Basis for Recognizing Phosphoarginine and Evolving Residue-Specific Protein Phosphatases in Gram-Positive Bacteria. Cell Reports 3, 1832–1839. https://doi.org/10.1016/j.celrep.2013.05.023

Fuhrmann, J., Schmidt, A., Spiess, S., Lehner, A., Turgay, K., Mechtler, K., Charpentier, E., Clausen, T., 2009. McsB Is a Protein Arginine Kinase That Phosphorylates and Inhibits the Heat-Shock Regulator CtsR. Science 324, 1323–1327. https://doi.org/10.1126/science.1170088

Fuhrmann, J., Subramanian, V., Kojetin, D.J., Thompson, P.R., 2016. Activity-Based Profiling Reveals a Regulatory Link between Oxidative Stress and Protein Arginine Phosphorylation. Cell Chemical Biology 23, 967–977. https://doi.org/10.1016/j.chembiol.2016.07.008

Fuhrmann, J., Subramanian, V., Thompson, P.R., 2015b. Synthesis and Use of a Phosphonate Amidine to Generate an Anti-Phosphoarginine-Specific Antibody. Angew. Chem. Int. Ed. 54, 14715–14718. https://doi.org/10.1002/anie.201506737

Fuhrmann, J., Subramanian, V., Thompson, P.R., 2013b. Targeting the Arginine Phosphatase YwlE with a Catalytic Redox-Based Inhibitor. ACS Chem. Biol. 8, 2024–2032. https://doi.org/10.1021/cb4001469

Fujisawa, M., Ito, M., Krulwich, T.A., 2007. Three two-component transporters with channel-like properties have monovalent cation/proton antiport activity. Proceedings of the National Academy of Sciences 104, 13289–13294. https://doi.org/10.1073/pnas.0703709104

Fujita, M., González-Pastor, J.E., Losick, R., 2005. High- and low-threshold genes in the Spo0A regulon of Bacillus subtilis. J. Bacteriol. 187, 1357–1368. https://doi.org/10.1128/JB.187.4.1357-1368.2005

Gajdosova, J., Benedikovicova, K., Kamodyova, N., Tothova, L., Kaclikova, E., Stuchlik, S., Turna, J., Drahovska, H., 2011. Analysis of the DNA region mediating increased thermotolerance at 58°C in Cronobacter sp. and other enterobacterial strains. Antonie van Leeuwenhoek 100, 279–289. https://doi.org/10.1007/s10482-011-9585-y

Gallegos-Monterrosa, R., Mhatre, E., Kovács, Á.T., 2016. Specific Bacillus subtilis 168 variants form biofilms on nutrient-rich medium. Microbiology 162, 1922–1932. https://doi.org/10.1099/mic.0.000371

Garcia-Garcia, T., Poncet, S., Derouiche, A., Shi, L., Mijakovic, I., Noirot-Gros, M.-F., 2016. Role of Protein Phosphorylation in the Regulation of Cell Cycle and DNA-Related Processes in Bacteria. Front. Microbiol. 7. https://doi.org/10.3389/fmicb.2016.00184

Garg, S.K., Kommineni, S., Henslee, L., Zhang, Y., Zuber, P., 2009. The YjbH Protein of Bacillus subtilis Enhances ClpXP-Catalyzed Proteolysis of Spx. Journal of Bacteriology 191, 1268–1277. https://doi.org/10.1128/JB.01289-08

Gerth, U., Kirstein, J., Mostertz, J., Waldminghaus, T., Miethke, M., Kock, H., Hecker, M., 2004. Fine-tuning in regulation of Clp protein content in Bacillus subtilis. J. Bacteriol. 186, 179–191.

Gilbert, P., Das, J., Foley, I., 1997. Biofilm Susceptibility to Antimicrobials. Adv Dent Res. 11, 160–167. https://doi.org/10.1177/08959374970110010701

Gill, A.C., 2000. Post-translational hydroxylation at the N-terminus of the prion protein reveals presence of PPII structure in vivo. The EMBO Journal 19, 5324–5331. https://doi.org/10.1093/emboj/19.20.5324

Glover, J.R., Lindquist, S., 1998. Hsp104, Hsp70, and Hsp40: a novel chaperone system that rescues previously aggregated proteins. Cell 94, 73–82. https://doi.org/10.1016/s0092-8674(00)81223-4

Goldberg, A.L., St. John, A.C., 1976. Intracellular Protein Degradation in Mammalian and Bacterial Cells: Part 2. Annu. Rev. Biochem. 45, 747–804. https://doi.org/10.1146/annurev.bi.45.070176.003531

Goloubinoff, P., Mogk, A., Zvi, A.P.B., Tomoyasu, T., Bukau, B., 1999. Sequential mechanism of solubilization and refolding of stable protein aggregates by a bichaperone network. Proceedings of the National Academy of Sciences 96, 13732–13737. https://doi.org/10.1073/pnas.96.24.13732

Gottesman, S., 2003. Proteolysis in bacterial regulatory circuits. Annu. Rev. Cell Dev. Biol. 19, 565–587. https://doi.org/10.1146/annurev.cellbio.19.110701.153228

Grass, G., Schierhorn, A., Sorkau, E., Müller, H., Rücknagel, P., Nies, D.H., Fricke, B., 2004. Camelysin is a novel surface metalloproteinase from Bacillus cereus. Infect. Immun. 72, 219–228. https://doi.org/10.1128/iai.72.1.219-228.2004

Groll, M., Huber, R., 2003. Substrate access and processing by the 20S proteasome core particle. The International Journal of Biochemistry & Cell Biology 35, 606–616. https://doi.org/10.1016/S1357-2725(02)00390-4

Grossman, A.D., 1995. Genetic Networks Controlling the Initiation of Sporulation and the Development of Genetic Competence in *Bacillus subtilis*. Annu. Rev. Genet. 29, 477–508. https://doi.org/10.1146/annurev.ge.29.120195.002401

Gupta, S.C., Sharma, A., Mishra, M., Mishra, R.K., Chowdhuri, D.K., 2010. Heat shock proteins in toxicology: How close and how far? Life Sciences 86, 377–384. https://doi.org/10.1016/j.lfs.2009.12.015

Gur, E., Sauer, R.T., 2008. Recognition of misfolded proteins by Lon, a AAA(+) protease. Genes Dev. 22, 2267–2277. https://doi.org/10.1101/gad.1670908

Guttenplan, S.B., Blair, K.M., Kearns, D.B., 2010. The EpsE flagellar clutch is bifunctional and synergizes with EPS biosynthesis to promote Bacillus subtilis biofilm formation. PLoS Genet. 6, e1001243. https://doi.org/10.1371/journal.pgen.1001243

Haijema, B.J., Hahn, J., Haynes, J., Dubnau, D., 2001. A ComGA-dependent checkpoint limits growth during the escape from competence. Mol. Microbiol. 40, 52–64.

Haldenwang, W.G., Losick, R., 1980. Novel RNA polymerase sigma factor from Bacillus subtilis. Proceedings of the National Academy of Sciences 77, 7000–7004. https://doi.org/10.1073/pnas.77.12.7000

Hamon, M.A., Stanley, N.R., Britton, R.A., Grossman, A.D., Lazazzera, B.A., 2004. Identification of AbrB-regulated genes involved in biofilm formation by Bacillus subtilis: AbrB regulated genes involved in biofilm formation. Molecular Microbiology 52, 847–860. https://doi.org/10.1111/j.1365-2958.2004.04023.x

Hantke, I., 2019. Protein quality control and antibiotics: the role of the small heat shock protein YocM and the disaggregase ClpC in B. subtilis. https://doi.org/10.15488/5491

Hartl, F.U., Hayer-Hartl, M., 2002. Molecular chaperones in the cytosol: from nascent chain to folded protein. Science 295, 1852–1858. https://doi.org/10.1126/science.1068408

Hashem, A., Tabassum, B., Fathi Abd_Allah, E., 2019. Bacillus subtilis: A plant-growth promoting rhizobacterium that also impacts biotic stress. Saudi Journal of Biological Sciences 26, 1291–1297. https://doi.org/10.1016/j.sjbs.2019.05.004

Haslberger, T., Zdanowicz, A., Brand, I., Kirstein, J., Turgay, K., Mogk, A., Bukau, B., 2008. Protein disaggregation by the AAA+ chaperone ClpB involves partial threading of looped polypeptide segments. Nat Struct Mol Biol 15, 641–650. https://doi.org/10.1038/nsmb.1425

Hausner, M., Wuertz, S., 1999. High rates of conjugation in bacterial biofilms as determined by quantitative in situ analysis. Appl. Environ. Microbiol. 65, 3710–3713.

Hayer-Hartl, M., Bracher, A., Hartl, F.U., 2016. The GroEL–GroES Chaperonin Machine: A Nano-Cage for Protein Folding. Trends in Biochemical Sciences 41, 62–76. https://doi.org/10.1016/j.tibs.2015.07.009

Hecker, M., Pané-Farré, J., Uwe, V., 2007. SigB-Dependent General Stress Response in *Bacillus subtilis* and Related Gram-Positive Bacteria. Annu. Rev. Microbiol. 61, 215–236. https://doi.org/10.1146/annurev.micro.61.080706.093445

Hecker, M., Schumann, W., Völker, U., 1996. Heat-shock and general stress response in Bacillus subtilis. Mol. Microbiol. 19, 417–428.

Hershko, A., Heller, H., Elias, S., Ciechanover, A., 1983. Components of ubiquitin-protein ligase system. Resolution, affinity purification, and role in protein breakdown. J. Biol. Chem. 258, 8206–8214.

Hilliard, J.J., Simon, L.D., Van Melderen, L., Maurizi, M.R., 1998. PinA inhibits ATP hydrolysis and energy-dependent protein degradation by Lon protease. J. Biol. Chem. 273, 524–527. https://doi.org/10.1074/jbc.273.1.524

Hitomi, M., Nishimura, H., Tsujimoto, Y., Matsui, H., Watanabe, K., 2003. Identification of a helix-turn-helix motif of Bacillus thermoglucosidasius HrcA essential for binding to the CIRCE element and thermostability of the HrcA-CIRCE complex, indicating a role as a thermosensor. J. Bacteriol. 185, 381–385. https://doi.org/10.1128/jb.185.1.381-385.2003

Hoch, J.A., 1993. Regulation of the Phosphorelay and the Initiation of Sporulation in Bacillus Subtilis. Annu. Rev. Microbiol. 47, 441–465. https://doi.org/10.1146/annurev.mi.47.100193.002301

Hoffmann, A., Bukau, B., Kramer, G., 2010. Structure and function of the molecular chaperone Trigger Factor. Biochimica et Biophysica Acta (BBA) - Molecular Cell Research 1803, 650–661. https://doi.org/10.1016/j.bbamcr.2010.01.017

Hoskins, J.R., Yanagihara, K., Mizuuchi, K., Wickner, S., 2002. ClpAP and ClpXP degrade proteins with tags located in the interior of the primary sequence. Proceedings of the National Academy of Sciences 99, 11037–11042. https://doi.org/10.1073/pnas.172378899

Huang, X., Fredrick, K.L., Helmann, J.D., 1998. Promoter recognition by Bacillus subtilis sigmaW: autoregulation and partial overlap with the sigmaX regulon. J. Bacteriol. 180, 3765–3770.

Huang, Yu.T., Kinsella, J.E., 1986. Functional properties of phosphorylated yeast protein: solubility, water-holding capacity, and viscosity. J. Agric. Food Chem. 34, 670–674. https://doi.org/10.1021/jf00070a020

Hunter, P., 2008. The mob response: The importance of biofilm research for combating chronic diseases and tackling contamination. EMBO Rep 9, 314–317. https://doi.org/10.1038/embor.2008.43

Ingmer, H., Vogensen, F.K., Hammer, K., Kilstrup, M., 1999. Disruption and analysis of the clpB, clpC, and clpE genes in Lactococcus lactis: ClpE, a new Clp family in gram-positive bacteria. J. Bacteriol. 181, 2075–2083.

Iosefson, O., Nager, A.R., Baker, T.A., Sauer, R.T., 2015. Coordinated gripping of substrate by subunits of a AAA+ proteolytic machine. Nature Chemical Biology 11, 201.

Ito, K., Akiyama, Y., 2005. CELLULAR FUNCTIONS, MECHANISM OF ACTION, AND REGULATION OF FTSH PROTEASE. Annu. Rev. Microbiol. 59, 211–231. https://doi.org/10.1146/annurev.micro.59.030804.121316

Jayaprakash, N.G., Surolia, A., 2017. Role of glycosylation in nucleating protein folding and stability. Biochemical Journal 474, 2333–2347. https://doi.org/10.1042/BCJ20170111

Jenal, U., Hengge-Aronis, R., 2003. Regulation by proteolysis in bacterial cells. Current Opinion in Microbiology 6, 163–172. https://doi.org/10.1016/S1369-5274(03)00029-8

Jiang, M., Shao, W., Perego, M., Hoch, J.A., 2000. Multiple histidine kinases regulate entry into stationary phase and sporulation in Bacillus subtilis. Mol Microbiol 38, 535–542. https://doi.org/10.1046/j.1365-2958.2000.02148.x

Kalamara, M., Spacapan, M., Mandic-Mulec, I., Stanley-Wall, N.R., 2018. Social behaviours by *Bacillus subtilis* : quorum sensing, kin discrimination and beyond: Social behaviours by Bacillus subtilis. Mol Microbiol 110, 863–878. https://doi.org/10.1111/mmi.14127

Kang, C.M., Vijay, K., Price, C.W., 1998. Serine kinase activity of a *Bacillus subtilis* switch protein is required to transduce environmental stress signals but not to activate its target PP2C phosphatase. Molecular Microbiology 30, 189–196. https://doi.org/10.1046/j.1365-2958.1998.01052.x

Karzai, A.W., Roche, E.D., Sauer, R.T., 2000. The SsrA-SmpB system for protein tagging, directed degradation and ribosome rescue. Nat. Struct. Biol. 7, 449–455. https://doi.org/10.1038/75843

Katikaridis, P., Meins, L., Kamal, S.M., Römling, U., Mogk, A., 2019. ClpG Provides Increased Heat Resistance by Acting as Superior Disaggregase. Biomolecules 9. https://doi.org/10.3390/biom9120815

Kearns, D.B., Chu, F., Branda, S.S., Kolter, R., Losick, R., 2005. A master regulator for biofilm formation by Bacillus subtilis. Mol. Microbiol. 55, 739–749. https://doi.org/10.1111/j.1365-2958.2004.04440.x

Kearns, D.B., Chu, F., Rudner, R., Losick, R., 2004. Genes governing swarming in Bacillus subtilis and evidence for a phase variation mechanism controlling surface motility: Genetic analysis of B. subtilis swarming. Molecular Microbiology 52, 357–369. https://doi.org/10.1111/j.1365-2958.2004.03996.x

Keiler, K.C., Waller, P.R.H., Sauer, R.T., 1996. Role of a Peptide Tagging System in Degradation of Proteins Synthesized from Damaged Messenger RNA. Science 271, 990–993. https://doi.org/10.1126/science.271.5251.990

Keller, A., Fritzsche, M., Yu, Y.-P., Liu, Q., Li, Y.-M., Dong, M., Besenbacher, F., 2011. Influence of Hydrophobicity on the Surface-Catalyzed Assembly of the Islet Amyloid Polypeptide. ACS Nano 5, 2770–2778. https://doi.org/10.1021/nn1031998

Kenniston, J.A., Baker, T.A., Sauer, R.T., 2005. Partitioning between unfolding and release of native domains during ClpXP degradation determines substrate selectivity and partial processing. Proceedings of the National Academy of Sciences 102, 1390–1395. https://doi.org/10.1073/pnas.0409634102

Kim, D., Yu, B.J., Kim, J.A., Lee, Y.-J., Choi, S.-G., Kang, S., Pan, J.-G., 2013. The acetylproteome of Gram-positive model bacterium *Bacillus subtilis*. Proteomics 13, 1726–1736. https://doi.org/10.1002/pmic.201200001

Kim, Y.I., Levchenko, I., Fraczkowska, K., Woodruff, R.V., Sauer, R.T., Baker, T.A., 2001. Molecular determinants of complex formation between Clp/Hsp100 ATPases and the ClpP peptidase. Nat. Struct. Biol. 8, 230–233. https://doi.org/10.1038/84967

Kinsinger, R.F., Shirk, M.C., Fall, R., 2003. Rapid Surface Motility in Bacillus subtilis Is Dependent on Extracellular Surfactin and Potassium Ion. Journal of Bacteriology 185, 5627–5631. https://doi.org/10.1128/JB.185.18.5627-5631.2003

Kirstein, J., Dougan, D.A., Gerth, U., Hecker, M., Turgay, K., 2007. The tyrosine kinase McsB is a regulated adaptor protein for ClpCP. EMBO J. 26, 2061–2070. https://doi.org/10.1038/sj.emboj.7601655

Kirstein, J., Hoffmann, A., Lilie, H., Schmidt, R., Rübsamen-Waigmann, H., Brötz-Oesterhelt, H., Mogk, A., Turgay, K., 2009a. The antibiotic ADEP reprogrammes ClpP, switching it from a regulated to an uncontrolled protease: Mechanism of ClpP targeting antibiotic. EMBO Molecular Medicine 1, 37–49. https://doi.org/10.1002/emmm.200900002

Kirstein, J., Molière, N., Dougan, D.A., Turgay, K., 2009b. Adapting the machine: adaptor proteins for Hsp100/Clp and AAA+ proteases. Nat. Rev. Microbiol. 7, 589–599. https://doi.org/10.1038/nrmicro2185

Kirstein, J., Schlothauer, T., Dougan, D.A., Lilie, H., Tischendorf, G., Mogk, A., Bukau, B., Turgay, K., 2006. Adaptor protein controlled oligomerization activates the AAA+ protein ClpC. EMBO J. 25, 1481–1491. https://doi.org/10.1038/sj.emboj.7601042

Kirstein, J., Strahl, H., Molière, N., Hamoen, L.W., Turgay, K., 2008. Localization of general and regulatory proteolysis in *Bacillus subtilis* cells. Molecular Microbiology 70, 682–694. https://doi.org/10.1111/j.1365-2958.2008.06438.x

Kirstein, J., Zühlke, D., Gerth, U., Turgay, K., Hecker, M., 2005. A tyrosine kinase and its activator control the activity of the CtsR heat shock repressor in B. subtilis. EMBO J. 24, 3435–3445. https://doi.org/10.1038/sj.emboj.7600780

Kobayashi, K., 2008. SlrR/SlrA controls the initiation of biofilm formation in Bacillus subtilis. Mol. Microbiol. 69, 1399–1410. https://doi.org/10.1111/j.1365-2958.2008.06369.x

Kobayashi, K., 2007a. Bacillus subtilis pellicle formation proceeds through genetically defined morphological changes. J. Bacteriol. 189, 4920–4931. https://doi.org/10.1128/JB.00157-07

Kobayashi, K., 2007b. Gradual activation of the response regulator DegU controls serial expression of genes for flagellum formation and biofilm formation in Bacillus subtilis. Mol. Microbiol. 66, 395–409. https://doi.org/10.1111/j.1365-2958.2007.05923.x

Kobayashi, K., Iwano, M., 2012. BslA(YuaB) forms a hydrophobic layer on the surface of Bacillus subtilis biofilms. Mol. Microbiol. 85, 51–66. https://doi.org/10.1111/j.1365-2958.2012.08094.x

Kobir, A., Shi, L., Boskovic, A., Grangeasse, C., Franjevic, D., Mijakovic, I., 2011. Protein phosphorylation in bacterial signal transduction. Biochimica et Biophysica Acta (BBA) - General Subjects 1810, 989–994. https://doi.org/10.1016/j.bbagen.2011.01.006

Kock, H., Gerth, U., Hecker, M., 2004. The ClpP Peptidase Is the Major Determinant of Bulk Protein Turnover in Bacillus subtilis. Journal of Bacteriology 186, 5856–5864. https://doi.org/10.1128/JB.186.17.5856-5864.2004

Konkol, M.A., Blair, K.M., Kearns, D.B., 2013. Plasmid-Encoded ComI Inhibits Competence in the Ancestral 3610 Strain of Bacillus subtilis. Journal of Bacteriology 195, 4085–4093. https://doi.org/10.1128/JB.00696-13

Koo, B.-M., Kritikos, G., Farelli, J.D., Todor, H., Tong, K., Kimsey, H., Wapinski, I., Galardini, M., Cabal, A., Peters, J.M., Hachmann, A.-B., Rudner, D.Z., Allen, K.N., Typas, A., Gross, C.A., 2017. Construction and Analysis of Two Genome-Scale Deletion Libraries for Bacillus subtilis. Cell Syst 4, 291-305.e7. https://doi.org/10.1016/j.cels.2016.12.013

Kovács, A.T., Kuipers, O.P., 2011. Rok regulates yuaB expression during architecturally complex colony development of Bacillus subtilis 168. J. Bacteriol. 193, 998–1002. https://doi.org/10.1128/JB.01170-10

Krüger, E., Hecker, M., 1998. The first gene of the Bacillus subtilis clpC operon, ctsR, encodes a negative regulator of its own operon and other class III heat shock genes. J. Bacteriol. 180, 6681–6688.

Krüger, E., Völker, U., Hecker, M., 1994. Stress induction of clpC in Bacillus subtilis and its involvement in stress tolerance. J. Bacteriol. 176, 3360–3367. https://doi.org/10.1128/jb.176.11.3360-3367.1994

Krüger, E., Witt, E., Ohlmeier, S., Hanschke, R., Hecker, M., 2000. The Clp Proteases of Bacillus subtilisAre Directly Involved in Degradation of Misfolded Proteins. Journal of Bacteriology 182, 3259–3265. https://doi.org/10.1128/JB.182.11.3259-3265.2000

Krüger, E., Zühlke, D., Witt, E., Ludwig, H., Hecker, M., 2001. Clp-mediated proteolysis in Gram-positive bacteria is autoregulated by the stability of a repressor. EMBO J 20, 852–863. https://doi.org/10.1093/emboj/20.4.852

Kumar, A., Singh, T.R., 2013. A quantitative study of gene regulatory pathways in Bacillus subtilis for virulence and competence phenotype by quorum sensing. Syst Synth Biol 7, 33–39. https://doi.org/10.1007/s11693-013-9105-7

Kumar, P., Bansal, M., 2016. Structural and functional analyses of PolyProline-II helices in globular proteins. Journal of Structural Biology 196, 414–425. https://doi.org/10.1016/j.jsb.2016.09.006

Kwon, H.-Y., Kim, S.-W., Choi, M.-H., Ogunniyi, A.D., Paton, J.C., Park, S.-H., Pyo, S.-N., Rhee, D.-K., 2003. Effect of Heat Shock and Mutations in ClpL and ClpP on Virulence Gene Expression in Streptococcus pneumoniae. Infection and Immunity 71, 3757–3765. https://doi.org/10.1128/IAI.71.7.3757-3765.2003

Lancelot, G., Mayer, R., Hélène, C., 1979. Models of interaction between nucleic acids and proteins Hydrogen bonding of arginine with nucleic acid bases, phosphate groups and carboxylic acids. Biochimica et Biophysica Acta (BBA) - Nucleic Acids and Protein Synthesis 564, 181–190. https://doi.org/10.1016/0005-2787(79)90217-X

Laufen, T., Mayer, M.P., Beisel, C., Klostermeier, D., Mogk, A., Reinstein, J., Bukau, B., 1999. Mechanism of regulation of hsp70 chaperones by DnaJ cochaperones. Proc. Natl. Acad. Sci. U.S.A. 96, 5452–5457. https://doi.org/10.1073/pnas.96.10.5452

LeDeaux, J.R., Yu, N., Grossman, A.D., 1995. Different roles for KinA, KinB, and KinC in the initiation of sporulation in Bacillus subtilis. J. Bacteriol. 177, 861–863. https://doi.org/10.1128/jb.177.3.861-863.1995

Lee, B.-G., Kim, M.K., Song, H.K., 2011. Structural insights into the conformational diversity of ClpP from Bacillus subtilis. Mol Cells 32, 589–595. https://doi.org/10.1007/s10059-011-0197-1

Lee, B.-G., Park, E.Y., Lee, K.-E., Jeon, H., Sung, K.H., Paulsen, H., Rübsamen-Schaeff, H., Brötz-Oesterhelt, H., Song, H.K., 2010. Structures of ClpP in complex with acyldepsipeptide antibiotics reveal its activation mechanism. Nat Struct Mol Biol 17, 471–478. https://doi.org/10.1038/nsmb.1787

Lee, C., Franke, K.B., Kamal, S.M., Kim, H., Lünsdorf, H., Jäger, J., Nimtz, M., Trček, J., Jänsch, L., Bukau, B., Mogk, A., Römling, U., 2018. Stand-alone ClpG disaggregase confers superior heat tolerance to bacteria. Proc Natl Acad Sci USA 115, E273–E282. https://doi.org/10.1073/pnas.1712051115

Lee, C., Schwartz, M.P., Prakash, S., Iwakura, M., Matouschek, A., 2001. ATP-Dependent Proteases Degrade Their Substrates by Processively Unraveling Them from the Degradation Signal. Molecular Cell 7, 627–637. https://doi.org/10.1016/S1097-2765(01)00209-X

Lee, S.-Y., Tsai, F.T.F., 2005. Molecular Chaperones in Protein Quality Control. BMB Reports 38, 259–265. https://doi.org/10.5483/BMBRep.2005.38.3.259

Leichert, L.I.O., Scharf, C., Hecker, M., 2003. Global Characterization of Disulfide Stress in Bacillus subtilis. JB 185, 1967–1975. https://doi.org/10.1128/JB.185.6.1967-1975.2003

Levchenko, I., Luo, L., Baker, T.A., 1995. Disassembly of the Mu transposase tetramer by the ClpX chaperone. Genes & Development 9, 2399–2408. https://doi.org/10.1101/gad.9.19.2399

Levchenko, I., Seidel, M., Sauer, R.T., Baker, T.A., 2000. A specificity-enhancing factor for the ClpXP degradation machine. Science 289, 2354–2356. https://doi.org/10.1126/science.289.5488.2354

Li, T., Weaver, C.L., Lin, J., Duran, E.C., Miller, J.M., Lucius, A.L., 2015. Escherichia coli ClpB is a non-processive polypeptide translocase. Biochemical Journal 470, 39–52. https://doi.org/10.1042/BJ20141457

Liberek, K., Marszalek, J., Ang, D., Georgopoulos, C., Zylicz, M., 1991. Escherichia coli DnaJ and GrpE heat shock proteins jointly stimulate ATPase activity of DnaK. Proceedings of the National Academy of Sciences 88, 2874–2878. https://doi.org/10.1073/pnas.88.7.2874

Liebman, S.W., Chernoff, Y.O., 2012. Prions in Yeast. Genetics 191, 1041–1072. https://doi.org/10.1534/genetics.111.137760

Lilge, L., Reder, A., Tippmann, F., Morgenroth, F., Grohmann, J., Becher, D., Riedel, K., Völker, U., Hecker, M., Gerth, U., 2020. The Involvement of the McsB Arginine Kinase in Clp-Dependent Degradation of the MgsR Regulator in Bacillus subtilis. Front. Microbiol. 11, 900. https://doi.org/10.3389/fmicb.2020.00900

Liu, J., Mei, Z., Li, N., Qi, Y., Xu, Y., Shi, Y., Wang, F., Lei, J., Gao, N., 2013. Structural Dynamics of the MecA-ClpC Complex: A TYPE II AAA $^{+}$ PROTEIN UNFOLDING MACHINE. Journal of Biological Chemistry 288, 17597–17608. https://doi.org/10.1074/jbc.M113.458752

Liu, Q., Wang, X., Qin, J., Cheng, S., Yeo, W.-S., He, L., Ma, X., Liu, X., Li, M., Bae, T., 2017. The ATP-Dependent Protease ClpP Inhibits Biofilm Formation by Regulating Agr and Cell Wall Hydrolase Sle1 in Staphylococcus aureus. Front. Cell. Infect. Microbiol. 7, 181. https://doi.org/10.3389/fcimb.2017.00181

Lopez, D., Fischbach, M.A., Chu, F., Losick, R., Kolter, R., 2009. Structurally diverse natural products that cause potassium leakage trigger multicellularity in Bacillus subtilis. Proceedings of the National Academy of Sciences 106, 280–285. https://doi.org/10.1073/pnas.0810940106

López, D., Kolter, R., 2010. Extracellular signals that define distinct and coexisting cell fates in *Bacillus subtilis*. FEMS Microbiol Rev 34, 134–149. https://doi.org/10.1111/j.1574-6976.2009.00199.x

Lopez, K.E., Rizo, A.N., Tse, E., Lin, J., Scull, N.W., Thwin, A.C., Lucius, A.L., Shorter, J., Southworth, D.R., 2020. Conformational plasticity of the ClpAP AAA+ protease couples protein unfolding and proteolysis. Nat Struct Mol Biol 27, 406–416. https://doi.org/10.1038/s41594-020-0409-5

Loquet, A., Saupe, S.J., Romero, D., 2018. Functional Amyloids in Health and Disease. Journal of Molecular Biology 430, 3629–3630. https://doi.org/10.1016/j.jmb.2018.07.024

Luscombe, N.M., 2001. Amino acid-base interactions: a three-dimensional analysis of protein-DNA interactions at an atomic level. Nucleic Acids Research 29, 2860–2874. https://doi.org/10.1093/nar/29.13.2860

Maaβ, S., Wachlin, G., Bernhardt, J., Eymann, C., Fromion, V., Riedel, K., Becher, D., Hecker, M., 2014. Highly Precise Quantification of Protein Molecules per Cell During Stress and Starvation Responses in *Bacillus subtilis*. Molecular & Cellular Proteomics 13, 2260–2276. https://doi.org/10.1074/mcp.M113.035741

Macek, B., Forchhammer, K., Hardouin, J., Weber-Ban, E., Grangeasse, C., Mijakovic, I., 2019. Protein post-translational modifications in bacteria. Nat Rev Microbiol 17, 651–664. https://doi.org/10.1038/s41579-019-0243-0

Magnuson, R., Solomon, J., Grossman, A.D., 1994. Biochemical and genetic characterization of a competence pheromone from B. subtilis. Cell 77, 207–216. https://doi.org/10.1016/0092-8674(94)90313-1

Mah, T.-F., 2012. Biofilm-specific antibiotic resistance. Future Microbiology 7, 1061–1072. https://doi.org/10.2217/fmb.12.76

Martin, A., Baker, T.A., Sauer, R.T., 2008. Protein unfolding by a AAA+ protease is dependent on ATP-hydrolysis rates and substrate energy landscapes. Nat Struct Mol Biol 15, 139–145. https://doi.org/10.1038/nsmb.1380

Martin, A., Baker, T.A., Sauer, R.T., 2007. Distinct Static and Dynamic Interactions Control ATPase-Peptidase Communication in a AAA+ Protease. Molecular Cell 27, 41–52. https://doi.org/10.1016/j.molcel.2007.05.024

Martin, D.D., Ciulla, R.A., Roberts, M.F., 1999. Osmoadaptation in Archaea. Appl. Environ. Microbiol. 65, 1815–1825. https://doi.org/10.1128/AEM.65.5.1815-1825.1999

Mayer, M.P., Bukau, B., 2005. Hsp70 chaperones: cellular functions and molecular mechanism. Cell. Mol. Life Sci. 62, 670–684. https://doi.org/10.1007/s00018-004-4464-6

Mayer, M.P., Bukau, B., 1998. Hsp70 chaperone systems: diversity of cellular functions and mechanism of action. Biol. Chem. 379, 261–268.

McLoon, A.L., Guttenplan, S.B., Kearns, D.B., Kolter, R., Losick, R., 2011. Tracing the Domestication of a Biofilm-Forming Bacterium. Journal of Bacteriology 193, 2027–2034. https://doi.org/10.1128/JB.01542-10

Miethke, M., Hecker, M., Gerth, U., 2006. Involvement of Bacillus subtilis ClpE in CtsR degradation and protein quality control. J. Bacteriol. 188, 4610–4619. https://doi.org/10.1128/JB.00287-06

Mijakovic, I., Grangeasse, C., Turgay, K., 2016. Exploring the diversity of protein modifications: special bacterial phosphorylation systems. FEMS Microbiology Reviews 40, 398–417. https://doi.org/10.1093/femsre/fuw003

Miller, M.B., Bassler, B.L., 2001. Quorum Sensing in Bacteria. Annu. Rev. Microbiol. 55, 165–199. https://doi.org/10.1146/annurev.micro.55.1.165

Min, K.-T., Hilditch, C.M., Diederich, B., Errington, J., Yudkin, M.D., 1993. σF, the first compartment-specific transcription factor of B. subtilis, is regulated by an anti-σ factor that is also a protein kinase. Cell 74, 735–742. https://doi.org/10.1016/0092-8674(93)90520-Z

Miras, M., Dubnau, D., 2016. A DegU-P and DegQ-Dependent Regulatory Pathway for the K-state in Bacillus subtilis. Front. Microbiol. 7. https://doi.org/10.3389/fmicb.2016.01868

Mogk, A., 1999. Identification of thermolabile Escherichia coli proteins: prevention and reversion of aggregation by DnaK and ClpB. The EMBO Journal 18, 6934–6949. https://doi.org/10.1093/emboj/18.24.6934

Mogk, A., Bukau, B., Kampinga, H.H., 2018. Cellular Handling of Protein Aggregates by Disaggregation Machines. Molecular Cell 69, 214–226. https://doi.org/10.1016/j.molcel.2018.01.004

Mogk, A., Deuerling, E., Vorderwülbecke, S., Vierling, E., Bukau, B., 2003a. Small heat shock proteins, ClpB and the DnaK system form a functional triade in reversing protein aggregation. Mol. Microbiol. 50, 585–595.

Mogk, A., Homuth, G., Scholz, C., Kim, L., Schmid, F.X., Schumann, W., 1997. The GroE chaperonin machine is a major modulator of the CIRCE heat shock regulon of Bacillus subtilis. EMBO J. 16, 4579–4590. https://doi.org/10.1093/emboj/16.15.4579

Mogk, A., Schlieker, C., Friedrich, K.L., Schönfeld, H.-J., Vierling, E., Bukau, B., 2003b. Refolding of substrates bound to small Hsps relies on a disaggregation reaction mediated most efficiently by ClpB/DnaK. J. Biol. Chem. 278, 31033–31042. https://doi.org/10.1074/jbc.M303587200

Mogk, A., Schlieker, C., Strub, C., Rist, W., Weibezahn, J., Bukau, B., 2003c. Roles of Individual Domains and Conserved Motifs of the AAA+ Chaperone ClpB in Oligomerization, ATP Hydrolysis, and Chaperone Activity. J. Biol. Chem. 278, 17615–17624. https://doi.org/10.1074/jbc.M209686200

Moliere, N., 2012. The Role of Bacillus subtilis Clp/Hsp100 Proteases in the Regulation of Swimming Motility and Stress Response. Leibniz Universität Hannover.

Molière, N., Hoßmann, J., Schäfer, H., Turgay, K., 2016. Role of Hsp100/Clp Protease Complexes in Controlling the Regulation of Motility in Bacillus subtilis. Front Microbiol 7. https://doi.org/10.3389/fmicb.2016.00315

Molle, V., Fujita, M., Jensen, S.T., Eichenberger, P., González-Pastor, J.E., Liu, J.S., Losick, R., 2003. The Spo0A regulon of Bacillus subtilis: The Spo0A regulon. Molecular Microbiology 50, 1683–1701. https://doi.org/10.1046/j.1365-2958.2003.03818.x

Moores, B., Drolle, E., Attwood, S.J., Simons, J., Leonenko, Z., 2011. Effect of Surfaces on Amyloid Fibril Formation. PLoS ONE 6, e25954. https://doi.org/10.1371/journal.pone.0025954

Mordini, S., Osera, C., Marini, S., Scavone, F., Bellazzi, R., Galizzi, A., Calvio, C., 2013. The Role of SwrA, DegU and PD3 in fla/che Expression in B. subtilis. PLoS ONE 8, e85065. https://doi.org/10.1371/journal.pone.0085065

Morikawa, M., Kagihiro, S., Haruki, M., Takano, K., Branda, S., Kolter, R., Kanaya, S., 2006. Biofilm formation by a Bacillus subtilis strain that produces gamma-polyglutamate. Microbiology (Reading, Engl.) 152, 2801–2807. https://doi.org/10.1099/mic.0.29060-0

Mostertz, J., Scharf, C., Hecker, M., Homuth, G., 2004. Transcriptome and proteome analysis of Bacillus subtilis gene expression in response to superoxide and peroxide stress. Microbiology 150, 497–512. https://doi.org/10.1099/mic.0.26665-0

Msadek, T., Kunst, F., Rapoport, G., 1994. MecB of Bacillus subtilis, a member of the ClpC ATPase family, is a pleiotropic regulator controlling competence gene expression and growth at high temperature. Proceedings of the National Academy of Sciences 91, 5788–5792. https://doi.org/10.1073/pnas.91.13.5788

Muffler, A., Fischer, D., Altuvia, S., Storz, G., Hengge-Aronis, R., 1996. The response regulator RssB controls stability of the sigma(S) subunit of RNA polymerase in Escherichia coli. EMBO J. 15, 1333–1339.

Mukherjee, S., Bree, A.C., Liu, J., Patrick, J.E., Chien, P., Kearns, D.B., 2015. Adaptor-mediated Lon proteolysis restricts *Bacillus subtilis* hyperflagellation. Proc Natl Acad Sci USA 112, 250–255. https://doi.org/10.1073/pnas.1417419112

Mukherjee, S., Kearns, D.B., 2014. The Structure and Regulation of Flagella in *Bacillus subtilis*. Annual Review of Genetics 48, 319–340. https://doi.org/10.1146/annurev-genet-120213-092406

Muntel, J., Fromion, V., Goelzer, A., Maaβ, S., Mäder, U., Büttner, K., Hecker, M., Becher, D., 2014. Comprehensive Absolute Quantification of the Cytosolic Proteome of *Bacillus subtilis* by Data Independent, Parallel Fragmentation in Liquid Chromatography/Mass Spectrometry (LC/MS ^{E}). Molecular & Cellular Proteomics 13, 1008–1019. https://doi.org/10.1074/mcp.M113.032631

Murray, E.J., Kiley, T.B., Stanley-Wall, N.R., 2009a. A pivotal role for the response regulator DegU in controlling multicellular behaviour. Microbiology (Reading, Engl.) 155, 1–8. https://doi.org/10.1099/mic.0.023903-0

Murray, E.J., Strauch, M.A., Stanley-Wall, N.R., 2009b. SigmaX is involved in controlling Bacillus subtilis biofilm architecture through the AbrB homologue Abh. J. Bacteriol. 191, 6822–6832. https://doi.org/10.1128/JB.00618-09

Musumeci, L., Bongiorni, C., Tautz, L., Edwards, R.A., Osterman, A., Perego, M., Mustelin, T., Bottini, N., 2005. Low-Molecular-Weight Protein Tyrosine Phosphatases of Bacillus subtilis. Journal of Bacteriology 187, 4945–4956. https://doi.org/10.1128/JB.187.14.4945-4956.2005

Nagorska, K., Ostrowski, A., Hinc, K., Holland, I.B., Obuchowski, M., 2010. Importance of eps genes from Bacillus subtilis in biofilm formation and swarming. J. Appl. Genet. 51, 369–381. https://doi.org/10.1007/BF03208867

Nakano, M.M., Corbell, N., Besson, J., Zuber, P., 1992. Isolation and characterization of sfp: a gene that functions in the production of the lipopeptide biosurfactant, surfactin, in Bacillus subtilis. Molec. Gen. Genet. 232, 313–321. https://doi.org/10.1007/BF00280011

Nakano, M.M., Nakano, S., Zuber, P., 2002. Spx (YjbD), a negative effector of competence in Bacillus subtilis, enhances ClpC-MecA-ComK interaction. Mol. Microbiol. 44, 1341–1349.

Nakano, S., Kuster-Schock, E., Grossman, A.D., Zuber, P., 2003. Spx-dependent global transcriptional control is induced by thiol-specific oxidative stress in Bacillus subtilis. Proceedings of the National Academy of Sciences 100, 13603–13608. https://doi.org/10.1073/pnas.2235180100

Nakayama, H., Kurokawa, K., Lee, B.L., 2012. Lipoproteins in bacteria: structures and biosynthetic pathways. FEBS J 279, 4247–4268. https://doi.org/10.1111/febs.12041

Narula, J., Fujita, M., Igoshin, O.A., 2016. Functional requirements of cellular differentiation: lessons from Bacillus subtilis. Current Opinion in Microbiology 34, 38–46. https://doi.org/10.1016/j.mib.2016.07.011

Nenninger, A.A., Robinson, L.S., Hultgren, S.J., 2009. Localized and efficient curli nucleation requires the chaperone-like amyloid assembly protein CsgF. PNAS 106, 900–905. https://doi.org/10.1073/pnas.0812143106

Nicolas, P., Mader, U., Dervyn, E., Rochat, T., Leduc, A., Pigeonneau, N., Bidnenko, E., Marchadier, E., Hoebeke, M., Aymerich, S., Becher, D., Bisicchia, P., Botella, E., Delumeau, O., Doherty, G., Denham, E.L., Fogg, M.J., Fromion, V., Goelzer, A., Hansen, A., Hartig, E., Harwood, C.R., Homuth, G., Jarmer, H., Jules, M., Klipp, E., Le Chat, L., Lecointe, F., Lewis, P., Liebermeister, W., March, A., Mars, R.A.T., Nannapaneni, P., Noone, D., Pohl, S., Rinn, B., Rugheimer, F., Sappa, P.K., Samson, F., Schaffer, M., Schwikowski, B., Steil, L., Stulke, J., Wiegert, T., Devine, K.M., Wilkinson, A.J., Maarten van Dijl, J., Hecker, M., Volker, U., Bessieres, P., Noirot, P., 2012. Condition-Dependent Transcriptome Reveals High-Level Regulatory Architecture in Bacillus subtilis. Science 335, 1103–1106. https://doi.org/10.1126/science.1206848

Nikolakaki, E., Drosou, V., Sanidas, I., Peidis, P., Papamarcaki, T., Iakoucheva, L.M., Giannakouros, T., 2008. RNA association or phosphorylation of the RS domain prevents aggregation of RS domain-containing proteins. Biochimica et Biophysica Acta (BBA) - General Subjects 1780, 214–225. https://doi.org/10.1016/j.bbagen.2007.10.014

Nye, T.M., Schroeder, J.W., Kearns, D.B., Simmons, L.A., 2017. Complete Genome Sequence of Undomesticated *Bacillus subtilis* Strain NCIB 3610. Genome Announc. 5, e00364-17, /ga/5/20/e00364-17.atom. https://doi.org/10.1128/genomeA.00364-17

Ogura, M., Tsukahara, K., 2010. Autoregulation of the *Bacillus subtilis* response regulator gene *degU* is coupled with the proteolysis of DegU-P by ClpCP. Molecular Microbiology 75, 1244–1259. https://doi.org/10.1111/j.1365-2958.2010.07047.x

Ogura, M., Yamaguchi, H., Kobayashi, K., Ogasawara, N., Fujita, Y., Tanaka, T., 2002. Whole-Genome Analysis of Genes Regulated by the Bacillus subtilis Competence Transcription Factor ComK. Journal of Bacteriology 184, 2344–2351. https://doi.org/10.1128/JB.184.9.2344-2351.2002

Ogura, T., Wilkinson, A.J., 2001. AAA+ superfamily ATPases: common structure-diverse function. Genes Cells 6, 575–597. https://doi.org/10.1046/j.1365-2443.2001.00447.x

Oh, J., Kim, J.-G., Jeon, E., Yoo, C.-H., Moon, J.S., Rhee, S., Hwang, I., 2007. Amyloidogenesis of Type III-dependent Harpins from Plant Pathogenic Bacteria. J. Biol. Chem. 282, 13601–13609. https://doi.org/10.1074/jbc.M602576200

Olsen, I., 2015. Biofilm-specific antibiotic tolerance and resistance. Eur J Clin Microbiol Infect Dis 34, 877–886. https://doi.org/10.1007/s10096-015-2323-z

Olsen, J.V., Blagoev, B., Gnad, F., Macek, B., Kumar, C., Mortensen, P., Mann, M., 2006. Global, In Vivo, and Site-Specific Phosphorylation Dynamics in Signaling Networks. Cell 127, 635–648. https://doi.org/10.1016/j.cell.2006.09.026

Ongena, M., Duby, F., Jourdan, E., Beaudry, T., Jadin, V., Dommes, J., Thonart, P., 2005. Bacillus subtilis M4 decreases plant susceptibility towards fungal pathogens by increasing host resistance associated with differential gene expression. Appl Microbiol Biotechnol 67, 692–698. https://doi.org/10.1007/s00253-004-1741-0

Otto, S.B., Martin, M., Schäfer, D., Hartmann, R., Drescher, K., Brix, S., Dragoš, A., Kovács, Á.T., 2019. Privatization of biofilm matrix in structurally heterogeneous biofilms (preprint). Microbiology. https://doi.org/10.1101/742593

Pak, M., Wickner, S., 1997. Mechanism of protein remodeling by ClpA chaperone. Proc Natl Acad Sci USA 94, 4901. https://doi.org/10.1073/pnas.94.10.4901

Pan, Q., Garsin, D.A., Losick, R., 2001. Self-reinforcing activation of a cell-specific transcription factor by proteolysis of an anti-sigma factor in B. subtilis. Mol. Cell 8, 873–883.

Pan, Q., Losick, R., 2003. Unique degradation signal for ClpCP in Bacillus subtilis. J. Bacteriol. 185, 5275–5278.

Park, S.-S., Kwon, H.-Y., Tran, T.D.-H., Choi, M.-H., Jung, S.-H., Lee, S., Briles, D.E., Rhee, D.-K., 2015. ClpL is a chaperone without auxiliary factors. FEBS J 282, 1352–1367. https://doi.org/10.1111/febs.13228

Perego, M., Cole, S.P., Burbulys, D., Trach, K., Hoch, J.A., 1989. Characterization of the gene for a protein kinase which phosphorylates the sporulation-regulatory proteins Spo0A and Spo0F of Bacillus subtilis. J. Bacteriol. 171, 6187–6196. https://doi.org/10.1128/jb.171.11.6187-6196.1989

Perrody, E., Abrami, L., Feldman, M., Kunz, B., Urbé, S., van der Goot, F.G., 2016. Ubiquitin-dependent folding of the Wnt signaling coreceptor LRP6. eLife 5, e19083. https://doi.org/10.7554/eLife.19083

Persuh, M., Mandic-Mulec, I., Dubnau, D., 2002. A MecA paralog, YpbH, binds ClpC, affecting both competence and sporulation. J. Bacteriol. 184, 2310–2313.

Petersohn, A., Brigulla, M., Haas, S., Hoheisel, J.D., Volker, U., Hecker, M., 2001. Global Analysis of the General Stress Response of Bacillus subtilis. Journal of Bacteriology 183, 5617–5631. https://doi.org/10.1128/JB.183.19.5617-5631.2001

Pettersen, E.F., Goddard, T.D., Huang, C.C., Couch, G.S., Greenblatt, D.M., Meng, E.C., Ferrin, T.E., 2004. UCSF Chimera?A visualization system for exploratory research and analysis. J. Comput. Chem. 25, 1605–1612. https://doi.org/10.1002/jcc.20084

Prepiak, P., Defrancesco, M., Spadavecchia, S., Mirouze, N., Albano, M., Persuh, M., Fujita, M., Dubnau, D., 2011. MecA dampens transitions to spore, biofilm exopolysaccharide and competence expression by two different mechanisms: MecA dampens developmental transitions. Molecular Microbiology 80, 1014–1030. https://doi.org/10.1111/j.1365-2958.2011.07627.x

Prepiak, P., Dubnau, D., 2007. A peptide signal for adapter protein-mediated degradation by the AAA+ protease ClpCP. Mol. Cell 26, 639–647. https://doi.org/10.1016/j.molcel.2007.05.011

Price, C.W., Fawcett, P., Cérémonie, H., Su, N., Murphy, C.K., Youngman, P., 2002. Genome-wide analysis of the general stress response in Bacillus subtilis: B. subtilis general stress regulon. Molecular Microbiology 41, 757–774. https://doi.org/10.1046/j.1365-2958.2001.02534.x

Ramakrishna, W., Yadav, R., Li, K., 2019. Plant growth promoting bacteria in agriculture: Two sides of a coin. Applied Soil Ecology 138, 10–18. https://doi.org/10.1016/j.apsoil.2019.02.019

Ranson, N.A., Farr, G.W., Roseman, A.M., Gowen, B., Fenton, W.A., Horwich, A.L., Saibil, H.R., 2001. ATP-bound states of GroEL captured by cryo-electron microscopy. Cell 107, 869–879. https://doi.org/10.1016/s0092-8674(01)00617-1

Rath, A., Davidson, A.R., Deber, C.M., 2005. The structure of unstructured regions in peptides and proteins: Role of the polyproline II helix in protein folding and recognition. Biopolymers 80, 179–185. https://doi.org/10.1002/bip.20227

Richter, A., Hölscher, T., Pausch, P., Sehrt, T., Brockhaus, F., Bange, G., Kovács, Á.T., 2018. Hampered motility promotes the evolution of wrinkly phenotype in Bacillus subtilis. BMC Evol Biol 18, 155. https://doi.org/10.1186/s12862-018-1266-2

Ripstein, Z.A., Vahidi, S., Houry, W.A., Rubinstein, J.L., Kay, L.E., 2020. A processive rotary mechanism couples substrate unfolding and proteolysis in the ClpXP degradation machinery. eLife 9, e52158. https://doi.org/10.7554/eLife.52158

Rodrigue, A., Quentin, Y., Lazdunski, A., Méjean, V., Foglino, M., 2000. Cell signalling by oligosaccharides. Two-component systems in Pseudomonas aeruginosa: why so many? Trends in Microbiology 8, 498–504. https://doi.org/10.1016/S0966-842X(00)01833-3

Romero, D., Aguilar, C., Losick, R., Kolter, R., 2010. Amyloid fibers provide structural integrity to Bacillus subtilis biofilms. Proceedings of the National Academy of Sciences 107, 2230–2234. https://doi.org/10.1073/pnas.0910560107

Romero, D., Vlamakis, H., Losick, R., Kolter, R., 2014. Functional Analysis of the Accessory Protein TapA in Bacillus subtilis Amyloid Fiber Assembly. Journal of Bacteriology 196, 1505–1513. https://doi.org/10.1128/JB.01363-13

Romero, D., Vlamakis, H., Losick, R., Kolter, R., 2011. An accessory protein required for anchoring and assembly of amyloid fibres in B. subtilis biofilms: B. subtilis amyloid fibre accessory protein. Molecular Microbiology 80, 1155–1168. https://doi.org/10.1111/j.1365-2958.2011.07653.x

Roncarati, D., Danielli, A., Scarlato, V., 2014. The HrcA repressor is the thermosensor of the heat-shock regulatory circuit in the human pathogen *H elicobacter pylori*: Thermoregulation in

Helicobacter pylori. Molecular Microbiology 92, 910–920. https://doi.org/10.1111/mmi.12600

Rosario, M.M.L., Ordal, G.W., 1996. CheC and CheD interact to regulate methylation of Bacillus subtilis methyl-accepting chemotaxis proteins. Mol Microbiol 21, 511–518. https://doi.org/10.1111/j.1365-2958.1996.tb02560.x

Rosenzweig, R., Moradi, S., Zarrine-Afsar, A., Glover, J.R., Kay, L.E., 2013. Unraveling the Mechanism of Protein Disaggregation Through a ClpB-DnaK Interaction. Science 339, 1080. https://doi.org/10.1126/science.1233066

Runde, S., Molière, N., Heinz, A., Maisonneuve, E., Janczikowski, A., Elsholz, A.K.W., Gerth, U., Hecker, M., Turgay, K., 2014. The role of thiol oxidative stress response in heat-induced protein aggregate formation during thermotolerance in Bacillus subtilis. Mol. Microbiol. 91, 1036–1052. https://doi.org/10.1111/mmi.12521

Ruvolo, M.V., Mach, K.E., Burkholder, W.F., 2006. Proteolysis of the replication checkpoint protein Sda is necessary for the efficient initiation of sporulation after transient replication stress in Bacillus subtilis. Mol. Microbiol. 60, 1490–1508. https://doi.org/10.1111/j.1365-2958.2006.05167.x

Saibil, H.R., Fenton, W.A., Clare, D.K., Horwich, A.L., 2013. Structure and allostery of the chaperonin GroEL. J. Mol. Biol. 425, 1476–1487. https://doi.org/10.1016/j.jmb.2012.11.028

Sauer, R.T., Baker, T.A., 2011. AAA+ Proteases: ATP-Fueled Machines of Protein Destruction. Annu. Rev. Biochem. 80, 587–612. https://doi.org/10.1146/annurev-biochem-060408-172623

Sauer, R.T., Bolon, D.N., Burton, B.M., Burton, R.E., Flynn, J.M., Grant, R.A., Hersch, G.L., Joshi, S.A., Kenniston, J.A., Levchenko, I., Neher, S.B., Oakes, E.S.C., Siddiqui, S.M., Wah, D.A., Baker, T.A., 2004. Sculpting the Proteome with AAA+ Proteases and Disassembly Machines. Cell 119, 9–18. https://doi.org/10.1016/j.cell.2004.09.020

Schäfer, H., Turgay, K., 2019. Spx, a versatile regulator of the Bacillus subtilis stress response. Curr. Genet. 65, 871–876. https://doi.org/10.1007/s00294-019-00950-6

Schirmer, E.C., Glover, J.R., Singer, M.A., Lindquist, S., 1996. HSP100/Clp proteins: a common mechanism explains diverse functions. Trends Biochem. Sci. 21, 289–296.

Schlieker, C., Tews, I., Bukau, B., Mogk, A., 2004. Solubilization of aggregated proteins by ClpB/DnaK relies on the continuous extraction of unfolded polypeptides. FEBS Letters 578, 351–356. https://doi.org/10.1016/j.febslet.2004.11.051

Schlothauer, T., 2004. Role of the MecA adaptor protein in regulation of the AAA + chaperone ClpC of Bacillus subtilis. https://doi.org/10.11588/HEIDOK.00004771

Schlothauer, T., Mogk, A., Dougan, D.A., Bukau, B., Turgay, K., 2003. MecA, an adaptor protein necessary for ClpC chaperone activity. Proc. Natl. Acad. Sci. U.S.A. 100, 2306–2311. https://doi.org/10.1073/pnas.0535717100

Schmidt, A., Ammerer, G., Mechtler, K., 2013. Studying the fragmentation behavior of peptides with arginine phosphorylation and its influence on phospho-site localization. Proteomics 13, 945–954. https://doi.org/10.1002/pmic.201200240

Schmidt, A., Trentini, D.B., Spiess, S., Fuhrmann, J., Ammerer, G., Mechtler, K., Clausen, T., 2014. Quantitative Phosphoproteomics Reveals the Role of Protein Arginine Phosphorylation in the Bacterial Stress Response. Molecular & Cellular Proteomics 13, 537–550. https://doi.org/10.1074/mcp.M113.032292

Schneider, C.A., Rasband, W.S., Eliceiri, K.W., 2012. NIH Image to ImageJ: 25 years of image analysis. Nat Methods 9, 671–675. https://doi.org/10.1038/nmeth.2089

Schulz, A., Schumann, W., 1996. hrcA, the first gene of the Bacillus subtilis dnaK operon encodes a negative regulator of class I heat shock genes. J. Bacteriol. 178, 1088–1093. https://doi.org/10.1128/jb.178.4.1088-1093.1996

Schweitzer, J.-E., 2008. Analyse des Substratspektrums der ClpCP-Protease aus Corynebacterium glutamicum, Schriften des Forschungszentrums Jülich Reihe Gesundheit. Forschungszentrum, Zentralbibliothek, Jülich.

Seminara, A., Angelini, T.E., Wilking, J.N., Vlamakis, H., Ebrahim, S., Kolter, R., Weitz, D.A., Brenner, M.P., 2012. Osmotic spreading of Bacillus subtilis biofilms driven by an extracellular matrix. Proceedings of the National Academy of Sciences 109, 1116–1121. https://doi.org/10.1073/pnas.1109261108

Serio, T., Lindquist, S., 2001. [PSI+], SUP35, and chaperones, in: Advances in Protein Chemistry. Elsevier, pp. 335–366. https://doi.org/10.1016/S0065-3233(01)57027-8

Serrano, M., Zilhão, R., Ricca, E., Ozin, A.J., Moran, C.P., Henriques, A.O., 1999. A Bacillus subtilis secreted protein with a role in endospore coat assembly and function. J. Bacteriol. 181, 3632–3643.

Seyffer, F., Kummer, E., Oguchi, Y., Winkler, J., Kumar, M., Zahn, R., Sourjik, V., Bukau, B., Mogk, A., 2012. Hsp70 proteins bind Hsp100 regulatory M domains to activate AAA+ disaggregase at aggregate surfaces. Nat Struct Mol Biol 19, 1347–1355. https://doi.org/10.1038/nsmb.2442

Shafikhani, S.H., Mandic-Mulec, I., Strauch, M.A., Smith, I., Leighton, T., 2002. Postexponential Regulation of sin Operon Expression in Bacillus subtilis. Journal of Bacteriology 184, 564–571. https://doi.org/10.1128/JB.184.2.564-571.2002

Shahnawaz, M., Park, K.-W., Mukherjee, A., Diaz-Espinoza, R., Soto, C., 2017. Prion-like characteristics of the bacterial protein Microcin E492. Sci Rep 7, 45720. https://doi.org/10.1038/srep45720

Shapiro, J.A., 1998. THINKING ABOUT BACTERIAL POPULATIONS AS MULTICELLULAR ORGANISMS. Annu. Rev. Microbiol. 52, 81–104. https://doi.org/10.1146/annurev.micro.52.1.81

Shu, Q., Krezel, A.M., Cusumano, Z.T., Pinkner, J.S., Klein, R., Hultgren, S.J., Frieden, C., 2016. Solution NMR structure of CsgE: Structural insights into a chaperone and regulator protein important for functional amyloid formation. Proc Natl Acad Sci USA 113, 7130–7135. https://doi.org/10.1073/pnas.1607222113

Sickmann, A., Meyer, H.E., 2001. Phosphoamino acid analysis. Proteomics 1, 200–206. https://doi.org/10.1002/1615-9861(200102)1:2<200::AID-PROT200>3.0.CO;2-V

Siligardi, G., Drake, A.F., 1995. The importance of extended conformations and, in particular, the PII conformation for the molecular recognition of peptides. Biopolymers 37, 281–292. https://doi.org/10.1002/bip.360370406

Sinderen, D., Luttinger, A., Kong, L., Dubnau, D., Venema, G., Hamoen, L., 1995. comK encodes the competence transcription factor, the key regulatory protein for competence development in Bacillus subtilis. Mol Microbiol 15, 455–462. https://doi.org/10.1111/j.1365-2958.1995.tb02259.x

Singh, S.K., Rozycki, J., Ortega, J., Ishikawa, T., Lo, J., Steven, A.C., Maurizi, M.R., 2001. Functional Domains of the ClpA and ClpX Molecular Chaperones Identified by Limited Proteolysis and Deletion Analysis. J. Biol. Chem. 276, 29420–29429. https://doi.org/10.1074/jbc.M103489200

Singhal, K., Vreede, J., Mashaghi, A., Tans, S.J., Bolhuis, P.G., 2015. The Trigger Factor Chaperone Encapsulates and Stabilizes Partial Folds of Substrate Proteins. PLoS Comput Biol 11, e1004444. https://doi.org/10.1371/journal.pcbi.1004444

Sivertsson, E.M., Jackson, S.E., Itzhaki, L.S., 2019. The AAA+ protease ClpXP can easily degrade a 31 and a 52-knotted protein. Sci Rep 9, 2421. https://doi.org/10.1038/s41598-018-38173-3

Solomon, J.M., Lazazzera, B.A., Grossman, A.D., 1996. Purification and characterization of an extracellular peptide factor that affects two different developmental pathways in Bacillus subtilis. Genes Dev. 10, 2014–2024. https://doi.org/10.1101/gad.10.16.2014

Soufi, B., Jers, C., Hansen, M.E., Petranovic, D., Mijakovic, I., 2008. Insights from site-specific phosphoproteomics in bacteria. Biochimica et Biophysica Acta (BBA) - Proteins and Proteomics 1784, 186–192. https://doi.org/10.1016/j.bbapap.2007.07.018

Sprangers, R., Gribun, A., Hwang, P.M., Houry, W.A., Kay, L.E., 2005. Quantitative NMR spectroscopy of supramolecular complexes: Dynamic side pores in ClpP are important for product release. Proceedings of the National Academy of Sciences 102, 16678–16683. https://doi.org/10.1073/pnas.0507370102

Stancik, I.A., Šestak, M.S., Ji, B., Axelson-Fisk, M., Franjevic, D., Jers, C., Domazet-Lošo, T., Mijakovic, I., 2018. Serine/Threonine Protein Kinases from Bacteria, Archaea and Eukarya Share a Common Evolutionary Origin Deeply Rooted in the Tree of Life. Journal of Molecular Biology 430, 27–32. https://doi.org/10.1016/j.jmb.2017.11.004

Stanley, N.R., Lazazzera, B.A., 2005. Defining the genetic differences between wild and domestic strains of Bacillus subtilis that affect poly-gamma-dl-glutamic acid production and biofilm formation. Mol. Microbiol. 57, 1143–1158. https://doi.org/10.1111/j.1365-2958.2005.04746.x

Steinberg, N., Rosenberg, G., Keren-Paz, A., Kolodkin-Gal, I., 2018. Collective Vortex-Like Movement of Bacillus subtilis Facilitates the Generation of Floating Biofilms. Front. Microbiol. 9, 590. https://doi.org/10.3389/fmicb.2018.00590

Stock, A.M., Robinson, V.L., Goudreau, P.N., 2000. Two-Component Signal Transduction. Annu. Rev. Biochem. 69, 183–215. https://doi.org/10.1146/annurev.biochem.69.1.183

Stock, J.B., Ninfa, A.J., Stock, A.M., 1989. Protein phosphorylation and regulation of adaptive responses in bacteria. Microbiol. Rev. 53, 450–490.

Storz, G., Hengge, R., American Society for Microbiology (Eds.), 2011. Bacterial stress responses, 2nd ed. ed. ASM Press, Washington, DC.

Stöver, A.G., Driks, A., 1999a. Control of synthesis and secretion of the Bacillus subtilis protein YqxM. J. Bacteriol. 181, 7065–7069.

Stöver, A.G., Driks, A., 1999b. Secretion, localization, and antibacterial activity of TasA, a Bacillus subtilis spore-associated protein. J. Bacteriol. 181, 1664–1672.

Strauch, M., Webb, V., Spiegelman, G., Hoch, J.A., 1990. The SpoOA protein of Bacillus subtilis is a repressor of the abrB gene. Proc. Natl. Acad. Sci. U.S.A. 87, 1801–1805. https://doi.org/10.1073/pnas.87.5.1801

Strauch, M.A., Bobay, B.G., Cavanagh, J., Yao, F., Wilson, A., Le Breton, Y., 2007. Abh and AbrB Control of Bacillus subtilis Antimicrobial Gene Expression. Journal of Bacteriology 189, 7720–7732. https://doi.org/10.1128/JB.01081-07

Studier, F.W., Rosenberg, A.H., Dunn, J.J., Dubendorff, J.W., 1990. [6] Use of T7 RNA polymerase to direct expression of cloned genes, in: Methods in Enzymology. Elsevier, pp. 60–89. https://doi.org/10.1016/0076-6879(90)85008-C

Suskiewicz, M.J., Hajdusits, B., Beveridge, R., Heuck, A., Vu, L.D., Kurzbauer, R., Hauer, K., Thoeny, V., Rumpel, K., Mechtler, K., Meinhart, A., Clausen, T., 2019. Structure of McsB, a protein kinase for regulated arginine phosphorylation. Nature Chemical Biology 15, 510–518. https://doi.org/10.1038/s41589-019-0265-y

Sutherland, I., 2001. The biofilm matrix – an immobilized but dynamic microbial environment. Trends in Microbiology 9, 222–227. https://doi.org/10.1016/S0966-842X(01)02012-1

Szabo, A., Langer, T., Schroder, H., Flanagan, J., Bukau, B., Hartl, F.U., 1994. The ATP hydrolysis-dependent reaction cycle of the Escherichia coli Hsp70 system DnaK, DnaJ, and GrpE. Proceedings of the National Academy of Sciences 91, 10345–10349. https://doi.org/10.1073/pnas.91.22.10345

Tan, I.S., Weiss, C.A., Popham, D.L., Ramamurthi, K.S., 2015. A Quality-Control Mechanism Removes Unfit Cells from a Population of Sporulating Bacteria. Developmental Cell 34, 682–693. https://doi.org/10.1016/j.devcel.2015.08.009

Tanner, A.W., Carabetta, V.J., Dubnau, D., 2018. ClpC and MecA, components of a proteolytic machine, prevent Spo0A-P-dependent transcription without degradation: ClpC and MecA prevent Spo0A-P-dependent transcription. Molecular Microbiology 108, 178–186. https://doi.org/10.1111/mmi.13928

Tao, L., Biswas, I., 2013. ClpL Is Required for Folding of CtsR in Streptococcus mutans. Journal of Bacteriology 195, 576–584. https://doi.org/10.1128/JB.01743-12

Teague, W.E., Dobson, G.P., 1999. Thermodynamics of the Arginine Kinase Reaction. J. Biol. Chem. 274, 22459–22463. https://doi.org/10.1074/jbc.274.32.22459

Terra, R., Stanley-Wall, N.R., Cao, G., Lazazzera, B.A., 2012. Identification of Bacillus subtilis SipW as a Bifunctional Signal Peptidase That Controls Surface-Adhered Biofilm Formation. Journal of Bacteriology 194, 2781–2790. https://doi.org/10.1128/JB.06780-11

Thompson, M.W., Singh, S.K., Maurizi, M.R., 1994. Processive degradation of proteins by the ATP-dependent Clp protease from Escherichia coli. Requirement for the multiple array of active sites in ClpP but not ATP hydrolysis. J. Biol. Chem. 269, 18209–18215.

Tjalsma, H., Bolhuis, A., van Roosmalen, M.L., Wiegert, T., Schumann, W., Broekhuizen, C.P., Quax, W.J., Venema, G., Bron, S., van Dijl, J.M., 1998. Functional analysis of the secretory precursor processing machinery of Bacillus subtilis: identification of a eubacterial homolog of archaeal and eukaryotic signal peptidases. Genes Dev. 12, 2318–2331. https://doi.org/10.1101/gad.12.15.2318

Trejo, M., Douarche, C., Bailleux, V., Poulard, C., Mariot, S., Regeard, C., Raspaud, E., 2013. Elasticity and wrinkled morphology of Bacillus subtilis pellicles. Proceedings of the National Academy of Sciences 110, 2011–2016. https://doi.org/10.1073/pnas.1217178110

Trentini, D.B., Fuhrmann, J., Mechtler, K., Clausen, T., 2014. Chasing Phosphoarginine Proteins: Development of a Selective Enrichment Method Using a Phosphatase Trap. Mol Cell Proteomics 13, 1953–1964. https://doi.org/10.1074/mcp.O113.035790

Trentini, D.B., Suskiewicz, M.J., Heuck, A., Kurzbauer, R., Deszcz, L., Mechtler, K., Clausen, T., 2016. Arginine phosphorylation marks proteins for degradation by a Clp protease. Nature 539, 48–53. https://doi.org/10.1038/nature20122

Tsilibaris, V., Maenhaut-Michel, G., Van Melderen, L., 2006. Biological roles of the Lon ATP-dependent protease. Research in Microbiology 157, 701–713. https://doi.org/10.1016/j.resmic.2006.05.004

Tu, G.F., Reid, G.E., Zhang, J.G., Moritz, R.L., Simpson, R.J., 1995. C-terminal extension of truncated recombinant proteins in Escherichia coli with a 10Sa RNA decapeptide. J. Biol. Chem. 270, 9322–9326. https://doi.org/10.1074/jbc.270.16.9322

Turgay, K., Hahn, J., Burghoorn, J., Dubnau, D., 1998. Competence in Bacillus subtilis is controlled by regulated proteolysis of a transcription factor. EMBO J. 17, 6730–6738. https://doi.org/10.1093/emboj/17.22.6730

Turgay, K., Hamoen, L.W., Venema, G., Dubnau, D., 1997. Biochemical characterization of a molecular switch involving the heat shock protein ClpC, which controls the activity of ComK, the competence transcription factor of Bacillus subtilis. Genes Dev. 11, 119–128.

Tyedmers, J., Mogk, A., Bukau, B., 2010. Cellular strategies for controlling protein aggregation. Nat Rev Mol Cell Biol 11, 777–788. https://doi.org/10.1038/nrm2993

Vabulas, R.M., Raychaudhuri, S., Hayer-Hartl, M., Hartl, F.U., 2010. Protein Folding in the Cytoplasm and the Heat Shock Response. Cold Spring Harbor Perspectives in Biology 2, a004390–a004390. https://doi.org/10.1101/cshperspect.a004390

Varmanen, P., Vogensen, F.K., Hammer, K., Palva, A., Ingmer, H., 2003. ClpE from Lactococcus lactis Promotes Repression of CtsR-Dependent Gene Expression. Journal of Bacteriology 185, 5117–5124. https://doi.org/10.1128/JB.185.17.5117-5124.2003

Verhamme, D.T., Kiley, T.B., Stanley-Wall, N.R., 2007. DegU co-ordinates multicellular behaviour exhibited by Bacillus subtilis. Mol. Microbiol. 65, 554–568. https://doi.org/10.1111/j.1365-2958.2007.05810.x

Verhamme, D.T., Murray, E.J., Stanley-Wall, N.R., 2009. DegU and Spo0A jointly control transcription of two loci required for complex colony development by Bacillus subtilis. J. Bacteriol. 191, 100–108. https://doi.org/10.1128/JB.01236-08

Vijay, K., Brody, M.S., Fredlund, E., Price, C.W., 2000. A PP2C phosphatase containing a PAS domain is required to convey signals of energy stress to the sigmaB transcription factor of

Bacillus subtilis. Mol Microbiol 35, 180–188. https://doi.org/10.1046/j.1365-2958.2000.01697.x

Vlamakis, H., Aguilar, C., Losick, R., Kolter, R., 2008. Control of cell fate by the formation of an architecturally complex bacterial community. Genes & Development 22, 945–953. https://doi.org/10.1101/gad.1645008

Vlamakis, H., Chai, Y., Beauregard, P., Losick, R., Kolter, R., 2013. Sticking together: building a biofilm the Bacillus subtilis way. Nature Reviews Microbiology 11, 157–168. https://doi.org/10.1038/nrmicro2960

Voelker, U., Voelker, A., Haldenwang, W.G., 1996. Reactivation of the Bacillus subtilis anti-sigma B antagonist, RsbV, by stress- or starvation-induced phosphatase activities. J. Bacteriol. 178, 5456–5463. https://doi.org/10.1128/jb.178.18.5456-5463.1996

Voges, D., Zwickl, P., Baumeister, W., 1999. The 26S Proteasome: A Molecular Machine Designed for Controlled Proteolysis. Annual Review of Biochemistry 68, 1015–1068. https://doi.org/10.1146/annurev.biochem.68.1.1015

Walker, J.E., Saraste, M., Runswick, M.J., Gay, N.J., 1982. Distantly related sequences in the alpha- and beta-subunits of ATP synthase, myosin, kinases and other ATP-requiring enzymes and a common nucleotide binding fold. EMBO J. 1, 945–951.

Wallace, E.W.J., Kear-Scott, J.L., Pilipenko, E.V., Schwartz, M.H., Laskowski, P.R., Rojek, A.E., Katanski, C.D., Riback, J.A., Dion, M.F., Franks, A.M., Airoldi, E.M., Pan, T., Budnik, B.A., Drummond, D.A., 2015. Reversible, Specific, Active Aggregates of Endogenous Proteins Assemble upon Heat Stress. Cell 162, 1286–1298. https://doi.org/10.1016/j.cell.2015.08.041

Wang, F., Mei, Z., Qi, Y., Yan, C., Xiang, S., Zhou, Z., Hu, Q., Wang, J., Shi, Y., 2009. Crystal Structure of the MecA Degradation Tag. J. Biol. Chem. 284, 34376–34381. https://doi.org/10.1074/jbc.M109.053033

Wang, J., Hartling, J.A., Flanagan, J.M., 1997. The Structure of ClpP at 2.3 Å Resolution Suggests a Model for ATP-Dependent Proteolysis. Cell 91, 447–456. https://doi.org/10.1016/S0092-8674(00)80431-6

Wang, S., Wu, H., Qiao, J., Ma, L., Liu, J., Xia, Y., Gao, X., 2009. Molecular mechanism of plant growth promotion and induced systemic resistance to tobacco mosaic virus by Bacillus spp. J. Microbiol. Biotechnol. 19, 1250–1258.

Weibezahn, J., Schlieker, C., Bukau, B., Mogk, A., 2003. Characterization of a trap mutant of the AAA+ chaperone ClpB. J. Biol. Chem. 278, 32608–32617. https://doi.org/10.1074/jbc.M303653200

Weibezahn, J., Tessarz, P., Schlieker, C., Zahn, R., Maglica, Z., Lee, S., Zentgraf, H., Weber-Ban, E.U., Dougan, D.A., Tsai, F.T.F., Mogk, A., Bukau, B., 2004. Thermotolerance Requires Refolding of Aggregated Proteins by Substrate Translocation through the Central Pore of ClpB. Cell 119, 653–665. https://doi.org/10.1016/j.cell.2004.11.027

Weinhäupl, K., Brennich, M., Kazmaier, U., Lelievre, J., Ballell, L., Goldberg, A., Schanda, P., Fraga, H., 2018. The antibiotic cyclomarin blocks arginine-phosphate-induced millisecond dynamics in the N-terminal domain of ClpC1 from Mycobacterium tuberculosis. J. Biol. Chem. 293, 8379–8393. https://doi.org/10.1074/jbc.RA118.002251

Wickner, R.B., Edskes, H.K., Shewmaker, F., Nakayashiki, T., 2007. Prions of fungi: inherited structures and biological roles. Nat Rev Microbiol 5, 611–618. https://doi.org/10.1038/nrmicro1708

Wickner, S., Gottesman, S., Skowyra, D., Hoskins, J., McKenney, K., Maurizi, M.R., 1994. A molecular chaperone, ClpA, functions like DnaK and DnaJ. Proceedings of the National Academy of Sciences 91, 12218–12222. https://doi.org/10.1073/pnas.91.25.12218

Wickner, S., Maurizi, M.R., Gottesman, S., 1999. Posttranslational quality control: folding, refolding, and degrading proteins. Science 286, 1888–1893.

Wilking, J.N., Zaburdaev, V., De Volder, M., Losick, R., Brenner, M.P., Weitz, D.A., 2013. Liquid transport facilitated by channels in Bacillus subtilis biofilms. Proceedings of the National Academy of Sciences 110, 848–852. https://doi.org/10.1073/pnas.1216376110

Winkler, J., Tyedmers, J., Bukau, B., Mogk, A., 2012. Hsp70 targets Hsp100 chaperones to substrates for protein disaggregation and prion fragmentation. The Journal of Cell Biology 198, 387–404. https://doi.org/10.1083/jcb.201201074

Woo, K.M., Chung, W.J., Ha, D.B., Goldberg, A.L., Chung, C.H., 1989. Protease Ti from Escherichia coli requires ATP hydrolysis for protein breakdown but not for hydrolysis of small peptides. J. Biol. Chem. 264, 2088–2091.

Wouters, M.A., Fan, S.W., Haworth, N.L., 2010. Disulfides as Redox Switches: From Molecular Mechanisms to Functional Significance. Antioxidants & Redox Signaling 12, 53–91. https://doi.org/10.1089/ars.2009.2510

Wozniak, D.J., Tiwari, K.B., Soufan, R., Jayaswal, R.K., 2012. The mcsB gene of the clpC operon is required for stress tolerance and virulence in Staphylococcus aureus. Microbiology (Reading, Engl.) 158, 2568–2576. https://doi.org/10.1099/mic.0.060749-0

Wynendaele, E., Gevaert, B., Stalmans, S., Verbeke, F., De Spiegeleer, B., 2015. Exploring the chemical space of quorum sensing peptides: *Quorum Sensing Peptides Space*. Biopolymers 104, 544–551. https://doi.org/10.1002/bip.22649

Xu, C., Ng, D.T.W., 2015. Glycosylation-directed quality control of protein folding. Nat Rev Mol Cell Biol 16, 742–752. https://doi.org/10.1038/nrm4073

Yang, X., Kang, C.M., Brody, M.S., Price, C.W., 1996. Opposing pairs of serine protein kinases and phosphatases transmit signals of environmental stress to activate a bacterial transcription factor. Genes & Development 10, 2265–2275. https://doi.org/10.1101/gad.10.18.2265

Ye, X., Lorimer, G.H., 2013. Substrate protein switches GroE chaperonins from asymmetric to symmetric cycling by catalyzing nucleotide exchange. Proc. Natl. Acad. Sci. U.S.A. 110, E4289-4297. https://doi.org/10.1073/pnas.1317702110

Yuan, A.H., Garrity, S.J., Nako, E., Hochschild, A., 2014. Prion propagation can occur in a prokaryote and requires the ClpB chaperone. eLife 3, e02949. https://doi.org/10.7554/eLife.02949

Yuan, A.H., Hochschild, A., 2017. A bacterial global regulator forms a prion. Science 355, 198–201. https://doi.org/10.1126/science.aai7776

Yuan, X., Yin, P., Hao, Q., Yan, C., Wang, J., Yan, N., 2010. Single Amino Acid Alteration between Valine and Isoleucine Determines the Distinct Pyrabactin Selectivity by PYL1 and PYL2. J. Biol. Chem. 285, 28953–28958. https://doi.org/10.1074/jbc.M110.160192

Zeigler, D.R., Pragai, Z., Rodriguez, S., Chevreux, B., Muffler, A., Albert, T., Bai, R., Wyss, M., Perkins, J.B., 2008. The Origins of 168, W23, and Other Bacillus subtilis Legacy Strains. Journal of Bacteriology 190, 6983–6995. https://doi.org/10.1128/JB.00722-08

Zellmeier, S., Schumann, W., Wiegert, T., 2006. Involvement of Clp protease activity in modulating the Bacillus subtilissigmaw stress response. Mol. Microbiol. 61, 1569–1582. https://doi.org/10.1111/j.1365-2958.2006.05323.x

Zhang, H., Kim, M.-S., Sun, Y., Dowd, S.E., Shi, H., Paré, P.W., 2008. Soil Bacteria Confer Plant Salt Tolerance by Tissue-Specific Regulation of the Sodium Transporter *HKT1*. MPMI 21, 737–744. https://doi.org/10.1094/MPMI-21-6-0737

Zhou, J., Xu, Z., 2005. The structural view of bacterial translocation-specific chaperone SecB: implications for function: Structure and function of chaperone SecB. Molecular Microbiology 58, 349–357. https://doi.org/10.1111/j.1365-2958.2005.04842.x

Zhou, Y., Gottesman, S., Hoskins, J.R., Maurizi, M.R., Wickner, S., 2001. The RssB response regulator directly targets sigma(S) for degradation by ClpXP. Genes Dev. 15, 627–637. https://doi.org/10.1101/gad.864401

Ziemienowicz, A., Skowyra, D., Zeilstra-Ryalls, J., Fayet, O., Georgopoulos, C., Zylicz, M., 1993. Both the Escherichia coli chaperone systems, GroEL/GroES and DnaK/DnaJ/GrpE, can reactivate heat-treated RNA polymerase. Different mechanisms for the same activity. J. Biol. Chem. 268, 25425–25431.

Zolkiewski, M., 1999. ClpB Cooperates with DnaK, DnaJ, and GrpE in Suppressing Protein Aggregation: A NOVEL MULTI-CHAPERONE SYSTEM FROM *ESCHERICHIA COLI*. Journal of Biological Chemistry 274, 28083–28086. https://doi.org/10.1074/jbc.274.40.28083

Curriculum vitae

Regina Maria Alver (geb. Kramer)

Geboren am 22.10.1990 in Paderborn, Deutschland

Ausbildung

Oktober 2015 – Oktober 2020	**Promotion in Biologie (PhD), Institut für Mikrobiologie, Leibniz Universität Hannover** Schwerpunkte: Charakterisierung von Proteinqualitätskontrollsystemen *in vitro*, Biofilmbildung
Oktober 2013 – September 2015	**Leibniz Universität Hannover, Master of Science in Pflanzenbiotechnologie** Masterarbeit zum Thema: Entwicklung von Methoden zur affinitätschromatographischen Reinigung von Peptidasen aus Basidiomyceten
Oktober 2010 – August 2014	**Leibniz Universität Hannover, Bachelor of Science in Pflanzenbiotechnologie**
August 2002 – Juni 2010	**Pelizaeus-Gymnasium Paderborn, Abitur**

Berufserfahrung

April 2019 – September 2020	**Max-Planck-Forschungsstelle für die Wissenschaft der Pathogene**, wissenschaftliche Mitarbeiterin, Berlin, Deutschland
Oktober 2015 – März 2019	**Leibniz Universität Hannover, Institut für Mikrobiologie**, wissenschaftliche Mitarbeiterin, Hannover, Deutschland

List of Publications

Anne Diehl, Yvette Roske, Linda Ball, Anup Chowdhury, Matthias Hiller, Noel Molière, Regina Kramer, Daniel Stöppler, Catherine L. Worth, Brigitte Schlegel, Martina Leidert, Nils Cremer, Natalja Erdmann, Daniel Lopez, Heike Stephanowitz, Eberhard Krause, Barth-Jan van Rossum, Peter Schmieder, Udo Heinemann, Kürşad Turgay, Ümit Akbey, Hartmut Oschkinat, (2018). Structural changes of TasA in biofilm formation of *Bacillus subtilis*. PNAS, 115 (13) 3237-3242; doi: 10.1073/pnas.1718102115

Hantke, I., Schäfer, H., Kramer, R., Turgay, K. (2019). The stressful life of *Bacillus subtilis*. BIOspektrum 02/2019. doi: 10.1007/s12268-019-1023-0

Dougan, D.A., Alver, R. and Turgay, K. (2020), Exploring a potential Achilles heel of *Mycobacterium tuberculosis*: defining the ClpC1 interactome. FEBS J. doi:10.1111/febs.15430

Manuscript in preparation:

Alver, R., Hantke, I., Gunka, K., Molière, N., Elsholz, A.K.W., Charpentier, E., and Turgay K., The role of protein arginine phosphorylation and dephosphorylation in protein homeostasis of *Bacillus subtilis* cells

Danksagung

Als erstes möchte ich mich bei Prof. Dr. Kürşad Turgay für die Betreuung und große Unterstützung während meiner Promotionszeit ausdrücklich bedanken. Insbesondere durch die fachlichen Ratschläge, die gewährte Freiheit bei den Projekten, sowie durch die anregenden Diskussionen, die immer spannende, neue Ideen lieferten, konnte ich viel lernen. Vielen Dank!

Prof. Dr. Brüser danke ich für die hilfreichen Diskussionen im Rahmen des Seminars, die Möglichkeit während des Laborumzuges nach Berlin weiter im Institut in Hannover arbeiten zu können und für die Erstellung des zweiten Gutachtens dieser Arbeit, sowie Prof. Dr. Braun für die Übernahme des Prüfungsvorsitzes.

Ein spezieller Dank gilt den Kollegen und Kolleginnen am Institut für Mikrobiologie, besonders Heinrich, Ingo und Michelle, für die großartige, oft amüsante Arbeitsatmosphäre und zugleich für viele hilfreiche, lebhafte Diskussionen. Für die große technische Unterstützung möchte ich Armgard danken, sowie Katrin, die mir sehr bei der Durchführung der unzähligen Experimente geholfen hat.

Des Weiteren möchte ich mich bei den Mitarbeitern des MPUSP Berlin dafür bedanken, dass sie mir beim Einzug in das neue Labor mit Rat und Tat zur Seite standen und direkt einen Austausch von Ideen und eine angenehme Zusammenarbeit ermöglichten. Prof. Emmanuelle Charpentier und Dr. Alexander Elsholz danke ich für die herzliche Aufnahme am Institut.

Für die erfolgreiche Zusammenarbeit und Kooperation, die das Biofilm-Projekt ermöglicht hat, möchte ich Dr. Anne Diehl, Prof. Dr. Hartmut Oschkinat (Leibniz-Forschungsinstitut für Molekulare Pharmakologie), Dr. Yvette Roske (Max-Delbrück-Centrum für Molekulare Medizin) und allen anderen Beteiligten danken.

Meiner Familie möchte ich besonders danken für die Unterstützung bei all meinen Ideen und Vorhaben. Danke, dass ihr immer für mich da seid!

Der letzte und größte Dank gilt meinem Mann Ufuk. Für die Unterstützung, die Geduld und dafür, dass du mir gezeigt hast, dass man ab und zu einfach mal etwas wagen muss. Egal wo es hin geht, du bist mir das Wichtigste.